CHARACTERIZATION OF THE PHEROMONE COMMUNICATION CHANNEL IN *MAMESTRA CONFIGURATA*, THE BERTHA ARMYWORM

A Thesis Submitted to the
College of Graduate and Postdoctoral Studies
In Partial Fulfillment of the Requirements
For the Degree of Doctor of Philosophy
In the Department of Biology
University of Saskatchewan
Saskatoon

By

EDYTA AGNIESZKA SIEMINSKA

PERMISSION TO USE

In presenting this thesis/dissertation in partial fulfillment of the requirements for a Postgraduate degree from the University of Saskatchewan, I agree that the Libraries of this University may make it freely available for inspection. I further agree that permission for copying of this thesis/dissertation in any manner, in whole or in part, for scholarly purposes may be granted by the professor or professors who supervised my thesis/dissertation work or, in their absence, by the Head of the Department or the Dean of the College in which my thesis work was done. It is understood that any copying or publication or use of this thesis/dissertation or parts thereof for financial gain shall not be allowed without my written permission. It is also understood that due recognition shall be given to me and to the University of Saskatchewan in any scholarly use which may be made of any material in my thesis/dissertation.

Requests for permission to copy or to make other uses of materials in this thesis/dissertation in whole or part should be addressed to:

Head of Department of Biology
University of Saskatchewan
112 Science Place
Saskatoon, Saskatchewan S7N 5E2 Canada

OR

Dean
College of Graduate and Postdoctoral Studies
University of Saskatchewan
116 Thorvaldson Building, 110 Science Place
Saskatoon, Saskatchewan S7N 5C9 Canada

ABSTRACT

The bertha armyworm (BAW), *Mamestra configurata,* is one of the major insect pests feeding on a wide range of plant species, including canola, across western Canada. The components of the sex pheromone blend specific to *M. configurata* were identified in the 1970's and are currently used in the pheromone trap monitoring system. However, there is evidence that geographic BAW populations develop at different rates and respond differently to the commercially prepared pheromone lures which affects our ability to accurately predict economic infestation levels for this pest. Collection of egg masses and pupae from several western Canada locations during the last BAW outbreak (2011-2014) presented a rare opportunity to investigate the genetics and biology of pheromone communication in *M. configurata* in field populations as compared to the long-term laboratory reared strain. My research encompassed aspects of both female pheromone production and male response to the female produced signal. I utilized next generation sequencing combined with bioinformatic analysis to identify and characterize genes involved in pheromone biosynthesis in females and chemosensory proteins involved in pheromone reception in males and females. I also used a novel single nucleotide polymorphism identification strategy to characterize genetic variation within pheromone specific chemosensory gene sequences among males from three BAW populations. The female pheromone gland analysis via gas chromatography coupled mass spectroscopy indicated that although, the amount of major and minor pheromone components varied greatly between individuals within a population, the pheromone blend ratios were not found to be significantly different between the two subpopulations investigated. Behavioural assays in the wind tunnel showed a marked difference in the ability of colony reared BAW males to take flight and reach the pheromone source as compared to field population males. Electrophysiological recordings obtained from colony and field population BAW male antenna showed significant loss of sensitivity to the minor pheromone component in the colony reared males. The knowledge gained from these studies will serve as a foundation for future research aimed at developing more effective integrated pest management strategies utilizing the pheromone communication channel for *M. configurata.*

ACKNOWLEDGMENTS

To my committee for their guidance and support while I pursued this degree.

To my supervisor Dr. Martin Erlandson for his willingness to take me on as a student and his patience as this project evolved and coalesced. I am thankful for his mentorship and his ability to strike a balance between exploration and focus. As a scientist, I will forever measure myself by his standard of knowledge, work ethic and humility.

To my co-supervisor Dr. Jack Gray for his support, enthusiasm and for continually challenging me to go back and learn more.

To Dr. Dwayne Hegedus, Dr. Art Davis and Dr. Neil Chilton for their time and encouragement. Special thanks to Dr. Hegedus for his thorough review of this thesis and his invaluable feedback.

To the members of the Erlandson and Hegedus labs with special thanks to Doug, Stephanie, Jen and Cathy for their help over the last five years. It has been a privilege to work with you.

To Dr. Matthew Links for his bioinformatics expertise and inspiration.

To Dr. Boyd Mori for his helpful advice and comments on electrophysiology and on experimental design.

To Dr. Gerhard Gries and Regine Gries from Simon Fraser University for their assistance on pheromone gland analysis and GC-EAD analysis and for allowing me to visit their laboratory to carry out these experiments.

To my parents for instilling curiosity in me and teaching me how to ask the right question.

To Remi for feeding, supporting and inspiring me.

To Stefan, for your smiles, falling stars and for reminding me of what is truly important.

I am very grateful for the joys and challenges that this experience has provided me.

DEDICATION

To my family

"Sell your cleverness and buy bewilderment.

Cleverness is mere opinion, bewilderment is intuition."

-Rumi-

TABLE OF CONTENTS

LIST OF TABLES

LIST OF FIGURES

LIST OF EQUATIONS

LIST OF ABBREVIATIONS

3HCD	3-hydroxyacyl-CoA dehydrogenase
AAFC	Agriculture and Agri-food Canada
ACB	Asian corn borer
ACC	acetyl-CoA carboxylase
ACD	acyl-CoA dehydrogenase
ACO	B-oxidase
ADO	aldehyde oxidases
AFLP	amplified fragment length polymorphism
AL	antennal lobe
ASS	alternative splice sites
BAW	bertha armyworm
cAMP	cyclic adenosine monophosphate
CDS	current source density
CNS	central nervous system
CoA	Coenzyme A
CSP	chemosensory proteins
DBG	de Bruijn graph
DES	desaturase
EAD	electroantennographic detection
EAG	electroantennograph
ECB	European cornborer
ECH	enoyl-CoA hydratase
F1	filial 1 hybrid
FAR	fatty acid reductases
FAS	fatty acid synthase
FAT	acetyl transferases
FID	flame ionization detector
FPKM	fragments per kilobase of transcripts per million fragments mapped
GC	gas chromatography
GC-MS	gas chromatography mass spectroscopy
GOBP	general odorant-binding proteins
GPCR	G-protein coupled receptor
GR	gustatory receptor
GSN	gustatory sensory neurons
iGluR	ionotropic glutamate receptor
ILPt	inferior lateral protocerebrum

IR	ionotropic receptor
KCT	acetoacetyl-CoA thiolase
l-APT	lateral antennoprotocerebral tract
LFP	local field potential
LN	local neurons
LP	lateral protocerebrum
m-APT	medial antennoprotocerebral tract
MBC	mushroom body calyces
McGl	macroglomerular complex
ml-APT	mediolateral antennoprotocerebral tract
OBP	odorant binding proteins
ODE	odorant-degrading enzyme
OR	olfactory receptors
ORCO	olfactory coreceptor
OSN	olfactory sensory neuron
PBAN	pheromone biosynthesis activating neuropeptide
PBANr	PBAN receptor
PBP	pheromone binding protein
pgFAR	pheromone gland fatty acyl reductase
PIPMN	Prairie Insect Pest Monitoring Network
PN	projection neurons
PR	pheromone receptor
QTL	quantitative trait locus
RNA-Seq	RNA sequencing
RSEM	RNA-Seq by expectation maximization
SNMP	sensory neuron membrane protein
SNP	single nucleotide polymorphism
TEP	transepithelial potential
TPM	transcripts per million
Z11-16Ac	(Z)-11-hexadecenyl acetate
Z11-16OH	(Z)-11-hexadecenyl alcohol
Z7-12Ac	(Z)-7-dodecenyl acetate
Z9-14Ac	(Z)-9-tetradecenyl acetate

CHAPTER 1. LITERATURE REVIEW AND OBJECTIVES

1.1 CHEMICAL COMMUNICATION

Chemical communication is a silent, ubiquitous language in nature [Ryan 2002; Mucignat-Caretta 2014]. Organisms across all phyla, from bacteria to vertebrates, have evolved the ability to interpret chemical cues carrying information about food sources, danger, orientation, kin and predator recognition and mate attraction [Wyatt 2014]. Chemical communication offers certain advantages over visual or auditory communication. Chemical messages can be very private and long lasting, travel over considerable distances when carried by air, and be effective even in the absence of light. The sensory modality of olfaction has evolved as a mechanism for deciphering the chemical messages in a multitude of ecological lifestyles [Hansson and Stensmyr 2011]. Arguably, among all organisms, insects present the greatest range of behaviours mediated by olfactory cues [Martin et al. 2011]. In the insect world, the olfactory information is encoded by volatile compounds called semiochemicals[1]. Specific semiochemicals or semiochemical mixtures provide fast and reliable environmental cues that elicit essential innate behaviours and may also lead to the establishment of adaptive behaviours[2] [de Bruyne and Baker 2008]. Whereas olfaction contributes to an insect's fitness and is critically important for its survival [Hansson and Stensmyr 2011], this form of chemoreception also plays a pivotal role in insect behaviours of particular interest to humans [Reisenman et al. 2016]. Olfaction-guided adaptive behaviours often determine an insect's environmental and economic importance, either as beneficial pollinator, agricultural pest or a vector of human disease [Wilson-Sanders 2011]. During the last century, the insect olfactory system has emerged as a prominent model for studies on olfaction [Hildebrand and Shepherd 1997; Kay and Stopfer 2006]. On one hand, the

[1] **semiochemicals**: chemical compound that conveys information from one organism to another so as to modify the behaviour of the recipient organism

[2] **adaptive behaviour**: behaviour that contributes directly or indirectly to an individual's reproductive success and thus it is subject to the forces of natural selection

accessibility and simplicity of the insect olfactory system design has allowed for detailed studies of its underlying anatomy, molecular architecture, function and general principles of sensory processing [de Bruyne and Baker 2008]. On the other hand, the vast diversity of olfactory systems within the order Insecta has allowed for comparative work based on species' natural histories and adaptation to their specific environments [Hansson and Stensmyr 2011]. One fundamental aim of insect olfaction research is to understand the underpinnings of neural mechanisms eliciting olfaction based behaviours [Cardé and Elkinton 1984; Suckling 2016]. Notably, the largest contribution to our current understanding of olfactory processes modulating insect behavioural responses comes from the research on pheromone communication commonly employed by insects in location of conspecific mating partners [Kuenen and Siegel 2015].

1.2 LEPIDOPTERAN SEX PHEROMONE COMMUNICATION CHANNEL

In the late 1800s, Jean-Henri Lafabre, the French naturalist and entomologist, observed the powerful attraction between the female and male giant peacock moths (*Saturnia pyri,* Saturniidae) [Willis and Baker 1988]. Lafabre speculated that the males must be attracted to an invisible signal emitted by the female. Lafabre's speculation was confirmed 84 years later by a German biochemist, Adolf Butendandt. Butendandt and his team extracted over 500,000 female pheromone glands from the domestic silk worm *Bombyx mori* (Bombycidae) to identify the first lepidopteran pheromone (*E,Z*)-10, 12-hexdecadienol (bombykol) [Butenandt et al. 1959; Wyatt 2014]. In parallel with Butenandt's discovery, the word pheromone was coined from the Greek words "pherein" meaning to carry or transfer and "hormone" to excite or stimulate [Karlson and Luscher 1959]. At approximately the same time, another German scientist, Dietrich Schneider, developed a technique for detecting neural responses from the insect antenna [Schneider 1957]. Both of these findings mark the beginning of almost 80 years of intense research on insect pheromones.

Pheromones are a class of semiochemicals defined as molecules that are produced and that elicit a response within the same species [Vogt and Chertemps 2005]. Pheromone signalling is considered one of the most sophisticated forms of chemical communication [Schneider 1992]. In the order Lepidoptera, emission of specific ratios of volatile compounds by adult females is required to attract conspecific males to ensure mating success and reproductive isolation of species [Gould et al. 2010]. Lepidoptera are currently classified into 53 superfamilies, 137

families, 15,648 genera and 157,424 species [van Nieukerken et al. 1999]. It is thought that pheromone communication may have contributed to the wide speciation and diversity observed within this order [Cardé and Haynes 2004]. As the second largest insect order, with the majority of its members being herbivorous, the Lepidoptera represent a large proportion of insect pests of food and crops worldwide. Olfactory processes underlying lepidopteran sex pheromone communication have been the subject of extensive research as potential targets for the development of pest control strategies [Baker et al. 2016]. Whether the strategies are indirect, such as pheromone trap monitoring for developing economic threshold models [McNeil 1991], or direct, such as mass trapping or mating disruption [Miller and Gut 2015], they rely on a comprehensive understanding of the female-produced signal and the male response to that signal [Pickett et al. 1997]. In particular, design of effective pest control strategies requires an in-depth understanding of the variation within pheromone communication and its underlying causes.

1.3 THE SIGNAL: LEPIDOPTERAN FEMALE PHEROMONE

1.3.1 Behaviour associated with pheromone signaling

In the majority of moth species, pheromones are produced by the females. The behaviour of female "calling" involves the female protruding her abdominal tip (ovipositor) to expose the pheromone gland (Figure 1-1A) to permit the evaporation of the pheromone blend components from the gland's external surface [Percy-Cunningham and Macdonald 1987]. The calling is associated with circadian rhythms and can be affected by a number of external factors such as temperature, relative humidity, light, wind speed, general weather conditions and presence of host plants [McNeil 1991; Groot 2014]. In addition, physiological factors, such as female's age, diet and mating status, can also contribute to the timing and quality of "calling" [McNeil 1991].

1.3.2 Structure and morphology of the female pheromone gland

In noctuid lepidopterans, the pheromone gland is ductless and commonly located in the intersegmental membrane between the eighth and ninth abdominal segments [Percy-Cunningham and Macdonald 1987]. At least in the subfamily Heliothinae, the glandular tissue was shown to have a complete ring structure when the ovipositor is fully protruded and a U-shaped fold when the ovipositor is retracted [Raina et al. 2000]. The U-shaped fold is thought to prevent spontaneous release of pheromone in the retracted state. The modified intersegmental membrane is a highly folded structure and is formed by a single cell layer composed of either one or two

types of cells depending on the species [Raina et al. 2000]. Type 1 cells are predominant with a columnar shape and prominent spherical nuclei at their base. They have been shown to exhibit marked opaque spherical bodies during the scotophase. The basal region of Type 1 cells below the nucleus is rich in Golgi complexes, lipid droplets, glycogen deposits, and rough endoplasmic reticulum, characteristic of cells involved in lipid accumulation and metabolism [Ma and Ramaswamy 2003]. These cells are also characterized by the presence of perforated outer epicuticle covered in cuticular hairs, which apparently enhances the diffusion of secretions from the surface of the gland [Raina et al. 2000]. Type 2 cells have a narrow shape with small lobed nuclei and, if present, can be found in the depressions of the prominent fold structures [Hallberg and Subchev 1997; Raina et al. 2000]. The modified epithelium contains extracellular spaces allowing for storage of secretions. The plasma membrane is differentiated both apically and basally contributing to the increased surface area for transport between the hemolymph, glandular cells and cuticle. The glandular cuticle acts as a storage and transport site for the pheromone components [Fleischer et al. 2018]. In several morphological studies, small opaque droplets were identified at the tips of cuticular hairs directly above the pheromone gland during the scotophase [Itagaki and Conner 1988; Raina et al. 2000]. Although these findings suggest that the pheromone molecules are excreted through these hairs, the exact mechanism of excretion is not known.

1.3.3 Lepidopteran pheromone biochemistry

To date, pheromone gland contents and composition have been identified from approximately 2000 lepidopteran species [Löfstedt et al. 2016]. In the majority of species, female moths produce species-specific sex pheromones as a multi-component blend with precise ratios of individual components. In addition to pheromone components which elicit excitation in conspecific males, female pheromone glands may contain a number of other substances referred to as constituents [Baker 2008]. Pheromone gland secretions often contain volatile compounds which serve to reduce attraction or prevent flight behaviour in males when detected in the presence of heterospecific pheromone blends [Linn et al. 2003]. Extensive research has been carried out on the sex pheromone biosynthetic pathway and the enzymes involved [Matsumoto 2010]. In 2004, Ando et al. proposed a classification of pheromones (Figure 1-1B) into three main types: Type I (75%), Type II (15%) and miscellaneous (10%) based on the chemical structure of compounds produced [Ando et al. 2004]. More recently, Löfstedt et al. proposed that

in addition to Type I and Type II pheromones, Type III and Type 0 pheromones should be added to the classification scheme based on recently identified novel structures [Löfstedt et al. 2016]. A comprehensive list of pheromones identified to date is maintained online as "The Pherobase" website (www.pherobase.com) [El-Sayed 2014].

1.3.3.1 Type I Pheromones

Type I pheromones are even-numbered C_{10}-C_{18} straight chain, unsaturated derivatives of fatty acids with the carbonyl carbon modified to form an oxygen-containing alcohol, aldehyde or ester functional group. This class of compounds is synthesized *de novo* in the female pheromone gland through modification of the fatty acid biosynthetic pathway (Figure 1-1C) [Matsumoto 2010]. Type I pheromone production is under direct control of the pheromone biosynthesis activating neuropeptide (PBAN) which upregulates pheromone synthesis in the pheromone gland. *De novo*-synthesized free saturated fatty acids are stored mostly as triglycerols, or associated with other glycerolipids or phospholipids. The three most common fatty acids produced in the lepidopteran pheromone glands are steric acid (18:CoA), palmitic acid (16:CoA) and myristic acid (14:CoA) although the enzymes responsible for generation of these saturated precursors have not been functionally assayed [Jurenka 2003]. The two initial steps in biosynthesis of Type I pheromones involve desaturation (introduction of double bonds) carried out by desaturases, followed by ß-oxidation to shorten or elongate the chain (2 carbons per cycle). Thus, the majority of Type I compounds have an even number of carbons (10-18). The resulting fatty acids containing a carboxy moiety (COOH) are first reduced via pheromone gland fatty acyl reductases (pgFARs) to alcohols (OH) [Morse and Meighen 1986]. Alcohols can be further converted to aldehydes by alcohol oxidase or to acetate esters (OAc) by acetyltransferases [Jurenka 2003]. In a small number of species the diversity of Type I pheromones is expanded with the inclusion of unusual functional groups such as nitro groups, esters and modified acetates [Ando et al. 2004].

1.3.3.2 Type II Pheromones

Type II pheromones are much less common and produced by highly evolved lepidopteran families such as Geometridae, Lymantriidae and Arctiidae [Ando et al. 2004]. This class of

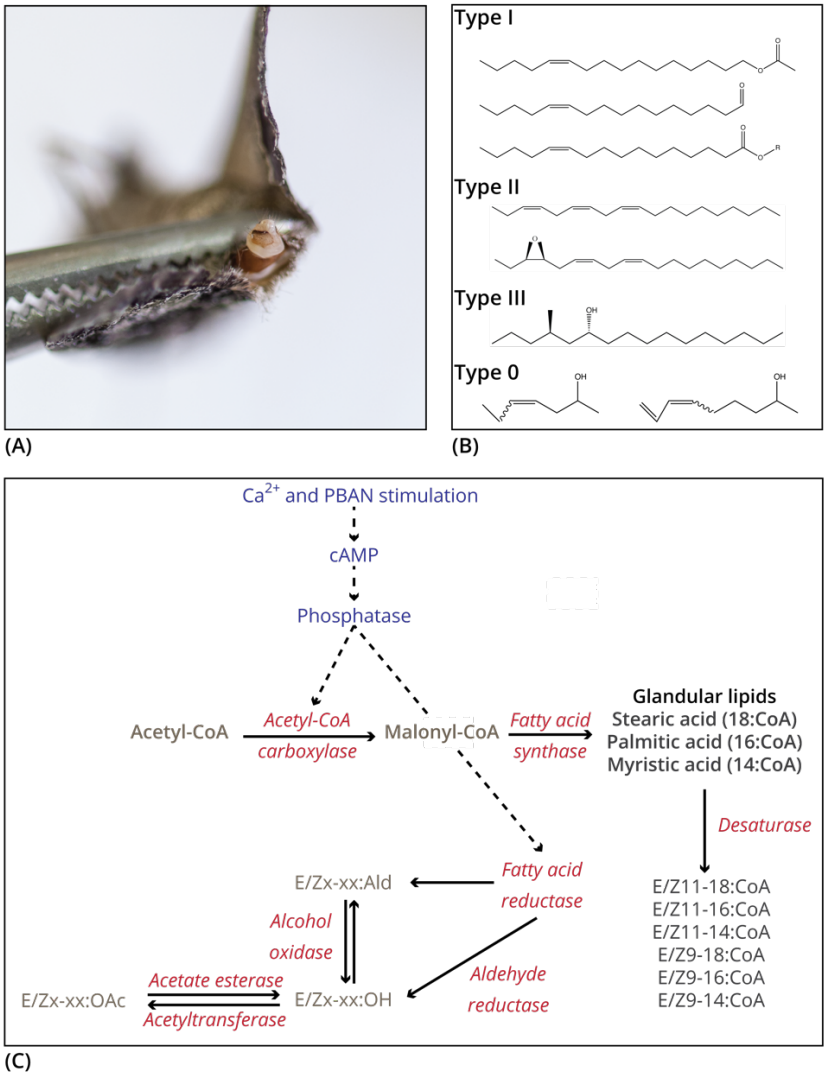

Figure 1-1 Lepidopteran pheromones. **(A)** Extruded female pheromone gland tissue of *Mamestra configurata*. **(B)** Structural representation of compounds belonging to the four pheromone classes. Type I pheromones constitute the largest class of lepidopteran pheromones and include straight chain unsaturated derivatives of fatty acids with respective functional group of either an ester, alcohol and aldehyde. Type II pheromones are polyunsaturated hydrocarbons or corresponding epoxide derivatives lacking functional groups and produced by the Geometridae, Lymantriidae and Arctiidae families. Type III pheromones are methyl branched compounds initially identified within the Arctiidae family. Type 0 structures correspond to short chain methylcarbinols and methylketones produced by species within Nepticulidae and Eriocraniidae. **(C)** Overview of biosynthetic pathway for Type I lepidopteran pheromones. Major enzymes participating in the synthesis are indicated in red. PBAN (biosynthesis activating neuropeptide), CoA (coenzyme A), Ald (Aldehyde), OAc (acetyl ester), OH (alcohol). Adapted from Ando et al. (2004) and Löfstedt et al. (2016).

compounds includes polyunsaturated hydrocarbons or corresponding epoxide derivatives with C_{17}-C_{25} unbranched carbon chains and often lacking a terminal functional group. Type II pheromones are synthesized from diet-derived linoleic or linolenic acid [Samuelson et al. 1988] in oenocyte[3] cells associated with the integument or fat body and transported to the pheromone gland via lipophorin carrier proteins in the hemolymph [Matsuoka et al. 2006]. Some of the compounds belonging to this class are released from the pheromone gland without any further modifications, whereasothers undergo further processing, such as epoxidation [Miyamoto et al. 1999], or addition of terminal functional groups [Kiyota et al. 2011]. In contrast to Type I pheromones, Type II pheromone synthesis is not under direct control of PBAN; however, it is thought that PBAN controls the uptake of pheromone precursors from the hemolymph to the pheromone gland [Fujii et al. 2007]. Some experimental evidence suggests that the synthesis of Type II pheromones may start in the early pupal stage rather than post eclosion [Rule and Roelofs 1989].

1.3.3.3 Type III Pheromones

More recently, methyl-branched pheromone molecules were discovered in the lichen moth, *Miltochrista calamine* [Yamakawa et al. 2011b], and confirmed in small number of other species [Löfstedt et al. 2016]. These Type III pheromones are synthesized *de novo*, but not in the pheromone gland [Schal et al. 1998]. Schal et al. (1998) provided evidence for the production of Type III precursors in oenocytes and their transport via lipophorin proteins through the hemolymph with the pheromone gland as their final destination. Subsequently, it was also shown that PBAN did not directly control the production of Type III compounds, but did up-regulate the epoxidation reactions in the pheromone gland [Jurenka 2004]. The methyl-branch structure is thought to originate from amino acid precursors, such as leucine or valine, with typical fatty acid biosynthesis or incorporation of methylmalonyl CoA in place of malonyl CoA [Blomquist et al. 2010]. No studies to date have directly addressed the details of the Type III pheromone biosynthetic pathway [Löfstedt et al. 2016].

[3] **Oenocytes**: large, straw-colored cells that are segmentally arranged in connection with the fat bodies and tracheae of most insects and may have important secretory functions

1.3.3.4 Type 0 Pheromones and Others

Recently, Löfsted et al. (2016) suggested that a fourth class of pheromone be added based on work in primitive moth species from the Nepticulidae [Toth et al. 1995] and Eriocraniidae families [Zhu et al. 1995]. Type 0 pheromones consist of short-chain methylcarbinols and methylketones. Information on these compounds and their biosynthesis is very limited. Their chemical structure suggests they may be related to Type I pheromones. A theoretical biosynthetic pathway was proposed with fatty acid precursors, such as myristic acid, followed by 2-3 cycles of ß-oxidation and reductive decarboxylation of ß-ketoacyl intermediates from the chain-shortening reactions [Löfstedt and Kozlov 1997].

In addition to the four pheromone classes mentioned thus far, a few of the pheromonal compounds eliciting classical sexual communication behaviours in males remain unclassified. For example, *Hemithea tritonaria* [Yamakawa et al. 2011a] and *Corcyra cephalonica* [Mori et al. 1991] utilize terpenoid-derived compounds not found in other pheromone blends. Several arctiine species (Lithosiini) utilize propionate esters of secondary alcohols [Fujii et al. 2013]. Overall, given the diversity of Lepidoptera, only a small portion of pheromone compounds has been identified. Currently, the majority of identified compounds correspond to pheromones of species considered to be major agricultural pests. As these studies are expanded to other lepidopteran species and novel compounds discovered, it is plausible that the overwhelming predominance of Type I pheromones may change.

1.3.4 Factors affecting pheromone blend composition

Although the first pheromone characterized in *B. mori* was a single compound, (10E,12Z)-10,12-hexadecadienol (bombykol) [Butenandt et al. 1959], the majority of moth species produce blends containing specific ratios of volatile molecules [Byers 2006]. Chemical specificity of an individual pheromone blend is achieved through several qualitative properties of the female-produced effluvium components. Pheromone constituents vary in chain length, double bond configuration, the presence or absence of functional moieties and their ratios [Allison and Cardé 2016a]. It is generally accepted that these differences contribute to the reproductive isolation within the species-rich order Lepidoptera. The variation in pheromone blend composition among individuals, populations or closely-related species is under the control of a number of physiological, environmental and genetic factors [Allison 2006; Allison and Cardé 2016a].

1.3.4.1 Physiological factors

The presence of multiple components in the pheromone blend introduces the possibility of variation in the ratios of compounds. The majority of studies carried out to date are based on female pheromone gland contents and only a small subset of those studies address the differences between gland composition and the actual emitted blend [Löfstedt et al. 2016]. Furthermore, understanding variation at an individual level is essential before attempting to study variance in pheromone production at the level of population. Several studies have addressed the consistency of the female-produced blend within an individual [Du et al. 1987; Svensson et al. 1997]. For example, each *Agrotis segetum* female could reproduce the most attractive ratio of pheromone components with a 0.82-0.9 repeatability value (highest being 1); however, the fidelity diminished with the age of the females [Svensson et al. 1997]. This age dependence for producing the most attractive blend ratio was found in a number of other moth species. In moths that mate shortly after eclosion, the titers of pheromone components are very low at eclosion, rise rapidly to peak for several days and then steadily decline until death [Schal 1986; Tang et al. 1992; Gemeno and Haynes 2000; Allison 2006].

The concentration and chemical ratios found in pheromone glands are not always an accurate predictor of the emitted pheromone blend during female calling [Hunt and Haynes 1990; Haynes and Hunt 1990a]. Generally, it is accepted that when the pheromone components are of the same chain length and contain same functional group, the ratios emitted are often comparable to the ratios present in the gland [Cardé et al. 1979; Collins and Cardé 1985; Lacey and Sanders 1992]. In *Trichoplusia ni*, the composition of the emitted blend was compared between the calling stage, early scotophase and photophase. Although the concentration of the main pheromone component, (Z)-7-dodecenyl acetate (Z7-12Ac), remained the same between the gland and captured emission during all three stages, the amount of the (Z)-9-tetradecenyl acetate (Z9-14Ac) component increased significantly relative to Z7-12Ac in the emission fraction, but remained constant in the gland during the calling stage [Hunt and Haynes 1990]. Consequently, the content between the gland and emitted blend is not consistent for blends with components of variable chain lengths and functional moieties. The differences observed are likely due to the discrete vapour pressures of each compound as determined by their respective chemical properties resulting in variable rates of evaporation from the gland's surface [Roelofs and Cardé 1977; Allison and Cardé 2016a]. To account for differences in vapour pressure of the individual

components from a calling female, a control mechanism would be required to mediate the synthesis and transport of these compounds to the surface of the female pheromone gland. To date, no evidence for such a control mechanism has been found [Allison and Cardé 2016a].

1.3.4.2 Environmental factors

In addition to physiological factors, a number of environmental factors, including variation in temperature during larval and pupal phases, wind speed, light intensity and diet can affect the pheromone gland production and discharge [McNeil 1991]. For example, in the potato tuberworm moth, *Phthorimaea operculella*, the sex pheromone consists of two compounds: (*E, Z, Z*)-4,7,10-tridecatrenyl acetate (triene) and (*E, Z*)-4,7-tridecadenyl acetate (diene) [Ono et al. 1990; Ono 1993]. Studies on laboratory-reared moths suggest that the biosynthesis of the triene occurs during pupal phase, whereas the diene is synthesized for a few days immediately post-eclosion. The variation of rearing temperature during these phases can alter the ratio of triene to diene in the final pheromone blend [Ono 1993]. In another species, *Heliothis virescens*, the feeding behaviour was shown to affect the titers of pheromone components in the gland [Foster and Anderson 2015].

1.3.5 Genetic basis of female pheromone variation

The diversification of species-specific pheromone signals in Lepidoptera is thought to be driven by genetic changes in loci coding for enzymes involved in the biosynthesis of female-produced pheromone components [Phelan and Baker 1987; Phelan 1992]. Studies probing the inheritance of genotypes corresponding to the differences in pheromone blend production have employed a number of techniques, including crossing experiments, parent-offspring correlation, sibling and half-sibling studies and quantitative trait locus (QTL) analysis [Haynes 2016]. Although mating between two genetically-differentiated strains or closely-related species is rare in nature, it is possible and has been exploited under laboratory conditions [Wang et al. 2005; Groot et al. 2009; Lassance et al. 2010]. Investigations exploring the genetic make-up of the offspring produced from interspecific crosses in moths have greatly contributed to our current knowledge of mechanisms responsible for pheromone signal differentiation. However, these studies have been limited to only a small number of persistent agricultural pest species for which genetic and molecular aspects of pheromone production have been delineated. A brief review of the four

major model species, along with the contributions made by each to our understanding of the genetics underlying pheromone signal variation are outlined below.

Pheromone signal production divergence has been extensively studied within the genus *Ostrinia* species (Crambidae) [Lassance 2016]. Due to its pest status, the European cornborer (ECB; *O. nublialis*) has received considerable research attention regarding its pheromone communication. Early studies revealed that ECB has two unique strains, the *E*-strain with a 99:1 ratio of (*E*)-11-tetradecenyl acetate (*E*11-14Ac) to (*Z*)-11-tetradecenyl acetate (*Z*11-14Ac) and the *Z*-strain with a 3:97 ratio. This polymorphism in the female-produced pheromone blend represented a unique opportunity to study the genetics, biochemistry and molecular biology intrinsic to the evolution of signal production [Lassance and Löfstedt 2013]. The difference between the blends from the *E* and *Z* strains has been correlated to a mutation in the fatty acyl reductase gene (*pgfar*) expressed in the pheromone gland which affects the enzyme's specificity [Zhu et al. 1996b; Lassance et al. 2010]. The F1 (filial 1 hybrid) generation from crosses between the two parental *Ostrinia* strains resulted in an intermediate pheromone phenotype of 65:35 *E*11-14Ac to *Z*11-14Ac confirming autosomal inheritance of the factor responsible for blend variation [Roelofs et al. 1987; Roelofs and Rooney 2003]. Zhu et al. showed that other alleles, and possibly other genes, might contribute to the impact of genotypic variation between the *E* and *Z*-strain desaturases [Zhu et al. 1996a]. Furthermore, a comparative study using hybrid offspring of ECB and Asian corn borer (ACB; *O. furnicalis*) showed that two different desaturases were responsible for the generation of respective pheromone components in each species. Both desaturase genes were present in each species, but only one or the other was expressed and biologically active [Roelofs and Rooney 2003].

Several species within the subfamily Heliothinae have been studied extensively and have emerged as model systems. The heliothine moths are distributed globally with an estimated 365 member species often occurring in sympatry across vast geographic areas [Cho et al. 2008]. Many of the species are persistent pests of economically-important crops [Fitt 1989]. For the majority of species within this subfamily, variation in the female-produced ratio of the major component, (Z)-11-hexadecenal (Z11-16Ald), and the two minor components, (Z)-9-tetradecenal (Z9-14Ald) and (Z)-9-hexadecenal, is sufficient to maintain the species-specific blend isolation [Hillier and Baker 2016]. A small number of other minor pheromone components were also

identified among various species and are known to enhance the species-specific blends. In addition to the female pheromone components, the majority of heliothine females also produce compounds that act as antagonists for heterospecific males [Domingue et al. 2007; Baker 2008]. Recent studies provide evidence for autosomal inheritance of pheromone blend production in heliothines. The difference in blend ratios produced by offspring of *Helicoverpa armigera* and *H. assulta* (Noctuidae) crosses was mapped to a single autosomal gene [Wang et al. 2008]; however, high genetic variation observed in the offspring from parental backcrosses suggested that more than one gene was involved. Other studies showed that trait loci from a single chromosome may affect multiple pheromone components and that epistatic interactions are possible between loci located on different chromosomes [Löfstedt 1990; Groot et al. 2006]. A chromosome mapping approach (Amplified Fragment Length Polymorphism) was used to study the genetic basis of the pheromone blend differences between *Heliothis virescens* and *H. subflexa* [Groot et al. 2004; 2006; 2009]. Since chromosome crossing over does not occur in Lepidoptera, a QTL can be localized to a specific chromosome [Sheck et al. 2006]. Out of 31 chromosomes (30 autosomal + 1 sex) in *H. virescens*, at least 9 were reported to have impact on the blend ratio in the pheromone gland [Groot et al. 2009]. In the same study, a detailed analysis of one of the QTLs identified, implicated this gene as a suppression factor for production of antagonist acetates in *H. virescens*.

In another pest species, the cabbage looper moth, *T. ni* (Noctuidae), females produce a six-component blend consisting of dodecyl acetate (12Ac), (Z)-5-dodecenyl acetate (Z5-12Ac), (Z)-7-dodecenyl acetate (Z7-12Ac), 11-dodecenyl acetate (11-12Ac), (Z)-7-tetradecenyl acetate (Z7-14Ac) and (Z)-9-tetradecenyl acetate (Z9-14Ac) [Linn et al. 1984]. Significant, but subtle, inter-population variation in pheromone blend composition has been described with multiple genes implicated as the basis for variation [Haynes and Hunt 1990a]. In addition, a recessive mutation in a colony-reared strain that dramatically affects the quantity of two of the pheromone components is linked to a single autosomal locus [Haynes and Hunt 1990b]. The difference between the mutant and original strain pheromone blends was correlated to a mutation the encoding a ß-oxidation (chain shortening) enzyme [Jurenka et al. 1994]. Further crossing experiments (half-sibling breeding) of the mutant laboratory strain with a wild-type laboratory strain established involvement of both autosomal and sex-linked genes in the observed pheromone blend variation [Gemeno et al. 2001].

Agrotis segetum (Noctuidae) has also attracted considerable research due to its pest status and marked geographic segregation of pheromone phenotypes [Löfstedt et al. 1985a; Hansson et al. 1990; Toth et al. 1992; Wu et al. 1998]. This species has a wide distribution throughout Eurasia and Africa. The three pheromone components (*Z*)-5-decenyl (*Z*5-10Ac), (*Z*)-7-dodecenyl (*Z*7-12Ac) and (*Z*)-9-tetradecenyl (*Z*9-14Ac) are produced in different ratios in females from various geographic locations. The most extreme blend ratios are found in populations from Sweden {12:59:29} [Löfstedt et al. 1985b] and Zimbabwe {78:20:2} [Wu and Baldwin 2010]. Specimens from Sweden {4:52:44}, France {47:40:13} [Löfstedt et al. 1986], Armenia {1:52:47} and Bulgaria {1:42:57} also exhibit a wide spectrum of pheromone blends [Hansson et al. 1990]. Crossing experiments were carried out on populations from Sweden and Zimbabwe revealed that the genetic basis underlying the pheromonal differences between the two populations is very complex [LaForest et al. 1997]. Incomplete dominance in one or more genes was reported for the Z5-12Ac and Z7-12Ac components, but the ratio of Z9-14Ac to Z7-12Ac was under dominant gene control in the Scandinavian strain.

Together, these studies indicate that pheromone production is under autosomal control with polygenic interactions. However, epigenetic interaction with the sex-linked chromosome cannot be excluded [Gemeno et al. 2001; Haynes 2016]. Each pheromone component and its titer in the pheromone gland may vary heritability [Gemeno et al. 2001; Sheck et al. 2006]. Genetic variation may be mapped to a single or multiple loci coding for various enzymes in the pheromone biosynthetic pathway. Genetic changes affecting the active site of enzymes critical to pheromone biosynthesis and having a large impact on the final blend composition are thought to represent changes underlying pheromone blend divergence and speciation [Roelofs et al. 2002; Bengtsson and Löfstedt 2007]. In contrast, smaller magnitude changes affecting catalytic rates, catalytic efficiency or transcriptional control of biosynthetic enzymes are thought to be responsible for more subtle variation, such as the variation often observed in populations of the same species distributed across a broad geographic range [Haynes and Hunt 1990a; Löfstedt et al. 2016]. What is not well-understood is the extent to which the environment affects the differentiation of genotypes corresponding to pheromone signal production. We currently do not understand how male preference for the signal or communication interference from sympatric species affects the variation in signal production [Bengtsson and Löfstedt 2007]. We also do not know if divergence events are responsible for speciation initiation or if they occur as an

"adjustment" once a speciation event has taken place [Löfstedt 1990]. A mechanism must exist by which the response of the male receiver adapts in parallel to the changes in the female-produced signal to maintain the effectiveness of the pheromone communication channel.

1.4 EVOLUTION OF PHEROMONE COMMUNICATION

Any change in the female-produced pheromone that renders the male unable to recognize her message and effectively decreases their chance of mating success should be selected against [Ritchie 1996]. Thus, sexual communication should be under strong stabilizing selection [Löfstedt 1990]. Conversely, species-specific pheromones maintain reproductive isolation and may contribute to speciation as outlined above. The evolutionary mechanism responsible for this apparent contradiction has been one of the longstanding questions in the field of lepidopteran pheromone research. One possible answer is that the signal production and response are genetically-linked due to pleiotropic effects[4] or linkage disequilibrium[5] [Allison and Cardé 2016b]. Although few examples of genetic coupling between pheromone signal and response have been reported [Fujii et al. 2010b], the majority of the studies contradict this notion [Roelofs et al. 1987; Bultin and Ritchie 1989; Löfstedt 1990]. The second possibility is that the traits responsible for signal production and signal reception co-evolve by complementary changes between the signal and the receiver due to drift or external directional selection [Löfstedt 1990]. Thus, the males must be able to "track" the changes in the female-produced blends and adapt to those changes over time [Phelan and Baker 1990; Phelan 1992].

1.5 THE RESPONSE: PHEROMONE RECEPTION IN LEPIDOPTERAN MALES

1.5.1 Pheromone-elicited behaviour in males

The ability of a male moth to detect the female-produced pheromone and track the odour back to its source is considered one of the most remarkable adaptations of Lepidoptera. The evolutionary advantage of specific and sensitive long-distance communication has allowed lepidopterans to maintain population levels with considerably lower density than insects that use visual or acoustic signals alone [Cardé 2016]. Even a single molecule of the female-produced pheromone can evoke a characteristic orientation behavior, referred to as optomotor anemotaxis [Kennedy and Marsh 1974], toward the pheromone source [Kaissling 2014]. All aspects of the pheromone-

[4] **pleiotropy**: occurs when one gene influences two or more seemingly unrelated phenotypic traits
[5] **linkage disequilibrium**: refers to the non-random association of alleles at two or more loci in general population

guided behaviour in lepidopteran males, from activation to pheromone source location, have been subject to intense investigation. Many experiments have shown that successful location of a pheromone source requires not only the presence of the odour, but also detection of the direction of the wind that carries the odour [Cardé and Willis 2008]. The wind direction is the primary cue used by flying insects and it allows them to orient their flight towards the odor source [Kennedy et al. 1980; Vickers and Baker 1992]. Upwind flight is mediated by the physical and chemical characteristics of the pheromone plume [Baker et al. 1985; Murlis et al. 1992]. The pheromone plume emitted from a single source and carried via air does not form a homogenous cloud, but is broken up by turbulence into discrete pockets of odour interspersed with pockets of odour-free air [Murlis and Jones 1981]. Thus, the odour plumes carry information on the identity, intensity and temporal content of the female-produced signal. The intermittent property of the odour plume (the ON and OFF zones) is required for eliciting arousal, undertaking of anemotactic flight, maintaining contact with the plume and successful navigation to the pheromone source by the male [Cardé and Willis 2008]. A constant and very high concentration of the pheromone is known to inhibit the flight and search for the signaling female, likely due to over-stimulation/ desensitization of the male's sensing mechanism [Baker et al. 1988]. The contact with the odour plume is maintained by integration of optomotor anemotaxis and "self-steered counter-turning" [David and Kennedy 1987], which continually orient the flying moth to the wind and produce the characteristic "zigzag" flight path observed in the majority of moths. Experimental evidence suggests that male moths can recognize a conspecific blend in 100 milliseconds [de Bruyne and Baker 2008] and initiate cross-wind "casting" in search of a lost plume within 300-500 milliseconds during flight [Baker and Vogt 1988].

1.5.2 Pheromone reception and perception

The olfactory processes mediating the male responses include reception in the periphery and perception at the level of the central nervous system (CNS). Uptake and reception are extracellular perireceptor events which lead to receptor activation. Intracellular transduction of a chemical message into an electrical potential via an activated receptor results in depolarization of the receptor neuron. The generated electrical signal "code" is read and integrated with information from the visual system via neural processes in the insect's CNS and brain.

1.5.2.1 Insect antenna is the primary olfactory organ

Detection of chemical signals in insects is achieved by means of specialized sensilla located primarily on the insect antennae, but also found in smaller numbers on the maxillary and labial palps [Hansson and Stensmyr 2011]. Although antennal morphology is highly varied among different insect orders, basic antennal design is based on common principles with characteristic sexual dimorphism often observed between males (Figure 1-2A) and females (Figure 1-2B) [Kaissling 2014]. In the order Lepidoptera, night-flying moths possess either long and slender filiform or comb-like pectinate antennae. The ventral surface of the antenna is covered by thousands of regularly-arranged, sensillar, bristle-like hairs of varying lengths, shapes and sizes. The spacing, arrangement and sensillar content on the antennae is sex- and species-specific. The sensilla are categorized based on their wall structure and morphology into 10 classes, including chaetica, trichodea (Type I-III), styloconica, auricillica, basiconica, coeloconica, ampulacea, campaniformia, placodea, scalopalia, scolopophora and squamiformia [Ryan 2002]. These types can be further classified as aporous, uniporous or multiporous sensilla. The thick-walled and aporous sensilla, such as chaetica, are thought to be mechano-, hygro- and thermo-sensitive rather than olfactory [Steinbrecht 1997; Faucheux 2011]. Basiconic sensilla are short and slender hairs with a very high number of cuticular pores and have been implicated in both pheromone and host odour detection [Grant et al. 1989; Hallberg et al. 1994]. The most abundant and longest multiporous trichoid sensilla are chemoreceptive and primarily implicated in pheromone reception in adult moth males [Steinbrecht 1997]. Each sensillum trichodeum forms a long hollow hairshaft encased in cuticle with a large number of very small pores [Hansson 1995]. The waxy surface of the cuticle covering the sensillar hair is thought to attract the lipophilic volatile compounds. The detection unit that mediates the olfactory response of males to female pheromones must be sensitive, fast and precise. Kaissling (1998a) proposed that male antennae detect a molecular flux of pheromone molecules rather than their concentration alone. Molecular flux is defined as molecules per second that come in contact with the antenna. In a pheromone plume, the flux encountered by the flying moth has varying degrees of intensity dependent on the abundance of the pheromone component, the speed of the pheromone molecules carried by air, and the additional air disturbance created by the moth's wings [Baker et al. 2012]. Thus, insect

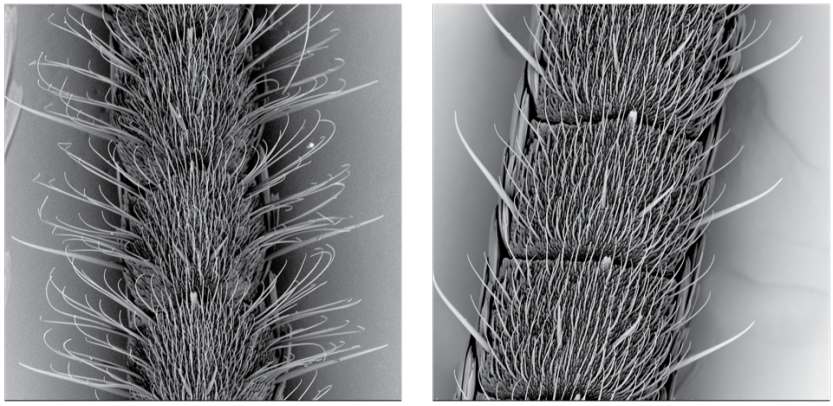

Figure 1-2 Scanning electron microscopic images of *M. configurata* antennae. **(A)** male antenna (magnification 560x) and **(B)** female antenna (magnification 520x). Images acquired at the Department of Biology, University of Saskatchewan.

antennae were suggested to function as a "magnifying lens" that directs and concentrates the signal molecules to the detection units (sensilla). The sensilla, in turn, amplify the signal prior to internal processing [Mafra-Neto and Cardé 1995].

1.5.2.2 Trichoid sensillum houses the olfactory detection unit

The specialized trichoid sensilla are innervated by at least two olfactory sensory neurons (OSN) and three associated auxiliary support cells [Kaissling 2014]. Insect OSNs can be assigned to several functional classes based on their response spectra and their expression pattern can be correlated to characteristic sensillum morphologies [Renou 2014]. The OSNs are bipolar with dendrites extending the entire length of the sensillar lumen and surrounded by sensillar lymph [Kaissling 2014]. The cell bodies are surrounded by three types of non-neuronal support cells: tormogen, trichogen and thecogen [Haupt et al. 2010]. The hollow sensillar shaft of the sensillum is formed by the trichogen and tormogen cells, which produce sensillar lymph and its components including the chemosensory proteins required for the odour perception [Pelosi et al. 2006; Forstner et al. 2008]. Thecogen is the innermost cell and wraps around the inner dendrite and soma of the OSN [Stengl and Hildebrand 1990]. In the OSNs tuned to pheromone signals, the diameter of the dendrite is correlated to the relative abundance of the component eliciting a response [Hallberg et al. 1994]. Thus, the OSNs responding to more abundant components have

a wider dendrite diameter and a larger action potential amplitude than those responding to minor pheromone components [Baker et al. 2012].

Comparative studies on species from different lepidopteran families suggest that the arrangement of two or more OSNs within a single sensillum is of functional importance [Baker and Hansson 2016]. In some families, including Tortricidae, Crambidae and Yponomeutidae, OSNs tuned to the two most critical pheromone components in a blend are co-housed as a pair in a single sensillum [Binyameen et al. 2014; Wicher 2018]. This colocalization of the major and minor pheromone components is thought to allow for simultaneous and accurate reporting of component ratios as the male encounters varying flux intensity in the plume. Interestingly, closely related species in these families often rely on very narrow differences in pheromone component ratios involving the same components [Löfstedt et al. 1991; Roelofs and Rooney 2003; Liénard et al. 2010; Regier et al. 2012; Lassance 2016]. In contrast, in other families, such as Noctuidae, co-localization of the OSNs tuned to the major and minor pheromone component has not been reported [de Bruyne and Baker 2008]. Many species of noctuid moths appear to have a high tolerance for large variation in the female-produced blend ratio and its precision is less critical for conspecific attraction [Baker and Hansson 2016].

1.5.2.3 Perireceptor events leading to receptor activation

The perireceptor events in the trichoid sensilla include uptake, binding, transport and inactivation of pheromones, as well as receptor activation and signal transduction [Leal 2013]. Much of the experimental evidence accumulated to date indicate that molecular events related to reception at the periphery (olfactory sensilla on the antennae) determine the sensitivity and kinetics of the male response [Kaissling 2013]. The first chemosensory event involves contact with and uptake of a volatile odorant from the environment and its transport or diffusion through the hydrophilic environment of the sensillar lymph [Brito et al. 2016]. As the odorant molecules enter the hair shaft of a sensillum trichoideum, they are bound by two different classes of proteins, including odorant binding proteins (OBPs) and the more recently discovered chemosensory proteins (CSPs) [Wanner et al. 2004]. A specialized class of pheromone-specific OBPs, called pheromone binding proteins (PBP), is thought to be responsible for pheromone detection and transport to the dendritic membrane of OSN [Leal 2013; Kaissling 2009]. While bound to PBP, the ligand is protected from odorant-degrading enzymes (ODE) also present in the sensillar lymph. The

second event in chemoreception is marked by the interaction of either the ligand or ligand:OBP complex with membrane bound olfactory receptor (OR) proteins that act as the bridge between the extracellular signal and the intracellular neurological response [Vogt and Chertemps 2005]. Generally, each OSN expresses only one ligand-specific OR, whereas OSNs expressing up to five different ORs have also been characterized [Goldman et al. 2005; Koutroumpa and Karpati 2014; Karner et al. 2015]. To function, ORs form heteromeric receptor complexes of unknown stoichiometry with the ubiquitous OR co-receptor (ORCO) [Benton et al. 2006; Vosshall and Hansson 2011]. Recent research suggests that although individual ORs can respond to multiple ligands and specific chemical compounds can activate multiple ORs [Hallem et al. 2004; Hallem and Carlson 2006], vital information, such as pheromone signal, is recognized by a specialized class of ORs and leads to activation of dedicated neuronal pathways often referred to as "labeled line pathways" [Berg et al. 2014; Zhang et al. 2015a]. As a subclass of ORs, pheromone receptors (PRs) exhibit a higher degree of sequence conservation and ligand specificity than other ORs. PRs also require the presence of a sensory membrane protein (SNMP) for their function [Benton et al. 2007].

The transduction of the chemical information carried by the odorant molecule into neural code requires several steps. The contact of the odorant molecule with the OR portion of the OR:ORCO dimer, whether alone or in an OBP:ligand complex, evokes a change in the dendritic transmembrane potential called the receptor potential [Kaissling 2014]. The sensillum lymph has an unusually high potassium concentration (200mM) [Kaissling 2009]. The difference in chemical composition between the sensillum lymph and hemolymph generates a transepithelial potential (TEP). A TEP of up to 40 mV contributes to the negative resting potential of the OSN and is thought to be the driving force for the receptor current [Kijima et al. 1995; Dolzer et al. 2001]. Prevailing experimental evidence supports a dual model for the OR signalling mechanism [Wicher et al. 2008; Nakagawa and Vosshall 2009]. Initially, the OR:ORCO complex forms an ion-gated channel and its interaction with the odorant generates a fast ionotropic response [Sato et al. 2008]. However, considerable evidence also supports a slower, but more sensitive, regulation of the channel via the metabotropic pathway utilizing the classical G-protein coupled receptor (GPCR) [Wicher et al. 2008; Deng et al. 2011]. Once the receptor potential reaches a threshold of -40 mV during the depolarization event, it elicits opening of voltage-gated ion channels required for generation of action potentials [Kaissling 2009].

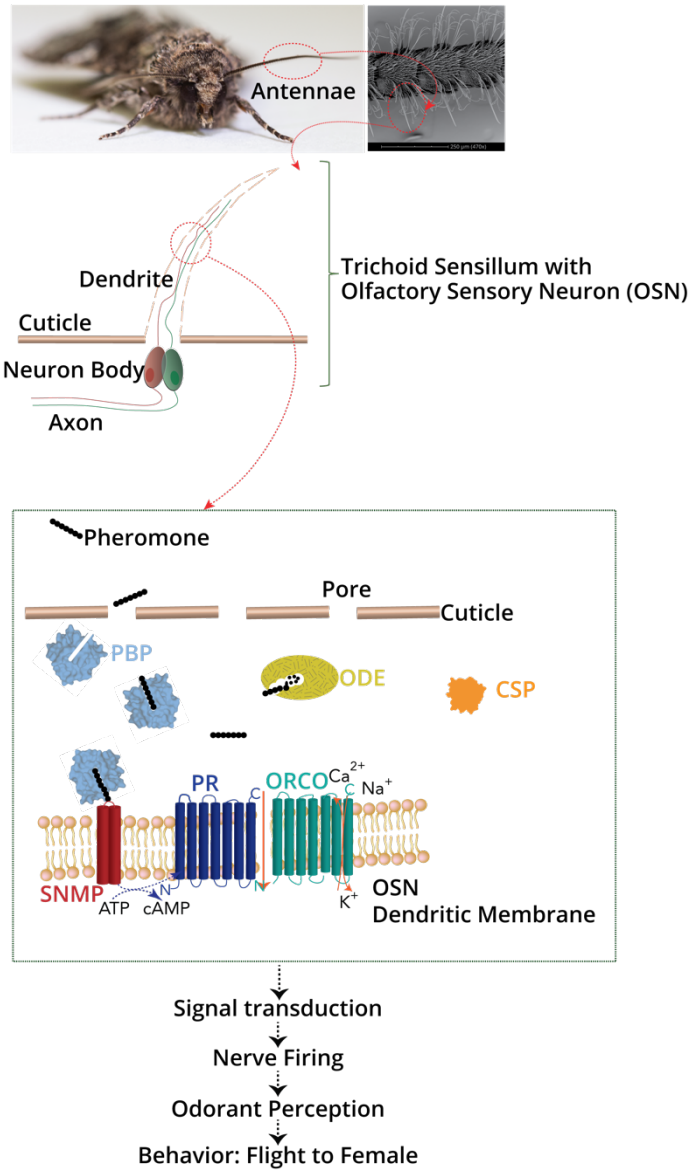

Figure 1-3 Pheromone reception in Lepidoptera. The trichoid sensilla located on the male antenna house the primary olfactory detection units called olfactory sensory neurons (OSN). The enlarged view shows several key protein factors contained within the sensillar lymph or localized to the OSN dendritic membrane that are thought to participate in perireceptor events. A pheromone molecule entering the lumen of a trichoid sensillum through a cuticular pore channel is bound to a pheromone binding protein (PBP) that transports the pheromone to the dendritic membrane. Another class of smaller binding proteins called chemosensory proteins (CSPs) is also present, although their function in pheromone reception is not fully understood. A sensory neuron membrane protein (SNMP) binds to the PBP-pheromone complex and directs the pheromone to the nearby pheromone receptor (PR). The pheromone binds to the PR-Orco heteromeric complex resulting in either very rapid recognition by means of an ionotropic activation pathway or a slower, prolonged detection via G-protein-mediated signal amplification. Odorant-degrading enzymes (ODEs) inactivate unbound pheromones. Modified and adapted from Gould et al. (2017).

To generate the fast, sensory response required for modulation of flight, a signal termination mechanism must exist that clears odour stimuli and resets the detection unit for the next round of sensing. Although the precise mechanism of signal termination is not fully understood, two different hypotheses have been proposed. In the first hypothesis, pheromone deactivation is postulated to be a non-enzymatic reaction [Kaissling 1998b; 2001]. During deactivation, the odour molecule remains chemically intact; however, it is prevented from continual excitation of the receptor either via a hypothetical "scavenger" enzyme or conformational changes in the PBP or PBP:OR interaction [Kaissling 2009]. In an alternate model, the degradation and clearing of the volatile compound is carried out by odorant-degrading enzymes (ODEs) [Ishida and Leal 2005; Leal et al. 2005; Ishida and Leal 2008]. Much less attention has been focused on the signal deactivation at the periphery compared to pheromone binding and receptor activation [Leal 2013].

1.5.2.4 Pheromone processing and integration in higher brain centers

The axons of pheromone-sensitive OSN project into the macroglomerular complex (McGl) located in the antennal lobes (AL) of the CNS (Figure 1-4) [Renou 2014]. The frequency[6] and temporal resolution[7] of generated action potentials transmitted along the axonal fibers is integrated as a neural code via the sex pheromone olfaction pathway in order to resolve the pheromone's position in both odour-space and odour-time [Baker and Hansson 2016]. The spherical glomeruli contained within the McGl of the AL function as a relay center where the axons of the OSN synapse with local interneurons (LNs) and projection neurons (PNs) that relay the odour information to higher-order regions of the brain. Multiple studies have shown that OSNs tuned to recognize a specific pheromone component project into the same area of the McGl [Galizia and Rössler 2010]. Insect OSNs are thought to be achromatic in that each OSN cannot by itself discriminate the stimulus quality (ie blend ratio) [Baker and Hansson 2016]. Instead, each OSN transduces the airborne abundance of only the pheromone component to which it is tuned into a level of action potential frequency (spikes per second). The reports from

[6] **Frequency coding (rate coding)** model of neuronal firing which states that as the intensity of odour concentration increases, OSN action potential frequency also increases

[7] **Temporal coding:** the precise spike timing or high frequency firing rate fluctuation of odour-elicited action potentials carrying information at the level of the neuronal population; temporal coding can also exist in single neurons

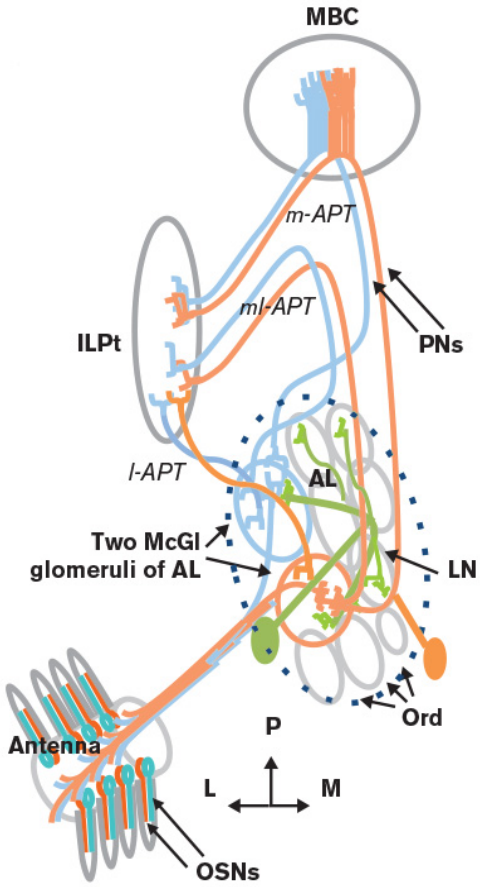

Figure 1-4 Schematic representation of neuronal architecture of the lepidopteran olfactory pathway for pheromone processing. Two types of OSN housed within a single sensillum are represented in orange and blue. The two OSNs report relative abundance of different pheromone components. Each of the two OSNs arborizes in its own pheromone component-specific glomerulus (blue and orange circles) in the macroglomerular complex (McGl) of the antennal lobe (AL). The AL is dealinated by dashed oval. At the McGl, the information is passed to a population of local neurons (LNs; green) that integrate the information before passing it to the protocerebrum via axons of the projection neurons (PNs). The axons of the PNs travel through the medial antennoprotocerebral tract (m-APT) to the mushroom body (MBC) before arborizing in the inferior lateral protocerebrum (ILPt). Some PNs travel through the mediolateral antennoprotocerebral tract (ml-APT) and lateral antennoprotocerebral tract (l-APT), bypassing the MBC. The grey ovals within the AL depict the general odour glomeruli (Ord). Adapted from Baker and Hansson (2016).

each of the individual OSNs are delivered to integrative neurons in the AL and beyond where they are analyzed with regard to the ratios of excitations that the OSNs are delivering. The ratio of excitation (ratios of spike frequencies), therefore, is what is correlated with the relative ratios of the components in the pheromone blend. The "blend-ratio sensitive" integrative neurons exiting the AL are only excited when the ratios of excitations coming from the differentially-tuned OSNs are "correct." Furthermore, areas in the McGl responsible for pheromone processing are distinct and separate from areas responsible for general odour processing [Kanzaki et al. 1991b]. Thus, each pheromone component in a blend is represented in a single glomerulus within the McGl and a specific pattern of activity across several different glomeruli represents the response to the pheromone blend [Vickers and Christensen 2003]. The information processed by either individual McGl glomeruli or their combinations is forwarded by PNs to the inferior lateral protocerebrum (ILPt) of the lateral protocerebrum (LP) via three distinct pathways. The first pathway travels medially through the brain with axon collaterals traversing the mushroom body calyces (MBCs) and arborizing in the ILPt. The other two pathways are project laterally and directly into the ILPt without traversing through the MBC.

It is at the level of the ILPt and the MBC where information is integrated to generate upwind flight behaviour. Although the details of the integrative processes resulting in pheromone induced flight in male moths are beyond the scope of this review, it is important to note that the act of flying is strictly a visual rather than an olfactory response [Baker and Hansson 2016]. Based on several landmark studies, it is currently accepted that presence of female pheromone stimulates and enhances a moth's attention to optical flow stimuli required for flight [Olberg and Willis 1990; Kanzaki et al. 1991a]. Thus, the behavioral response requires integration and cross-talk of both olfactory and visual systems.

1.5.3 Variation in the male response to the female pheromone

1.5.3.1 Environmental factors

In contrast to the number of studies on female pheromone production and pheromone variation, only a few studies are available that address the male's pheromone blend preference and the variation in male response [Allison and Cardé 2016a]. The male response profile may be influenced by the same environmental factors affecting the female pheromone production, especially temperature, relative humidity, wind speed, light levels and possibly odours produced

by plants and sympatric species [Baker and Linn 1984; Linn et al. 1987; 1988; Karpati et al. 2013]. Temperature plays a role in pheromone-mediated flight because at lower temperatures the energetic cost of flight is higher, especially for smaller moths [Vickers 2006a; Crespo et al. 2012]. For example, males of *Grapholita molesta* and *Pectinophora gossypiella* (Tortricidae) were attracted to a narrower range of pheromone blend ratios at 20°C than at 26°C [Linn et al. 1988]. The *Z*-strain males of *O. nubilalis* are typically attracted to a narrow range of their conspecific female pheromone blend ratio in wind tunnel conditions [Linn et al. 1997]. However, early pre-exposure to the optimal *Z*-strain blend prior to plume navigation allowed the males to navigate to sub-optimal blend ratios that would typically be not attractive [Karpati et al. 2013].

1.5.3.2 Genetic basis of male pheromone response

In contrast to genetic studies on variation in female pheromone blend composition, genetic analysis of male response is inherently more difficult. Whereas identity of pheromone components, pheromone titre or component ratios are quantifiable, male response is not. Simply not completing a series of events that would lead the male to finding the female cannot be easily correlated to a specific pheromone response phenotype [Haynes 2016]. Generally, we would expect that statistically more males should respond to an optimal blend produced by a conspecific female. However, in many lepidopteran species, some males exhibit a broad window of response [Dopman 2010; Haynes 2016]. Rigorous experimental design is complicated by the fact that in the majority of cases males cannot be tested repeatedly since a single exposure may affect their subsequent behaviour or result in adaptation [Allison and Cardé 2016a]. Not surprisingly, the current knowledge of the genetic basis for variation in the male pheromone response comes from model systems used to investigate variation in the female-produced signal.

The existence of two sympatric strains, ECB-*E* and ECB-*Z* (*E*- and *Z*-strain), within the genus *Ostrinia*, each utilizing opposite isomer ratios of the same compound (*E*- and *Z*-isomer), provides a unique system for studies of the genetic basis of male pheromone response (See section 1.3.5). The male behaviour is a product of peripheral events and integration of these events at the level of the CNS [Kaissling 2014]. Although to date, the genetic factors responsible for behaviour [Glover et al. 1990; Dopman et al. 2005], sensillar morphology [Hansson et al. 1987; Olsson et al. 2010], OR phenotype [Wanner et al. 2010; Lassance et al. 2011] and functional organization of the McGl [Kárpáti et al. 2008; 2010] has been determined for ECB strains, a complete

understanding of the genetic mechanism guiding the male pheromone response is still lacking. At the level of behaviour, male response to the female ECB pheromone was found to be under the control of the sex-linked factor *Resp* [Glover et al. 1990; Dopman et al. 2004]. However, whether *Resp* corresponds to a single gene or multiple genes and how it guides the behavioral response to pheromone are currently not known [Dopman et al. 2010; Lassance 2016]. At the level of the antenna, three different types of sensilla trichoidea (A-C) have been identified for both ECB strains [Hallberg et al. 1994]. The pheromone-sensitive trichoid sensilla B, found in both strains, contain a large spike (action potential)-amplitude OSN responding to the major component and a small spike-amplitude OSN responding to the minor pheromone component [Roelofs et al. 1987]. The differences between the two spike amplitudes correspond to the diameter of the dendrite containing ORs specific for each isomer [Hansson et al. 1994]. Initial crossing experiments and electrophysiological investigation indicated that that the morphology of the pheromone-sensitive olfactory sensilla is controlled by a single autosomal factor [Roelofs et al. 1987]. Further analysis of males with an antennal transplant corresponding to one strain, but exhibiting the behavioral responses of the other strain appeared to support the initial finding that there is no correlation between genetic control of the behavioral response and genetic control of sensillar physiology [Cossé et al. 1995; Linn et al. 1997; 1999]. However, a more recent re-examination of the inheritance pattern of sensillar physiology established that, in addition to the autosomal locus, another sex-linked locus exhibiting *E*-strain dominance and involved in epistatic interaction with the autosomal locus is involved [Kárpáti et al. 2010; Olsson et al. 2010]. Moreover, gross antennal response representing the sum of all OSNs responding to the pheromone stimulus was also determined to be under sex-linked inheritance [Kárpáti et al. 2010]. At the molecular level in the sensillum trichodeum, the two ECB strains were determined to be genetically differentiated at three distinct OR loci mapping to sex-linked chromosomes. In contrast, examination of variation at loci encoding PBP did not find any fixed differences between the strains [Willett and Harrison 1999]. At the level of the CNS, both strains contain a pheromone response center McGl composed of two larger and one smaller glomeruli (neuropil bundles) [Kárpáti et al. 2008]. Recent neuroanatomical studies have shown that each ECB strain exhibits reversed expression of ORs tuned into major and minor pheromone components in OSN axons projecting to McGl glomeruli [Kárpáti et al. 2010]. Thus, the topology of the McGl

glomeruli was also found to be reversed for the two strains and genetic factors responsible have been mapped to the sex-linked chromosome.

Male heliothine moths exhibit a high degree of sensitivity and specificity to precise ratios of female-emitted pheromone blends [Hillier and Baker 2016]. Much of the current knowledge accumulated on the genetic principles guiding heliothine male response comes from behavioural [Baker et al. 2006; Vickers 2006b; c], neuroanatomical [Große-Wilde et al. 2007; Gould et al. 2010] and genetic analysis [Gould et al. 2010; Wang et al. 2011; Vasquez et al. 2013] with hybrids from closely-related species. Collectively these studies have established that the phenotypic variation observed in the male response was found to be modulated by autosomal inheritance. The pheromone response in heliothine moths is altered by shifts in expression levels of either one or more OR genes. The changes in OR gene expression patterns in turn affect the tuning of the OSNs and result in novel behavioral responses as an adaptation to changes in female-produced pheromone blends. For example, in *H. virescens* and *H. subflexa* a QTL approach, similar to that used in determination of genetic factors underlying female-produced pheromone divergence, was applied [Gould et al. 2010]. Four OR genes mapped to chromosome 27 in both species. In *H. virescens*, the factor from chromosome 27 was shown to control specificity for *Z*9-14Ald (*H. virescens*-specific) and in *H. subflexa* to *Z*9-16Ald (*H. subflexa*-specific). Another factor from the same chromosome affected positive (*H. subflexa*) or negative (*H. virescens*) responses to Z11-16Ac. One marked characteristic of the response of heliothine males is the tuning of OSNs, not only to the pheromone components of their conspecific females, but also to the antagonists produced by heterospecific species [Baker 2008]. Thus, the evolution within the heliothine pheromone communication channel is often referred to as "adaptive response to heterospecific blends in which different species-specific blends have diverged during a reproductive character displacement[8] process in zones of sympatry of two established species" [Hillier and Baker 2016].

In studies of *Trichoplusia ni*, the discovery of a mutation affecting female pheromone production allowed the authors to track the changes in male pheromone response over multiple generations [Linn et al. 1984; Liu and Haynes 1994a](also see section 1.3.5). Although initially males did

[8] **reproductive character displacement**: differences among similar species whose distributions overlap geographically are accentuated in regions where the species co-occur, but are minimized or lost where the species distributions do not overlap

not respond to the mutant blend, their response adapted over 50 generations. Electrophysiological investigation found that the sensitivity of the OSN tuned to *Z*9-14Ac was attenuated in the mutant males [Domingue et al. 2009]. This attenuation caused the spike amplitudes from both *Z*9-14Ac and *Z*7-12Ac to be approximately equal, which in turn translated into mutant males being able to detect both mutant and original pheromone blends equally. Subsequent analysis revealed that although the mutant males were able to respond equally to both pheromone blends, overall their sensitivity was lower than in wild-type males [Hemmann et al. 2008]. To test whether the wild-type colony had heritable variation, father-son regression technique was used Evenden et al. (2002) and revealed that the heritability of male response within the wild type colony was 0.25, but near 0 in the mutant colony. The authors concluded that additive genetic variance[9] underlies the male response; however, the low heritability of the response of mutant males to the mutant pheromone could indicate that the additive genetic variance is limited by selection [Evenden et al. 2002].

Together these studies suggest that the genetic factors underlying the male response at the behavioral and physiological level are complex and elucidation of details remains a major challenge. The evidence from the model systems suggests that the olfactory circuitry is similar among various lepidopteran species, thus the changes at the periphery must be responsible for accommodating shifts in the male response over time. The factors guiding OR choice in each pheromone-sensitive OSN are not well understood [Ray et al. 2007; Fujii et al. 2011]. However, OR gene choice, along with OR diversity in the OR gene repertoire, may represent the key elements in evolutionary changes of male behavioral response to pheromone signals. Understanding how much genotype and the environment affects pheromone production and pheromone reception can further our understanding of the evolutionary mechanism guiding pheromone communication. Understanding variation in signal production and response is also crucial in the design of effective, long-term pest management strategies.

1.6 *MAMESTRA CONFIGURATA* (BERTHA ARMYWORM; BAW)

The bertha armyworm (BAW), *Mamestra configurata* Walker (Lepidoptera: Noctuidae), is a polyphagous insect pest native to North America [Turnock 1985; Erlandson 2013]. In Canada,

[9] **additive genetic variance**: involves the inheritance of a particular allele from a parent and the allele's independent effect on the specific phenotype which will cause the phenotype deviation from the mean phenotype

BAW has a univoltine life cycle and its populations are found spanning the western provinces from Manitoba to British Columbia [Mason et al. 2002]. Although, limited information is available on BAW native host plant range prior to its first recorded outbreak in western Canada, it is thought to have included various plants from the Chenopodiaceae and Brassicaceae [Mason et al. 1998]. In the American Pacific North West, BAW is bivoltine and feeds mostly on Brassicaceae [Landolt 2000].

1.6.1 BAW biology

In western Canada, BAW adults (Figure 1-5A) emerge from the soil from early to mid-June until early August [Turnock 1985]. The adult moths are nocturnal and are attracted to host plant fields in bloom. The females start to display calling behaviour 2-3 nights after emergence and during the last two-thirds of scotophase, and remain *in copula* for approximately 17 h [Howlader and Gerber 1986a; b; Gerber and Howlader 1987]. The frequency and duration of the calling behaviour, as well as the number of females calling, is influenced by temperature [Gerber and Howlader 1987]. Mated females lay single-layered masses of 20-200 eggs (Figure 1-5B) on the underside of the host plant leaves [Bracken 1984; Ulmer et al. 2001; Weeraddana and Evenden 2018]. After approximately one week, the eggs hatch into pale green larvae with light yellow stripes and characteristic black heads. The larvae (Figure 1-5C) are mostly active at night and feed on host plant foliage until the fourth instar (1^{st} - 4^{th}) [Bracken 1984]. The final two BAW instars (5^{th} and 6^{th}) preferentially feed on the developing plant seedpods [Bracken and Bucher 1977; Bracken 1987]. During the 6^{th} instar stage, larvae consume 70-80% of the total food intake during all larval stages [Bracken 1987]. Under natural conditions, larvae take 6-7 weeks to complete development. As the larvae mature, their coloring darkens and varies from dark green to brown to black. It is at this stage that the larvae can be easily detected on the host plants. In the late summer, the larvae drop from host plants and burrow 5-16 cm below the soil surface where they pupate and overwinter [Mason et al. 1998]. The reddish brown BAW pupae (Figure 1-5D) undergo facultative diapause induced by photoperiod and temperature changes during the last two larval instars [Hegdekar 1983]. Pupal survival during winter is affected by duration of exposure to temperatures near or below freezing [Lamb et al. 1985; Turnock and Braken 1989; Mason et al. 2002]

1.6.2 BAW as pest

Across the Canadian prairies, only sporadic BAW outbreaks were reported on various crops prior to 1940. The bertha armyworm is attracted to the native weed, lamb's quarters (*Chenopodium album*), but feeds on canola (*Brassica napus* and *Brassica rapa*), flax (*Linum usitatissimum*), sweet clover (*Melilotus officinalis*) and alfalfa (*Medicago sativa*) [Bracken 1984; Turnock 1985]. Since the 1970's, the major BAW infestations have been primarily confined to canola fields most likely due to the rapid increase in the amount of land planted to canola varieties with low isothiocyanate and glucosinolate levels [McCloskey and Isman 1993; Weeraddana and Evenden 2018]. The major economic damage to canola caused by BAW results from larvae feeding on seedpods, thereby reducing seed yield and affecting seed quality [Bracken and Bucher 1977; Bracken 1984; 1987]. The bertha armyworm outbreaks are typically cyclic and localized, occurring every six to eight years and can persist up to four years [Mason et al. 1998]. The factors responsible for the onset of BAW outbreaks and the mechanism underlying outbreak dispersal are not well understood [Wylie and Bucher 1977]. Small populations of BAW are encountered during non-outbreak years and it is thought that the increase in population numbers is dependent on favourable environmental conditions [Mason et al. 1998]. Although, causes of outbreak collapse have not been thoroughly investigated, pathogens, including baculoviruses [*Mamestra configurata* nucleopolyhedrovirus-A and -B] [Erlandson 1990; 2013] and entomopathogenic fungi [Erlandson 2013; Hokkanen and Menzler-Hokkanen 2017], as well as the native parasitoids *Trichogramma inyoense* (Hymenoptera: Trichogrmmatidae) and *Banchus flavescens* (Hymenoptera: Ichneumonidae)), likely contribute to curtailing BAW populations.

The components of the sex pheromone blend specific to BAW are (*Z*)-11-hexadecenyl acetate (*Z*11-16:OAc) and (*Z*)-9-tetradecenyl acetate (*Z*9-14:OAc) in a 19:1 blend ratio [Chisholm et al. 1975; Underhill et al. 1977a]. The corresponding synthetic pheromone blend is exploited in pheromone traps employed for the BAW monitoring program coordinated by the Prairie Insect Pest Monitoring Network (PIPMN; westernforum.org/IPMNMain.html) [Steck et al. 1979]. Synthetic pheromone-baited traps are used to document changes in pest density and develop action thresholds based on prediction of larval infestation levels by the PIPMN. Currently, the cyclical BAW outbreaks are controlled by aerial application of broad-spectrum chemical insecticides, which is associated with high economic cost [Mason et al. 1998] and may carry negative human and environmental impacts [Hill et al. 2017]. The pheromone trap counts are

also used as an assessment tool for the timing and level of insecticide application during outbreaks. However, in practice, pheromone trap catches do not always accurately reflect the larval infestation level to follow. Observations from the most current outbreaks suggested that not all males from the different geographic BAW populations are equally attracted to the synthetic pheromone blends used in the pheromone traps across western Canada (Western Committee of Crop Pests Annual Meeting 2011; www.westernforum.org).

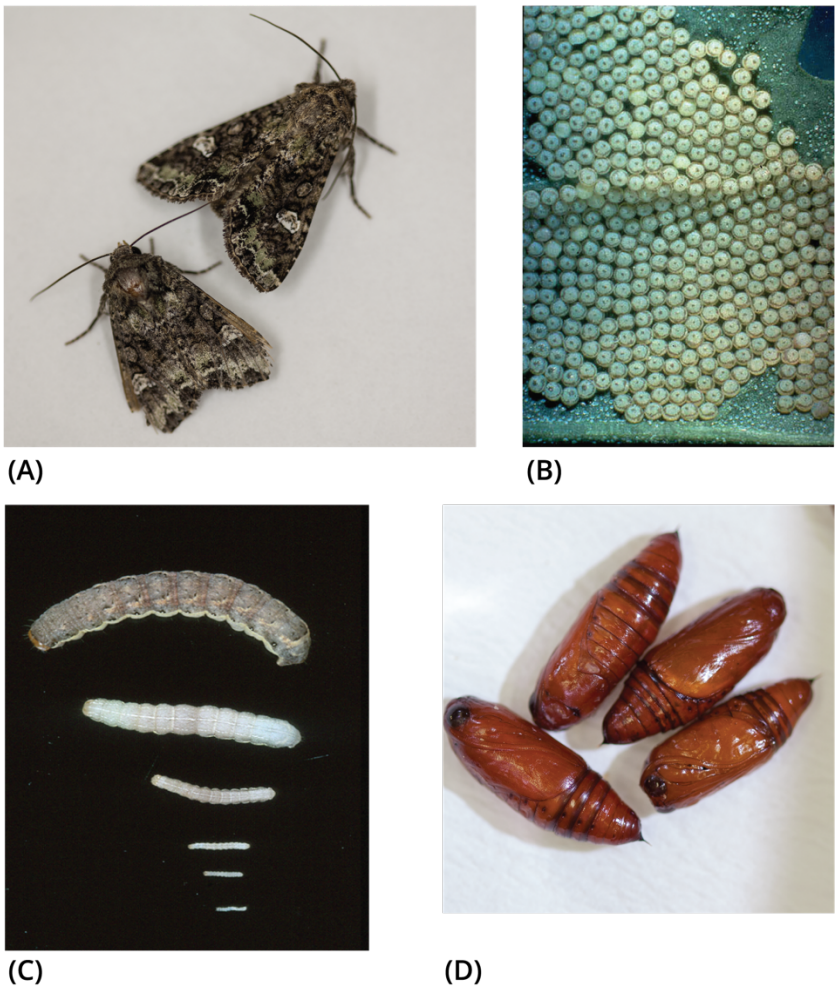

Figure 1-5 Life stages of *M. configurata*. **(A)** Adult male moths. **(B)** Eggs. **(C)** Larval instars 1-6 (from bottom up). **(D)** Pupae.

1.6.3 Characterization of the pheromone communication channel in BAW

At the peak of the last major BAW outbreak (2011-2014), a concerted and extensive effort by staff from Agriculture and Agri-food Canada in Saskatoon (AAFC-Saskatoon) and the PIPMN was undertaken to collect adult male moths from across the BAW geographic range (Figure 1-6A). This collection was aimed at generation of a BAW genome sequence, as well as investigation of genetic diversity and population structure of BAW across its geographic range [Erlandson et al. 2019]. In addition, egg masses and pupae were collected from a number of distinct geographic locations (Figure 1-6B). Both egg masses and pupae were reared under laboratory conditions in an effort to establish strain colonies representative of the geographic outbreak populations.

The majority of our current knowledge on BAW genetics and biology is based on studies carried out with a laboratory-reared colony established at AAFC-Saskatoon in 1976. However, research concerning pheromone communication involving laboratory-reared colonies may not provide an accurate representation of field populations. The selective pressure maintaining the consistency of the pheromone blend may not be the same for laboratory-reared insects as for the wild populations [Haynes 2016], for example, the requirement for males to find females is not relevant in cages and, thus, the selective forces acting on female pheromone production may relax and lead to higher variation in the pheromone blend ratios. Moreover, the colonies are often established from only a few individuals and pass through a population "bottleneck" [Kim et al. 2007]. Generally, population bottlenecks are thought to decrease genetic variation in laboratory-reared populations [Hill and Armando 1992]. Some experimental evidence also suggests that colony inbreeding increases the level of heritable variation [Buskirk and Willi 2006]. At least for some species, similar levels of variation were found among wild-type and laboratory-reared strains [Miller and Roelofs 1980; Haynes et al. 1984]. The availability of both males and females of BAW from the second generation of two outbreak population strains presented a rare opportunity to comparatively investigate both genetic and biological aspects of pheromone communication in BAW geographic populations.

Despite the economic and environmental importance of BAW, our knowledge of its biodiversity with respect to genotypes and phenotypes that occur across its geographical range is limited. The genetic architecture underlying pheromone production in females and pheromone reception in

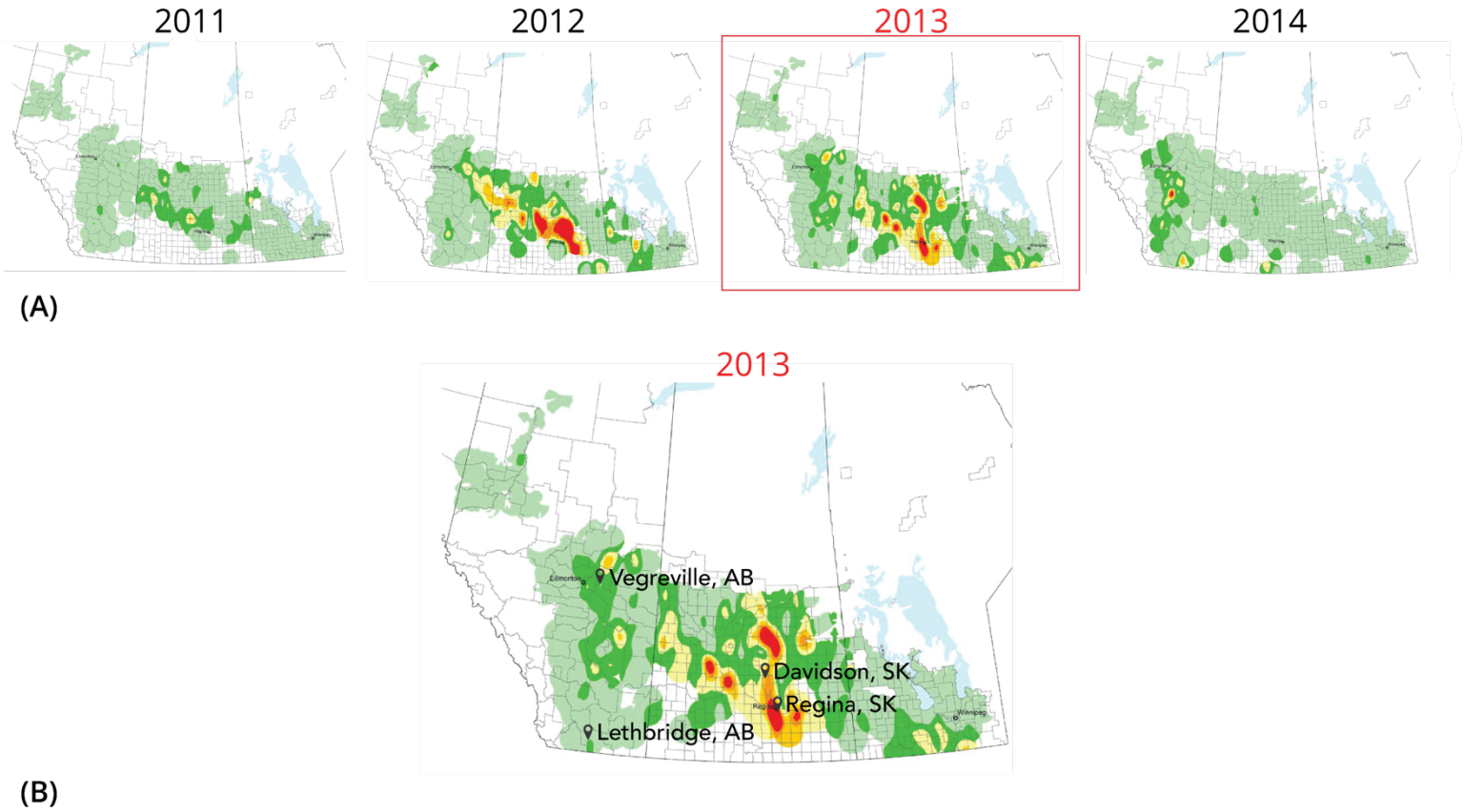

Figure 1-6 BAW outbreak 2011-2014. **(A)** Pheromone trap monitoring data showing BAW infestation levels between 2011-2014 during the last major BAW outbreak in western Canada. The colour of localities indicates cumulative moth counts; 0-300 (pale green), 300-600 (dark green), 600-900 (yellow), 900-1200 (pale orange), 1200-1500 (dark orange) and 1500+ (red). **(B)** The four geographic locations used as collection sites for either egg masses or pupae material during the summer of 2013 are indicated. The materials collected were used to establish geographic BAW colonies at Agriculture and Agri-food Canada in Saskatoon.

males and the level of associated genetic variation has not been explored. Although, a large project has been undertaken to delineate the population structure of geographic BAW populations [Erlandson et al. 2019], focus on the pheromone channel is warranted by recent findings suggesting that genetic differentiation may exist at only a few loci coding for high impact genes related to the phenotypic variants observed [Lassance 2016; Coates et al. 2018]. In the determination of genetic diversity among geographic populations "frequencies of neutral genetic markers [may] fail to discriminate between the intraspecific phenotypic variants, [however] markers associated with strongly selected loci underlying species-specific traits may be capable of defining lineages when genomic regions are in linkage disequilibrium with those loci" [Coates et al. 2018]. For example, in the model *Ostrinia* spp , for which two morphologically indistinguishable ECB strains exhibit large phenotypic differences in the pheromone blend ratios, genetic analysis has demonstrated that a very limited number of loci show significant genetic differentiation and these loci are associated with pheromone communication [Lassance 2016].

Until recently, the type of genetic analysis required to address the questions above was limited to only a small number of model species [Ekblom and Galindo 2011]. The development of next generation sequencing (NGS) techniques has opened the possibility of expanding these studies to non-model organisms, such as *M. configurata*. Advancement of NGS and bioinformatic analysis tools [Levy and Myers 2016] has led to a reduction in sequencing costs [van Dijk et al. 2014] and prompted a vast increase of genomic and transcriptomic studies in a large number of lepidopteran species [Große-Wilde et al. 2011; Liu et al. 2012; Xu et al. 2015; Perera et al. 2015; Feng et al. 2017; Silva-Brandão et al. 2017; Zhong et al. 2017; Grapputo et al. 2018]. NGS, also called high-throughput sequencing, encompasses a number of massive, parallel, deep sequencing platforms [van Dijk et al. 2014]. NGS applications can be categorized as genomic DNA sequencing and RNA sequencing. Over the last decade, high-throughput RNA sequencing (RNA-Seq) technology has become the method of choice for transcriptome profiling. In particular, RNA-Seq has become an invaluable tool in studies on non-model organisms for which genome sequence information is lacking or incomplete and molecular biology tools for altering the expression of a specific gene in a specific tissue do not exist [Ekblom and Galindo 2011]. Since only 1-2% of all genes are coding and 80-90% of transcribed genes are not translated to proteins, transcriptomic analysis offers more focused and rapid technique for examination of tissue-specific coding gene content of the genome [Anamika et al. 2016]. RNA-Seq data is

highly sensitive and specific and allows for generation of comprehensive libraries of tissue-specific expressed genes coding for proteins. The technique permits for quantification of genes and isoforms, as well as the detection of transcripts with very low abundance. Accurate mapping of reads back to *de novo* assembled transcripts can be considered unambiguous and sufficient for identification of sequence polymorphisms, such as alternative splicing sites, single nucleotide polymorphisms (SNPs) and tandem repeats [Sacomoto et al. 2012]. Recently, RNA-Seq has become the preferred technique for characterization of genes involved in pheromone signal production and pheromone olfaction [Strandh et al. 2008; Ekblom and Galindo 2011; Montagné et al. 2015]. Based on these advantages and the absence of genome information for BAW, I have chosen transcriptomics as a suitable methodology for characterization of genes involved in pheromone communication as a basis for subsequent structural, functional and evolutionary studies.

We currently do not understand BAW interactions with other sympatric lepidopteran species with similar host plant ranges. A number of related armyworm and cutworm pest species, including *Agrotis orthogonia* (pale western cutworm), *Euxoa auxiliaris* (army cutworm), *Euxoa ochrogaster* (redback cutworm), *Feltia jaculifera* (dingy cutworm) and *Lacinipolia renigera* (bristly cutworm), share overlapping geographic areas in western Canada and utilize the same unsaturated acetates as their pheromone blend components. During the massive collection effort undertaken in 2011-2014 outbreak, CO1 barcode sequence analysis showed that at least 10 other Lepidoptera: Noctuidae taxa were found in BAW pheromone traps [Erlandson et al. 2019]. The trap catches included *Apamea cogitata* Smith*, Apamea commoda* Walker, *Apamea devastator*, *Chersotis juncta*, *Enargia spp.*, *Euxoa spp.*, *Feltia jaculifera*, *Leucania anteroclara* Smith, *Mniotype spp.* Franclemont, *Peridroma saucia* and *Xestia smithii*. The presence of other species utilizing the same pheromone components as BAW or attracted to similar pheromone blends may exert different selective pressure in different geographic regions. As chemosensory gene repertoires from different species are characterized, comparative analysis may prove to be useful in increasing our understanding of these interspecific relationships with respect to pheromone communication.

Research presented in this thesis aimed to investigate whether genetic differentiation exists among geographic populations of BAW with respect to pheromone communication.

I characterized the genes involved in pheromone synthesis by BAW females and carried out chemical analysis of the contents of female pheromone gland. I also characterized the genes involved in BAW male response to pheromones. Subsequently, I explored the level of genetic polymorphism present among current populations in regions/loci more susceptible to shifts that lead to genetic differentiation in the male response. In addition to genetic characterization of factors underlying pheromone communication in BAW, I investigated potential differences in pheromone biosynthesis and reception among BAW populations. Initial identification of BAW female pheromones was aimed at their utilization in pheromone traps for insect monitoring purposes [Steck et al. 1979]. Since the early experiments were primarily carried out during 1970's, only a few field-trapping bioassays were done to confirm the biological activity of the identified compounds and optimize the synthetic blend ratios used in the pheromone lure [Steck et al. 1984; Mason et al. 2002]. With respect to female pheromone biosynthesis, there have been no studies on the level of variation in BAW pheromone component production among individuals and among geographic populations. It was also of interest to determine whether any differences existed at the behavioural or electrophysiological response level in BAW males from distinct populations. From a practical application standpoint, characterization of the pheromone communication channel in BAW is necessary for designing more effective, integrated, pest management strategies for this species. However, my work will also serve as a foundation for future comparative investigation of the interaction and competition with closely-related species. The long-term goal of this research is to combine the knowledge of genes and their expression patterns with behavioural and electrophysiological studies together with knowledge gained from model species and statistical analysis for the development of olfactory processing models applicable to non-model species.

OBJECTIVES

CHAPTER 2. CHEMICAL AND GENETIC ANALYSIS OF THE FEMALE PHEROMONE GLAND

1. To characterize female BAW pheromone signal production in colony and geographic populations via:
    - **a.** Investigation of the variation in pheromone component production among individual BAW females and between a long-term reared colony and geographic populations.
    - **b.** Generation and characterization of BAW female pheromone gland transcriptome.

CHAPTER 3. GENETIC CHARACTERIZATION OF BAW MALE RESPONSE TO THE FEMALE-PRODUCED PHEROMONES

2. To characterize the male BAW pheromone response in colony and geographic populations via:
    - **a.** Identification and characterization of the candidate chemosensory genes involved in pheromone communication.
    - **b.** Assessment of the frequency of natural polymorphism among colony and geographic strains through comparison of the Illumina sequencing libraries corresponding to each distinct geographic BAW population.

CHAPTER 4. BAW MALE RESPONSE TO SYNTHETIC PHEROMONES AND FEMALE-PRODUCED PHEROMONE BLEND

3. To characterize the degree of variation between the colony and geographic populations with respect to:
    - **a.** Navigation to pheromone source under wind tunnel conditions.
    - **b.** Electrophysiological responses from the antenna to the pheromone blend components.
    - **c.** Electrophysiological responses from the antenna to the synthetic pheromone components at various concentrations.

CHAPTER 2. CHEMICAL AND GENETIC ANALYSIS OF THE FEMALE PHEROMONE GLAND

2.1 INTRODUCTION

Studies of sex pheromones produced by females have revealed tremendous diversity in the lepidopteran mating communication systems [Löfstedt et al. 2016]. Approximately 75% of all lepidopteran pheromones identified to date belong to the Type 1 class of fatty acid derivatives with carbon chain lengths of C_{10}-C_{18}, a number of double bonds ranging from 0 to 4 and an oxygenated alcohol, aldehyde or acetate ester functional group [Ando et al. 2004]. The majority of moths use a blend of at least two or more of these biosynthetically-related compounds in a species-specific ratio. It is the relative ratios of the pheromone components that determine the blend quality and ensure successful intraspecific mating [Allison and Cardé 2016b]. Thus, research on female pheromone biosynthesis has primarily focused on the chemical properties of the pheromones, how the ratios of compounds are produced by the lepidopteran females and how changes to blend quality affect the male response [Tillman et al. 1999; Ando et al. 2004; Jurenka 2004; Blomquist et al. 2012; Yew and Chung 2015; Foster 2016; Löfstedt et al. 2016]. Although we currently have a general knowledge of the pheromone biosynthesis pathway, much of that knowledge has been inferred from our understanding of general fatty acid metabolism.

2.1.1 Overview of the Type 1 pheromone biosynthesis pathway

The biosynthesis of the Type 1 pheromones in the female pheromone gland to a large extent resembles "general" fatty acid biosynthesis (Figure 2-1). The pathway is regulated by pheromone biosynthesis-activating neuropeptide (PBAN) released from the subesophageal ganglion complex of adult female moths [Rafaeli and Jurenka 2003; Jurenka and Rafaeli 2011]. PBAN interacts with the PBAN receptor (PBANr) belonging to the G-protein coupled receptor (GPCR) class [Jurenka and Rafaeli 2011]. In all moth species studied to date, PBAN activation of the receptor induces influx of extracellular calcium followed by an increase of cytosolic calcium [Jurenka et

al. 1991; Jacquin et al. 1994]. Elevated levels of cytosolic calcium activate a calcium/calmodulin-sensitive adenylate cyclase, which subsequently stimulates production of cyclic-AMP and activation of kinase and phosphatase enzymes [Jurenka and Rafaeli 2011]. Activation with PBAN via a calcium-dependent signal cascade is thought to affect the rate-limiting step of fatty acid biosynthesis catalyzed by acetyl-CoA carboxylase (ACC) [Jurenka et al. 1991] and in some species, fatty acid reductase [Fang et al. 1995a]. Studies in model species have identified up to 3 isoforms of PBANr (A, B and C) [Kim et al. 2008]. All three sequences appear to be nearly identical and show variation only in the C-terminal portion of the protein. However, only PBANr-C was identified in the tissues of the adult female pheromone gland from *Heliothis virescens*, whereas PBANr-A and B were found in the larval central nervous system [Kim et al. 2008].

The Type 1 pheromone biosynthetic pathway can be divided into three distinct stages: (i) fatty acid synthesis, (ii) modification of the carbon chain, and (iii) modification of the carboxyl group [Foster 2016]. During fatty acid synthesis, ACC produces malonyl-CoA from acetyl-CoA. Fatty acid synthase (FAS) condenses malonyl-CoA with successive units of acetyl-CoA to produce a medium chain fatty acid precursor, such as hexadecanoate or octadecenoate. To date, neither ACC or FAS specific to pheromone production have been identified [Ding and Löfstedt 2015]. Our current knowledge of this biosynthetic stage is inferred from analysis of labelled precursor in crude pheromone gland extracts [Jurenka et al. 1991; Jacquin et al. 1994] and inhibitory studies with the herbicide diclofop, which acts as an inhibitor of ACC [Eliyahu et al. 2003].

The fatty acid pheromone precursors undergo a series of catalytic reactions during the carbon chain modification stage [Jurenka 2003]. This stage is thought to be responsible for generating the diversity of Type 1 pheromone compounds among Lepidoptera [Lienard et al. 2008; Löfstedt et al. 2016] and is mediated by a multi-enzyme complex, including a conserved family of Δ9 and Δ11 desaturases (DESs) and β-oxidation enzymes [Jurenka 2004]. Insect DESs are homologous to the Δ9 acyl-CoA DESs from fungi, plants and vertebrates [Bjostad et al. 1987]. Fatty acid DESs are region-selective and stereo-selective enzymes that catalyze the introduction of double bonds to the acyl chain precursor [Hashimoto et al. 2008]. In this class of enzymes, at least four groups can be distinguished based on the region-selective activity of the enzyme. DESs from the

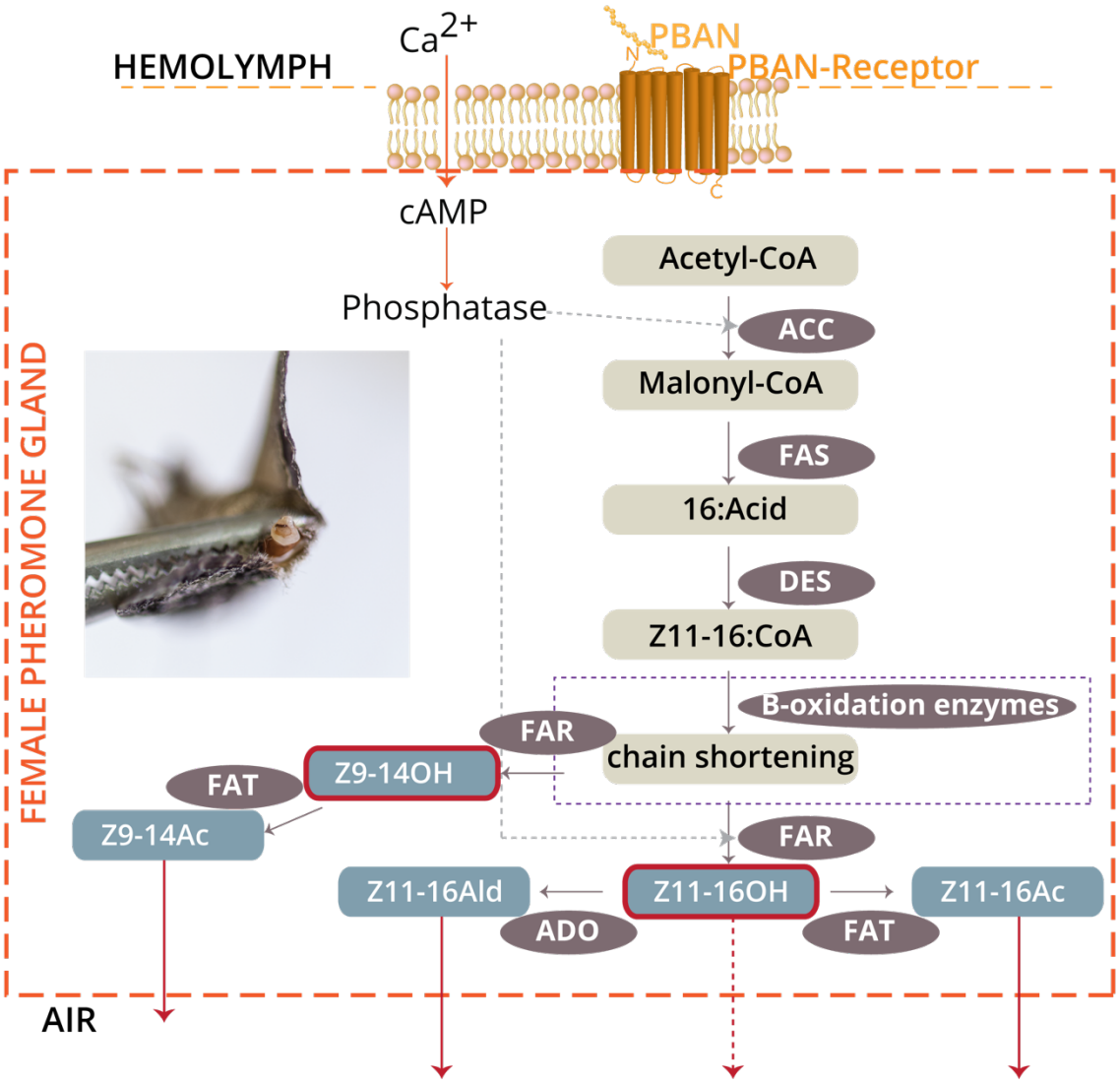

Figure 2-1 Overview of the Type 1 pheromone biosynthesis pathway in Lepidoptera. Activation of the pheromone biosynthesis-activating neuropeptide receptor (PBANr) by PBAN and subsequent activation of calcium-dependent cascades is the rate limiting step for the pathway. The first step is carboxylation of the acetyl-coenzyme A (CoA) precursor by acetyl-CoA carboxylase (ACC). Fatty acid synthase (FAS) catalyzes the condensation of malonyl-CoA with successive units of acetyl-CoA to produce the fatty acid precursor. Desaturase (DES) specific for medium chain fatty acids introduces double bonds into the acyl-CoA chain prior to chain shortening via the β-oxidation enzyme complex. The carboxyl group is modified by fatty acid reductases (FARs) to produce fatty alcohols. The fatty alcohols can be emitted as pheromone components or undergo further modification by acyltransferases (FAT) to produce acetyl esters or by aldehyde oxidases (ADO) to produce aldehydes. The enzymes are represented as purple ovals. The pheromone components are represented by grey rectangles. The special role of the fatty alcohols Z9-14OH and Z11-16 OH as precursors of pheromones is indicated by the red border framing the label. Adapted from Ding and Löfstedt (2015); He et al. (2017).

first group insert double bonds into the saturated acyl chain, whereasthe remaining DESs belong to the following three classes: (i) front-end DESs which introduce a double bond between an existing double bond and carboxylic end, (ii) omega DESs which insert double bonds between an existing double bond and the methyl end, and (iii) sphingolipid desaturases which modify sphingolipid components of the eukaryotic plasma membrane. The front-end DESs can be further divided into several subclasses based on the four-letter key motif associated with the location of the inserted double bond [Jeong et al. 2003]. The most common subclasses of front-end DESs includeΔ9-KPSE DES (C16>C18), Δ9-NPVE DES (C18>C16) and Δ10/Δ11-xxxQ or -xxxE DES. Although 9-KPSE DES and Δ9-NPVE DES (C18>C16) are homologous to DESs participating in general cellular fatty acid metabolism, their functional role in sex pheromone biosynthesis in moths is well-documented [Knipple et al. 2002]. However, molecular evolution studies of this gene family suggest that the majority of pheromone structures produced in moths are a result of a Δ11 DES unique to lepidopterans and absent from other insect orders [Liénard et al. 2014].

The unsaturated fatty acid derivative can subsequently enter one or more rounds of limited chain shortening through β-oxidation processes. The first reaction involves conversion of acyl-CoA into E2-enoyl-CoA. This conversion is catalyzed by β-oxidases (ACO) in peroxisomes, whereas in mitochondria it is carried out by acyl-CoA dehydrogenases (ACD). Dehydrogenases are further classified into short (C_4-C_6), medium (C_6-C_{10}), long (>C_8) and very long chain (C_{20}-C_{24}) dehydrogenases based on the length of their substrate [Ikeda et al. 1985]. The second reaction of β-oxidation involves hydration of E2-enoyl-CoA to L-3-hydroxyacyl-CoA by enoyl-CoA hydratase (ECH), followed by reversible dehydrogenation of L-3-hydroxyacyl-CoA to 3-ketoacyl-CoA by 3-hydroxyacyl-CoA dehydrogenase (3HCD). During the final step, the 3-ketoacyl-CoA substrate is cleaved by acetoacetyl-CoA thiolase (KCT) between the α and β carbon atoms to produce a molecule shortened by two carbons. The differences in the chain-shortening outcome between peroxisomes and mitochondria point to peroxisomes as the site for pheromone biosynthesis [Jurenka 2004]. In mitochondria, the acyl substrates are systematically degraded into a two-carbon product. In peroxisomes, however, the specificity of the acyl-CoA oxidase is limited to substrates with eight carbon atoms or more resulting in the production of medium-chain fatty acyl-CoAs [Hashimoto 1996]. Mutations in ACOs specific to pheromone

β-oxidation were shown to contribute to pheromone variation in *T. ni* [Jurenka et al. 1994; Gemeno et al. 2001]. As a large number of Type 1 pheromones have carbon chains of C_{12}-C_{16}, additional factors may participate in the pheromone-specific chain shortening in the female pheromone glands [Ding and Löfstedt 2015].

In the third and final stage of the pheromone biosynthesis, the carboxyl group of the fatty acyl precursor is modified to alcohol and then to acetyl ester or aldehyde (Figure 2-1) [Jurenka 2003]. The reduction of fatty-acyl precursors is catalyzed by fatty-acyl reductases (FARs) [Moto et al. 2003; Lienard et al. 2008; Hagström et al. 2012]. Along with DESs and β-oxidation enzymes, FARs are known to contribute to the pheromone variation observed in moths as illustrated by studies in *Ostrinia nublialis* [Zhu et al. 1996a; Lassance et al. 2010]. Among the FARs in moths, substrate specificity for the respective pheromone component precursor acid ranges from very high to moderate [Foster 2016]. For example, in *Agrotis segetum*, a single pheromone gland FAR (pgFAR) is responsible for reducing all three fatty-acyl precursors Z5-10CoA, Z7-12CoA and Z9-14CoA [Ding and Löfstedt 2015]. Although some species do utilize pheromone alcohols, these compounds typically undergo either acetylation or oxidation reactions in most species [Jurenka 2003]. The acetylation of fatty pheromone alcohols is catalyzed by a class of acetyltransferases (FATs) [Morse and Meighen 1987]. Due to the ubiquitous role of acetyltransferases in eukaryotes, the cloning of pheromone-specific FAT has been unsuccessful thus far [Fujii et al. 2010a; Ding and Löfstedt 2015]. The conversion of fatty alcohol pheromone precursors to their corresponding aldehyde pheromones is carried out by a cuticular aldehyde oxidase (ADO) [Teal and Tumlinson 1987; 1988; Fang et al. 1995b]. The oxidases that participate in pheromone biosynthesis show broad specificity to primary alcohols and do not show preferences for chain length or position and geometry of the double bond.

In addition to enzymes involved in pheromone biosynthesis, transcriptomic studies in *Spodoptera litura* [Zhang et al. 2015b], *A. segetum* [Strandh et al. 2008] and *Sesamia inferens* [Zhang et al. 2013] have also reported the presence of OBPs and CSPs in female pheromone glands. Their function in non-sensory organs has not been studied extensively, but it was suggested that CSPs participate in pheromone storage and delivery [Jacquin-Joly et al. 2001]. Although the catalytic framework for pheromone biosynthesis is well-established, many details pertaining to the molecular mechanism specific to pheromone synthesis and emission remain poorly understood.

Development of strategies to link the ever-increasing genetic information produced by NGS approaches with chemistry and molecular biology is necessary, but requires an in-depth understanding of all three of these areas.

2.1.2 Analyses of lepidopteran sex pheromones by coupled gas chromatography mass spectrometry (GC-MS)

Quantification of pheromone components involves determination of the titer at a specific point in time [Foster 2016]. Analysis of the components of the female pheromone blend can be carried out based on extraction of the gland's contents in organic solvent. Subsequent identification of compounds and determination of the ratios is routinely achieved with GC-MS [Ando and Yamakawa 2011]. Alternatively, pheromone gland emissions can be captured on adsorbent material and either extracted or directly analyzed with GC-MS depending on the analytical technique used for capturing the volatile compounds.

The identification of pheromone compounds is typically carried out in the electron ionization (EI) mode. The characteristic structure of monounsaturated Type I pheromones allows for relatively easy compound identification [Ando et al. 2004]. The molecular ions M^+ from Type I pheromones are relatively hard to detect by EI at 70ev; however, their molecular weights (mass-to-charge ratio; m/z) can be estimated from $[M\text{-}H_2O]^+$ for alcohols (m/z 138, 166, 194, 222 and 250) and aldehydes (m/z 136, 164, 192, 220 and 248), and from $[M\text{-}AcOH]^+$ for acetates (m/z 138, 166,194, 222 and 250) for carbon chains of C_{10}, C_{12}, C_{14}, C_{16} and C_{18}, respectively [Ando and Yamakawa 2011]. Fatty acid alcohol- and acetate ester-derivatives with the same length of carbon chain show the same fragment atom, but acetates can be distinguished by the presence of the characteristic $[AcOH+1]^+$ m/z of 61, which is absent for alcohols. Furthermore, pheromone compounds with two (dienyl) or three (trienyl) double bonds can be identified by their M^+ ion. For example, a C_{16} carbon chain acetate is represented with m/z 280 for dienyl and m/z 278 for trienyl compounds. The relative intensity of M^+ ion originating from a compound with conjugated double bonds is stronger than the intensity from a compound with isolated double bonds. The major contaminants found in pheromone gland extracts are *n*-alkanes present in insect cuticles; however, their presence can be easily omitted based on their characteristic spectral patterns [Ando and Yamakawa 2011].

Struble et al. (1984) carried out GC-MS EI and chemical ionization (CI:isobutane) analysis of 365 pooled BAW female pheromone glands [Struble et al. 1984]. The GC-MS analysis produced full spectra for 12:Ac, Z9-14:Ac, 16:Ac, Z9-16:Ac and Z11-16:Ac and partial spectra for Z7-12:Ac and 14:Ac. The estimated relative quantities of the components in the extract were 1 (12:Ac); 1 (Z7-12:Ac); <0.6 (14:Ac); 7 (Z9-14:Ac); <0.6 (Z9-14:OH); < 2 (16:Ac); 0.6 (Z7-16:Ac); 0.9 (Z9-16:Ac); 100 (Z11-16:Ac); and <0.6 (Z11-16:OH) . The amount of Z11-16:Ac from one gland was estimated to be 5 ng. Analysis of inter-individual variation has never been carried out for BAW, but it is required for future investigations on geographic inter-population differences.

2.1.3 Transcriptomic analysis of female pheromone glands

Modern pheromone research has moved beyond simple identification of pheromones for exploitation in pest control strategies [Ruther 2014]. A major contribution towards this shift can be attributed to development of NGS. In particular, RNA-Seq has become an invaluable tool in studies on non-model organisms for which the genome sequence is lacking or incomplete [Wang et al. 2009; Ozsolak and Milos 2011]. As gene repertoires from different species and insect orders are characterized from transcriptomic data, our knowledge of the complex architecture underlying pheromone communication is no longer limited only to a few model species.

The quality of the transcriptome assembly defines our ability to perform downstream analyses, such as novel transcript identification, isoform detection, transcript quantification and detection of sequence variation [Conesa et al. 2016; Huang et al. 2016]. For non-model organisms for which genomic information is not available, evaluation of the transcriptomic assembly can be particularly challenging. Assembly errors can be introduced in several ways during the assembly process [Conesa et al. 2016]. One of the most common errors is fragmentation producing several smaller contigs instead of one sequence. In contrast, large chimera contigs can also be found when several transcripts are strung together. Fragmentation is often associated with variable read coverage along the length of the transcript, whereas chimeric sequences tend to originate from ambiguities in the overlap of shorter reads and the tendency of the assembly software to choose the longest contigs possible. Three factors directly affect the quality of *de novo* assembled transcripts: (i) type of transcripts, (ii) sequencing technology, and (iii) bioinformatic workflow [Smith-Unna et al. 2016]. The type of transcript is affected by the overall complexity of the

organism (e.g. ploidy level and GC content), as well as the presence of repeats, polymorphisms and splicing events. The sequencing technology used involves library preparation and the sequencing strategy which can affect sequencing accuracy. The workflow requires consideration of assembly algorithms and data handling software, such as annotation or abundance estimation.

Transcriptome assembly can be carried out as a reference-guided or *de novo* process [Grabherr et al. 2011; Haas et al. 2013]. In the reference-guided assembly, the RNA-Seq reads are aligned to a reference genome and merged based on overlapping alignment to form longer contigs. Since no genome information was available for *M. configurata,* my analysis required *de novo* transcriptome assembly [Haas and Zody 2010]. At the time my thesis project was initiated, a few *de novo* assemblers were in the early stages of development and refinement [Robertson et al. 2010; Grabherr et al. 2011; Schulz et al. 2012; Xie et al. 2014]. However, there were no formal comparisons of either RNA-Seq experimental design practices, comparisons of assembler efficiencies or tools and documented pipelines for building *de novo* transcriptome assemblies. The Trinity package offered several technical advantages, including its ability to handle large RNA-Seq read libraries and operation in the computing grid system where the memory-intensive assembly process could be broken up into many smaller jobs allowing for lower overall memory requirement and faster job completion [Haas et al. 2013]. Analysis of RNA-Seq data is a multi-step process that involves raw data clean up and assessment, assembly, transcriptome evaluation, coding region prediction, functional annotation and gene quantification (Figure 2-2) [Conesa et al. 2016].

2.1.3.1 RNA-Seq data preprocessing

Prior to transcriptome assembly, the raw RNA-Seq reads must be assessed based on base quality distribution, kmer frequencies and adapter contamination. Erroneous k-mers arising from sequencing errors should be corrected or removed altogether [Conesa et al. 2016]. The sequencing pipeline may incompletely remove adapter sequences and low-quality bases; thus, general clean up must also be carried out. FASTQC (www.bioinformatics.babraham.ac.ukprojectsfastqc) and Trimmomatic [Bolger et al. 2014] algorithms can facilitate the required data preprocessing and are commonly utilized for Illumina RNA-Seq data. FASTQC is a rapid assessment tool that carries out basic quality analysis on the raw RNA-Seq and identifies errors originating from the sequencing process or the library

preparation. Trimmomatic is an algorithm that carries out a number of read-trimming and processing steps with its main focus being the removal of technical sequences, such as adapters and low quality bases [Bolger et al. 2014].

2.1.3.2 De novo Trinity assembly

As a *de novo* assembler, Trinity generates contigs directly from RNA-Seq reads. The program utilizes a structure called a De Bruijn graph, which is also used by a number of genome and transcriptome assemblers [Grabherr et al. 2011]. A De Bruijn graph is a mathematical representation of a node in the form of a substring of letters of length *k* [Zerbino and Birney 2008]. For *de novo* sequence solution, such as genome and transcriptome assembly, a node is represented by a sequence of a fixed length of *k* nucleotides, also referred to as *k*-mer. Multiple nodes can be connected by edges if the *k*-mer sequence content creates an exact k-1 overlap between the nodes. In a transcriptome assembly, the short RNA-Seq reads are broken up into short *k*-mers (typically k=25). De Bruijn graph structures are built by connecting nodes with overlap between the last k-1 nucleotide of one substring with the first *k*-1 nucleotides of the subsequent substring. During graph extension, identical overlaps between nodes are merged and counted, whereasnodes with differences result in branches in the graph. The presence of single nucleotide differences between sequences results in generation of "bubble" structures in the graph [Grabherr et al. 2011; Sacomoto et al. 2012; Conesa et al. 2016]. The structure of the bubbles may correspond to the presence of alternative splicing or alternative transcription start and end sites. Single nucleotide discrepancies may indicate the presence of single nucleotide polymorphisms (SNPs) or sequencing errors [Sacomoto et al. 2012]. Although, the main goal of Trinity is to resolve sequence conflicts and linearize the bubbles, these structures carry important information for downstream analysis (Section 3.4.1).

2.1.3.3 Transcriptome evaluation

The quality of the assembled transcriptome can be evaluated via several different methods, including traditional assembly metrics, RNA-Seq read representation, full-length reconstructed protein content and assembly evaluation software. Metrics based on contig count and length, which were historically used in genome assemblies, can also be considered for transcriptomes [Conesa et al. 2016]. However, these metrics are of limited use since the length of the assembled

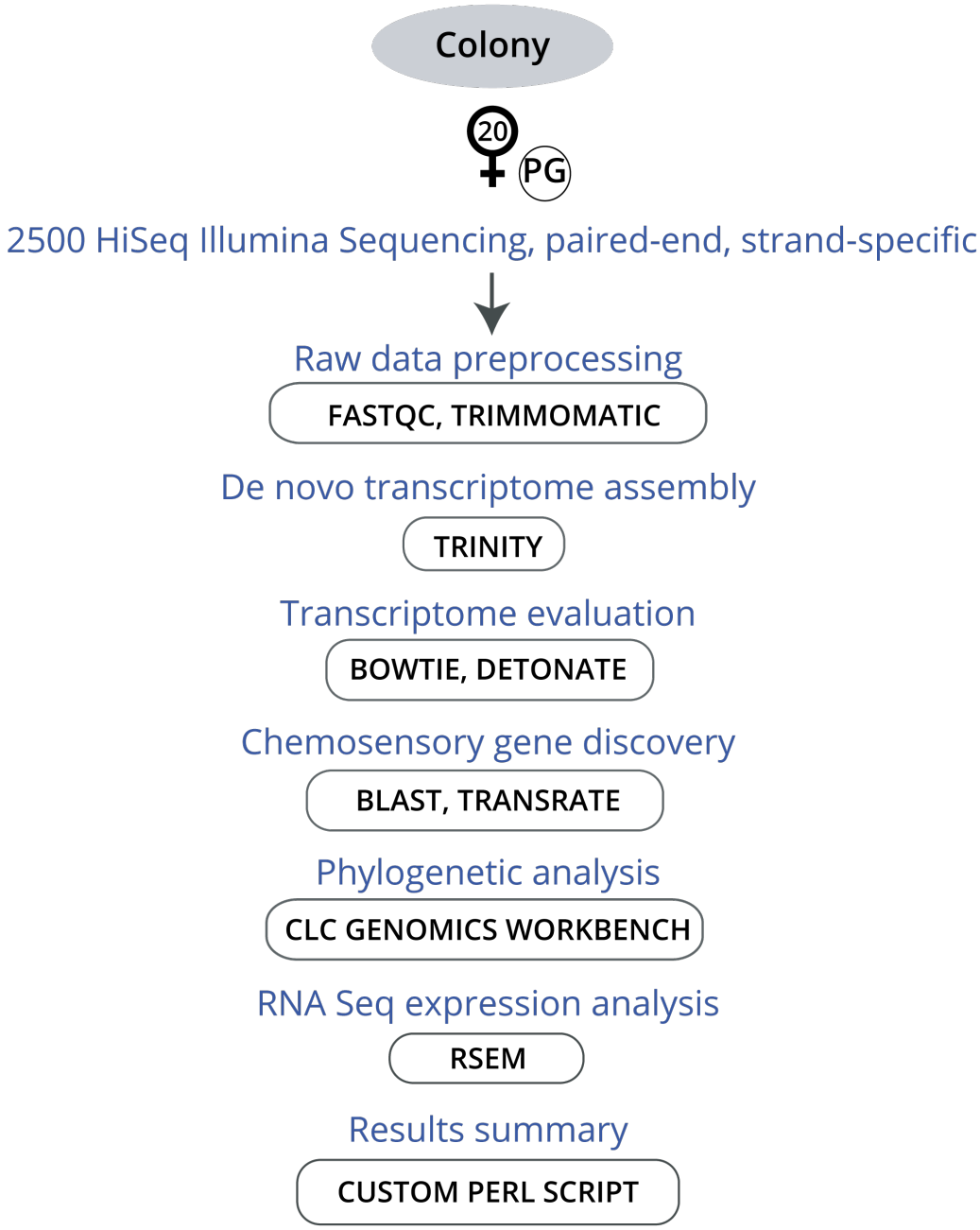

Figure 2-2 Bioinformatic workflow for *de novo* assembly and analysis. Total RNA from the female pheromone gland (PG) tissue was subjected to HiSeq Illumina sequencing. The raw RNA-Seq reads were preprocessed and their quality evaluated prior to carrying out *de novo* assembly with Trinity. Transcriptome evaluation involved the assessment of aligned read representation, full-length protein content and TransRate statistics. The transcriptome was mined for genes encoding proteins implicated in pheromone biosynthesis and transport. The sequences obtained were analyzed with a custom bioinformatic workflow, which included phylogenetic analysis and transcript abundance determination.

contigs varies depending on the length of the transcripts being assembled and specific to the tissue and organism. A more useful statistic is the Ex90N50 statistic [Haas et al. 2013]. The N50 statistic corresponds to a value for which at least 50% of the assembled transcript nucleotides are found in contigs of at least the N50 length value. For the E90N50 statistic, the N50 is limited to the most highly-expressed transcripts. Exclusion of many low-expressed contigs, which often tend to be very short due to the nature of the assembly, provides a more useful evaluation statistic. Another helpful parameter can be obtained by aligning the input RNA-Seq reads to the assembly [Haas et al. 2013]. In a high-quality assembly, approximately 80% of the total RNA-Seq reads should be represented by the transcriptome. The number of full-length reconstructed proteins obtained from searching the transcriptome against databases of known and related protein sequences provides an indication of the fragmentation and depth of content of the assembly. More recently, software, such as Detonate [Li et al. 2014] and TransRate [Smith-Unna et al. 2016], were developed to aid in the evaluation process. Denotate provides an overall score and is helpful in comparing assembly outcomes based on the same input RNA-Seq data, but is performed with different assembly parameters. TransRate provides a number of descriptive statistics that can be used for comparison of the transcriptomes. Ultimately, effective evaluation requires a combination and assessment of several, if not all, of the methods mentioned.

2.1.3.4 Analysis of gene content and functional annotation

The initial search for full-length reconstructed proteins provides an estimate of the proportion of the transcriptome corresponding to functionally-identifiable gene content. The Trinity package includes an open reading frame predictive software called Transdecoder for coding region identification [Haas et al. 2013]. The output from Transdecoder is also a useful estimate of the coding content of the transcriptome. Additional searches based on conserved ortholog content (BUSCO) [Simão et al. 2015] and eukaryotic Orthologous Groups (KOG), gene ontology (GO), protein structure and conserved domains (Swiss-Prot, Pfam, TMHMM) allow for characterization of the transcriptomic content [Conesa et al. 2016; Bryant et al. 2017]. Characterization of coding content has a dual function as it allows for assessment of the transcriptome, while also providing a starting point for discovery and identification of novel proteins.

2.1.3.5 Transcript quantification

The Trinity assembly can be subjected to either alignment-based or alignment-free transcript quantification algorithms. The alignment-based methods, such as RSEM (RNA-Seq by Expectation Maximization) [Li and Dewey 2011] and eXpress [Zhang et al. 2017], provide an indication of the RNA-Seq read representation and, thus, the quality of the transcriptome assembly [Haas et al. 2013]. The output of the quantification algorithms provides transcript level estimates of the count of RNA-Seq fragments that were derived from each transcript, as well as a normalized measure of transcript expression that takes into account the transcript length, the number of reads mapped to the transcript and the total number of reads that mapped to reads within the transcriptome. The two most commonly reported normalized expression metrics are "fragments per kilobase of transcript per million fragments mapped" (FPKM) or "transcripts per million" (TPM) [Conesa et al. 2016]. The FPKM measure is an estimate of number of fragments that are derived from a given transcript. The TPM metric represents the estimated fraction of transcripts made up by a given gene or isoform. The TPM measure is independent of the mean expressed transcript length and conveniently, all TPM values within a data set sum up to 1 million, which allows for cross data sample comparisons.

My work in this study aimed to characterize the chemical composition of BAW female pheromone gland and the genetic architecture of the pheromone biosynthesis pathway. Although, sex pheromones and the blend ratios for BAW were previously reported, the investigation did not involve intraspecific and inter-specific population analysis of variation in pheromone production. The transcriptomic analysis was carried out on the pheromone glands from the long-term laboratory reared colony (AAFC-Saskatoon) with the aim of identification and characterization of genes directly implicated in pheromone biosynthesis and transport. The analysis of pheromone gland tissues is complicated by a large proportion of the transcriptome's coding content corresponding to catalytic proteins carrying out general metabolic functions. For catalytic proteins for which some biological and functional information exists, such as fatty acid DESs or pgFAR, assignment of transcripts to different functional groups is possible. However, for several of the enzyme classes, the linking of a specific gene to a catalytic protein with biological function implicated in pheromone biosynthesis is currently unattainable. Nevertheless, as the genetic data becomes available for other closely-related non-model species and the quality of that data improves, additional information can be obtained through comparative transcriptomics.

Characterization of the genetic framework underlying pheromone biosynthesis constitutes an important step towards design of molecular and functional studies aiming at closing the gap between the genetic characterization and biological function of gene products involved. The knowledge gained, in turn, can contribute to improved design of monitoring strategies for BAW.

2.2 MATERIALS AND METHODS

2.2.1 Insect rearing

In addition to a long-term (35 years in culture) laboratory *M. configurata* colony (AAFC-Saskatoon), four colonies established from individuals collected in the summer season of 2013 from Davidson, SK [N51.29987 W105.71261] (AAFC-Davidson; 7 moths and 5 egg masses), Vegreville, AB [N53.44340 W112.36830] (AAFC-Vegreville; 4 moths and 16 egg masses), Regina, SK [N50.28770 W104.65240] (AAFC-Regina; 4 egg masses) and Lethbridge, AB [N49.6819 W112.78] (AAFC-Lethbridge; 14 pupae) were used in the experiments. The laboratory colony from the AAFC-Saskatoon population was reared using a standard protocol [Bucher and Bracken 1976]. Briefly, larval instars (1-6) were reared on artificial alfalfa-soy-agar diet at 22°C and under 16-hour light (photophase): 8-hour dark (scotophase) cycle. Following pupation, pupae were sexed and transferred to clear 500 mL plastic tubs lined with a filter paper disk and covered with a mesh lid, and stored at the same temperature (22°C), but with a reversed light cycle with scotophase beginning at 8:00 am. Male and female adults were collected daily following the beginning of scotophase and transferred to separate cages (36 x 26 x 26 cm). Sucrose-honey solution (10% v/v) was provided as a food source in a small vial with a lid and a filter paper wick. Unless otherwise stated, adult moths at 48-72 hours post-eclosion were used in experiments. The geographic BAW populations corresponding to AAFC-Davidson, AAFC-Vegreville, AAFC-Regina and AAFC-Lethbridge were also reared according to the above protocol; however, larval instars 1-4 were reared on canola plants. Late 4^{th} or early 5^{th} instar larvae were transferred to artificial diet from the plant to complete the larval stages and pupate. For behavioural and electrophysiological experiments, males and females were kept in isolated incubators to ensure males would not be pre-exposed to the female-produced pheromones.

2.2.2 Semiochemicals

Previously identified pheromones of BAW, namely (Z)-11-hexadecenyl acetate and (Z)-9-tetradecenyl acetate [Chisholm et al. 1975; Underhill et al. 1977a], were obtained as synthetic neat solutions from Bedoukian Research, Connecticut, USA. Hexane (HPLC grade >97%), GC calibration standards, titanium tetrachloride, and plant volatiles including cis 3-hexenyl acetate (3HAC) and ethyl caproate (ECAP), were purchased from Sigma Aldrich, USA.

2.2.3 Female pheromone gland extracts

Adult BAW females (2-3 days old) were transferred to a dark container at 4°C, 2-3 hours after the onset of scotophase. The abdominal tip containing the pheromone gland was extruded by gently pressing the female's abdomen. The tip was immediately dissected with micro-scissors (World Precision Instruments) and placed in a glass vial containing 50 µL of hexane for 15-20 min at room temperature. For pooled gland extracts, the volume of hexane was adjusted to 15 µL of hexane per gland. The gland extract was either used immediately for GC-EAD or GC-MS analysis or sealed in glass ampule and stored at -20°C for later analysis.

2.2.4 Chemical analysis of pheromone gland components with GC-MS

The chemical analysis of the female pheromone gland extracts was carried out at Simon Fraser University with assistance of Regine Gries. The glands were dissected as described in Section 2.2.3 and immediately transferred to 50 µL of HPLC grade hexane (Sigma Aldrich, USA). Each individual gland extract (1 gland equivalent) was concentrated under a stream of nitrogen gas at room temperature to a volume of 2 µL. Aliquots (2 µL) were analyzed on a Varian Saturn 2000 Ion Trap GC-MS fitted with a DB-5MS column (30 m × 0.25 mm ID; Agilent Technologies Inc., Santa Clara, USA) and operated in full scan electron impact (EI) mode. The flow rate of the helium carrier gas was set at 35 cm/sec. The injector port of the GC–MS was kept at 250 °C, the transfer line at 280 °C, and the ion trap at 180 °C. The GC oven program was as follows: 50 °C (5 min), then 20 °C per minute to 280 °C and 280 °C (5 min). Mass spectra of compounds in the pheromone gland extracts were obtained and selected ion monitoring carried out focusing on ions characteristic of the pheromone components. The retention times for the major and minor pheromone components were determined by injecting a multi-component standard containing 10 ng of synthetic Z9-14Ac, Z11-16Ac and Z10-15Ac as internal standards. The quantity of each compound was calculated according to Equation 2-1.

Equation 2-1 Quantity of compound

$$Q_C = cf\,\frac{A_C Q_I}{A_I}$$

Where Q_c is the quantity of compound, A_c is the area of the peak corresponding to the compound, Q_I is the quantity of the internal standard, A_I is the area of the internal standard peak and *cf* is the correction factor. The *cf* is the ratio of the area of the internal standard to the area of the compound peak obtained from injection of the multi-component standard and was calculated according to Equation 2-2.

Equation 2-2 Correction factor

$$cf = \frac{A_{I'}}{A_{C'}}$$

Where $A_{I'}$ is the peak area of 10 ng of internal standard and $A_{C'}$ is the peak area of 10 ng of the compound. Extracts from individual glands collected from AAFC-Saskatoon (16 females) and AAFC-Davidson (10 females) were analyzed. One gland equivalent of a pooled gland extract from 10 AAFC-Saskatoon females was also analyzed according to the method described above.

2.2.5 Statistical analysis

The amounts of major and minor pheromone components present in the pheromone extracts of individual females from the AAFC-Saskatoon and AAFC-Davidson colonies obtained from GC-MS quantification were tested for normality with Shapiro-Wilk normality test. Wilcoxon rank sum test (significance level p =0.05) was performed on the amounts (ng) of Z9-14Ac and Z11-16Ac detected for each population (STATISTIX 10, Tallahassee, FL, USA). The pheromone blend ratios were compared using $\chi 2$ test of independence with reading values of zero (0 ng) for Z9-14Ac omitted from the analysis.

2.2.6 RNA isolation, library construction and sequencing

All tissue collections were carried out on 20 unmated adult female insects 48 h post-eclosion and 3-4 hours into the scotophase. The glandular tissues were transferred immediately upon excision into TRIzol (Invitrogen, Carlsbad, USA) and RNA extracted according to the manufacturer's protocol. Total RNA pellets were resuspended in 50 µL of ultrapure DEPC-treated water (Sigma Aldrich, USA). Each sample was subjected to DNase treatment with an Illustra RNAspin Mini Kit (GE Healthcare, Mississauga, Ontario, Canada) and total RNA was eluted with 100 µL of ultrapure RNase free water. RNA was quantified with a Nanodrop UV spectrophotometer

(Techno Scientific, Wilmington, USA) and Qubit 2.0 Fluorometer (Life Technologies, Burlington, Ontario, Canada). The quality and integrity of the total RNA samples were tested using an Agilent 2100 Bioanalyzer (Agilent Technologies, Santa Clara, USA). Total RNA for each tissue type (4 µg at 40 ng/µL) was submitted for cDNA library construction (Illumina TruSeq mRNA stranded library preparation) and Illumina 2500 Hi-Seq paired-end strand specific sequencing at the McGill University and Genome Quebec Innovation Centre, Quebec, Canada.

2.2.7 Transcriptome assembly and annotation

Quality trimming of raw reads was performed with Trimmomatic v0.36 [Bolger et al. 2014]. Quality trimming and removal of sequencing adapters was carried out with the following settings: LEADING:5, TRAILING:5, SLIDINGWINDOW:4:15, MINLEN:36, PHRED:5. *De novo* assembly was performed on the clean read library with Trinity v.2.5.1 (k-mer size of 25, min_kmer_cov set to 2 and all other parameters set to default) [Grabherr et al. 2011; Haas et al. 2013]. The transcriptome assembly quality was assessed with Transrate v1.0.3 software [Smith-Unna et al. 2016]. The RNA-Seq read representation analysis on the assembled transcriptome was performed with Bowite2 v2.3.5.1 [Langmead and Salzberg 2012].

The transcriptome assembly was scanned for open reading frames (ORFs) with Transdecoder v2.0.1 with minimum peptide length set to a default value of 100 amino acids [Haas et al. 2013]. Gene function was annotated by homology searches with Blast2Go v5.1 against the NCBI non-redundant protein (Nr) database, NCBI nucleotide (Nt) database, Swiss-Prot protein database, euKaryotic Orthologous Groups (KOG), Kyoto Encyclopedia of Genes and Genomes (KEGG), Gene Ontology (GO) and Protein family (Pfam) database [Conesa et al. 2005]. Targeted searches using BLAST were carried out on the ORF subset of the BAW sequences with manually-created lists of orthologous sequences of genes of interest. Similarity searches using BLASTx (E-value $1e^{-10}$ and Blosum62 Matrix) against a nucleotide database containing output ORF sequences from Transdecoder were carried out with CLC Genomics Workbench (Qiagen Bioinformatics; versions v9.0-current).

2.2.8 Abundance estimation

Gene expression levels for each sample were estimated using RSEM v1.2.15 [Li and Dewey 2011]. Isoform expression for each transcript was measured as the expected number of transcripts per million (TPM) normalized for gene length and sequencing depth.

2.2.9 Phylogenetic analyses

Transcripts encoding putative chemosensory proteins identified in the BLAST searches were imported into CLC Genomics Workbench (Qiagen Bioinformatics; versions v9.0-current). Alignments of amino acid sequences with other previously reported lepidopteran protein sequences (Table A-1) were carried out with the CLUSTALO algorithm in CLC [Larkin et al. 2007]. Phylogenetic trees were assembled in CLC based on the Jones-Taylor-Thornton model with nearest neighbour interchange [Arenas 2015]. Maximum Likelihood Phylogeny analysis was carried out with the Neighbor-Joining method. Branch support was estimated by bootstrap analysis based on 1000 replicates with approximate likelihood-ratio test (aLRT) in CLC Genomics Workbench (Qiagen Bioinformatics; versions v9.0-current). Phylogenetic trees were created in iTOL:Interactive Tree of Life web server (www. itol.embl.de) [Letunic and Bork 2007]. Graphical representations were edited in Adobe Illustrator and exported as png formats.

2.3 RESULTS

2.3.1 Chemical composition of BAW female pheromone glands

Extracts from individual pheromone glands were analyzed using GC-MS. The peaks eluting from the DB5-MS column were identified based on their retention times and integrated for quantification of the major and minor pheromone component with Z10-15Ac as an internal standard (Figure 2-3 and Table 2-1). For all individual glands, the following set of peaks were detected: 16.15 min (Z9-14Ac), 16.2 min (14Ac), 17.2 min (Z11-16OH), 18.2 min (Z11-16Ac) and 18.3 min (16Ac) with the exception of two AAFC-Saskatoon and one AAFC-Davidson females for which the Z9-14Ac peak was below the limit of detection (Figure 2-3A). The mass spectra showed the characteristic diagnostic ions for C_{16} acetate $[M\text{-}AcOH]^+$ at m/z 222 and C_{14} $[M\text{-}AcOH]^+$ at m/z 194 for Z11-16Ac and Z9-14Ac respectively (Figure 2-3B, C). The acetate ion $[AcOH+1]^+$ was also detected at m/z 61. Large variation was observed in the amount of the major and minor pheromone components produced among females from AAFC-Saskatoon [Z11-16Ac (0.28 - 42.10 ng), Z9-14Ac (0 - 1.70 ng)] and AAFC-Davidson [Z11-16Ac (0.14 – 20.80 ng), Z9-14Ac (0 – 0.45 ng)]. However, the mean amount produced by each female for both Z11-16Ac [$Z=1.24$; $p > 0.05$ ($p=0.22$)] and Z9-14Ac [$Z=1.66$; $p > 0.05$ ($p=0.09$)] was not statistically different between the two populations (Figure 2-4A and B).

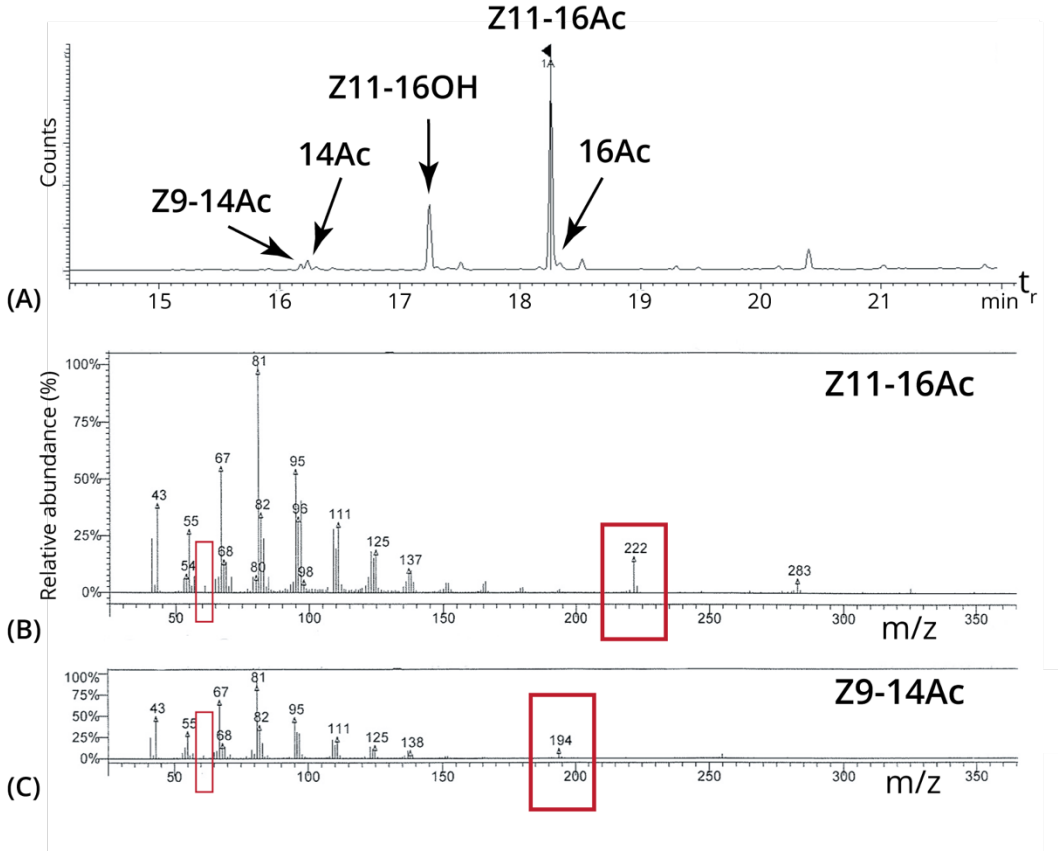

Figure 2-3 GC-MS analysis of the BAW female pheromone gland. **(A)** Gas chromatogram showing peaks detected from 1 gland equivalent from an AAFC-Saskatoon colony BAW female. Retention times (t_r) were detected at 16.15 min (Z9-14Ac), 16.2 min (14Ac), 17.2 min (Z11-16OH), 18.2 min (Z11-16Ac) and 18.3 min (16Ac). **(B)** Z11-16Ac mass spectrum showing the characteristic diagnostic ions for C_{16} acetate $[M\text{-}AcOH]^+$ at m/z 222 and acetate $[AcOH+1]^+$ at m/z 61 (red boxes). **(C)** Z9-14Ac mass spectrum showing the characteristic diagnostic ions for C_{14} $[M\text{-}AcOH]^+$ at m/z 194 and acetate $[AcOH+1]^+$ at m/z 61 (red boxes).

The blend ratios for individual females from the AAFC-Saskatoon population ranged from 5:1 to 47:1, whereas the ratios from AAFC-Davidson females ranged from 9:1 to 51:1. When females with no Z9-14Ac were excluded from the analysis and a χ^2 test of independence performed on the blend ratios between AAFC-Davidson (mean = 29:1) and AAFC-Saskatoon (mean = 30:1), no statistically significant difference was detected [$\chi^2(1)=0.0038$; $p=0.9507$] (Figure 2-4C). No additional peaks were detected when 1 gland equivalent of pooled gland extracts from 10 AAFC-Saskatoon females were analyzed. The mean (5 technical replications) amount of Z11-16Ac and Z9-14Ac in the pooled sample was calculated to be 4.41 ng and 0.14 ng, respectively, producing a blend ratio of 32:1.

Table 2–1 Comparison of BAW pheromone gland content based on results from this study and previously reported compounds.

Compounds	Struble et al. 1984[1]	AAFC-Saskatoon	AAFC-Davidson
12Ac	+	+	+
Z7-12Ac	+[2]	-	-
Z9-14Ac[3]	+	+	+
14Ac	+[2]	+	+
Z9-16Ac	+	-	-
Z11-16OH	-	+	+
Z11-16Ac[3]	+	+	+
16Ac	+	+	+

[1] [Struble et al. 1984]
[2] indicates incomplete spectra reported
[3] active BAW pheromone components are highlighted in bold, blue font

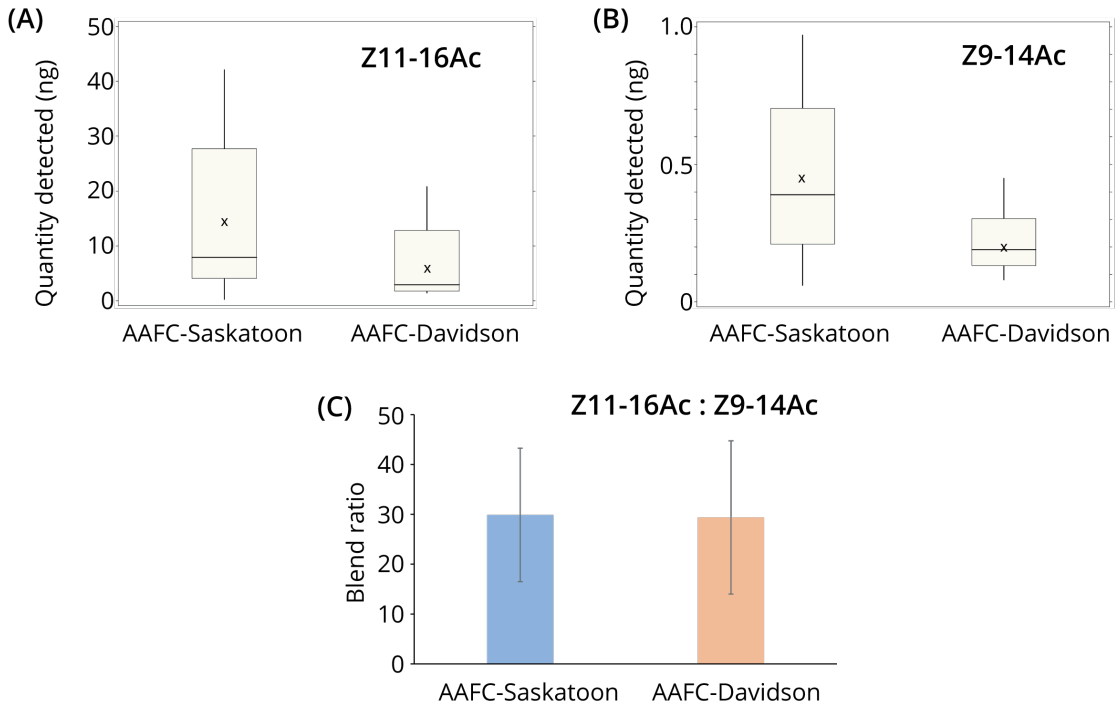

Figure 2-4 Quantities of major and minor pheromone components in BAW pheromone glands. Box and whiskers plots for quantity (ng) of **(A)** Z11-16Ac and **(B)** Z9-14Ac detected via GC-MS quantification of individual pheromone gland extracts from AAFC-Saskatoon and AAFC-Davidson females. The horizontal line within the box indicates the median, the boundaries of the box indicate the 25th- and 75th -percentile, and the whiskers indicate the highest and lowest values of the results. Means are indicated with the x symbol. The inter-individual variation was large within each population. **(C)** Mean blend population ratios with error bars corresponding to 1 standard deviation.

2.3.1 Pheromone gland transcriptome

Illumina RNA-Seq from the pheromone gland library resulted in 38,690,187 raw reads. After processing and trimming, the BAW reference pheromone gland data set contained 37,621,978 reads with 97.3 % of the reads determined as high quality reads (Q20) via FastQC analysis. The Trinity assembly of the BAW pheromone gland transcriptome produced 100,558 transcripts and 75,564 unigenes (Table 2-2). Standard assembly statistics provided N50 length estimates for unigenes and transcripts as 2271 and 1398 base pairs, respectively. The E90N50 statistic was determined to be 2596 base pairs. Bowtie2 analysis indicated that 82% of the clean reads aligned back to the transcriptome assembly with 75% being concordantly paired, 7% discordantly paired and 18% not aligning to the transcriptome (Table 2-3). The transcriptome was assembled three times. The statistics for each assembly were compared with Transrate and assembly with the best statistics was selected for downstream analysis. The Blast2Go platform was used to assess the pheromone gland transcriptome gene content. The BLASTX algorithm applied against the NCBI non-redundant (nr) protein data base (cut-off E-value of 10^{-10}) resulted in 33,377 hits (45% of the total number of unigenes). Homology analysis identified *Amyelois transitella* (21.3%), *Bombyx mori* (18.5%) and *Papilio machaon* (7.8%) as the top three most closely-related species in BLASTX results. GO annotation assigned GO terms to 41,798 (55%) of the 75,564 unigenes. The assigned unigenes were categorized into 60 GO terms, including 26 (43%) biological process terms, 14 (23%) molecular function terms and 20 (34%) cellular component terms (Figure 2-5). In the biological process category, cellular process (14,101), metabolic process (13,105) and biological regulation (6,116) were the most represented subcategories. Binding (13,070), catalytic activity (12,163) and transporter activity (1,852) were the top three subcategories in the molecular activity category. For the cellular component group, membrane (10,034), cell (9,580) and cell part (9,412) were the most commonly identified subcategories.

2.3.2 Candidate biosynthetic enzymes

The content of the BAW pheromone gland transcriptome was mined for genes encoding proteins implicated in pheromone biosynthesis and transport. BLAST searches with BLASTx and custom-curated chemosensory protein data sets from previously-characterized lepidopteran species resulted in identification of a subset of genes implicated in the pheromone biosynthetic

Table 2–2 Trinity assembly statistics for pheromone gland transcriptome

	Total contigs	Min Contig Length	Mean Contig Length	Median Contig Length	Max Contig Length	N50	E90N50
Trinity transcripts	100,558	201	752	364	39,933	1,398	---
Trinity "unigenes"	75,564	201	1,060	452	39,933	2,271	2,596

[1] Contig length, N50 and E90N50 statistic values are expressed as a number of base pairs (bp)

Table 2–3 Bowtie2 read coverage assessment of the pheromone gland transcriptome

	Number of reads	%[1]
Proper pairs	3,7621,978	100
Aligned concordantly 0 times	9,257,702	25
Aligned concordantly 1 time	8,536,249	23
Aligned concordantly >1	19,828,027	53
Total aligned concordantly	28,364,276	75
Aligned discordantly	2,468,599	7
Did not align	6,789,103	18
Total aligned		82

[1] % value corresponds to a percentage of total reads aligned or not aligned to the transcriptome

Table 2–4 Summary of gene annotation results for the pheromone gland transcriptome

	Number of unigenes	%[1]
Total	75,564	
CD-HIT (98)	73,412	97
Open Reading Frames (ORFs)	19,246	26
Annotated with		
BlastX	33,377	45
GO2Blast	41,798	55
GO Annotations	33,142	44

[1] % value corresponds to a percentage of total unigenes assembled (75,564)

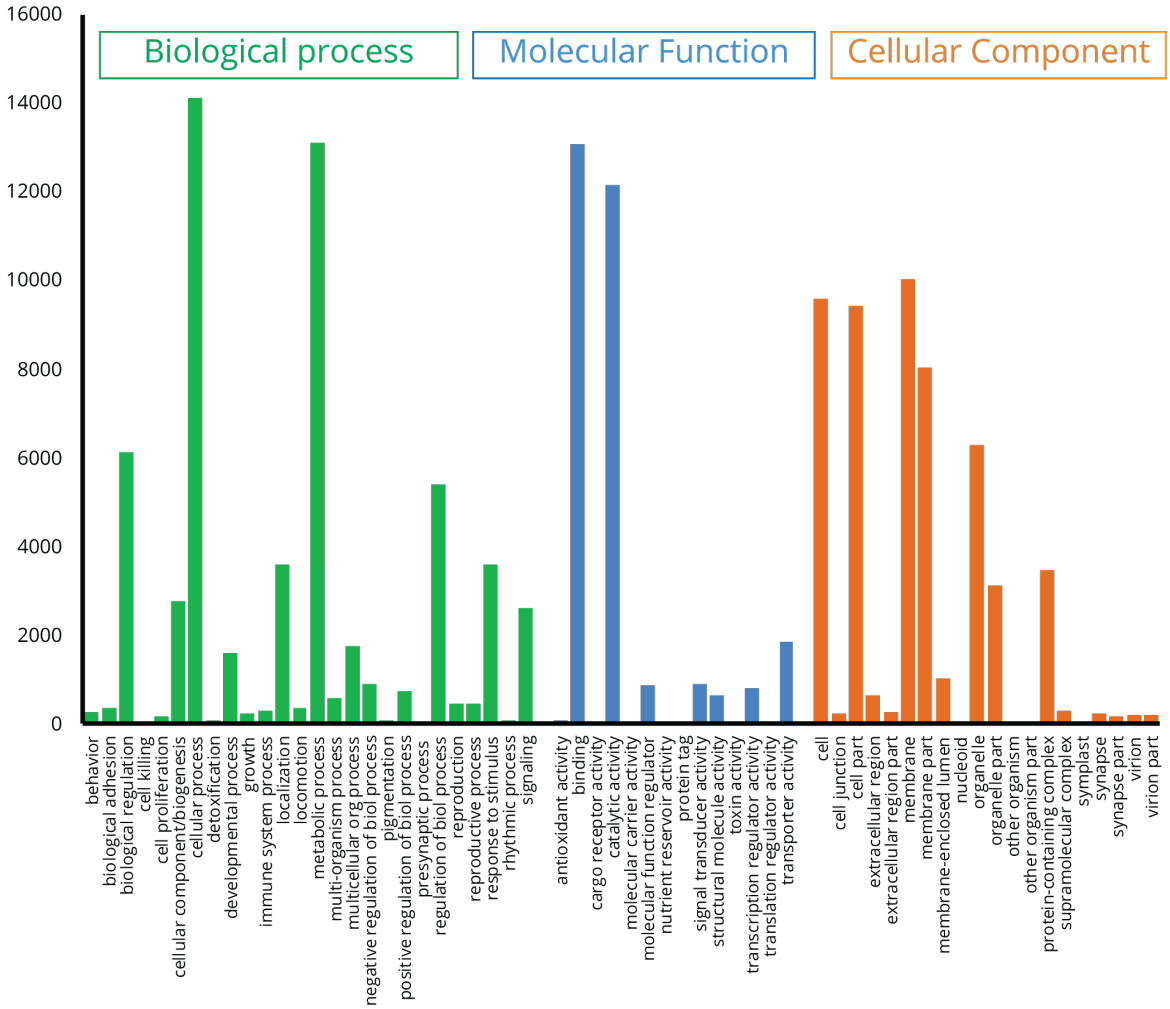

Figure 2-5 Gene ontology (GO) classification of BAW pheromone gland transcripts. GO categories (60) displayed on the x-axis are assigned into three main ontologies: biological process, molecular function and cellular component. The y-axis corresponds to the number of genes from the total transcripts (100,558) assigned to each GO category.

pathway (Table 2-5, Table A-2). The search produced one transcript coding for ACC with 85% amino acid identity to *Agrotis segetum* ACC. Five unique transcripts were identified as putative MconFAS genes; however, three out of the five genes had abundance values of 1 or less TPM and were, therefore, expressed at very low levels. Transcripts coding for MconFAS1 were the most abundant (494 TPM).

An important step in pheromone synthesis is the introduction of double bonds by DES enzymes. The search for orthologues of DES enzymes in the BAW pheromone gland transcriptome produced nine distinct transcripts, including one encoding sphingolipid DES, two encoding Δ11 DES, four encoding Δ9 DES and two encoding undescribed DESs (Table 2-5 and Figure 2-6). Based on the four-letter amino acid code motif descriptor, MconDES7 is a LPAQ-Δ11 DES and the only full length Δ11 DES detected in BAW pheromone gland. The four Δ9 DESs include MconDES5 and MconDES4 as NPVE-Δ9 DESs, MconDES1 as a KPSE-Δ9 DES, MconDES3 as a GATD-Δ9 DES and MconDES2 as a KSVE-Δ9 DES. MconDES6 displays sequence similarity to sphingolipid-Δ4 DES from *A. segetum* (95%) and sphingolipid-Δ4 DES from *Spodoptera litura* (95%). The open reading frames for MconDES9 and MconDES8 encoded for only partial enzyme sequences. MconDES9 displays high amino acid sequence similarity to MPVE-Δ11 DES from *S. litura* (89%) and *Trichoplusia ni* (86%). MconDES8 was found to be highly similar to a Δ11 DES from *Helicoverpa armigera* (87%) and a FADS-like-Δ9 DES from *A. segetum* (89%). The MconDES8 four-letter motif was found to correspond to amino acids PPDS based on the DES protein alignment. The four Δ9 DESs are the most abundant gene transcripts among the DES transcripts discovered (Table 2-5 and Figure 2-6). *MconDES7* transcripts, which encode a protein belonging to the Δ11 DES clade, were detected at 4.83 TPM, in contrast to the most abundant KSVE-Δ9 *MconDES2* transcript detected at 64 TPM.

The search for orthologous sequences produced putative protein sequences corresponding to enzymes catalyzing β-oxidation chain shortening reactions, including eight putative peroxisomal ACO, eight ECH, eight ACD, two KCT and three 3HCD sequences (Table 2-5). The most abundant peroxisomal transcript was derived from *MconACO4* (190 TPM) and encoded a protein with 86% amino acid sequence identity to *A. segetum* ACO. Transcripts from the three ECH genes, including *MconECH1*, *MconECH5* and *MconECH8*, were detected at 83.8, 62.9 and 83.7 TPM, respectively (Table 2-5). Among the MconACD transcripts, *MconACD2* and *MconACD3*

were found to encode a short acyl chain specific ACD with transcript from *MconACD3* being the most abundant (38.4 TPM). MconACD4 displayed high similarity to a very long acyl chain specific ACD from *S. litura* (87%) and its corresponding transcript was detected at 79.3 TPM. MconACD5 and MconACD6 were identified as medium acyl chain specific ACDs; however, only *MconACD5* transcript had a significant gene abundance (116.6 TPM). Similarly, although two MconKCT sequences were detected, only *MconKCT2* transcripts were abundant (102.0) TPM. This protein showed highest sequence similarity to *A. armigera* KCT (84%). Of the three Mcon3HCD sequences detected, *Mcon3HCD2* transcripts were the most abundant at 89 TPM and encoded a protein that was highly similar to *A. segetum* 3HCD (91%).

The FARs converting fatty-acyl precursors into their corresponding fatty alcohols represent another important step in the pheromone biosynthetic pathway. Searches within the BAW transcriptome identified eight putative FAR transcripts (Table 2-5 and Figure 2-7). Transcripts derived from *MconFAR2*, *MconFAR3* and *MconFAR7* were the most abundant with 58.9, 73.8 and 146.5 TPM expression levels, respectively. Phylogenetic analysis of pheromone gland FARs from other lepidopteran species indicated that MconFAR7 belongs to the pgFAR clade of FAR enzymes (Figure 2-7). MconFAR8, MconFAR6 and MconFAR5 were also grouped in the pgFAR clade; however, transcripts from their respective genes were detected below 5TPM. In BAW, the fatty alcohol precursors of Z11-16OH and Z9-14OH are acetylated to produce acetyl esters. In total total, 18 *MconFAT* transcripts were identified from the BAW pheromone gland transcriptome. *MconFAT5*, *MconFAT10*, *MconFAT17* and *MconFAT18* were expressed at the highest levels of 70.0, 244.5, 102.0 and 161.8 TPM, respectively.

In addition to catalytic proteins involved in pheromone biosynthesis, transcripts from eight CSP and four OBP genes with significant expression were identified in the BAW pheromone gland transcriptome. Transcripts encoding MconCSP1, 2, 4, 6, 8, 11-14, identified initially from the whole-head antennal transcriptome, were also detected in the pheromone gland and have 100% amino acid sequence identity with their antennal counterparts (nomenclature from BAW whole-head transcriptome; Chapter 3). Five MconCSP transcripts had relatively high gene expression levels, including *MconCSP3* (6104 TPM), *MconCSP8* (5676 TPM), *MconCSP7* (4325 TPM), *MconCSP9* (3822 TPM) and *MconCSP1* (3233 TPM). Nine OBP sequences discovered in the

Table 2–5 Putative BAW enzymes implicated in pheromone biosynthesis

Gene Name	Enzyme Name	Top Hit Species	Top Hit Accession	E-value[1]	% AA[2] Identity	Transcript Abundance (TPM[3])
Acetyl-CoA Carboxylase (ACC)						
ACC	acetyl-CoA carboxylase	*Agrotis segetum*	KJ622074.1	0	85.8	73.2
Fatty Acid Synthase (FAS)						
FAS1	fatty acid synthase	*Agrotis ipsilon*	JX989151.1	0	91.7	494.7
FAS2	fatty acid synthase	*Helicoverpa armigera*	KP237904.1	0	92.0	0.4
FAS3	fatty acid synthase	*Helicoverpa armigera*	XM_021338376.1	0	94.6	22.9
FAS4	fatty acid synthase-like	*Sodoptera litura*	XP_022827106.1	6.94 E-55	88.6	1.0
FAS5	fatty acid synthase-like	*Helicoverpa armigera*	XP_021181024.1	4.65 E-91	73.2	1.2
Desaturase (DES)						
DES1	acyl-CoA delta 9 desaturase	*Mamestra brassicae*	EU285579.1	0	99.3	2.2
DES2	desaturase 6	*Sesamia inferens*	KF960743.1	0	86.8	64.0
DES3	GATD desaturase	*Agrotis segetum*	KJ622057.1	0	91.6	14.8
DES4	NPVE desaturase	*Agrotis segetum*	KJ622049.1	0	92.5	51.8
DES5	NPVE desaturase	*Agrotis segetum*	KJ622049.1	0	91.5	50.4
DES6	sphingo desaturase	*Agrotis segetum*	KJ622050.1	0	85.9	2.5
DES7	acyl-CoA delta 11 desaturase	*Mamestra brassicae*	EU285580.1	0	99.5	4.8

Table 2-5 con't…

[1] E-value (BLAST) is the number of expected hits of similar quality (score) that could be found just by chance
[2] AA amino acid
[3] TPM transcripts per million

DES8	acyl-CoA Delta (11) desaturase.	*Helicoverpa armigera*	XM_021327954.1	0	79.7	0.8
DES9	acyl-CoA desaturase	*Helicoverpa assulta*	KP008122.1	1.56 E-149	83.2	1.1
β-Oxidation enzymes						
Acyl-CoA oxidase (ACO)						
ACO1	peroxisomal acyl-CoA oxidase	*Agrotis segetum*	KJ622088.1	0	87.3	23.6
ACO2	probable peroxisomal acyl-coenzyme A oxidase 1, variant1	*Ostrinia furnacalis*	XM_028300525.1	1.78 E-71	73.8	6.7
ACO3	peroxisomal acyl-coenzyme A oxidase 1, variant X3	*Spodoptera litura*	XM_022965916.1	0	80.4	29.0
ACO4	putative peroxisomal acyl-CoA oxidase	*Agrotis segetum*	KJ622089.1	0	87.0	190.9
ACO5	probable peroxisomal acyl-coenzyme A oxidase 1	*Agrotis segetum*	XM_021339857.1	0	82.0	11.1
ACO6	putative peroxisomal acyl-CoA oxidase	*Agrotis segetum*	KJ622094.1	0	83.8	14.4
ACO7	putative peroxisomal acyl-CoA oxidase 1	*Agrotis segetum*	KJ622094.1	0	84.3	9.1
ACO8	peroxisomal acyl-coenzyme A oxidase 3	*Spodoptera litura*	XM_022963703.1	0	85.6	5.8
Enoyl-CoA hydratase (ECH)						
ECH1	enoyl-CoA hydratase	*Agrotis segetum*	KJ622099.1	0	90.8	83.8
ECH2	enoyl-CoA delta isomerase 2	*Agrotis segetum*	KJ622112.1	3.34 E-100	84.1	11.8
ECH3	enoyl-CoA hydratase domain-containing protein 3, mitochondrial variant X1,	*Spodoptera litura*	XM_022966847.1	0	81.3	9.8
ECH4	putative enoyl-CoA hydratase	*Agrotis segetum*	KJ622096.1	0	83.0	16.6
ECH5	methylglutaconyl-CoA hydratase	*Agrotis segetum*	XM_021336574.1	4.06 E-144	79.8	62.9
ECH6	delta(3,5)-delta(2,4)-dienoyl-CoA isomerase	*Agrotis segetum*	KJ622095.1	0	87.8	20.5
ECH6	putative enoyl-CoA hydratase	*Helicoverpa armigera*	KJ622113.1	0	86.4	0.3

Table 2-5 con't…

ECH7	3-hydroxyisobutyryl-CoA hydrolase, mitochondrial variant X1	*Helicoverpa armigera*	XM_021342645.1	0	84.6	9.5
ECH8	enoyl-CoA hydratase	*Agrotis segetum*	KJ622099.1	0	90.8	83.8
Acyl-CoA dehydrogenase (ACD)						
ACD1	isovaleryl-CoA dehydrogenase, mitochondrial	*Helicoverpa armigera*	XM_021332708.1	0	83.8	16.8
ACD2	short-chain specific acyl-CoA dehydrogenase	*Agrotis segetum*	KJ622077.1	0	86.5	2.5
ACD3	short-chain specific acyl-CoA dehydrogenase	*Agrotis segetum*	KJ622078.1	0	90. 5	38.5
ACD4	very long-chain specific acyl-CoA dehydrogenase, mitochondrial	*Spodoptera litura*	XM_022966731.1	0	86.6	79.3
ACD5	putative medium-chain specific acyl-CoA dehydrogenase	*Agrotis segetum*	KJ622080.1	0	90.0	116.6
ACD6	putative medium-chain specific acyl-CoA dehydrogenase	*Agrotis segetum*	KJ622080.1	0	91.9	1.8
ACD7	acyl-CoA dehydrogenase	*Agrotis segetum*	KJ622081.1	0	81.4	7.6
ACD8	short/branched chain specific acyl-CoA dehydrogenase	*Agrotis segetum*	KJ622079.1	0	89.5	48.4
Ketoacyl-CoA thiolase (KCT)						
KCT1	3-ketoacyl-CoA thiolase, mitochondrial-like	*Helicoverpa armigera*	XM_021339793	0	83.3	3.4
KCT2	3-ketoacyl-CoA thiolase, mitochondrial-like	*Helicoverpa armigera*	XM_021339794.1	0	84.0	102.0
3-Hydroxyacyl-CoA dehydrogenase (3HCD)						
3HCD1	3-hydroxyacyl-CoA dehydrogenase	*Agrotis segetum*	KJ622105.1	0	87.5	5.2
3HCD2	3-hydroxyacyl-CoA dehydrogenase	*Agrotis segetum*	KJ622104.1	0	91.8	89.2

Table 2-5 con't…

3HCD3	3-hydroxyacyl-CoA dehydrogenase	*Agrotis segetum*	KJ622102.1	0	87.6	12.8
Fatty Acyl Reductase (FAR)						
FAR1	fatty acyl reductase	*Agrotis segetum*	KJ622064.1	0	85.4	27.2
FAR2	fatty acyl reductase	*Agrotis segetum*	KJ622062.1	0	81.3	58.9
FAR3	fatty acyl reductase	*Agrotis segetum*	AID66649.1	0	86.8	73.8
FAR4	fatty acyl reductase	*Agrotis segetum*	KJ622066.1	0	84.1	11.2
FAR5	fatty acyl reductase 14	*Helicoverpa armigera*	MF687541.1	0	87.6	0
FAR6	fatty acyl reductase	*Helicoverpa armigera*	MF687541.1	0	87.7	4.3
FAR7	fatty acyl reductase 1	*Helicoverpa armigera*	ATJ44471.1	0	76.9	146.5
FAR8	fatty-acyl CoA reductase 6	*Agrotis ipsilon*	JX989157.1	0	82.1	2.1
Acetyltransferase (FAT)						
FAT1	fatty alcohol acetyltransferase	*Agrotis segetum*	KJ579235.1	0	82.7	10.3
FAT2	fatty alcohol acetyltransferase	*Agrotis segetum*	KJ579209.1	0	90.6	13.1
FAT3	fatty alcohol acetyltransferase	*Agrotis segetum*	KJ579225.1	0	85.0	13.9
FAT4	fatty alcohol acetyltransferase	*Agrotis segetum*	KJ579212.1	0	91.7	70.0
FAT5	fatty alcohol acetyltransferase	*Agrotis segetum*	KJ579234.1	0	86.3	11.4
FAT6	N-alpha-acetyltransferase 20	*Helicoverpa armigera*	XM_021339596.1	6.97 E-178	88.5	16.1
FAT7	fatty alcohol acetyltransferase	*Agrotis segetum*	KJ579216.1	0	92.2	29.4
FAT8	fatty alcohol acetyltransferase	*Agrotis segetum*	KJ579229.1	0	86.2	11.1
FAT9	fatty alcohol acetyltransferase	*Agrotis segetum*	KJ579218.1	0	84.0	27.4
FAT10	fatty alcohol acetyltransferase	*Agrotis segetum*	KJ579231.1	0	92.7	244.5
FAT11	fatty alcohol acetyltransferase	*Agrotis segetum*	KJ579228.1	0	89.1	1.5
FAT12	fatty alcohol acetyltransferase	*Agrotis segetum*	KJ579222.1	0	92.8	1.4

Table 2-5 con't…

FAT12	fatty alcohol acetyltransferase	*Agrotis segetum*	KJ579232.1	0	86.7	11.6
FAT14	acetyltransferase	*Agrotis ipsilon*	KC007358.1	0	90.0	21.5
FAT15	fatty alcohol acetyltransferase	*Agrotis segetum*	KJ579206.1	0	87.8	1.0
FAT16	lysophospholipid acyltransferase 2	*Spodoptera litura*	XM_022979074.1	0	82.7	18.7
FAT17	fatty alcohol acetyltransferase	*Agrotis segetum*	KJ579213.1	0	87. 6	102.0
FAT18	fatty alcohol acetyltransferase	*Agrotis segetum*	KJ579224.1	0	80.8	161.8

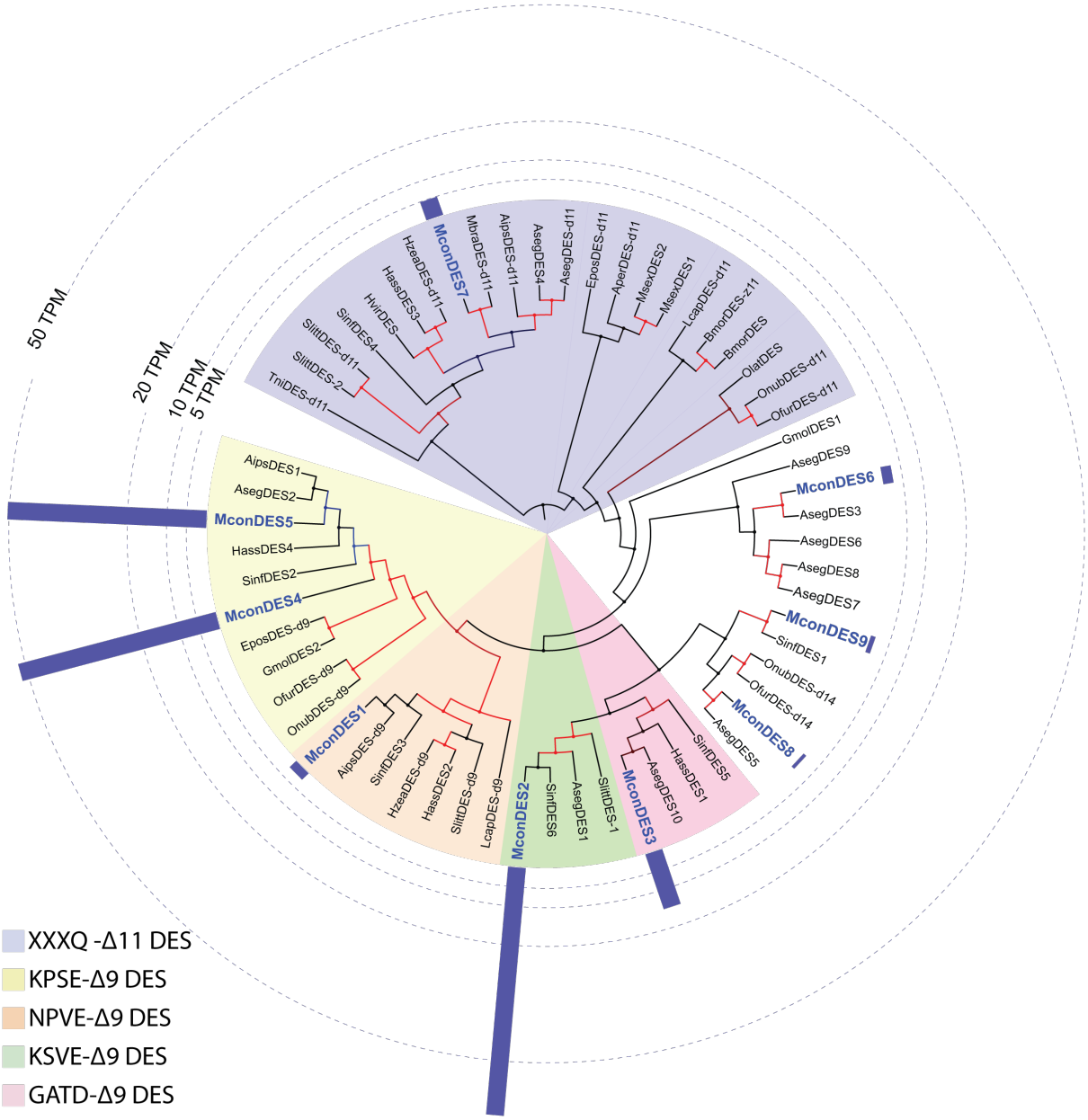
50 TPM
20 TPM
10 TPM
5 TPM
MconDES7
MconDES5
MconDES4
MconDES1
MconDES2
MconDES3
MconDES6
MconDES9
MconDES8
XXXQ -Δ11 DES
KPSE-Δ9 DES
NPVE-Δ9 DES
KSVE-Δ9 DES
GATD-Δ9 DES

Figure 2-6 Maximum likelihood tree for putative desaturases (DES) whose corresponding genes are expressed in BAW female pheromone gland. The candidate BAW desaturase (DES) proteins are indicated with dark blue text. Each subclass of DES proteins based on the four letter motif present within the sequence (XXXQ, KPSE, NPVE, KSVE, GATD) is indicated in the colour legend. The dark blue bars show relative transcript abundance from each desaturase gene in transcripts per million (TPM) values. Sequence abbreviations correspond to the following species names used in the analysis: Aips (*Agrotis ipsilon*), Aper (*Antheraea pernyi*), Aseg (*Agrotis segetum),* Asel (*Ascotis selenaria cretacea*), Avel (*Argyrotaenia velutinana*), Bmor (*Bombyx mori),* Cpar (*Choristoneura parallela*), Cpom (*Cydia pomonella*), Dpun (*Dendrolimus punctatus*), Epos (*Epiphyas postvittana*), Gmol (*Grapholita molesta*), Hass (*Helivoverpa assulta*), Hvir (*Heliothis virescens*), Hzea (*Helicoverpa zea*), Lcap (*Lampronia capitella*), Mbra (*Mamestra brassicae*), Mcon (*Mamestra configurata*), Msex (*Manduca sexta*), Ofur (*Ostrinia furnicalis*), Olat (*Ostrinia latipennis*), Sinf (*Sesamia inferens*), Slit (*Spodoptera littoralis*), Tni (*Trichoplusia ni*), Tpit (*Thaumetopoea pityocampa*). Branches supported by bootstrap values of 75% or higher are indicated in red. (See Table A-1; tab DES for the list of sequences and accession numbers).

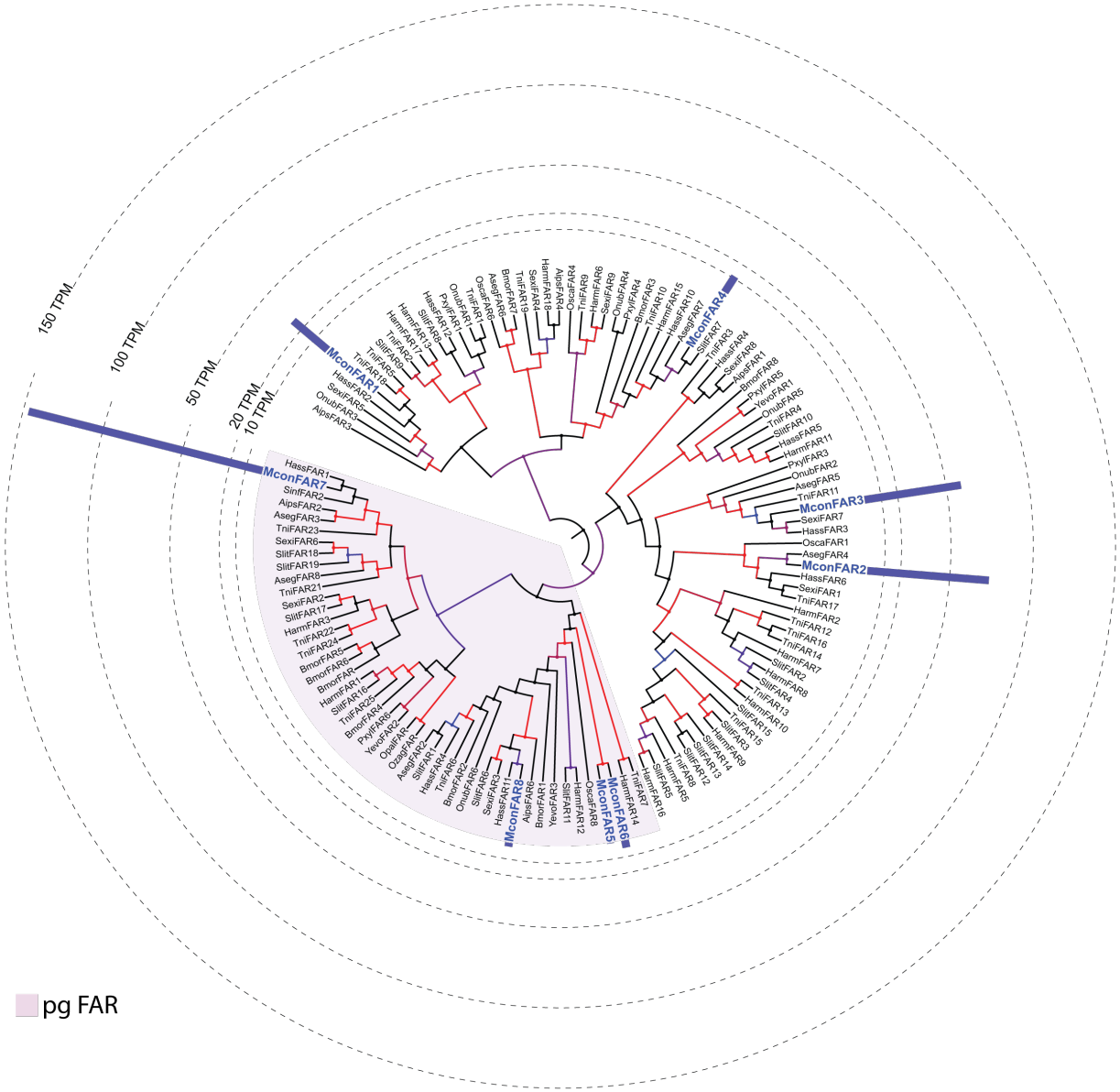
150 TPM
100 TPM
50 TPM
20 TPM
10 TPM
MconFAR1
MconFAR2
MconFAR3
MconFAR4
MconFAR5
MconFAR6
MconFAR7
MconFAR8
pg FAR

Figure 2-7 Maximum likelihood tree for putative BAW fatty acid reductase proteins in the female pheromone gland. The candidate BAW fatty-acid reductase (FAR) proteins are indicated with dark blue text. The dark blue bars show relative abundance of each reductase gene in transcripts per million (TPM). The pgFAR clade highlighted in light purple corresponds to a subset of FARs known to be involved in pheromone biosynthesis. Sequence abbreviations correspond to the following species names used in the analysis: Aips (Agrotis ipsilon), Aseg (*Agrotis segetum),* Bmor (*Bombyx mori),* Harm (*Helicoverpa armigera*), Hass (*Helivoverpa assulta*), Mcon (*Mamestra configurata*), Onub (Ostrinia *nubilalis*), Osca (*Ostrinia scapulalis*), Ozag (*Ostrinia zaguliaevi),* Pxyl (*Plutella xylostella*), Sexi (*Spodoptera exigua*), Slit (*Spodoptera litura*), Tni (*Trichoplusia ni*), Yevo (*Yponomeuta evonymellus*). Branches supported by bootstrap values of 75% or higher are indicated in red. (See Table A-1; tab FAR for the list of sequences and accession numbers).

pheromone gland had identical protein sequences to the transcripts retrieved from the whole-head BAW transcriptome. However, only three OBP genes, including *OBP3*, *OBP14* and *OBP23*, had notable expression levels with 398, 1278 and 398 TPM, respectively. MconOBP14 displayed the closest amino acid identity to OBPs from *Mythimna separata* (79%), *H. armigera* (71%) and *Agrotis ipsilon* (69%).

2.4 DISCUSSION

The chemical composition profile of the BAW female pheromone gland obtained from GC-MS analysis in this study was similar to previous results [Struble et al. 1984]. The two ion spectra not detected in this analysis, but reported by Struble et al, were Z7-12Ac and Z9-16Ac. In addition, the presence of Z11-16OH was not mentioned specifically in the GC-MS analysis reported previously, but this compound was listed as present in the BAW female pheromone gland extracts based on electroantennographic experiments with other species. [Struble et al. 1984]. Struble et al. (1984) also reported that addition of Z11-16OH to lures inhibited capture of BAW males in field trapping experiments. During the GC-MS analysis carried out in this study, I detected Z11-16OH and very small amounts of palmitic acid and octadecanol. The pheromone glands were excised from BAW females 2-3 hours into the scotophase and about 1-3 hours before their expected calling time. Thus, the presence of small amounts of all three precursors in the gland extracts observed in this study is not surprising. Large intraspecific variation was observed in the quantity of the major and minor pheromone components among individual females from each population; however, the mean amounts of pheromone components and the blend ratio were not significantly different. The blend ratios calculated from the amounts of the two pheromone components present in the gland extracts (AAFC-Saskatoon 30:1; AAFC-Davidson 29:1) were different from the blend ratio of 19:1 reported as the optimal attraction blend for use in pheromone trap lures in previous reports [Underhill et al. 1977a; b; Struble et al. 1984]. This difference between blend ratios from this study and the published literature may be accounted for by differences between the composition within the gland and the emissions [Hunt and Haynes 1990]. Male moths can detect a range of female-produced ratios, but the success of their flight to the female may be impacted by blend component ratios deviating from the mean population ratio [Willis and Baker 1988]. Thus, future analysis should investigate the composition of the emitted female blend rather than the composition of the pheromone gland. Together, these results suggest that BAW males should be attracted to an optimal median pheromone blend [Allison and

Cardé 2016b], but also that they have a wide response spectrum to accommodate the highly varied pheromone signal produced by con-specific females.

The importance of precise component production in the female pheromone glands has been extensively investigated [Löfstedt 1990]. Differences of only a few percent in component ratios in some moth species were found to have a pronounced impact on the male response [Cardé et al. 1977a]. For example, when pheromone components from glands of *Argyrotaenia velutinana* females were quantified, they were found to be precisely regulated with virtually no variation among individual gland extracts [Miller and Roelofs 1980]. In contrast, the attractive ratios produced can vary widely [Löfstedt et al. 1985a; Groot et al. 2014] in some species. In the field trapping experiments with *A. segetum* males, traps baited with a wide range of ratios of pheromones specific for this species were equally attractive to males, suggesting that female pheromone production is not as tightly-regulated as in *A. velutinana* [Löfstedt et al. 1985a]. Only a handful of studies to date address intraspecific variation in pheromone production [Miller and Roelofs 1980; Anglade et al. 1984; Löfstedt et al. 1985a; Duménil et al. 2014]. We currently do not understand how the inter-individual variation affects female competition for males or ability of males to successfully locate females. However, understanding of intraspecific variation is a prerequisite for studies on inter-population variation and how such variation arises.

As no differences were discovered in the chemical composition and overall blend ratios between the long-term reared colony and a geographic field population, the genetic analysis of the female pheromone gland tissue was carried out on AAFC-Saskatoon females only. The transcriptomic analysis of the pheromone gland tissue identified a subset of catalytic proteins as a starting point for future genetic and functional studies. The number of transcripts identified for each category is in agreement with the pheromone gland transcriptomes of *A. segetum* [Ding and Löfstedt 2015] and *S. litura* [Zhang et al. 2015b]. Although the TPM values reported for BAW transcript abundance are also within a similar range to values reported for homologous sequences in other species, direct comparison of values cannot be made as each study differs in the methods used for sample preparation, sequencing and bioinformatic analyses. Homology protein searches and gene expression analyses resulted in a list of putative BAW pheromone gland enzymes. Genes targeted for future functional analysis include those encoding four putative DESs, one ACO, two ACDs and three FARs. Among the four DESs, two were classified as NPVE-Δ9 DESs with their

respective genes being expressed at relatively higher levels than those encoding KPSE-Δ9 DES and LPAQ-Δ11 DES. All four of the DES enzymes have been shown to play an active role in pheromone biosynthesis in other species [Knipple et al. 2002]. However, the low abundance of transcripts encoding LPAQ-Δ11 DES, in contrast to the two Δ9 DESs is interesting, considering that the major pheromone component is a product of Δ11 rather than Δ9 DES.

In addition to the enzymes, two classes of odorant-binding proteins were detected in the pheromone gland. OBPs and CSPs were proposed to act as pheromone transport proteins in the pheromone gland, but their function has not been investigated [Jacquin-Joly et al. 2001]. In contrast to the bioinformatic analysis of the BAW whole-head transcriptome in which *MconCSP6* transcripts were detected in both males (2478 TPM) and females (1990 TPM), it was expressed at very low levels in the pheromone gland (49.4 TPM). Interestingly, transcripts from *MconCSP8* and *MconCSP9*, which were the two most abundant CSP transcripts in the BAW male and female whole-head transcriptomes, were also detected at comparable levels in the female pheromone gland; this suggests a more global role for these two proteins. *MconCSP1* and *MconCSP3* did not have significant expression in the head or antenna of BAW, but they had significant expression in the pheromone gland, 3233 and 6105 TPM, respectively. Transcripts from *MconCSP3* were the most abundant CSP transcripts in the BAW pheromone gland. This suggests that MconCSP3 may play a specific role in this tissue, although a global tissue screen is required to confirm this result. Whereas the transcript abundance for CSPs was comparable between the head and pheromone gland transcriptomes, OBP transcript abundance in the pheromone gland was considerably lower than in the whole-head. Among the nine OBP transcripts, only three were expressed at appreciable levels. *MconOBP14* was predominantly expressed in male (1335 TPM) and female (1244 TPM) antennal tissue and had a comparable expression in the pheromone gland (1278 TPM). Unlike CSP genes that have a global expression across different tissues, OBP genes are predominantly expressed in the antenna and insect reproductive tissues [Wanner et al. 2004; Pelosi et al. 2006; Brito et al. 2016; Pelosi et al. 2018]. Thus, MconOBP14 is an interesting candidate for future functional studies on pheromone transport in the moth female pheromone gland.

2.5 CONCLUSION

The chemical analysis of the BAW female pheromone gland extracts from the AAFC-Saskatoon and AAFC-Davidson populations did not show differences in the compounds present. Although, large inter-individual differences were detected within each population in terms of major and minor pheromone production, no statistically-significant differences were observed in the mean amounts of each pheromone component present or the mean blend ratios between the two populations. A pheromone gland transcriptome was assembled and mined for sequences corresponding to the main enzymes implicated in pheromone biosynthesis and carrier proteins involved in protein transport. The transcriptomic analysis resulted in identification of a subset of 70 sequences coding for enzymes from each step of the biosynthetic pathway along with estimates of gene expression. Phylogenetic analysis for DESs and FARs allowed for functional assignment of six DES transcripts and a major pheromone gland FAR. The data will aid in the design of future studies for lure composition and attractiveness, as well as molecular and functional analysis of the proteins involved in pheromone biosynthesis.

CHAPTER 3. GENETIC CHARACTERIZATION OF BAW MALE RESPONSE TO THE FEMALE-PRODUCED PHEROMONES

3.1 INTRODUCTION

An observation that even a single molecule of the female-produced pheromone can elicit flight orientation behaviour in males has inspired fundamental research on the insect olfactory system. Experimental evidence indicates that molecular events associated with reception at the periphery, rather than signal transduction and integration, determine the specificity and kinetics of the male response [Kaissling 2013]. These perireceptor events include uptake, binding, transport, receptor activation and pheromone removal [Leal 2013]. Several classes of proteins present either in the sensillar lymph or embedded in the membrane of the OSN mediate the steps leading to the translation of a chemical message into an electrical nerve impulse (Figure 3-1A). RNA-Seq analysis has expedited our ability to identify and characterize multiple classes of chemosensory genes involved in the perireceptor events. The available sequences for chemosensory genes from various species have accumulated rapidly in sequence repositories; however, our ability to correlate the identified sequences to the function and mechanism of the insect olfactory system remains limited.

3.1.1 Soluble binding proteins

3.1.1.1 Odorant binding proteins (OBPs)

The first chemosensory event involves the contact and uptake of a volatile odorant from the environment and its transport or diffusion through the hydrophilic sensillar lymph [Brito et al. 2016]. Two classes of proteins, which can mediate this process, were found in the chemosensory organs of insects; these include odorant binding proteins (OBPs) [Pelosi et al. 2006; 2014], and the more recently-discovered chemosensory proteins (CSPs) (Figure 3-1A) [Wanner et al. 2004]. Generally, OBPs are found in the lymph of chemosensory sensilla, but they are also found in

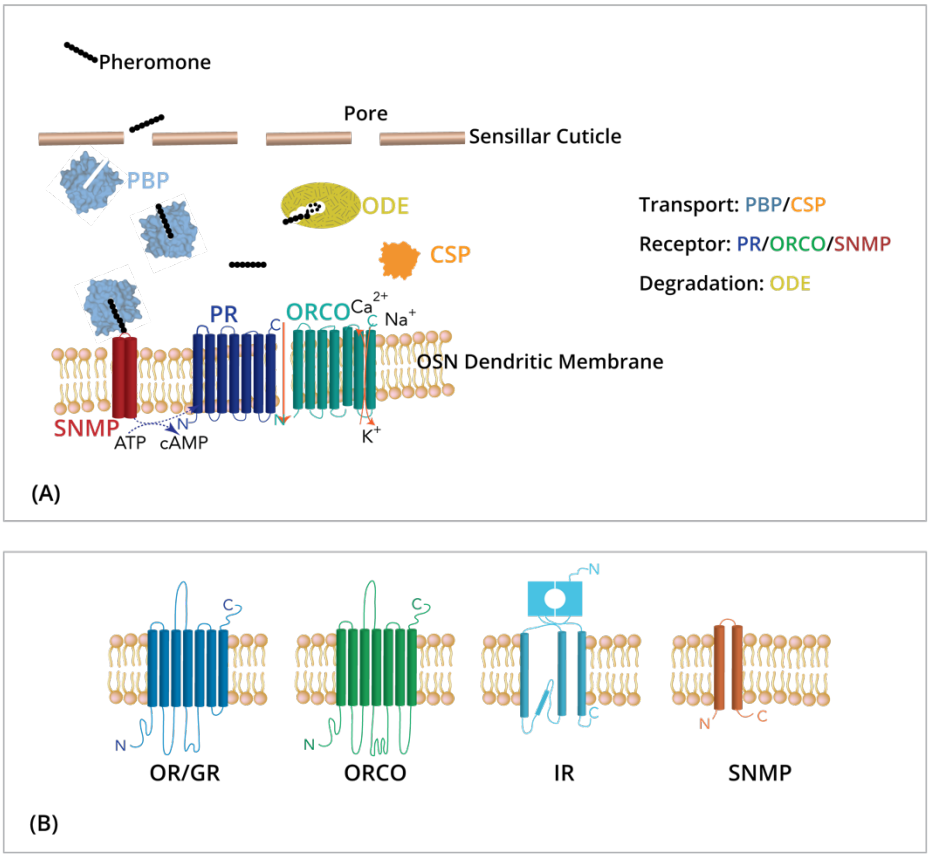

Figure 3-1 Insect chemosensory proteins. **(A)** Graphical overview of the different protein classes mediating perireceptor events near the olfactory sensory neuron (OSN) dendritic membrane in the trichoid sensillum of a male moth. Pheromone-binding proteins (PBPs-blue) and chemosensory proteins (CSPs-orange) bind and transport the hydrophobic pheromone compounds across the hydrophilic sensillar lymph. Sensory neuron membrane proteins (SNMPs-red) are implicated in aiding the transfer of the pheromone from the PBP or CSP to the highly specific pheromone receptor protein (PR). PR co-dimerize with olfactory co-receptor (ORCO) to form ligand-gated ion channels. Any unbound pheromone must be removed from the sensillar lymph to maintain the sensitivity and responsiveness of the system. Odorant-degrading enzymes have been implicated in this removal process. Modified and adapted from Gould et al. (2017) **(B)** Secondary structure prediction models for the different classes of transmembrane proteins. Olfactory receptors (ORs), gustatory receptors (GRs) and ORCO have a similar 7-transmembrane domain structure with the N-terminus of the protein located intracellularly. Ionotropic receptors (IRs) are similar in structure to ionotropic glutamate receptors (iGluRs) with bipartite ligand binding domains separated by an ion channel domain. SNMPs contain two transmembrane domains and belong to a class of lipoprotein binding proteins. Figure based on information from de Bruyne and Baker (2008).

tissues, such as mouthparts [Ishida et al. 2013], pheromone producing glands [Li et al. 2008] and reproductive organs [Sun et al. 2012]. OBPs are compact (120-150 aa), water-soluble, extracellular proteins characterized by a conserved 6-cysteine motif forming three interlocking disulfide bridges [Tegoni et al. 2004]. OBPs that contain either fewer or more than the 6 conserved cysteines have also been identified and, thus, the number of cysteine residues is currently used as means of OBP classification [Brito et al. 2016]. In chemosensory sensilla, OBPs are expressed in non-neuronal support cells (trichogen and techogen) and are localized, often in very high concentrations, in the extracellular space surrounding the sensory dendrites [Steinbrecht et al. 1995; Jacquin-Joly et al. 2001; Maida et al. 2003; Nardi et al. 2003]. The majority of our current knowledge on OBP structure and function comes from studies on pheromone-binding proteins (PBPs) and general odorant-binding proteins (GOBPs) [Vogt et al. 2015]. PBPs are present in pheromone-specific sensilla trichodea that respond to pheromones, whereas GOBPs are present in sensilla basicona that respond to plant volatiles and other insect-relevant odours [Leal 2013; Vogt et al. 2015]. Extensive structural and binding studies carried out with PBP from a number of insect species confirm that these proteins act as carriers for odour molecules and contribute to the specificity and sensitivity of the insect olfactory system; however, the details of their mode of action remain controversial [Pelosi et al. 2006].

3.1.1.2 Chemosensory proteins (CSPs)

CSPs are expressed more broadly across a variety of tissues, including the gut [Ribeiro et al. 2014], legs, wings [Wanner et al. 2004] and reproductive tissues [Picimbon et al. 2001], as well as the chemosensory organs [Mosbah et al. 2003; Pelosi et al. 2014]. CSPs are smaller (100 amino acid) water-soluble polypeptides that contain a 4-cysteine conserved motif forming two disulfide bridges [Angeli et al. 1999]. Protein alignments for CSPs from six different insect orders indicated three conserved motifs at the N-terminal YTTKYDN(V/I)(N/D)(L/V)DEIL, central DGKELKXX(I/L)PDAL and C-terminal KYDP regions [Wanner et al. 2004]. However, in several orders, including Lepidoptera, CSP sequences show various degrees of divergence within these motifs. The diverse pattern of CSP expression in non-chemosensory tissues suggests multiple functions for this class of proteins. The extent to which CSPs contribute to the perireceptor events and their mechanism of action at the antenna is currently unknown.

3.1.2 Receptor proteins

3.1.2.1 Olfactory receptors (ORs)

The second event in chemoreception is marked by the interaction of either the ligand or ligand:OBP complex with the membrane-bound olfactory receptor (OR) proteins that act as the bridge between the extracellular signal and the intracellular neurological response (Figure 3-1A and B) [Vogt and Chertemps 2005]. The contact of the odorant molecule with the OR, whether alone or in an OBP:ligand complex, evokes a change in the dendritic transmembrane potential called the receptor potential [Kaissling 2014]. Insect ORs are characterized by 7-transmembrane domains (TMDs) [Wicher et al. 2008; Sato et al. 2008] and an inverted protein topology compared to vertebrate ORs wherein the amino terminus is located intracellularly (Figure 3-1 B) [Benton et al. 2006]. Insect ORs are thought to have evolved from a distant lineage of insect gustatory receptors [Robertson et al. 2003; Gardiner et al. 2009] and are not related to the vertebrate G-protein coupled receptors (GCPR) that initially served as basis for insect OR identification [Benton et al. 2006]. Generally, each OSN expresses one OR [Hallem et al. 2004]; however, exceptions to this general rule have been found in moths [Koutroumpa and Karpati 2014]. Co-expression of OR genes within a single OSN is thought to affect the tuning of the OSN [Andersson et al. 2015]. In the model species *O. nubilalis*, specialized OSN in sensilla trichoidea have been found to co-express up to five different OR genes. An OSN expressing multiple ORs is broadly tuned to a variety of antagonistic pheromone compounds and was suggested to play a role in inhibition of cross-attraction to hetero-specific and sympatric species [Koutroumpa and Karpati 2014]. The mechanism controlling the co-expression of several OR genes within the same OSN is currently unknown. In *Anopheles gambiae*, OR genes co-expressed within the same OSN were shown to be clustered in the genome [Karner et al. 2015b]. It is unknown if similar clustering is present in moths.

ORs require hetero-dimerization with a highly conserved insect co-receptor called ORCO [Benton et al. 2007] for their localization to the OSN dendritic membrane and activity [Vosshall and Hansson 2011]. Although ORCO does not share significant sequence similarity to other ORs, it is itself highly conserved across insect species [Stengl and Funk 2013]. ORCO is ubiquitously-expressed in the majority of OSNs expressing ORs, and it has an inverted membrane topology like canonical ORs [Lundin et al. 2007]. Unlike ORs, ORCO does not participate in ligand binding [Wicher et al. 2008; Sato et al. 2008], but its absence in OSN cells

impairs ligand detection by the ORs and, thus, the signal transduction mechanism [Larsson et al. 2004]. The function of OR/ORCO complexes has been controversial due to conflicting reports regarding their mode of action in signal transduction [Fleischer et al. 2018]. In one scenario, OR/ORCO complexes function as odorant-activated (ligand-gated) ionotropic channels with both proteins contributing to the permeability of the ion channel [Sato et al. 2008]. However, in some species, the OR can also function as a non-canonical GPCRs via G-protein cascades [Talluri et al. 1995; Laue et al. 1997; Jacquin-Joly et al. 2002; Miura et al. 2005]. As a third option and in the absence of OR, ORCO units homo-dimerize to form spontaneously-opening cation channels permeable to Ca^{2+},Na^{+} and K^{+} cations [Wicher et al. 2008; Jones et al. 2011]. This suggests that ORCO homo-dimers may contribute to the spontaneous electrical activity observed [Hallem et al. 2004; Joseph et al. 2012]. In moths, a dual-activation model of a fast ionotropic and slower metabotropic (G-protein) activation has been proposed [Wicher et al. 2008]. Utilization of both activation pathways in parallel in flying moths makes sense in terms of satisfying the requirement for sensitivity and specificity in following a rapidly changing odour stimulus, such as a conspecific-produced pheromone.

Functional studies indicate that insect ORs respond to a range of odorants and that one odorant can activate multiple ORs [Hallem et al. 2004]. This type of overlap in detection spectra is observed for general odorants and is consistent with the principles of combinatorial coding of the odours present in vertebrates [Touhara and Vosshall 2009]. However, pheromones have been shown to activate a narrowly-tuned subset of ORs leading to activation of dedicated neural pathways often referred to as labeled-line pathways [Berg et al. 2014; Zhang et al. 2015a]. This specialized subset of ORs forms a distinct clade of conserved pheromone receptors (PRs) [Zhang and Löfstedt 2015] among the large and highly-divergent family of insect ORs [Krieger et al. 2004; 2005; Wanner et al. 2010]. The high degree of conservation among PRs suggests strong negative selection pressure on this subset of receptors [Zhang and Löfstedt 2015] and it may correspond to the high degree of similarity of the pheromone compounds utilized by the majority of lepidopteran insects [Yew and Chung 2015]. In addition to ORs, two other receptor classes are expressed within the antennal tissue. Although not implicated in pheromone reception, these receptor families also play a role in detection of chemical compounds.

3.1.2.2 Gustatory receptors (GRs)

Insect ORs are thought to have evolved from a distant lineage of insect gustatory receptors (GRs) [Robertson et al. 2003; Gardiner et al. 2009]. GRs are expressed in gustatory sensory neurons (GSN) localized to several tissues, including mouthparts, tarsi, wings and ovipositors (Figure 3-1 B) [Jørgensen et al. 2006; Hallem et al. 2006]. Although the lepidopteran antenna's primary function is as an olfactory organ, it also contains GSNs expressing genes encoding GRs involved in olfactory processes [Hallem et al. 2006; Jacquin-Joly et al. 2012]. Despite considerable sequence divergence between ORs and GRs, GRs are also membrane-bound proteins containing seven TMDs [Agnihotri et al. 2016]. A subset of GRs have been shown to detect CO_2 and in *D. melanogaster* a specific GR is implicated in pheromone detection [Jones et al. 2007; Watanabe et al. 2011]. Recent studies on two GRs in *B. mori* provided evidence for a reverse topology of GRs similar to ORs [Zhang et al. 2011]. Unlike ORs, GRs detect soluble chemicals, such as sugars, salts, inositol and plant alkaloids, via contact with the substrate and their function is not dependent on hetero-dimerization with ORCO [Benton et al. 2006; Fleischer et al. 2018].

3.1.2.3 Ionotropic receptors (IRs)

Insect IRs were identified through a bioinformatics approach in *D. melanogaster* and form a divergent subfamily of ionotropic glutamate receptors (iGluRs) with unique chemosensory functions and are not related to ORs and GRs [Benton et al. 2009]. IRs are similar to iGluRs in their molecular organization with bipartite ligand-binding domains separated by an ion channel domain; however, they lack the characteristic glutamate-interacting residues (Figure 3-1B) [Rytz et al. 2013]. In *D. melanogaster*, IRs are exclusively expressed in sensilla coeloconica and have been confirmed to play an olfactory role in detecting acids, amines and aldehydes [Silbering et al. 2011]. Orthologues of the majority of antennal IRs from *D. melanogaster* have been identified in lepidopterans [Olivier et al. 2011; Xu et al. 2015]. However, lepidopteran-specific IRs were also identified, but their function is currently unknown [Xu et al. 2015].

3.1.2.4 Sensory neuron membrane proteins (SNMPs)

In addition to the three classes of receptors, another membrane protein class identified as sensory neuron membrane proteins (SNMPs) plays a role in insect chemoreception. SNMPs contain two TMDs and belong to a family of lipoprotein-binding proteins that are expressed in sensilla implicated in pheromone detection (Figure 2-1A, B) [Benton et al. 2007; Jin et al. 2008]. In

Heliothis virescens, SNMP1 was required for the activation of PR but not necessary for activation of general ORs responding to common plant volatiles [Benton 2009]. In *Antheraea polyphemus*, *H. virescens* and *Spodoptera exigua*, SNMP1 was found in the dendritic membrane of OSNs, but SNMP2 was localized to OSN support cells [Forstner et al. 2008; Liu et al. 2014]. The role of SNMPs in lepidopteran pheromone detection is currently unknown [Fleischer et al. 2018]; however, significantly higher abundance of SNMP1 in dendritic membranes of OSNs tuned to pheromones and their co-localization with PRs is a compelling argument in favour of their participation in pheromone-mediated molecular events.

3.1.3 Odorant-degrading enzymes

To generate the fast, sensory response required for modulation of flight, a signal termination mechanism must exist that clears out odour stimuli and resets the detection unit for the next round of sensing. Although the precise mechanism of signal termination is not fully understood, two different hypotheses have been proposed. In the first hypothesis, pheromone deactivation was postulated to be a non-enzymatic reaction [Kaissling 1998b; 2001]. During deactivation, the odour molecule remains chemically intact; however, it is prevented from continual excitation of the receptor either via hypothetical "scavenger" enzyme or conformational changes in the PBP or PBP:OR interaction [Kaissling 2009]. In a competing view, the degradation and clearing of the volatile compound is carried out by odorant-degrading enzymes (ODEs) (Figure 3-1 A) [Ishida and Leal 2005; Leal et al. 2005; Ishida and Leal 2008]. A small number of ODEs have been identified in the insect antenna, including carboxylesterases (CXE), antennal oxidases (AOX), cytochrome P450 oxidases (450CYPs), glutathione-S-transferases (GSTs) and fatty acyl reductases (FARs) shown to degrade a volatile odour molecule [Ishida and Leal 2005; Chertemps et al. 2012; Choo et al. 2013; Durand et al. 2014]. As compared to pheromone binding and receptor activation, much less attention has been focused on the signal deactivation at the periphery [Leal 2013]. However, understanding the molecular mechanism of signal deactivation is of particular importance to the development of effective pest control strategies.

3.1.4 Investigation of genetic variation within chemosensory genes

3.1.4.1 KisSplice algorithm for de novo variant calling from RNA-Seq reads

The rapid evolution of RNA-Seq technologies has inspired the development of tools for downstream analysis of the transcriptome content. In addition to the transcriptomic pipeline

described in Chapter 2, genetic variant identification has been made possible with a KisSplice algorithm capable of predicting alternative splice sites (ASS) and single nucleotide polymorphisms (SNPs) directly from RNA-Seq reads and without the need for a reference genome [Sacomoto et al. 2012]. In this approach, only SNPs from transcribed regions can be identified; however, typically these SNPs are thought to have direct functional impact. Since the sequencing libraries are often generated from a pool of individuals, genotypes cannot be derived from the KisSplice approach [Sacomoto et al. 2012; Lopez-Maestre et al. 2016]. Instead, allele frequency in the population, also referred to as allelotype, is reported. Although individual SNPs are deemed less informative than multi-allelic markers, their identification from RNA-Seq libraries is rapid and has a low frequency of errors [Sacomoto et al. 2012].

KisSplice allows for *de novo* calling of SNPs from RNA-Seq reads, SNP annotation and SNP mapping onto genes of interest [Sacomoto et al. 2012; Lopez-Maestre et al. 2016]. Differential analysis of SNPs is also possible, although not applied in the work presented in this chapter. In brief, the KisSplice algorithm, like the Trinity *de novo* transcriptome assembler, utilizes a de Bruijn graph (DBG). The KisSplice algorithm takes advantage of the characteristic DBG structure feature called a "bubble" that is generated by sequence differences between the forward and reverse paths of the graph (Figure 3-2A-D). In contrast to the transcriptome assembly process, which aims to resolve and linearize bubbles with the aim of producing long sequence contigs, KisSplice utilizes the DBG structures to identify sites of putative genetic variation. Variation in the transcribed portion of the genome can arise from alternative splicing, SNPs and the presence of tandem repeats. The shape, as well as size, of the DBG bubbles and read coverage of the forward and reverse paths was shown to correlate to the type of polymorphism present [Sacomoto et al. 2012; Lopez-Maestre et al. 2016]. Large bubbles, for which the length of the forward and reverse sequence path is different, have been correlated to alternative-splicing sites or tandem repeats. Small bubbles, for which the length of the forward and reverse path is equal, typically correspond to SNPs, but may also indicate sequencing errors. However, sequencing errors are often characterized by poor read coverage of one of the sequence paths in the DBG bubble and, thus, can be distinguished from SNPs for which both paths have similar read coverage. The typical KisSplice analysis has three distinct stages. During the first stage, the DBG is built from RNA-Seq reads. During the second stage, all bubbles are enumerated and assigned based

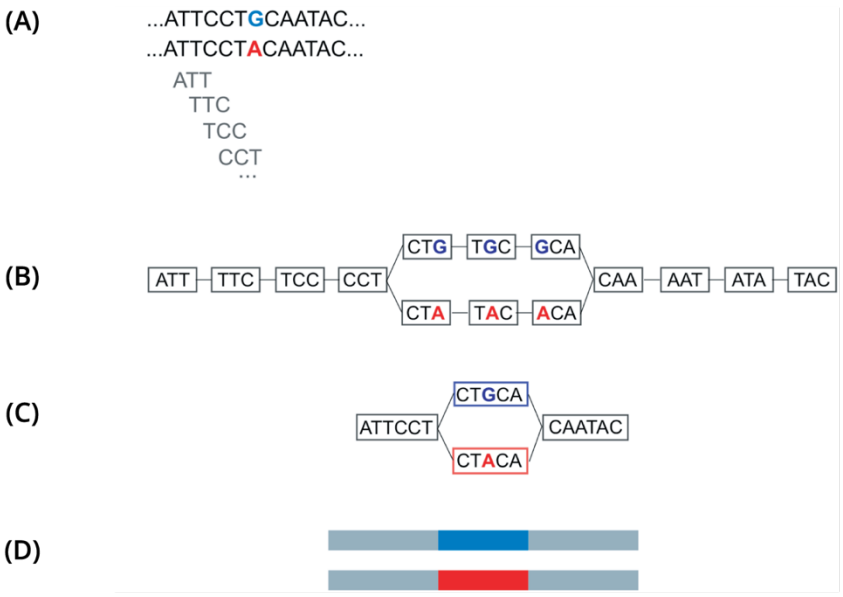

Figure 3-2 Graphical representation of a SNP as de Bruijn graph "bubble" structure. **(A)** an example of a SNP present in 2 alleles in RNA-Seq data. **(B)** The de Bruijn graph derived from the RNA-Seq data. The example illustrates a case in which *k*-mer size is set to 3 for simplicity. KisSplice algorithm utilizes *k*=41 as default value. **(C)** A compressed de Bruijn graph can be obtained by merging nodes with a single outgoing edge with nodes with a single incoming edge. No data is lost doing the compression step. **(D)** The two paths in the compressed de Bruijn graph correspond to the two alleles of the SNP. Adapted from Lopez-Maestre et al. (2016).

on their structure to alternative splice sites, SNPs or bubbles that cannot be assigned to either of the two categories. In the last stage, the reads are mapped to each path of each bubble to quantify the frequency of each variant. The predicted SNPs are mapped onto Trinity-predicted transcripts with BLAT or similar platform designed for alignment of very short sequences. The coding potential of the transcripts is predetermined with Transdecoder and, thus, each SNP can be classified as either located within an open reading frame (ORF) or not. SNPs located within ORFs are classified as either synonymous or non-synonymous, with non-synonymous SNPs potentially affecting the protein structure and function. A major advantage of calling the SNPs directly from RNA-Seq reads is that the analysis avoids biases associated with reference-guided SNP identification [Sacomoto et al. 2012].

3.1.4.2 Genetic variation among BAW populations

Collection of egg masses or pupae during the last BAW outbreak (2011-2014) from two distinct locations in western Canada presented a rare opportunity to investigate the genetic basis for olfactory processes in the context of pheromone communication in BAW field populations. Focus on the pheromone channel is warranted by recent findings suggesting that genetic differentiation may exist at only a few loci coding for high impact genes related to the phenotypic variants observed [Lassance 2016; Coates et al. 2018]. In determining the genetic diversity among geographic populations, markers associated with strongly-selected loci coding for species-specific traits may be capable of defining genetic lineages [Coates et al. 2018]. The study in Chapter 3 summarizes my findings with respect to the molecular architecture underlying pheromone reception in males and the level of associated genetic variation among three BAW populations. The identification and characterization of the different chemosensory gene families is carried out based on comparative analysis with other closely-related lepidopteran species, as well as differential gene expression between BAW males and females. The genetic variation analysis provides further insights into which chemosensory genes are under strong, stabilizing selection, and which are candidates for loci amenable to differentiation within the pheromone reception system.

3.2 MATERIALS AND METHODS

3.2.1 Insect collection and rearing

To establish laboratory colonies, BAW egg masses or pupae collected in 2013 from canola fields near Davidson, SK [(N51.29987 W105.71261); AAFC-Davidson] and Vegreville, AB [(N53.44340 W112.36830); AAFC-Vegreville] were reared to adult moths under a modified rearing protocol outlined in Chapter 2. In addition, individuals from a long-term (35-year old), laboratory colony at AAFC-Saskatoon were also used in this study. Once colonies were established, rearing was carried out at 22°C under a 16:8 light:dark cycle and according to standard protocol outlined in Chapter 2 [Bucher and Bracken 1976]. The pupae were sexed and transferred to separate cages prior to emergence for assignment to mating groups.

3.2.2 RNA isolation, library construction and sequencing

Antennae and heads were collected from second generation AAFC-Davidson (n=20 males; 19 females) and AAFC-Vegreville (n=26 males; 25 females) BAW populations, as well as from

individuals from the long-term AAFC-Saskatoon colony (n=20 males; 20 females). All tissue collections were carried out on unmated adult male and female insects 48 h post-eclosion. The antennae were excised at the pedicel, whereas the heads were severed between the ocellus and patagium. The tissues (head and antennae separately) were transferred immediately upon excision into TRIzol (Invitrogen, Carlsbad, USA). RNA extraction and determination of concentration were carried out according to the protocol outlined in Chapter 2 (Section 2.2.6). Total RNA for each tissue type (4 μg at 40 ng/μL) was submitted for cDNA library construction (Illumina TruSeq mRNA stranded library preparation) and Illumina 2500 Hi-Seq paired-end sequencing to the National Research Council of Canada, Saskatoon, Saskatchewan.

3.2.3 Transcriptome assembly and annotation

Quality-trimming of raw read data sets was performed with Trimmomatic v0.36 on each individual library [Bolger et al. 2014]. Quality-trimming and removal of sequencing adapters was carried out with the following Trimmomatic settings: LEADING:5, TRAILING:5, SLIDINGWINDOW:4:15, MINLEN:36, PHRED:5. The 12 read libraries were combined to obtain a reference read library containing 181,128,957 processed reads representing the whole BAW head transcriptome. The quality of the reads resulting from Trimmomatic processing was assessed with FastQC [Conesa et al. 2016]. *De novo* assembly was performed on the combined read library with Trinity v.2.1.1 (kmer size of 25, min_kmer_cov set to 2 and all other parameters set to default) [Grabherr et al. 2011; Haas et al. 2013]. The overall transcriptome assembly quality was assessed with Transrate v1.0.3 software [Smith-Unna et al. 2016]. The RNA-Seq read representation analysis was performed with Bowtie v1.1.2 [Langmead and Salzberg 2012]. BUSCO v3 (Benchmarking Universal Single Copy Orthologs) (www. Busco.ezlab.org) analysis was carried out using a virtual machine Busco_3_Ubuntu_VM [Simão et al. 2015]. The analysis was performed using the Arthropoda (ap;1066), Eukaryota (ek; 303) and Insecta (it; 1658) data sets.

3.2.4 Annotation and representation of full-length reconstructed protein-coding genes.

The transcriptome assembly was scanned for open reading frames (ORFs) with Transdecoder v2.0.1 with minimum peptide length set to a default value of 100 amino acids [Haas et al. 2013]. Gene function was annotated by homology searches with Blast2Go v5.1 and Trinotate v3.0.0 against the NCBI non-redundant protein (Nr) database, NCBI nucleotide (Nt) database, Swiss-

Prot protein database, euKaryotic Orthologous Groups (KOG), Kyoto Encyclopedia of Genes and Genomes (KEGG), Gene Ontology (GO) and Protein family (Pfam) database [Conesa et al. 2005]. Targeted searches using BLAST were carried out on the ORF subset of the BAW whole-head transcriptome with a manually-created list of orthologous sequences of genes of interest from *Agrotis ipsilon, Agrotis segetum, Antheraea polyphemus, Amyelois transitella, Bombyx mori, Conogethes punctiferalis, Diaphania indica, Helicoverpa armigera, Helicoverpa assulta, Heliothis virescens, Helicoverpa zea, Manduca sexta, Mamestra brassicae, Ostrinia furnicalis, Ostrinia latipennis, Ostrinia nubilalis, Ostrinia scapulalis, Plutella xylostella, Sesamia inferens, Sesamia nonagroides, Spodoptera littoralis, Spodoptera litura* and *Spodoptera exigua* (Table A-1). Lepidopteran chemosensory protein sequences were obtained from searches in the NCBI (https://blast.ncbi.nlm.nih.gov/Blast.cgi), Butterfly Genome (http://butterflygenome.org/) and LepidoDB databases (https://bipaa.genouest.org/is/lepidodb/). Similarity searches using tBLASTn (E-value $1e^{-10}$ and Blosum62 Matrix) against a nucleotide database containing output ORF sequences from Transdecoder were carried out with CLC Genomics Workbench (Qiagen Bioinformatics; versions v9.0-current) (Table A-3). Transmembrane predictions were conducted with TOPCONS v2.0 and visualized with PROTTER v1.0 [Bernsel et al. 2009; Omasits et al. 2013].

3.2.5 Abundance estimation

Gene expression levels for each sample were estimated using RSEM v1.2.15 [Li and Dewey 2011]. Gene expression was measured as expected number of transcripts per million (TPM) normalized for gene length and sequencing depth. Since the sum of all TPM values for each tissue library is the same, this approach offers a plausible platform for comparing the proportion of reads that mapped to a gene of interest in each sample [Conesa et al. 2016]. RSEM was carried out on the whole-head reference transcriptome as well as four read libraries including male antenna only, male head only, female antenna only and female head only. A custom script was used to extract TPM values from RSEM results for each class of putative chemosensory genes (Table A-3).

3.2.6 Phylogenetic analyses

Phylogenetic analysis was carried out according to methods outlined in Chapter 2 (Section 2.2.9)

3.2.7 Draft genome mapping

The putative chemosensory gene sequences were mapped onto the BAW draft genome v1 prepared in-house and deposited in the NCBI genome database (https://www.ncbi.nlm.nih.gov/genome/; accession NDFZ00000000).

3.2.8 Digital droplet PCR (ddPCR)

A subset of genes encoding BAW ORs was selected for expression analysis with ddPCR. Primers and probes were designed using the Integrated DNA Technologies (www.idtdna.com) primer Quest Tool and purchased from IDT (Table A-4). One µg of total RNA (same material as used for Illumina sequencing) was reverse-transcribed using the qScript kit (BioRad Laboratories Inc., Mississauga, Ontario, Canada). ddPCR was performed using a QX100 droplet generator and droplet reader (BioRad Laboratories Inc, Mississauga, Ontario, Canada). Each PCR reaction was carried out in a 20 µL volume containing 10 µL of 2X ddPCR Supermix, 2uL of cDNA, 1µL of primers, 1 µL of 5'-FAM labeled probe and 7 µL of nuclease free water. The reactions were amplified on a C1000 Touch Thermal Cycler (BioRad Laboratories, Mississauga, Ontario, Canada) with 50 cycles, starting annealing temperature of 58.3ºC and temperature ramp of 2ºC/s for 60 seconds. The ddPCR results were processed in QuantaSoft (BioRad Laboratories, Mississauga, Ontario, Canada). Three control sequences, *EF-1* (elongation factor 1), *RPS13* (ribosomal protein synthesis 13), and *RPS20* (ribosomal protein synthesis 20), were included as controls for each amplification experiment.

3.2.9 Single nucleotide polymorphism (SNP) analysis

The KisSplice v2.4.0 program was used for SNP analysis [Sacomoto et al. 2012; Lopez-Maestre et al. 2016]. Briefly, KisSplice was used to call SNPs directly from reads and the resulting SNP predictions were mapped back to the reference transcriptome. The coding potential of each SNP was determined by cross-referencing the aligned SNPs with the Transdecoder output. The frequency of each SNP was evaluated based on read sequence alignments. A custom script was used to search the KisSplice output file and identify SNPs contained within the chemosensory gene sequences. Only SNPs with read coverage of 10 reads or more were considered significant. The raw SNP data is provided in Table A-3 listing allelic frequencies and read counts for the forward and reverse read libraries. Allelic frequency, reported as percentage for each population,

is provided as a statistical average of the allelic frequency for the forward and reverse read libraries.

3.3 RESULTS

3.3.1 Transcriptome assemblies

Illumina RNA-Seq from the 12 tissue libraries resulted in 190,365,892 raw reads. The average library size for the antennal tissues and head tissue was 15.3 million (SE ± 0.9 million) and 16.4 million (SE ± 0.9 million) reads, respectively. After processing and trimming the individual libraries, the libraries were catenated to give a BAW reference whole-head data set containing 181,128,957 reads with 99.8 % of the reads determined as Q20 (high quality reads) via FastQC analysis.

The Trinity assembly of the BAW whole-head transcriptome produced 180,224 transcripts and 144,364 unigenes (Table 3-1). Standard assembly statistics provided N50 length estimates for unigenes and transcripts as 884 and 1,584 base pairs, respectively. Alignment of the clean reads to the Trinity assembly with Bowtie indicated that 95.5% of the clean reads aligned back to the transcriptome assembly with 77.5% being properly paired, 18.0% being improperly paired reads and 4.5% being either only forward or reverse reads (Table 3-2 and 3-3). In addition, the quality of the transcriptome was evaluated with Transrate. The BUSCO assessment results for the whole-head transcriptome indicated 98.7% completeness for the Arthropoda set and 97.3% completeness for the Insecta set.

Table 3–1 Trinity assembly statistics for whole-head BAW transcriptome.

	Total contigs	**Min Contig Length**	**Mean Contig Length**	**Median Contig Length**	**Max Contig Length**	**N50**
Trinity transcripts	180,224	201	785	364	17,953	1,584
Trinity "unigenes"	144,364	201	607	328	17,953	884

[1] Contig length and N50 statistic values are expressed as a number of base pairs (bp)

Table 3–2 Read counts and RSEM RNA-Seq statistics for individual and combined tissue libraries.

Library Name	Raw Reads	Clean Reads	Aligned Reads[1]	%[2]	Not Aligned Reads[1]	%[2]
AAFC-Saskatoon Female Antenna	17,079,845	16,333,909	13,949,023	85	2,384,886	15
AAFC-Saskatoon Female Head	15,850,132	15,026,400	12,922,704	86	1,780,738	14
AAFC-Saskatoon Male Antenna	13,308,364	12,719,560	10,770,480	85	1,949,080	15
AAFC-Saskatoon Male Head	15,260,447	14,475,518	12,883,211	89	1,592,307	11
AAFC-Davidson Female Antenna	1,4491,547	13,863,906	11,391,437	82	2,472,469	18
AAFC-Davidson Female Head	16,043,126	15,264,360	12,974,706	85	2,289,654	15
AAFC-Davidson Male Antenna	13,180,135	12,588,492	10,300,322	82	2,288,170	18
AAFC-Davidson Male Head	17,208,357	16,343,532	14,055,437	86	2,288,094	14
AAFC-Vegreville Female Antenna	15,336,546	14,621,804	11,961,153	82	2,660,651	18
AAFC-Vegreville Female Head	18,217,121	17,115,282	14,719,142	86	2,396,139	14
AAFC-Vegreville Male Antenna	18,539,622	17,705,069	14,429,631	81	3,275,438	19
AAFC-Vegreville Male Head	15,850,650	15,071,125	12,961,167	86	2,109,958	14
Females Whole-Head	97,018,317	92,225,661	78,600,045	85	13,625,616	15
Males Whole-Head	93,347,575	88,903,296	75,901,668	85	13,001,628	15
Combined Whole-Head	190,365,892	181,128,957	164,831,473	91	16,296,979	9

[1] reads aligned to the transcriptome with Bowtie algorithm during transcript quantification
[2] % value corresponds to a percentage of reads aligned or reads not aligned to the transcriptome

Table 3–3 Bowtie read coverage assessment of the whole-head transcriptome

	Number of reads	%[1]
Proper pairs	255,516,080	77.5
Improper pairs	59,485,666	18.0
Left only	7,350,361	2.23
Right only	7,330,600	2.22
Total aligned	329,682,907	

[1] % value corresponds to a percentage of total clean reads which aligned to the transcriptome

Table 3–4 Summary of gene annotation results for the whole-head transcriptome.

	Number of Unigenes	
Total 'trinity' transcripts	180, 224	
Total unigenes	144,364	
Open reading frames	35,481	
Annotated with		**%[1]**
NCBI Nr	48,550	34
Swiss-Prot	20,694	14
Pfam	15,922	11
TMHMM	3,924	2.7
KEGG	2,650	1.8
KOG	2,438	1.7
GO	3,566	2.5

[1] % value corresponds to a percentage of total unigenes obtained during the Trinity transcriptome assembly

Blast2Go and Trinotate platforms were used to assess the whole-head transcriptome gene content (Table 3-4). The BLASTX algorithm applied against the NCBI non-redundant (nr) protein database (cut-off E-value of 10^{-10}) resulted in 48,550 hits (33.6% of the total number of unigenes). Homology analysis identified *A. transitella* (19.5%), *B. mori* (15.8%) and *P. machaon* (8.3%) as the top three most closely-related species in BLASTX results. Searches performed against the UniProtKB/SwissProt database produced 20,694 hits and searches against the Pfam and TMHMM databases resulted in 15,922 and 3,924 hits, respectively. GO annotation assigned GO terms to 37,398 (26%) of the 144,427 unigenes. The assigned unigenes were categorized into 59 GO terms, including 28 (47%) biological process terms, 14 (24%) molecular function terms and 17 (29%) cellular component terms (Figure 3-3). In the biological process category, cellular process (14,284), metabolic process (13,064) and biological regulation (6,267) were the most represented subcategories. Binding (13,289), catalytic activity (12,357) and transporter activity (1,613) were the top three subcategories in the molecular activity category. For the cellular component group, membrane (9,707), cell (9,291) and cell part (9,228) were most commonly-identified subcategories.

3.3.2 Candidate chemosensory proteins

The content of the reference transcriptome was mined for genes encoding proteins implicated in lepidopteran olfaction. BLAST searches with custom-curated chemosensory protein data sets from previously-characterized lepidopteran species resulted in identification of 130 genes encoding putative, chemosensory proteins (Table A-3). Expression levels for genes identified are reported, highlighting sexually-dimorphic gene expression. I also carried out a SNP analysis applying a novel approach for SNP calling directly from RNA-Seq reads to assess possible genetic variation within the chemosensory gene repertoire among three BAW populations. Although, I was initially interested in detecting genetic variation in ORs implicated in pheromone detection and expanded the SNP analysis to the other chemosensory gene classes.

3.3.2.1 Odorant binding proteins (OBPs)

A total of 25 putative OBP and 13 CSP gene sequences were identified via searches of the BAW whole-head transcriptome. An initial sequence similarity search within the transcriptome produced 37 transcripts encoding candidate OBPs. Removal of redundant sequences

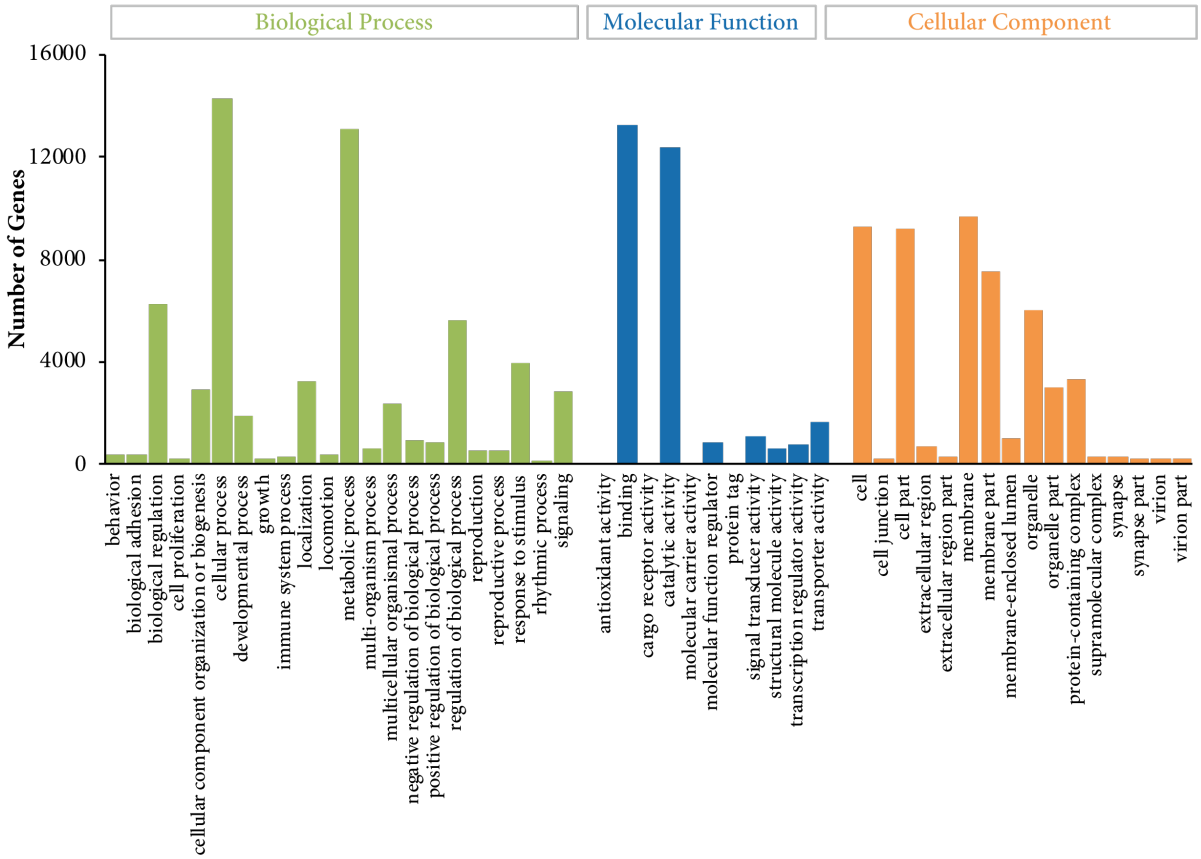

Figure 3-3 Gene ontology (GO) classification of whole-head BAW transcripts.
GO categories (49) displayed on the x-axis are assigned to the three main ontologies of biological process, molecular function and cellular component. The y-axis corresponds to the number of genes from the total 144,364 unigenes assigned to each GO category. For clarity, GO terms with very low sequence assignments (>10 sequences) were omitted and only 49 of the 59 GO terms assigned are shown.

(2 sequences) and transcripts with a TPM value of less than 1 (10 sequences) produced 25 putative OBP open reading frames, including 2 GOBPs, 3 PBPs and 20 putative OBPs (Table A-3; tab OBP). Nearly all of the transcripts identified encoded proteins with hallmark characteristics of OBPs, including a signal peptide and a highly conserved 4-6 cysteine motif. A phylogenetic tree of the BAW OBP and related lepidopteran sequences categorized the OBPs into 5 subfamilies (Figure 3-4). In agreement with other reports from noctuid antennal transcriptomes, GOBP1 and GOBP2 and the three PBPs were grouped as members of the same clade [Gong et al. 2009; Vogt et al. 2015]. Expression analysis shows that transcripts encoding

PBPs and GOBPs were expressed in antennal tissues rather than in the head (Figure 3-5). Among the 20 putative OBP-encoding genes, only 8 were found to be expressed in antennal tissue and at considerably lower levels than either PBP- or GOBP-encoding genes. In addition, *OBP13* and *OBP23* transcripts were also detected in the head tissue of both males and females. Expression analysis for the 3 putative PBP-encoding genes suggests that *PBP1* and *PBP2* are predominantly expressed in males with TPM values of 21033 and 28512, respectively, as compared to 5282 and 18603 in females. *PBP3* transcripts were less abundant than those derived from *PBP1* and *PBP2* in both sexes; however, its expression was higher in females (7946 TPM) than in males (4357 TPM). Transcripts from two other OBP-encoding genes, *OBP1* and *OBP23*, had significant expression in the antenna. *OBP1* transcripts were more abundant in females (12620 TPM) as compared to males (7498 TPM). *OBP23* was expressed at similar levels in the head and antenna for both males and females (6343 and 5162 TPM, respectively). Transcripts from *GOBP2* were the most abundant OBP transcript in male (30106 TPM) and females (33362 TPM) antennae. The three PBPs and two GOBPs contain the classic conserved six-cysteine motif present in most insect OBPs. The other 20 OBPs belong to the C-minus OBP category having 4 or 5 conserved cysteines [Vogt et al. 2015]. No OBPs were identified as belonging to the C-plus OBP category. Mapping of OBP transcripts onto the BAW draft genome showed that OBP genes were clustered on a small number of scaffolds with the majority of the OBP genes assigned to only 4 scaffolds (Table A-3; tab OBP). All three genes encoding PBPs and *GOBP2* mapped to the same scaffold (scaffold 7704), whereas *GOBP1* mapped to a different location in the genome (scaffold 5682).

Nucleotide variation between the three BAW populations for the chemosensory gene sequences of interest was investigated with the KisSplice algorithm. SNP analysis within the OBP protein family produced only 10 non-synonymous SNP locations within *OBP7*, *OBP15*, *OBP16*, *OBP17*, *OBP23* and *GOBP2*. However, for *OBP15*, *OBP16*, *OBP17*, the number of reads mapping to the detected SNP positions was found to be lower than the acceptable threshold of 10 due to their low levels of expression. The relatively abundant transcripts corresponding to *OBP23* had one non-synonymous SNP. Here, the frequency of occurrence represented by the number of reads containing variant 1 SNP versus variant 2 SNP among the three BAW populations indicated that variant 1 corresponding to amino acid residue 20 (A; AAT=asparagine) was present with 100%

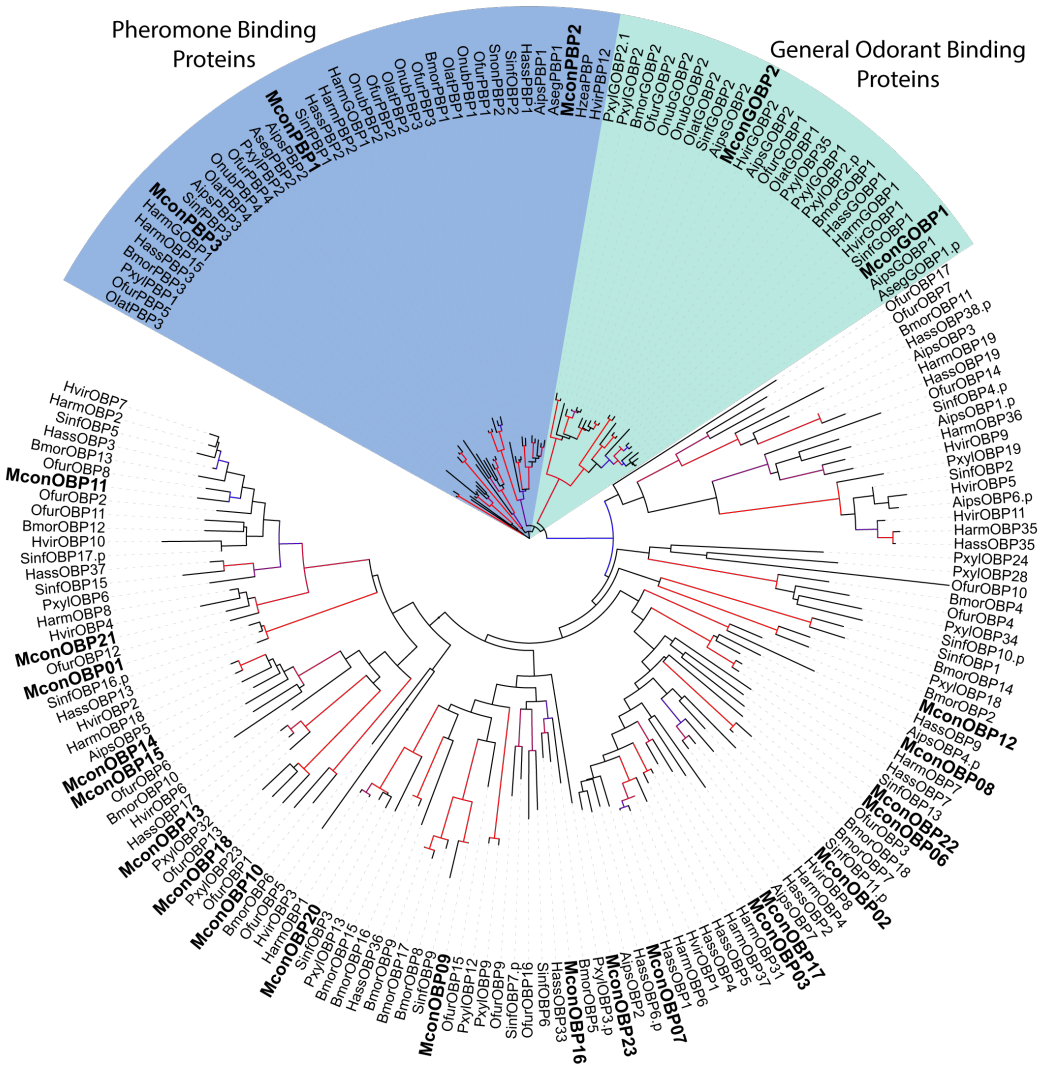

Figure 3-4 Maximum likelihood tree of lepidopteran odorant binding proteins (OBPs). The three pheromone binding proteins (PBPs) and two general odorant binding proteins (GOBPs) are a members of single monophyletic clade, whereasthe other 20 OBPs are distributed among at least 4 other distinct clades. The tree was constructed with lepidopteran sequences from Aips (*Agrotis ipsilon),* Aseg (*Agrotis segetum),* Bmor (*Bombyx mori),* Harm (*Helicoverpa armigera),* Hass (*Helicoverpa assulta),* Hvir (*Heliothis virescens),* Hzea (*Helicoverpa zea),* Mcon *(Mamestra configurata),* Ofur (*Ostrinia furnicalis),* Olap (*Ostrinia latipennis),* Onub (*Ostrinia nubilalis),* Osca (*Ostrinia scapulalis),* Pxyl (*Plutella xylostella),* Sinf (*Sesamia inferens)*. Branches supported by bootstrap values of 75% or higher are indicated by a color range from blue (75%) to red (100%). (See Table A-1; tab OBP for the list of sequences and accession numbers)

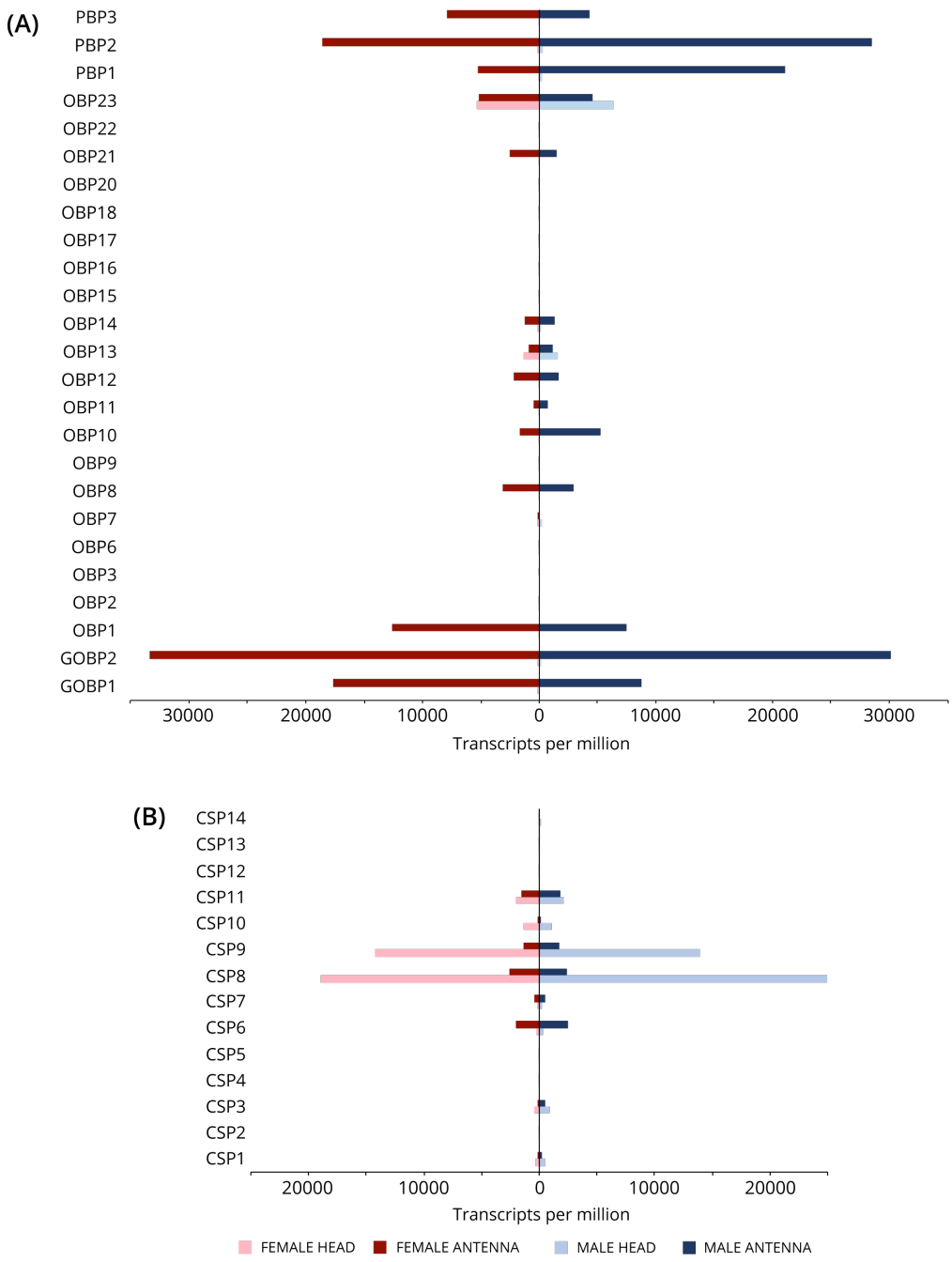

Figure 3-5 Transcript expression analysis for odorant binding proteins (OBPs) and chemosensory proteins (CSPs). **(A)** Gene expression for odorant binding proteins (OBPs) including pheromone binding proteins (PBPs) and general odorant binding proteins (GOBPs). **(B)** Gene expression for chemosensory binding proteins (CSPs). Gene expression values are represented as transcripts per million. The light red and blue bars correspond to female and male head tissue libraries, respectively, whereas the dark red and blue bars correspond to female and male antennal tissue libraries, respectively.

frequency in the AAFC-Saskatoon population, but only 51% in the AAFC-Vegreville population, whereas variant 2 (T; TAT= tyrosine) had 100% frequency in the AAFC-Davidson population.

Two SNPs were reported for *OBP7* gene. The first SNP was identical to the SNP identified for *OBP23* gene, since it occurred at a position corresponding to amino acid 20 with an A to T substitution and was present at the same allelic frequency for all three populations. The second SNP with variant 1 (C; CCC=proline) and variant 2 (T; TCC=serine) corresponding to amino acid residue 35 was found in all three populations with 100% frequency for AAFC-Saskatoon, 90% frequency for AAFC-Davidson and 50% frequency for AAFC-Vegreville populations. The position of the SNP reported for *GOBP2* corresponded to amino acid 7 where leucine (T; TTG=leucine) instead of valine (G; GTG=valine) was called with 100%, 74% and 99 % frequencies in the AAFC-Saskatoon, AAFC-Davidson and AAFC-Vegreville populations, respectively. No SNPs were identified in *PBP1-3* or *GOBP1*.

3.3.2.2 Chemosensory proteins (CSPs)

Of the 30 candidate genes initially identified as encoding proteins belonging to the CSP family, 13 full open reading frames encoded proteins with both a signal peptide and a conserved four cysteine motif. Phylogenetic analysis of these 13 CSPs showed a high degree of sequence similarity to other lepidopteran CSPs (Figure 3-6). CSP3 showed high sequence conservation to several *M. brassicae* CSPs. Abundance estimation suggested that only seven genes were expressed at detectable levels in adult heads and antennae (Figure 3-5). *CSP8* and *CSP9* were the most highly expressed CSP genes and were predominantly expressed in the heads of males and females. *CSP8* transcripts were the most abundant among all CSP transcripts with TPM values of 24947 in males and 18984 in females. Transcripts corresponding to *CSP9* were detected at similar levels in both males (14001 TPM) and females (14253 TPM). Although almost 10-fold less abundant than *CSP8*, *CSP6* transcripts were predominantly detected in the antennae of males (2478 TPM) and females (1990 TPM), indicating that *CSP6* is antenna-specific. Transcripts from another antenna-specific gene, *CSP7*, were detected in males at 520 TPM and 396 TPM in females. CSP7 and CSP6 share only 37% amino acid sequence identity, suggesting different olfactory functions for these two proteins. ClustalO-guided alignment of the BAW CSPs indicated that CSP2, CSP11, CSP12 and CSP13 did not contain conserved motifs shared by the

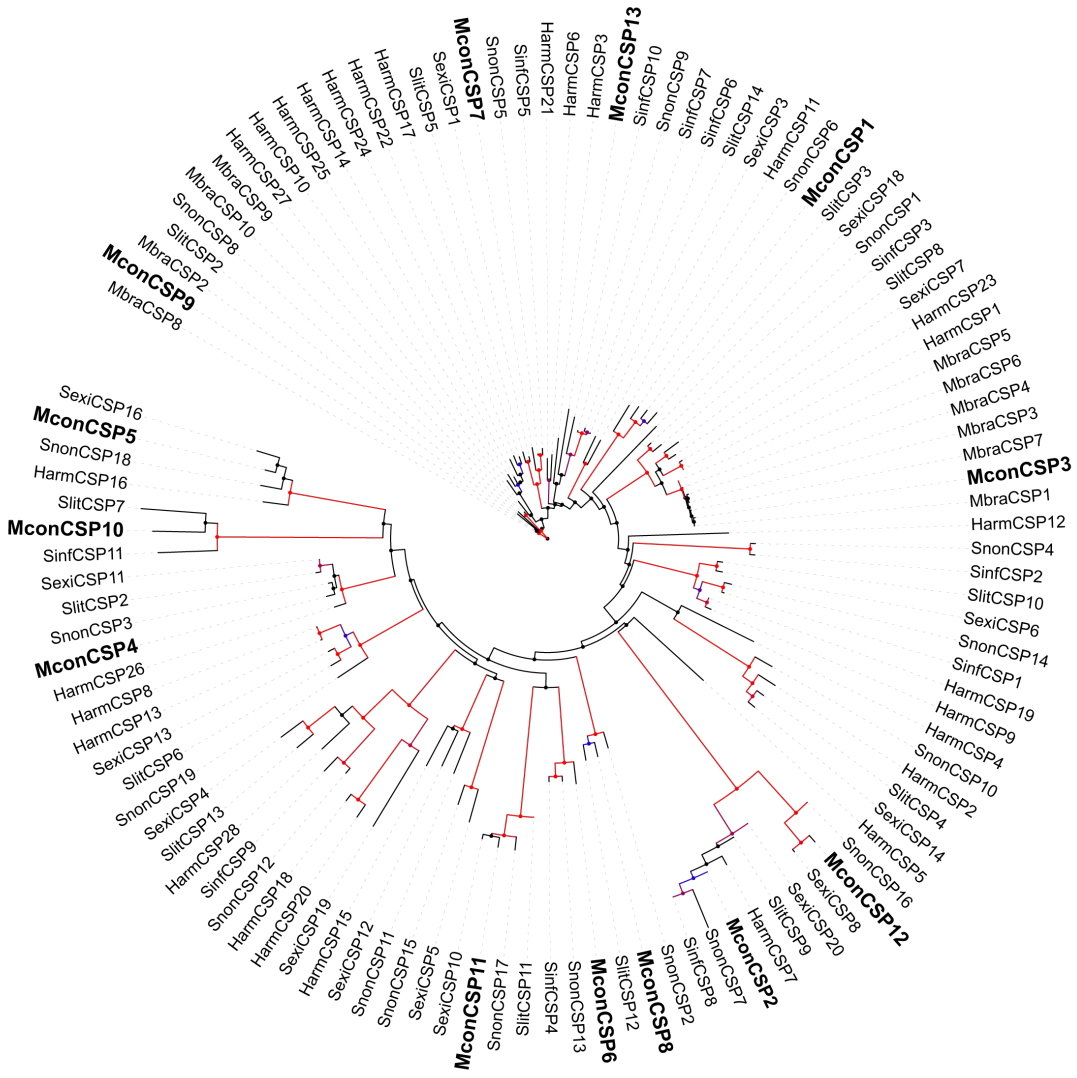

Figure 3-6 Maximum likelihood tree of lepidopteran chemosensory proteins (CSPs). The tree was constructed with lepidopteran sequences including: Harm (*Helicoverpa armigera*), Mbra (*Mamestra brassicae*), Mcon (*Mamestra configurata*), Sinf (*Sesamia inferens*), Snon (*Sesamia nonagroides*), Slitt (*Spodoptera littoralis*), Slit (*Spodoptera litura*), Sexi (*Spodoptera exigua*). Branches supported by bootstrap values of 75% or higher are indicated by a color range from blue (75%) to red (100%). (See Table A-1; tab CSP for the list of sequences and accession numbers)

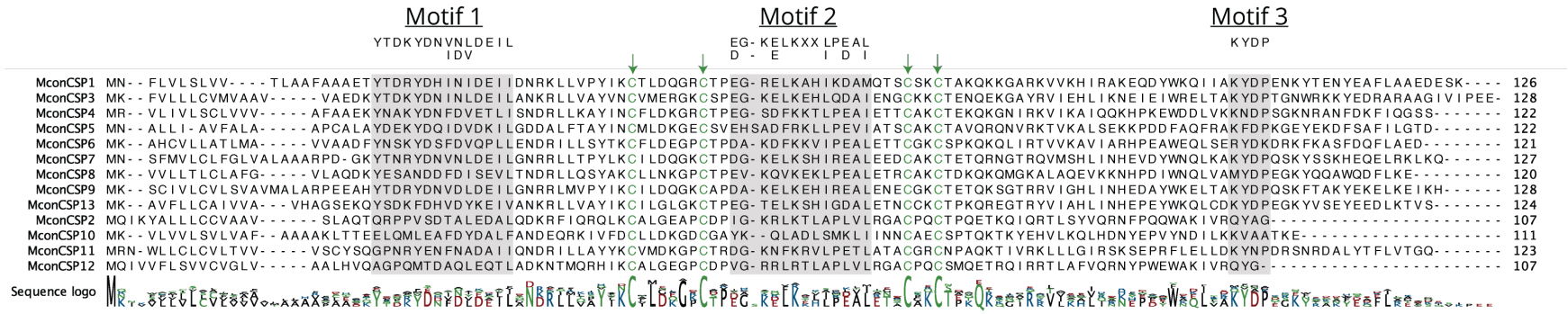

Figure 3-7 BAW chemosensory protein (CSPs) sequence alignment. In addition to the four conserved cysteine residues (red arrows), three conserved sequence regions denoted as Motif 1-3 (light blue) have been identified. CSP2, CSP10, CSP11 and CSP12 do not contain Motif1-3 but the four conserved cysteine residues are present.

majority of the CSP family members, including the N-terminal YTTKYDN(V/I)(N/D)(L/V)DEIL, the central DGKELKXX(I/L)PDAL and the C-terminal KYDP domain (Figure 3-7) [Wanner et al. 2004]. All 13 CSP sequences, however, had the highly conserved four-cysteine motif (C1-X_{6-8}-C2-X_{16-21}-C3-X_2-C4) common for this class of proteins. With the exception of *CSP2* and *CSP12*, all CSP genes mapped to two scaffolds in the BAW draft genome suggesting their genomic organization is similar to that of OBP genes (Table A-3; tab CSP). In *CSP1*, *CSP4*, *CSP8* and *CSP10*, the SNPs mapped to codons encoding amino acids following the C-terminal KYDP motif (Table A-3; tab CSP). In CSP1, aspartic acid (D; GAT) occurred at position 114 with 100% frequency in the AAFC-Saskatoon colony; however, an asparagine (N; AAC) was present in the AAFC-Davidson (100%) and AAFC-Vegreville (98%) populations. In CSP4, a valine (V; GTT) occurs at low frequency in the AAFC-Davidson (34%) and AAFC-Vegreville (22%) populations. Two non-synonymous SNPs were mapped to *CSP8*. At the corresponding amino acid position 92 within CSP8, an asparagine (N; AAC) was found with 34% and 16% frequencies in the AAFC-Davidson and AAFC-Vegreville populations, respectively. The second SNP mapped to a codon encoding an amino acid at position 106 and corresponds to a proline (P; CCT) variant that occurs at high frequency in all three populations [AAFC-Saskatoon (100%), AAFC-Davidson (58%) and AAFC-Vegreville (74%)]. However, an arginine (R; CGT) is also present in variants from the AAFC-Davidson (42%) and AAFC-Vegreville (26%) populations. In *CSP10*, a SNP was detected corresponding to amino acid 100 at which glutamic acid (E; GAG) occurs at lower frequencies of 20% and 6% in the AAFC-Davidson and AAFC-Vegreville populations. *CSP6* was an exception among the CSP-encoding genes, as the SNP corresponding to amino acid 3 [valine (V; GTT) instead of alanine (A; GCT)] is found at 47% frequency in the Davidson and at 11% frequency in the Vegreville populations.

3.3.2.3 Olfactory receptors (ORs)

A search of the BAW whole-head transcriptome identified 50 candidate olfactory receptor (OR) encoding genes. Of the 50 putative sequences, 43 were determined to contain complete open reading frames. The predicted number of BAW OR genes is in agreement with that reported in other lepidopterans, including 43 in *S. litorallis* [Jacquin-Joly et al. 2012], 47 in *M. sexta* [Große-Wilde et al. 2010], and 51 in *H. assulta* and *H. armigera* [Xu et al. 2015]. Phylogenetic analysis of OR protein sequences from 17 lepidopteran species identified OR15, OR27, OR29, OR42 and OR48 as putative BAW PRs (Figure 3-8). Furthermore, when the putative BAW PRs were

aligned with other deorphanized lepidopteran PRs, OR15 was classified as a Group 1 PR, whereasOR27, OR29, OR42 and OR48 were all assigned to Group 2 (Figure 3-9). Based on previous work from Xu et al. (2015), the PRs assigned to Group 1 typically detect the major sex pheromone and are expressed only in the male antennae. PRs classified as Group 2 were found to mainly detect the minor pheromone component, although some show affinity for major sex pheromone components as well [Zhang and Löfstedt 2013]. Group 3 PRs tend to have variable ligand and sensitivity spectra and are found to respond to both major and minor pheromone components. OR27 and OR29 are closely related to *A. segetum* PRs, which have several known ligands, including Z9-14:OAc (minor sex component in the BAW pheromone blend). Abundance estimation from the RNA-Seq data indicated that *OR15*, *OR27*, *OR29*, *OR42* are predominantly expressed in the male antenna (Figure 3-10). The most abundant, male-specific PR transcript encodes OR42 (127.7 TPM) and is closely related to AsegOR5 and HvirOR14 which are activated by Z9-14:OAc and Z11-16:OAc, respectively. The sequences of OR27 and OR29 have a high degree of amino acid identity (89%) and exhibit male-biased gene expression in antenna of 20.3 and 30.5 TPM, respectively. *OR29* transcript was also detected in female antenna at an of abundance only 4.9 TPM. The *OR15* gene was exclusively expressed in males (7.4 TPM), whereas the *OR48* gene, which also encodes a putative PR, was expressed in both males (23.8 TPM) and females (60.3 TPM) with a higher expression in the female antenna. The only female specific OR gene, *MconOR12* (7.3 TPM), was not assigned to the PR clade in the phylogenetic analysis. Recent investigation of ORs closely related to MconOR12 from *H. armigera*, *H. assulta* and *H. virescens* found that this receptor is tuned to six structurally-related plant volatiles [Cao et al. 2016]. The gene encoding the OR co-receptor ORCO was expressed at a level approximately twice that of the gene encoding the major male-biased PR MconOR42 (251.2 TPM) (Figure 3-8). Droplet digital PCR was carried out on a selected number of OR genes and confirmed the sex-biased expression of PR genes (Figure 3-11).

SNP analysis was carried out to explore the genetic variation within OR genes among the three BAW populations resulting in the identification of 70 non-synonymous SNP positions among the 50 OR gene sequences. The results below focus on the 5 putative PR genes, whereas the complete list of identified SNPs can be found in Table A-3. SNPs were found in three BAW PR genes, *OR15* and *OR27* and *OR29*, but not in *OR42* or *OR48* (Table 3-5). SNPs were mapped

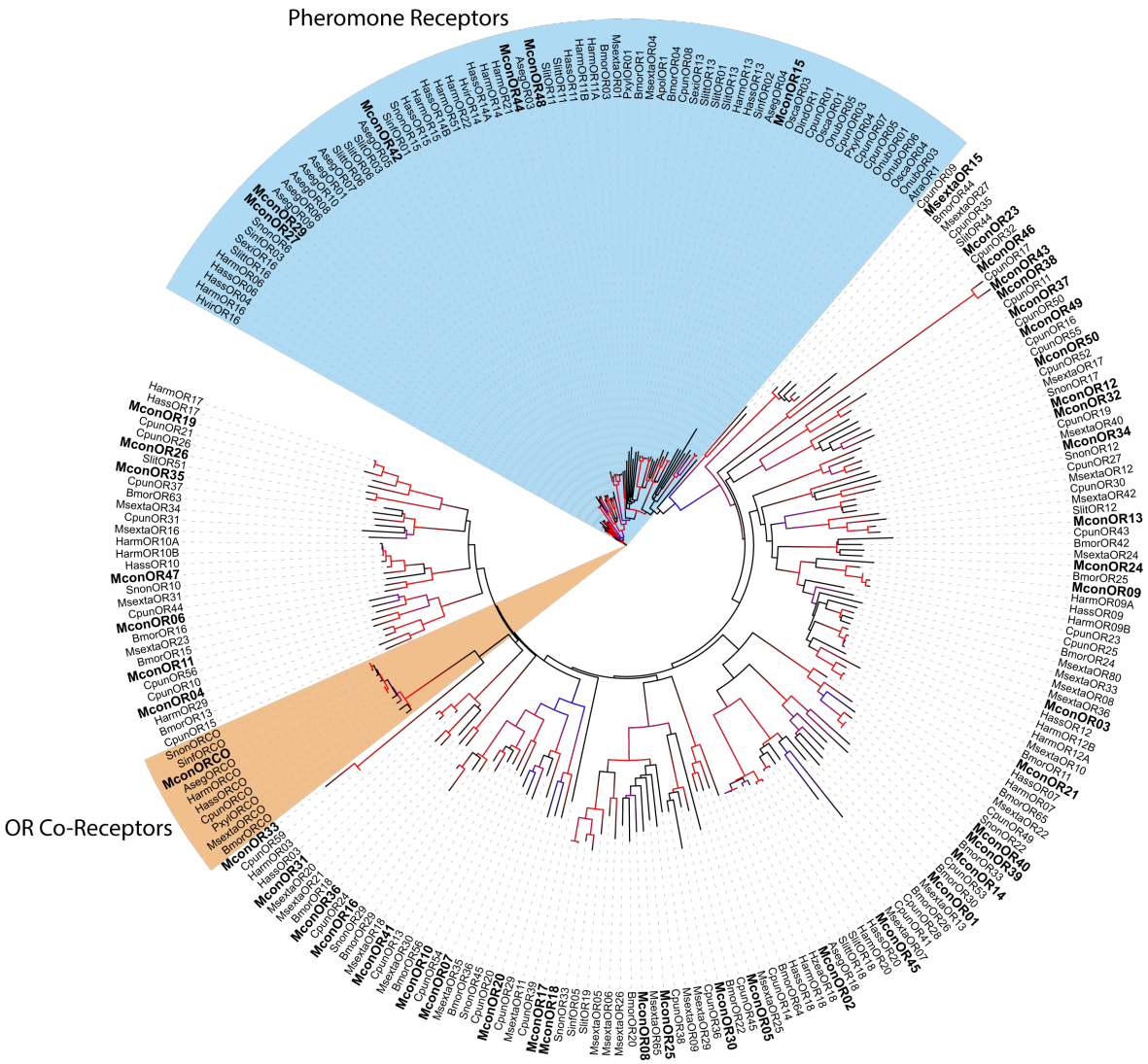

Figure 3-8 Maximum likelihood tree of lepidopteran olfactory receptor (OR) proteins. Pheromone olfactory receptors (PRs) (blue) form a distinct clade. MconOR15, OR27, OR29, OR42 and OR48 were identified as putative PRs. MconOR44 and MconOR28 were also assigned to the PR family and had expression values of less than 1 TPM in the abundance estimation analysis. The conserved olfactory co-receptor (ORCO) is shown in orange. The tree was constructed with the following lepidopteran sequences: Aseg (*Agrotis segetum),* Apol (*Antheraea polyphemus),* Atra (*Amyelois transitella),* Bmor (*Bombyx mori),* Cpun *(Conogethes punctiferalis),* Dind (*Diaphania indica),* Harm (*Helicoverpa armigera),* Hzea (*Helicoverpa zea),* Hass (*Helicoverpa assulta),* Hvir (*Heliothis virescens),* Msex (*Manduca sexta),* Mcon *(Mamestra configurata),* Ofur (*Ostrinia furnicalis),* Onub (*Ostrinia nubilalis),* Osca (*Ostrinia scapulalis),* Pxyl (*Plutella xylostella),* Sinf (*Sesamia inferens),* Snon (*Sesamia nonagroides),* Slit *(Spodoptera litura),* Slitt *(Spodoptera littoralis).* Branches supported by bootstrap values of 75% or higher are indicated by a color range from blue (75%) to red (100%). (See Table A-1; tab OR for the list of sequences and accession numbers)

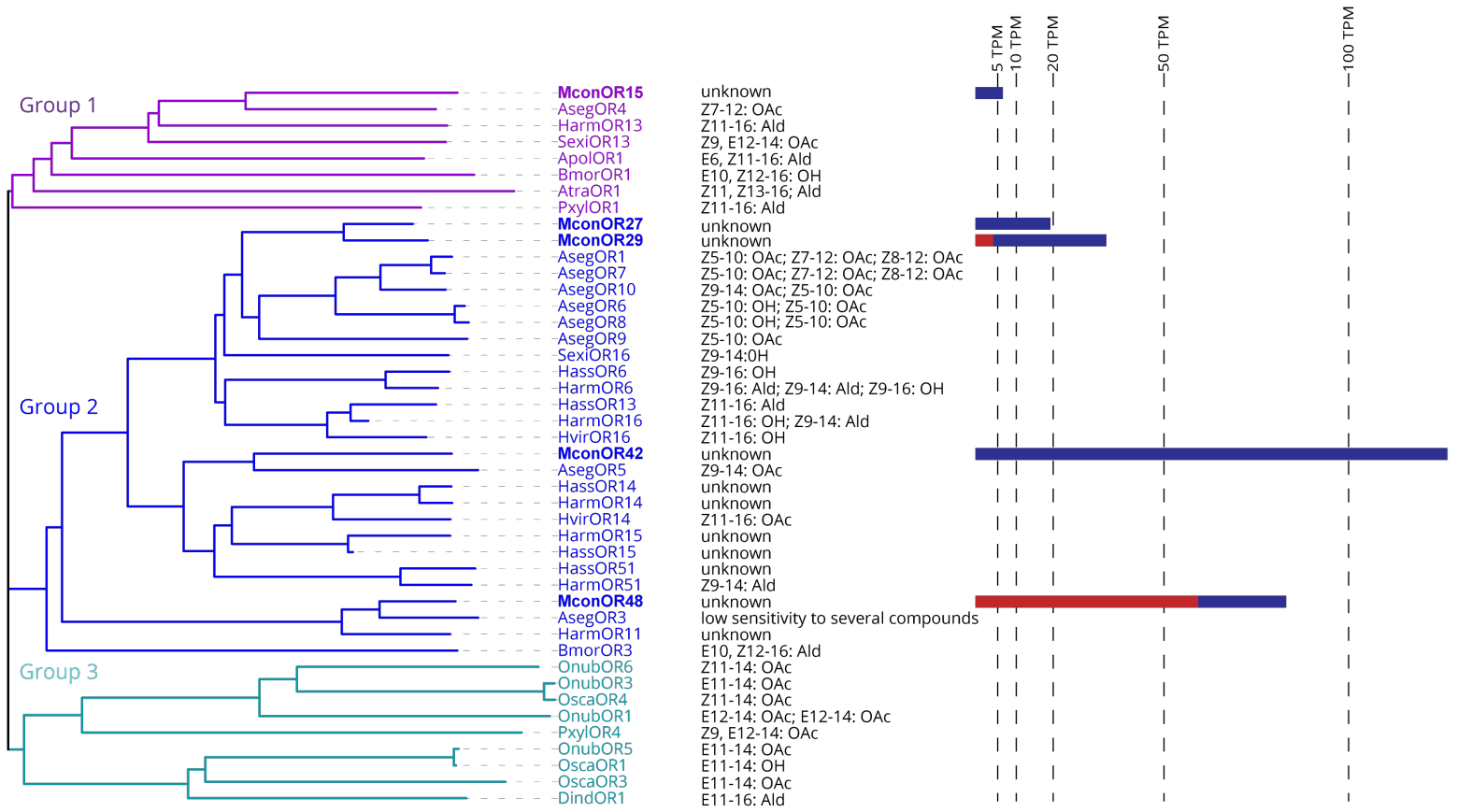

Figure 3-9 Maximum likelihood tree of lepidopteran pheromone olfactory receptors (PRs). For several lepidopteran species, PRs have been deorphanized and their activating ligands are known. The most abundant PR male biased (blue) transcript product, MconOR42, was assigned to Group 2 PRs along with MconOR27, MconOR29 and female biased (red) MconOR48. The male-biased, but least abundant OR based on transcript abundance, MconOR15 was categorized as a Group1 PR. The transcript abundance corresponding to each PR is expressed in transcripts per million (TPM). The tree was generated with PR sequences from lepidopteran species including Aseg (*Agrotis segetum),* Apol (*Antheraea polyphemus),* Atra (*Amyelois transitella),* Bmor (*Bombyx mori),* Dind (*Diaphania indica),* Harm (*Helicoverpa armigera),* Hass (*Helicoverpa assulta),* Hvir (*Heliothis virescens),* Mcon *(Mamestra configurata)*, Onub (*Ostrinia nubilalis),* Osca (*Ostrinia scapulalis),* Pxyl (*Plutella xylostella),* Sexi (*Spodoptera exigua).*

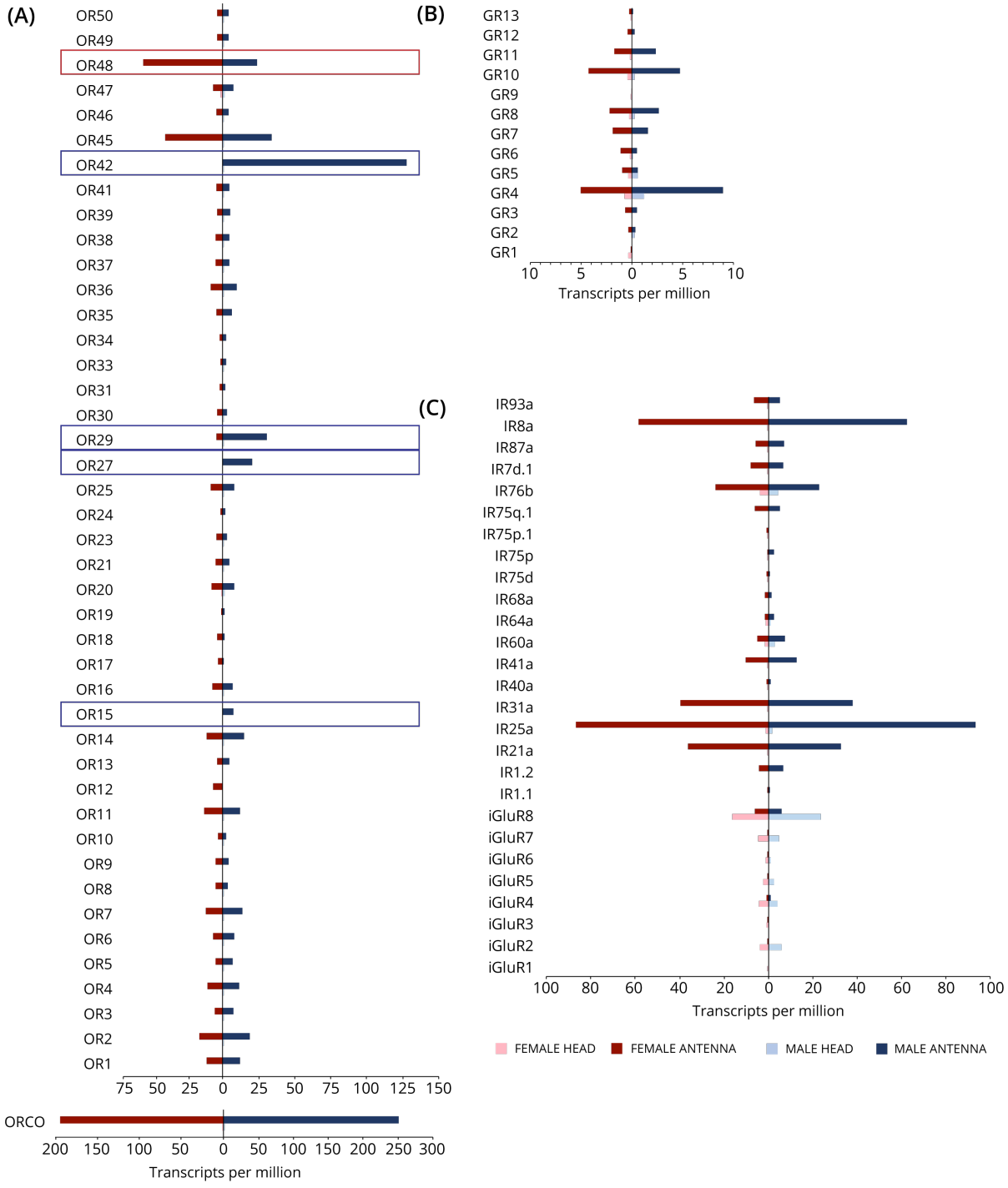
(A)
OR50
OR49
OR48
OR47
OR46
OR45
OR42
OR41
OR39
OR38
OR37
OR36
OR35
OR34
OR33
OR31
OR30
OR29
OR27
OR25
OR24
OR23
OR21
OR20
OR19
OR18
OR17
OR16
OR15
OR14
OR13
OR12
OR11
OR10
OR9
OR8
OR7
OR6
OR5
OR4
OR3
OR2
OR1
75 50 25 0 25 50 75 100 125 150
ORCO
200 150 100 50 0 50 100 150 200 250 300
Transcripts per million
(B)
GR13
GR12
GR11
GR10
GR9
GR8
GR7
GR6
GR5
GR4
GR3
GR2
GR1
10 5 0 5 10
Transcripts per million
(C)
IR93a
IR8a
IR87a
IR7d.1
IR76b
IR75q.1
IR75p.1
IR75p
IR75d
IR68a
IR64a
IR60a
IR41a
IR40a
IR31a
IR25a
IR21a
IR1.2
IR1.1
iGluR8
iGluR7
iGluR6
iGluR5
iGluR4
iGluR3
iGluR2
iGluR1
100 80 60 40 20 0 20 40 60 80 100
Transcripts per million
FEMALE HEAD
FEMALE ANTENNA
MALE HEAD
MALE ANTENNA

Figure 3-10 Expression analysis for the three classes of chemosensory receptors identified. Gene expression values are represented as transcripts per million (TPM). The light red and blue bars correspond to female and male head libraries, respectively; the dark red and blue bars correspond to female and male antennal libraries, respectively. **(A)** Expression analysis for olfactory receptors (ORs). Phylogenetic analysis identified OR15, OR27, OR29, OR42 and OR48 as putative PRs (male biased expression (blue frame); female biased expression (red frame). The expression of olfactory receptor co-receptor ORCO is shown below but was omitted from the OR graph due to its high expression level. (**B)** Expression analysis for gustatory receptors (GRs). (**C)** Expression analysis for ionotropic receptors (IRs).

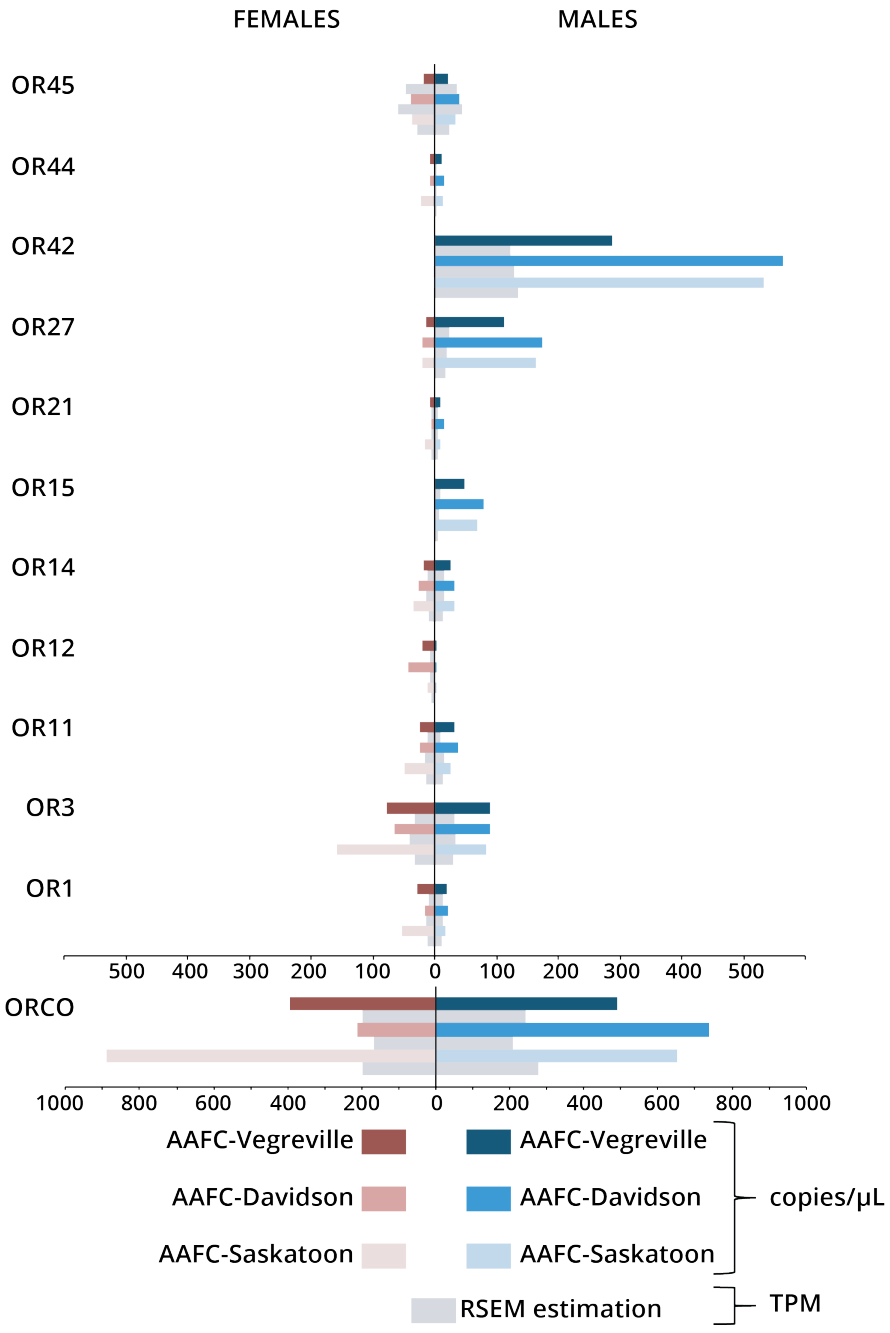

Figure 3-11 Digital droplet PCR survey of selected OR gene expression levels in three BAW populations and comparison to RSEM transcript abundance estimation. AAFC-Saskatoon males (light blue) and females (light red); AAFC-Davidson males (medium blue) and females (medium red); and AAFC-Vegreville males (dark blue) and females (dark red). The values represented by the coloured bars are given in copies/µL. The theoretical transcript abundance values calculated with RSEM are given in transcripts per million (TPM).

onto the transmembrane regions for OR15, OR27 and OR29 (Fig 3-12) and affected amino acids within the extracellular loops (ECLs), intracellular loops (ICLs) and transmembrane domains (TMDs).

Two SNPs corresponding to amino acid positions 49 and 122 within OR15 resided within the ICLs close to the amino terminus of the protein. At position 49, leucine (L; TTA) was predicted with 50% frequency in the AAFC-Vegreville population, but valine (V; GTA) occurred with 100% frequency in AAFC-Davidson and AAFC-Saskatoon populations. At position 122, phenylalanine (F; TTC) was more common in the AAFC-Davidson (94%) and AAFC-Vegreville (88%) populations than isoleucine (I; ATC), which was predominant in the AAFC-Saskatoon population (74%). Three SNPs were identified and mapped to amino acid positions 200, 219 and 347 located within the ECL1 and ECL2 of OR15. At position 200, valine (V; GTT) was found at low frequencies of 29% and 6% in the AAFC-Davidson and AAFC-Vegreville populations, respectively, whereas alanine (A; GCT) was predominant in all three populations. At position 219, arginine (R; AGA) was found with high frequency in all three populations, but lysine (K; AAA) (Q; GAG) to a histidine (H; CAT) substitution was detected with histidine observed at 23% and 41% in the AAFC-Davidson and AAFC-Vegreville populations, respectively. The SNP detected at OR15 position 424 falls within the 7th TMD with leucine (L; TTG) being predominant, whereas valine (V; GTG) was observed with 16% frequency in the AAFC-Davidson and 47% in AAFC-Vegreville populations.

From the three SNPs identified in *OR27* gene, the SNP resulting in an asparagine (N; AAT) to threonine (T; ACT) substitution corresponding to amino acid position 180 falls within ECL2. At this location, the AAFC-Saskatoon colony had threonine with 100% frequency, whereas the AAFC-Vegreville and AAFC-Davidson populations had asparagine with 100% and 62% frequencies, respectively. Another interesting SNP was found at a codon corresponding to amino acid 268 within ICL2. At this position, a phenylalanine (F; TTC) was present in the AAFC-Davidson (100%) and AAFC-Vegreville (89%) colonies, whereas tyrosine (Y; TAC) was present with 100% frequency in the AAFC-Saskatoon colony. The last SNP in *OR27* corresponded to amino acid position 342 and within TMD6 and in close proximity to ECL3; this corresponded to a valine (V; GTG) which was predominant in the AAFC-Saskatoon (100%) colony, or an alanine

(A; GCG) which was found at 5% frequency in the AAFC-Davidson population and at 41% frequency in the AAFC-Vegreville population.

Five putative SNPs were found within the *OR29* gene. In contrast to *OR15* and *OR27*, no SNPs were found in *OR29* corresponding to the ECL regions; however, three SNPs were found in regions corresponding to TMD 1, 3 and 6. At amino acid position 58 in TMD1, phenylalanine (F; TTT) was present instead of leucine (L; TTG) with 5% and 21% frequencies in the AAFC-Davidson and AAFC-Vegreville populations, respectively. At amino acid position 155 in TMD3, valine (V; GTT) was present with 43% frequency in the AAFC-Saskatoon colony in contrast to alanine (A; GCT) which was present with 100% frequency in both the AAFC-Davidson and AAFC-Vegreville colonies. At amino acid position 340 in TMD6, an alanine (A; GCG) was present at 5% and 41% frequencies in the AAFC-Davidson and AAFC-Vegreville colonies, respectively, instead of valine (V; GTG) which was found with 100% frequency in the AAFC-Saskatoon colony. This last SNP was at a position very similar to the SNP in the region of *OR27* encoding TMD6. The remaining two SNPs for *OR29* were predicted in the regions encoding ICL1 (position 106) and ICL2 (position 290). For the SNP affecting amino acid 106, the threonine (T; ACT) variant had 100% and 38% frequency in the AAFC-Saskatoon and AAFC-Davidson populations, respectively, whereas the asparagine (N; AAT) variant was present in the AAFC-Vegreville population with 100% frequency. This SNP occurs at a position very similar to the SNP in the region of *OR15* encoding ICL1. The SNP affecting amino acid 290 resulted in isoleucine (I; ATT) and was present with 34% and 5% frequencies in the AAFC-Saskatoon and AAFC-Vegreville populations, respectively, as compared to leucine (L; CTT) which was predominant in all three populations. Mapping of the OR gene sequences onto the BAW draft genome indicated that the majority of the OR sequences were scattered among 36 different scaffolds in contrast to genes encoding OBPs which were concentrated on only few scaffolds. However, *MconOR27* and *MconOR42* were found on the same scaffold (Table A-3; tab OR).

Table 3–5 Summary of single nucleotide polymorphism (SNP) predictions genes encoding for sequences identified as putative BAW pheromone olfactory receptors (PRs).

Gene	Amino Acid Position	Variant Codon1	Variant Codon2	Amino Acid 1	Amino Acid 2	Variant 1 Frequency (%)			Variant 2 Frequency (%)		
						C[1]	D[1]	V[1]	C	D	V
OR15	49	TTA	GTA	L	V	0	0	50	100	100	50
OR15	122	TTC	ATC	F	I	26	94	88	74	6	12
OR15	200	GTT	GCT	V	A	0	29	6	100	71	94
OR15	219	AAA	AGA	K	R	0	0	17	100	100	83
OR15	347	CAG	CAT	Q	H	100	77	59	0	23	41
OR15	424	TTG	GTG	L	V	100	84	53	0	16	47
OR27	180	AAT	ACT	N	T	0	62	100	100	38	0
OR27	268	TTC	TAC	F	Y	0	100	89	100	0	11
OR27	342	GCG	GTG	A	V	0	5	41	100	95	59
OR29	58	TTG	TTT	L	F	0	5	21	100	95	79
OR29	106	AAT	ACT	N	T	0	62	100	100	38	0
OR29	155	GTT	GCT	V	A	43	0	0	57	100	100
OR29	290	CTT	ATT	L	I	66	100	95	34	0	5
OR29	340	GCG	GTG	A	V	0	5	41	100	95	59

[1] C = AAFC-Saskatoon, D = AAFC-Davidson, V= AAFC-Vegreville.

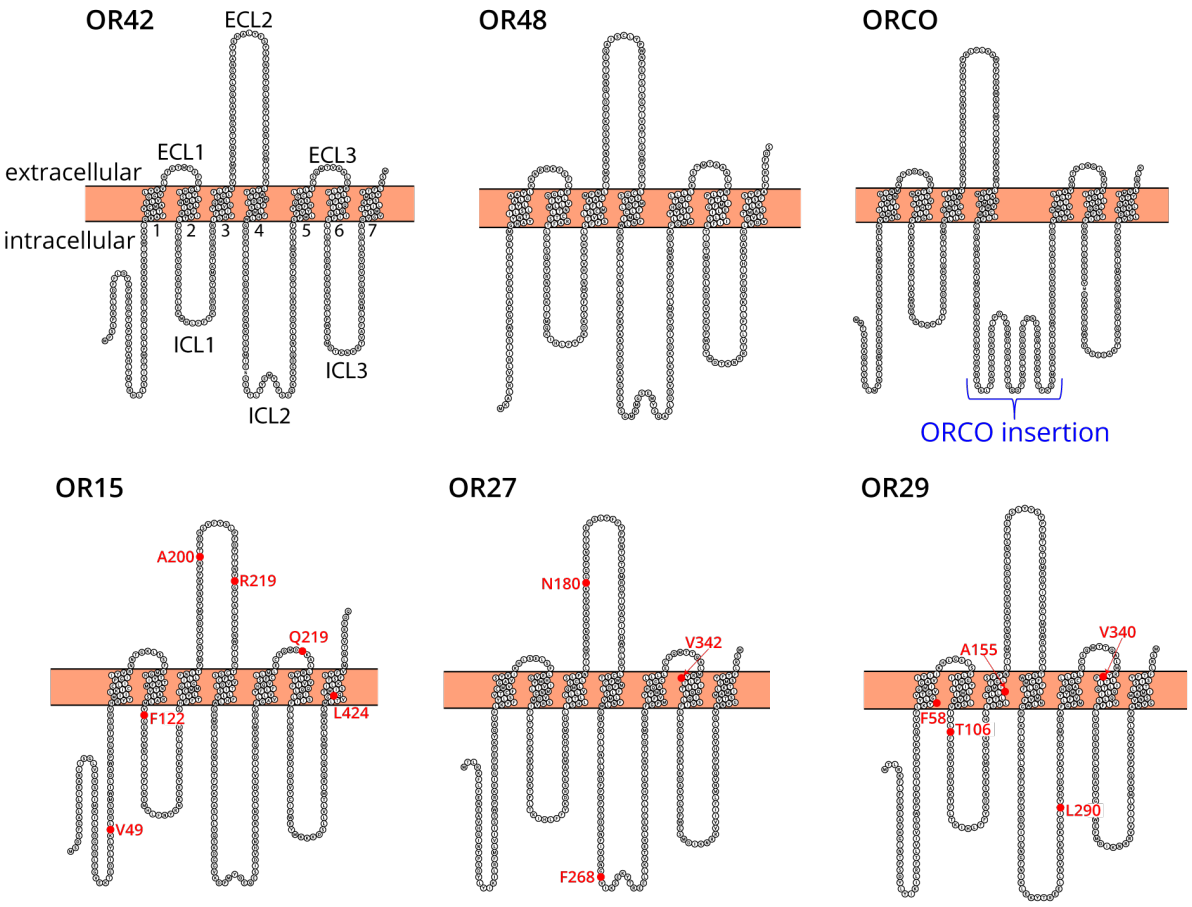

Figure 3-12 Transmembrane predictions for the five pheromone receptors (PRs) and OR-coreceptor (ORCO) identified in the BAW whole-head transcriptome. The orientation of the receptors is described for MconOR42 showing the intracellular and extracellular space outside of the dendritic membrane. The seven transmembrane domains (TMD) are labelled 1-7 below each domain, extracellular loops are marked as ECL1-3 and intracellular loops as ICL1-3. The locations of amino acid altered by SNPs are indicated with red circles. No SNPs were identified in *OR42*, *OR48* sequences or *ORCO*. The transmembrane prediction for ORCO shows the well-conserved insertion in ORCO's ICL2 (blue) which is not present in the other ORs.

3.3.2.4 Gustatory receptors (GRs)

The presence of GR gene expression in antennae was reported previously for several lepidopteran species [Jacquin-Joly et al. 2012]. Transcripts derived from 13 putative GR genes were found in the whole-head BAW transcriptome from males and females. Phylogenetic analysis grouped GR1, GR2, GR6, GR7 and GR10 with known lepidopteran sugar GRs (Figure 3-13), whereasGR4, GR5 and GR8 were identified as putative CO_2 receptors. Expression analysis indicates that, at least in the antenna of both males and females, the GR genes are expressed at low levels with all 13 sequences falling below 10 TPM (Figure 3-10). The most abundant GR transcript, derived from *GR4*, was found at 9 TPM in males and 5 TPM in females. Although 4 SNPs were detected within the GR-genes, the number of reads mapped and supporting each SNP was insufficient for further analysis. Similar to OR genes, GR genes were found scattered across the genome rather than clustered on a single scaffold (Table A-3; tab GR).

3.3.2.5 Ionotropic receptors (IRs)

A BLAST search identified transcripts encoding 32 putative IRs including 8 iGluRs, 22 antennal IRs and 2 ubiquitous IR co-receptors (Table A-3; tab IR). The naming convention for orthologous genes previously reported in *Drosophila*, *Spodoptera* and *Helicoverpa* species [Xu et al. 2015; Croset et al. 2010] was used. With the exception of contigs corresponding*MconGluR1*, *MconGluR8* and *MconIR75p.1*, all others possessed complete open reading frames. Phylogenetic analysis assigned each of the putative IRs to clusters of lepidopteran IRs (Figure 3-14) [Jacquin-Joly et al. 2012; Xu et al. 2015]. MconIR1.1, MconIR1.2 and MconIR87a clustered with lepidopteran specific IRs [Olivier et al. 2011]. Expression analysis shows that all of the genes encoding iGluRs were predominantly expressed in the head, whereas the IR genes were expressed in antennae (Figure 3-10). This is consistent with the role of iGluRs in synaptic transmission in the insect brain [Benton et al. 2009]. The expression levels for IR genes reported from other lepidopteran species are in agreement with the low expression determined in BAW [Xu et al. 2015]. The two most abundant transcripts corresponded to the genes encoding the ubiquitous IR co-receptors IR25a and IR8a. *IR25a* transcript abundance was determined to be 93.2 and 86.7 TPM in males and females, respectively, whereas*IR8a* was at 62.3 and 58.4 TPM in males and females, respectively. In addition to the two co-receptor genes, the expression level of *IR76b*, *IR31a* and *IR21a*, was also elevated compared to the other IR genes. With the

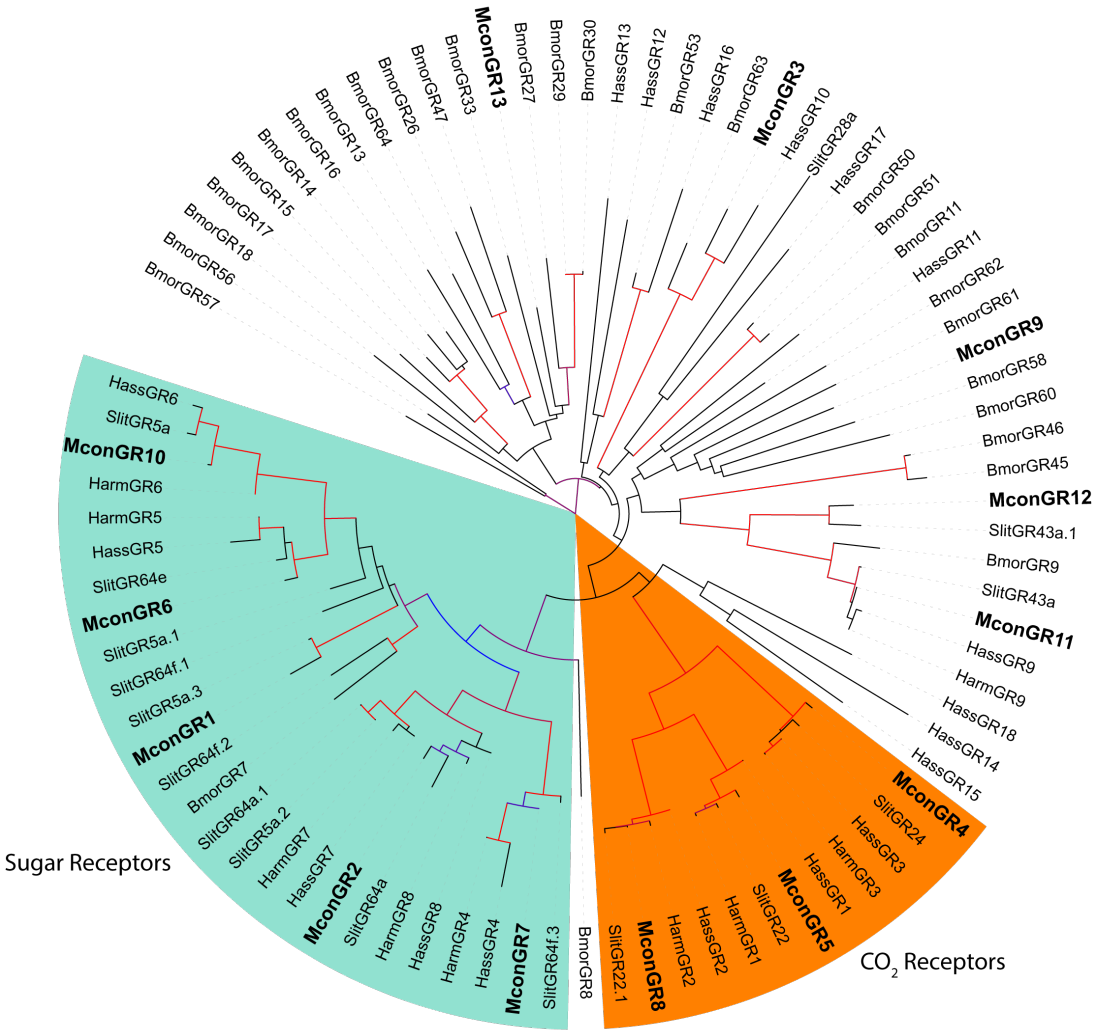

Figure 3-13 Maximum likelihood tree of lepidopteran gustatory receptors (GRs). The sugar (green) and CO_2 (orange) receptors are members of the same clade. The function of the remaining GRs is unknown. The tree was generated with lepidopteran sequences from Bmor (*Bombyx mori*), Harm (*Helicoverpa armigera*), Hass (*Helicoverpa assulta*), Mcon (*Mamestra configurata*), Slit (*Spodoptera litura).* Branches supported by bootstrap values of 75% or higher are indicated by a color range from blue (75%) to red (100%). (See Table A-1; tab GR for the list of sequences and accession numbers)

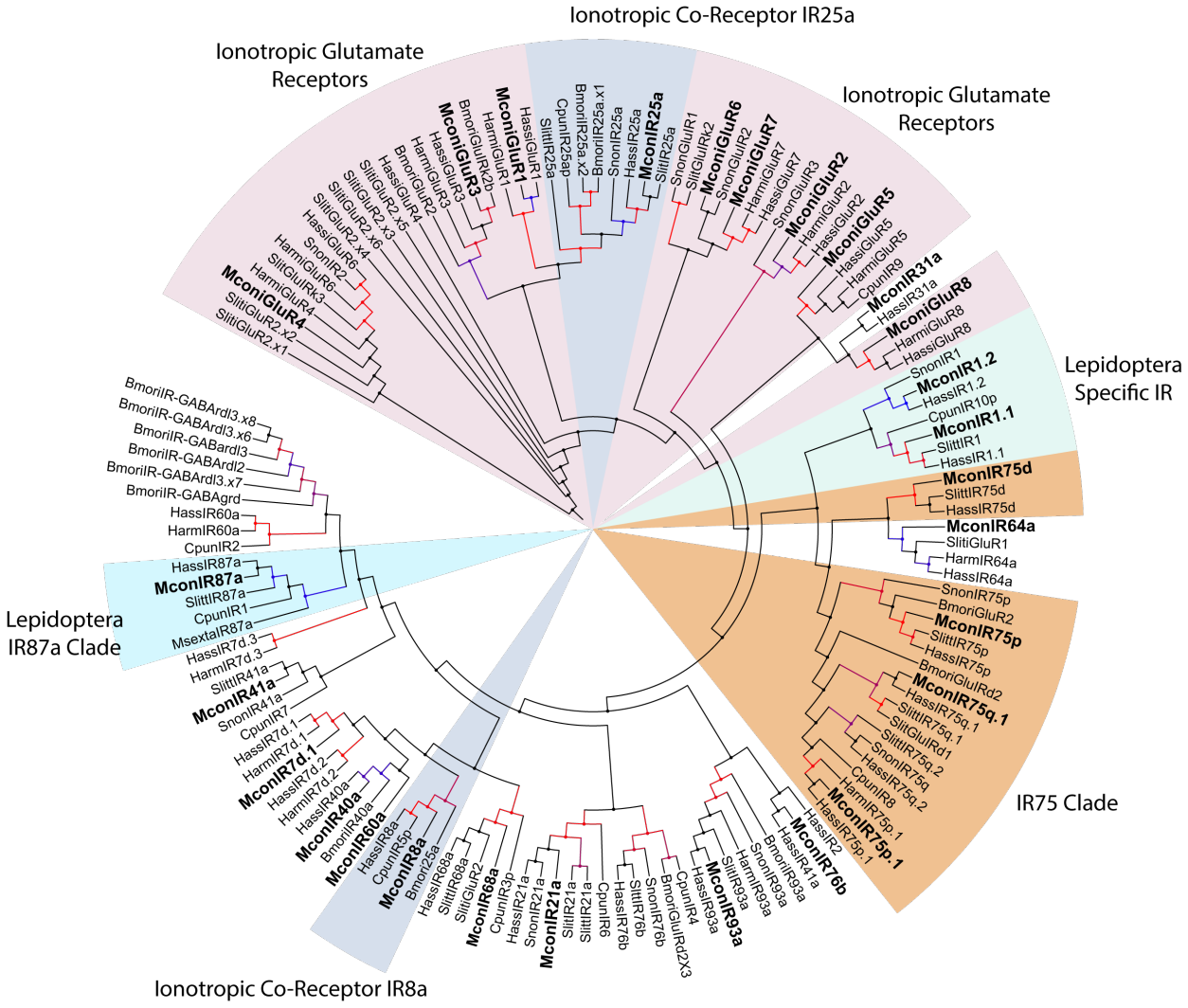

Figure 3-14 Maximum likelihood tree of lepidopteran antennal ionotropic receptors (IRs) and ionotropic glutamate receptors (iGluRs). The ionotropic glutamate receptors (iGluRs) are indicated in light pink and the ubiquitous ionotropic co-receptors IR25a and IR8a are highlighted in dark blue. The Lepidoptera specific IRs (light green) and IR87a clade (light blue) are Lepidoptera specific. The IR75 clade is conserved among all insects [Rytz et al. 2013]. The tree was generated with lepidopteran sequences from Bmor (*Bombyx mori*), Cpun (*Conogethes punctiferalis*), Harm (*Helicoverpa armigera*), Hass (*Helicoverpa assulta*), Mcon (*Mamestra configurata*), Snon (*Sesamia nonagroides*), Slitt (*Spodoptera littoralis*), Slit (*Spodoptera litura*). Branches supported by bootstrap values of 75% or higher are indicated by a color range from blue (75%) to red (100%). (See Table A-1; tab IR for the list of sequences and accession numbers)

exception of *iGluR8* and *iGluR2*, the expression of IR genes was similar between males and females. Transcripts from the lepidopteran-specific *IR1*.2 gene were found at 6.7 TPM in males and 4.4 TPM in females, whereas those from *IR87a* were found at 7.2 and 5.9 TPM in males and females, respectively. The other lepidopteran-specific IR transcript, *IR1.1*, was expressed at a very low level.

Analysis with KisSplice identified 48 putative SNPs within the protein coding regions of BAW IR genes. The highest number of SNPs (11) was recorded for the lepidopteran-specific *IR1.2*. Seven of the eleven SNPs reported were located in the region encoding the first ligand binding domain, two in transmembrane region 1, one in the second ligand binding domain region and one in the intracellular domain region close to the C-terminus of the protein (Table A-3; tab IR).

3.3.2.6 Sensory neuron membrane proteins (SNMPs)

Two putative SNMP sequences have been described in lepidopterans to date [Rogers et al. 1997; 2001; Forstner et al. 2008]. A BLAST search identified two SNMP genes in BAW, that were annotated as *MconSNMP1* and *MconSNMP2* (Table A-3; tab SNMP). Transcripts derived from *SNMP2* were more abundant than from *SNMP1* in the antennal tissue with TPM values of 1496 reported for males and 1012 for females. The *SNMP1* gene was expressed in the antenna of males at 515 TPM and females at 352 TPM. Interestingly, *SNMP2* transcripts were also detected in the head tissue at 77.2 TPM in males and 54.3 TPM in females, whereas *SNMP1* expression was not significant in this tissue. No SNPs were identified for either *MconSNMP1* or *MconSNMP2* further supporting the high level of conservation observed during BLAST analysis for the *SNMP* sequences. Mapping of *SNMP* genes onto the BAW draft genome shows that *SNMP1* is located on a different scaffold than *SNMP2*.

3.3.2.7 Candidate odorant degrading enzymes (ODEs)

As suggested by the Blast2Go analysis with respect to the distribution of GO terms, the BAW whole-head transcriptome had a high number of genes assigned to catalytic activity in the molecular function category. In agreement with this finding, 24 genes encoding putative enzyme implicated in odorant clearing and degradation were identified (Table A-3; tab ODE). These results are in agreement with reports from other lepidopteran species [Oakeshott et al. 1999; Durand et al. 2014]. Among the identified sequences, 12 corresponded to CXEs as candidates for degradation of acetate pheromones in the sensillar lymph. Alignment of the carboxylesterase

sequences showed that 10 of these contained a serine residue within the conserved *Gly-X-Ser-X-Gly* active site commonly shared by the α-/β hydrolase protein family [Oakeshott et al. 1999]. Phylogenetic analysis with CXE protein sequences from other lepidopteran species suggested that MconCXE4 and MconCXE11 belong to a clade of lepidopteran CXE proteins implicated in pheromone degradation (Figure 3-15). Transcript abundance evaluation with RSEM indicated that *CXE4* and *CXE11* transcripts were antennae-specific in both males and females (Figure 3-16). *CXE4* was expressed at a similar level in both males (145 TPM) and females (128 TPM), as was *CXE11*, although at lower levels of 26.9 TPM in males and 25.6 TPM in females. *CXE2*, *CXE3*, and *CXE5*-9 genes were expressed in both antennae and head with *CXE5* being expressed at higher levels in the head than in the antennae. Genes encoding a number of other enzymes, including one oxidase, two cytochrome P450 oxidases, two glutathione-S-transferases and seven reductases, were also identified. Analysis of the transcript abundance for sequences encoding the aforementioned enzymes revealed that they were antenna-specific and expressed at similar levels in both males and females (Table A-3; tab ODE).

SNP analysis identified 49 putative SNPs among genes encoding odorant-degrading enzymes (Table A-3; tab ODE). The highest number of SNPs (11) was found in the sequence of *CXE4*. Mapping of the SNPs to the *CXE4* sequence indicated that 9 of the 11 SNPs were located at positions within the protein sequence C-terminal to the serine active site (Figure 3-16).

3.5 DISCUSSION

A comprehensive chemosensory gene data set was obtained through bioinformatic analysis of the BAW whole-head transcriptome. The data set encompasses 130 putative chemosensory genes encoding 25 OBPs, 13 CSPs, 50 ORs, 13 GRs, 32 IRs, 2 SNMPs and 24 ODEs. The number of OBP sequences expressed in the BAW antennae is in agreement with other published results [Liu et al. 2012; Glaser et al. 2013; He et al. 2017]. The majority of OBP genes were expressed in the antenna, with the exception of two that were expressed in both head and antennal tissue. Twelve OBP genes were expressed at a low abundance in adult antennae, but may play a role prior to the adult phase or in another sensory tissue [Wanner et al. 2004]. Genes encoding PBPs and GOBPs were the most abundant transcripts among OBPs. Although all three PBP genes were expressed in both males and females, the expression of *PBP1* and *PBP2* was higher in males, whereas the

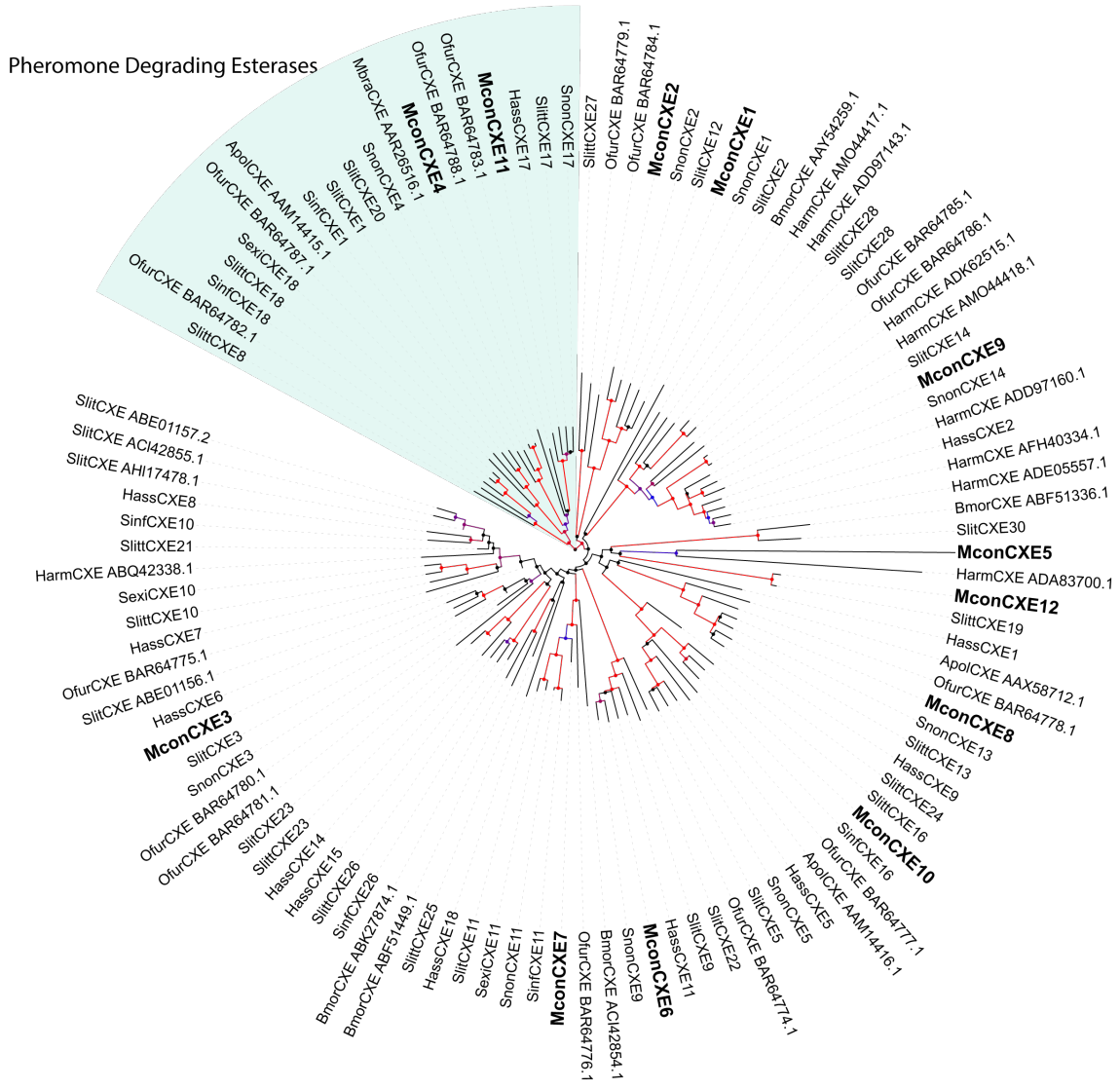

Figure 3-15 Maximum likelihood tree of lepidopteran carboxylesterases (CXEs). MconCXE4 and MconCXE11sequences were assigned to a clade (light green) containing several antennal esterases shown to degrade sex pheromones *in vitro* [Ishida and Leal 2005a]. The bootstrap values are indicated according to the heat color legend. Sequence abbreviations correspond to the following species names used in the analysis Apol (*Antheraea polyphemus),* Bmor (*Bombyx mori),* Harm (*Helicoverpa armigera),* Hass (*Helicoverpa assulta),* Mbra (*Mamestra brassicae*), Mcon *(Mamestra configurata)*, Ofur (*Ostrinia furnicalis*), Snon (*Sesamia nonagroides),* Sinf (*Sesamia inferens*), Sexi (Spodoptera exigua), Slitt (*Spodoptera littoralis),* Slit (*Spodoptera litura).* Branches supported by bootstrap values of 75% or higher are indicated by a color range from blue (75%) to red (100%). (See Table A-1; tab ODE for the list of sequences and accession numbers)

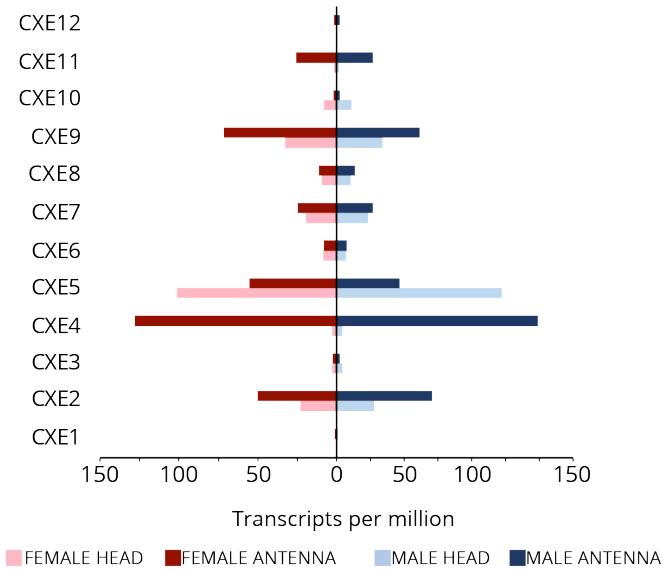

Figure 3-16 Expression analysis of genes encoding carboxylesterases (CXEs) based on the BAW whole-head transcriptome. Gene expression values are represented as transcripts per million. The light red and blue bars correspond to female and male head libraries, respectively, whereas the dark red and blue bars correspond to female and male antennal libraries, respectively. Transcript abundance is expressed in transcripts per million (TPM).

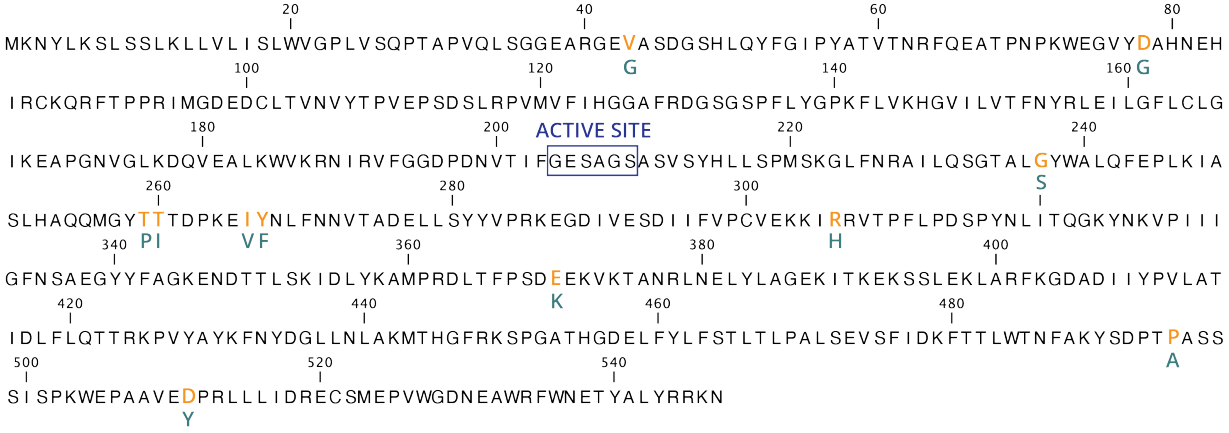

Figure 3-17 SNPs mapping to MconCXE4 sequence. CXE4 protein sequence with variant amino acids corresponding to SNPs predicted within CXE4 transcript. Variant amino acids are shown in orange with the second variant indicated below in blue. The active site sequence is indicated by the blue box.

abundance of *PBP3* was higher in females. The PBP gene expression profiles are consistent with reports from other lepidopteran species [Callahan et al. 2000]. The expression of *PBP3* in female antennae suggests that either BAW females detect their own pheromone components or pheromone produced by males [Schneider et al. 1998]. However, no male pheromone has been discovered for this species to date. A recent study of PBPs in *Maruca vitrata* showed that PBP3 was similar to GOBP2 with respect to affinity and binding energies for both pheromones and plant volatiles [Mao et al. 2016]. These results indicate that PBPs may have a dual role in transporting volatiles in sensilla tuned to pheromones and in sensilla tuned to plant volatiles. Several factors including the large number of OBP genes, their high levels of expression in antennae, and high degree of conservation (PBPs and GOBPs), imply that that these proteins contribute to the selectivity of the olfactory system [Brito et al. 2016]. Future studies in this area should include investigation of not only ligand spectra for OBPs, but also synergy between OBPs and the more specialized PBP and GOBPs.

In contrast to OBP genes, CSP genes were expressed in both the head and antennae with higher levels in the head. CSPs are a relatively newly-characterized family of chemosensory proteins and only a few studies have attempted to examine their biochemical properties. CSP19 from *S. inferens,* expressed as a recombinant protein, was shown to have a high affinity for the major pheromone components *in vitro* [Zhang et al. 2014]. The CSP encoded by the most highly expressed antennal BAW gene, MconCSP6, has 85% amino acid sequence identity to SinfCSP19, which was shown to bind all three female pheromones (Z11-16:OAc, Z11-16:OH, Z11-16:Ald) and a variety of plant volatiles. Considering that 19 CSPs were identified in *S. nonagrioides* [Glaser et al. 2013], 18 in *B. mori* [Gong et al. 2007], 21 in *S. littoralis* [Jacquin-Joly et al. 2012] and 21 in *M. sexta* [Große-Wilde et al. 2011], the number for BAW (13) is low and additional CSPs may exist. However, none of these reports included a study of the expression levels for the identified CSP genes and as my results suggest the number of active, biologically-relevant, antennal CSPs may be lower than the numbers reported for various lepidopteran species. Although, CSPs have been shown to bind odorants, such as pheromones and plant volatiles, their role in insect olfaction remains elusive [Fleischer et al. 2018].

Fifty putative OR genes were identified from the BAW transcriptome, including 5 PR genes and the OR co-receptor ORCO. Only two pheromone components of the female pheromone blend

have been found to evoke the stereotypical behavioral responses in BAW males [Struble et al. 1984a]. Thus, the presence of four male-specific PRs suggests that the BAW PRs have overlapping specificities, that more than one receptor can detect the same pheromone component, or that some of the PRs are tuned to pheromone antagonists. Three out of the four PR genes were expressed exclusively in males (*MconOR15, Mcon OR27,* and *MconOR42*). *MconOR29* transcripts were detected at very low level in females. The protein sequences of MconOR27 and MconOR29 are 89% conserved. In *D. melanogaster*, genes encoding ORs responding to pheromones were clustered in close proximity on the genome [Robertson et al. 2003]. Interestingly, *MconOR27* and *MconOR42* were on the same scaffold in the BAW draft genome, whereas genes encoding other ORs (including MconOR29) were scattered across different scaffolds. The discovery of a female-biased PR gene (*OR48*), suggests that BAW females may also be able to detect either their own pheromones or a male-produced pheromone. An SEM study of the BAW female and male antennae established that females possess Type 1 and 2 sensilla trichodea implicated in olfaction, but lack the Type 3 sensilla trichodea present in males [Liu and Liu 1984]. Further studies on BAW PR sensillar localization and ligand specificity are necessary.

As ORs are thought to be primarily responsible for the specificity of odorant recognition in insect olfactory processes, I was interested in whether any differences existed in the sequences and expression levels of these genes in BAW [Su et al. 2009; Zhang and Löfstedt 2015]. I did not find any significant variation in the expression levels of the five putative PR and ORCO genes among the three BAW populations. Progress in understanding the structural basis of insect OR function has been hampered by a lack of sequence similarity to known gated ion channel proteins and technical difficulties surrounding expression of recombinant transmembrane proteins for tertiary structure solution [Hughes et al. 2014]. Currently, our knowledge is limited to several studies involving mutagenesis-based screens for amino acid residues that vary between homologues, but occur within functionally distinct receptor subunits [Nakagawa et al. 2012; Leary et al. 2012; Kumar et al. 2013; Hughes et al. 2014; Yang et al. 2017]. In the OR TMD regions, amino acid polymorphism resulting from single point mutations were found to alter the selectivity and ligand binding kinetics of the receptor protein [Pellegrino et al. 2011; Leary et al. 2012]. For example, in two *O. nublialis* populations a single tyrosine to alanine (T148A) substitution in TMD3 altered the pheromone recognition specificity of the PR-ORCO channel

[Leary et al. 2012]. In *D. melanogaster*, a naturally-occurring polymorphism resulting in valine to alanine substitution (V91A) in TMD2 was found to alter N,N-diethyl-meta-toluamide (DEET) sensitivity of the OR [Pellegrino et al. 2011]. Although a change in the side chain from valine to alanine would seemingly be of little consequence to the structure of the channel, an example of this type was also reported in vertebrates where an alanine to valine mutation altered the function of a gated ion channel in the cardiac muscle [Laish-Farkash et al. 2010]. Thus, the SNPs affecting residues within the MconOR15 TMD7 region, the MconOR27 TMD6 region and the TMD1, 3 and 7 regions of OR29 could represent functionally-important residues. Furthermore, TMD6 and TMD7 were implicated in interaction of the OR with its co-receptor ORCO in *D. melanogaster* [Nakagawa et al. 2012]. In the only known 3D model of OR and ORCO using *D. melanogaster* proteins, the ECL2 was suggested to act as a lid interacting with the ligand active site of the heteromeric OR:ORCO complex [Hopf et al. 2015]. In the same study, the long extracellular loop of the OR was shown to be under strong evolutionary constraint suggesting its functional importance. My SNP analysis reported two SNPs for the *OR15* ECL2 region (A200V, R219K) and one in *OR27* (N180). Amino acid changes in the ICL2 and ICL3 region were also reported to affect PR ligand selectivity in two *Helicoverpa* species [Yang et al. 2017]. A tyrosine to isoleucine and phenylalanine to isoleucine substitutions in the ICLs were found responsible for the pheromone-binding profile of the receptor. In BAW, a SNP was detected in the ICL2 coding region of both *OR27* (F268T) and *OR29* (L290I). I did not find any SNPs in the ICL3 coding region, which has been suggested to form a molecular interface essential for ORCO interaction and, thus, any variation in this region would be detrimental to heteromeric complex formation [Hopf et al. 2015]. I also did not detect any SNPs in the sequences of *OR42* and *OR48* suggesting that these genes are under strong evolutionary selection. The localization of SNPs in BAW PR genes to residues and sequence motifs shown to be of consequence to the function of the protein is interesting in that it may indicate inherent points of sequence flexibility that allow males to adapt to changes in the female chemical signals over time. Another important observation provided by the SNP analysis was that much of the variation reported for the field-collected populations from AAFC-Davidson and AAFC-Vegreville is not present in the long-term AAFC-Saskatoon colony. The majority of the SNPs reported for the alleles in the AAFC-Saskatoon colony are fixed (invariant) in contrast to the 2nd generation of the field-collected individuals that have variable frequencies of each variant. If the variation in wild populations

predicted by the KisSplice algorithm does indeed exist in wild BAW populations, this may contribute to the variation observed with respect to the varied pheromone responses observed in wild populations. Confirmation of biological relevance for the predicted SNPs in the BAW populations, localization studies on OR expression in specific sensilla and odour profiles for each OR are required to further understand the various aspects of OR-mediated olfaction in this species.

A small number of GR genes were also identified that were expressed in both male and female antennae. Phylogenetic analysis categorized five of the protein sequences as putative sugar receptors and three as CO_2 receptors. In moths, CO_2 is an important volatile cue for localization of appropriate food sources [Xu and Anderson 2015; Ning et al. 2016]. *MconGR12*, which was expressed in BAW males and females at very low levels, is closely related to *S. littoralis GR4*, which is enriched in females and the corresponding receptor suggested to play a role in female oviposition [Jacquin-Joly et al. 2012]. I did not, however, detect a bias in *MconGR12* expression in females. All BAW GR genes expressed in the antennae had expression levels below 10 TPM, therefore, any conclusions with regard to their function in this organ will require further analysis.

Insect IRs are closely related to iGluRs and are thought to have evolved from this receptor family [Benton et al. 2009]. BAW was found to express 8 putative iGluR genes and 24 IRs. In *D. melanogaster*, IRs within the IR20a and the closely related IR52c/d clades have been implicated in pheromone detection and male courtship behaviour [Koh et al. 2014]. My analysis, however, did not find any IRs related to these two clades expressed in the BAW antennae, although most *D. melanogaster* antennal IR clades do have orthologues in lepidopterans. Functional characterization of moth IRs is still lacking. This analysis identified IR members of the highly conserved IR87a and IR75 clades, as well as the less conserved, Lepidoptera-specific IR1 clade; however, their ligands and functions are unknown at this time. In agreement with the SNP analysis for OR genes, analysis of the AAFC-Davidson and AAFC-Vegreville populations showed much higher diversity than the AAFC-Saskatoon colony.

The presence of SNMP1 proteins in the sensory neuron membrane of pheromone sensitive sensilla along with ORCO suggests their importance in pheromone signal transduction [Rogers et al. 1997; 2001]. Previous studies in *S. exigua* suggested that SNMP2 was present in the supporting neuronal cells and SNMP1 in the pheromone-sensitive OSNs [Liu et al. 2014]. In

D. melanogaster, SNMP1 is proposed to act as a membrane bound co-receptor with its ectodomain acting as a funnel that helps to unload the pheromone molecule from the PBP to its PR [Gomez-Diaz et al. 2016]. A similar role for SNMP1 has been proposed in moths based on differential tissue expression of *SNMP1* and *SNMP2*. *SNMP2* was found to be co-expressed with PBP genes in supporting neuronal cells of OSNs in pheromone-sensitive sensilla and, thus, proposed to participate in pheromone transport relay from the sensillar lymph; however, experimental evidence is still lacking [Forstner et al. 2008]. Interestingly, my analysis did show that *SNMP2*, but not *SNMP1*, was also expressed in the head, although at much lower level. Further functional studies are required to investigate the mechanism by which SNMPs mediate the interaction of odorants with their respective ORs.

The function of ODEs is well-established in the female pheromone gland; however, much less is known about their mode of action in the male antenna [Leal 2013]. From a repertoire of 27 putative ODE genes, I identified 2 encoding CXEs,3 encoding acyl-CoA reductases, one oxidase, two cytochrome P450 oxidases and two glutathione-S-transferases that had antennae-specific expression patterns in agreement with a previous report in *S. littoralis* [Durand et al. 2014]. In comparison to pheromone-binding proteins, the expression of genes encoding CXEs and reductases is several orders of magnitude lower in the antennae. Having different CXEs in the antenna would suggest that these enzymes may interact with different types of odorant molecules. However, my analysis did not identify a male-biased CXE gene in the antennae suggesting that degradation of pheromone components does not require the specificity observed for pheromone recognition steps by PBPs. Interestingly, the most highly expressed antennae-specific CXE gene in BAW also showed the highest degree of variation among the three populations. Out of the 49 SNPs detected for all ODE coding transcripts, 11 were found in the sequence of *MconCXE4*. In *D. melanogaster*, a specific CXE was shown to modulate the physiology and behaviour of the fly in response to its pheromone [Chertemps et al. 2012]. Many transcriptomic analyses to date focus on the genes encoding PBPs and PRs as potential targets for pest control. Odorant degradation is often overlooked, but this area requires particular focus as it can identify potential targets for the disruption of sexual communication as possible means of pest control.

3.6 CONCLUSION

This study generated a "whole-head" transcriptome reference for a persistent canola pest, BAW. The analysis was focused on cataloguing the olfactory genes with emphasis on the major chemosensory proteins involved in pheromone detection and deactivation. The results provide a starting point for functional and mechanistic studies of the key proteins and enzymes implicated in BAW olfaction. In addition, characterization and annotation of sequences from BAW will serve as a foundation for comparative studies with several other noctuid lepidopteran pest species across the Canadian prairie provinces. The novel approach for SNP determination directly from high throughput sequencing reads can be used as an accessible platform for future studies on genetic variation among geographic populations. The results also suggest that, at least with respect to the chemosensory genes, the colony-reared individuals exhibit less genetic variation than wild populations. As our knowledge of the pheromone communication in lepidopterans increases, it is becoming apparent that both signal production and detection are shaped by the unique insect environment and, thus, studies of genetic variation in non-model species is likely to play an important role in increasing our understanding of insect olfaction.

CHAPTER 4. BAW MALE RESPONSE TO SYNTHETIC PHEROMONES AND FEMALE-PRODUCED PHEROMONE BLEND

4.1 INTRODUCTION

For a semiochemical to be classified as a pheromone, the compound must be produced by a conspecific individual and elicit a behavioural response [Karlson and Luscher 1959; Vogt and Chertemps 2005]. The sex pheromone glands of noctuid female moths typically contain a mixture of compounds; however, not all of the components produced elicit a physiological response [Linn et al. 2003; Baker 2008]. In addition, some components may produce a large electro-physiological response, but do not elicit the relevant behaviour [Löfstedt et al. 2016]. As the biological relevance of the female-produced sex gland components must be determined based on the male response to those compounds [Baker 2008], rigorous studies of the electro-physiological response to individual compounds or compound mixtures should be complemented by behavioural bioassays to verify the pheromone status of the candidate odorants [de Bruyne and Baker 2008; Millar 2014]. Field-trapping and wind tunnel bioassays have been employed to study the male response to sex pheromones of their conspecific females [Allison and Cardé 2016b]. Although field-trapping bioassays evaluate the attractiveness of the pheromone blend under natural conditions, they rarely allow for the observation of insect behaviour [Cardé and Elkinton 1984]. Wind tunnel bioassays can also serve as an evaluative tool for attractiveness of pheromone blends, but in addition allow for observation and analysis of insect behaviour [Baker and Linn 1984]. Electroantennographic detection, either alone [Roelofs 1984] or coupled to gas chromatography [Struble and Arn 1984], allows for investigation of the electrophysiological response from the male antenna to individual pheromone components and other pheromone gland constituents. Together, the behavioural bioassays with electrophysiological recordings provide a powerful tool for studying the male response to pheromones.

4.1.1 Wind tunnel bioassays

Wind tunnels have been used in a wide range of studies including pheromone component isolation and identification [Hill and Roelofs 1981], determination of the behavioural roles of pheromone components and blends [Miller and Roelofs 1978; Linn and Gaston 1981], the response profiles of blends and concentrations [Baker and Cardé 1979; Linn and Roelofs 1981; 1983], habituation, sensory adaptation and disruption orientation [Kuenen and Baker 1981; Linn and Roelofs 1981; Phelan and Miller 1982], and the neural basis of the flight mechanism [Tobin 1981; Baker and Linn 1984; Willis and Baker 1984; Willis et al. 1994; Crespo et al. 2013]. Wind tunnels utilized for neuroethological[11] research serve as physical models of the field conditions encountered by flying insects [Baker and Linn 1984]. Although field bioassays involving capture of the males in response to a chemical lure are the ultimate test for a pheromone blend's activity, it is often desirable to conduct similar types of experiments in a controlled environment where observation of insect behaviour is also possible. In contrast to field-trapping bioassays, experiments carried out in the wind tunnel permit the manipulation of one experimental variable at a time, while controlling temperature, humidity, wind velocity and chemical plume characteristics [Allison and Cardé 2016a]. A wind tunnel bioassay allows for observation of a repertoire of male behaviours from pheromone activation and stereotypic wing fanning, upwind flight initiation, locking on the plume and source location [Baker and Linn 1984]. Characteristics associated with each of the behaviours can provide information on the quality and completeness of the pheromone blend used [Witzgall 1997]. Lack of activation and wing fanning may indicate complete blend mismatch or missing blend components [Baker and Vickers 1997; Baker 2008]. If release rates, concentration of the blend or the ratios of components deviate from the natural source, the activation may take place; however, accurate flight and source location may be inhibited [Kuenen and Baker 1982a; Willis and Baker 1984; Kuenen and Siegel 2015]. Inaccurate concentrations and ratios have been shown to induce prolonged flights or slower flights with males never reaching the source [Kuenen and Baker 1982a; Kuenen et al. 2014]. Flight accuracy may also be assessed by male flight characteristics, such as flying too high, too low or in an exaggerated zig-zag pattern indicating an inability to "lock on" to the odour plume properly [Allison and Cardé 2016a]. In field-trapping bioassays, the location of the pheromone

[11] neuroethology: evolutionary and comparative approach to the study of animal behaviour and its underlying mechanistic control by the nervous system

source may be more accurate as the males are already in flight and exposed to other sensory information which may aid in subsequent source finding [Cardé and Willis 2008; Cardé 2016]}. In contrast, during the wind tunnel experiments, the male moths are introduced into the tunnel in a quiescent state and often never having flown before. Experiments with nocturnal moths have shown that many species require a minimum acclimatization time to wind tunnel conditions, especially the light lux, for normal flight behaviour [Baker and Linn 1984]. If the acclimatization time is omitted, poor flight performance or even flight inhibition may result [Linn and Gaston 1981]. Experimental evidence also suggests that initial exposure of males to the pheromone source does sensitize them and improves their ability to orient to the source in subsequent exposures [Anderson et al. 2003]. In addition to insect handling, optimization of factors, such as temperature, humidity, wind speed, light levels and contamination, must be considered during the experimental design [Baker and Vickers 1997].

4.1.2 Electrophysiological bioassays

4.1.2.1 Electroantennography (EAG)

The electroantennogram (EAG) is postulated to represent the summed slow receptor potential generated across the sensory epithelium of the antenna by a population of olfactory sensory neurons (OSNs) simultaneously responding to the odour stimulus [Schneider 1969; Roelofs 1984]. A classical EAG experiment records a potential difference between the recording electrode placed at the distal end (the antennal tip) and the reference electrode placed at the proximal end (base of the antenna) [Schneider 1969]. The EAG signal represents changes in the slow receptor potential of the antenna as a function of time [Schneider 1969]. For most insects, absolute values of the EAG signal range between a few microvolts (μV) to several millivolts (mV), and rarely exceed 5 mV [Olsson and Hansson 2013]. The shape of the EAG signal corresponds to a quick hyper-polarization occurring within ~100 ms of stimulus application, followed by a much slower recovery [de Kramer et al. 1984]. The amplitude of the signal deflection and the half-time decay of the EAG are used to assess the potency of the stimulus [Roelofs 1984; Olsson and Hansson 2013]. Since its introduction by Schneider [Schneider 1957], the EAG bioassay has been widely applied in entomological research for rapid detection and characterization of insect olfactory responses to chemically-active compounds [Roelofs 1984; Bigiani et al. 1989; Lucas and Renou 1992; Hansson et al. 1994; Sasaerila et al. 1997; Malo et al. 2000; Crnjar et al. 2011; Jacob et al. 2017]. In particular, whole antenna EAGs have

been instrumental in predicting the absolute isomeric configuration of the sex-pheromone components [Roelofs 1984] and evaluation of relative antennal response to compounds which cannot be isolated or identified due to their low natural abundance [Miller et al. 1977; Cardé et al. 1977b]. However, despite the widespread use of this technique, the full theoretical understanding of the mechanism responsible for generation of EAGs during electrophysiological recording in insect antennae is lacking [Kaissling 1995].

At least in part, the observable EAG changes due to olfactory stimulation can be interpreted from our understanding of the bioelectric properties of the OSN [Kaissling 1995]. OSNs exhibit inherent structural asymmetry with the slender dendrites projecting into the lumen of sensillar hair and the corresponding globular soma lying below the multi-laminar cuticle of the antennae (Figure 4-1A) [de Kramer 1985]. Excitation of the receptor proteins embedded in the dendritic membrane of the OSN elicits opening of ion channels and influx of cations into the dendrite [Kaissling 1986]. Subsequent accumulation of negative charges in the sensillar lymph surrounding the dendrite results in the generation of an electrical dipole between the negatively charged distal sensillum and the positively charged OSN soma (Figure 4-1B) [Nicholson 1973]. The organization of sensilla along the same plane and orientation on the surface of the antenna is thought to further accentuate the dipole differential (Figure 4-1C) [Kaissling 1995]. In early experiments on olfactory stimulation, a gradient in response potential generated along the length of the whole antenna was found to become more negative towards the distal end of the antenna [Nagai 1981; 1983a] and proposed to be responsible for the negative charging of the recording electrode [Kaissling 1995]. In EAG recording from *O. nublialis* antennae, for which the distribution of the sensillar hair types is approximately uniform throughout the whole length of the antenna, the relationship between the initial negative potential and the length of the antenna was found to be linear [Nagai 1981]. The amplitude of the deflection was shown to increase with increasing concentration of the stimulus until saturation was observed [Roelofs 1984]. Furthermore, stimulation of various segments of the antenna showed that sensilla located near one of the electrodes contribute more to the EAG than sensilla located further away [Nagai 1983b]. Nagai also suggested that the fast negative initial charge observed with the voltage

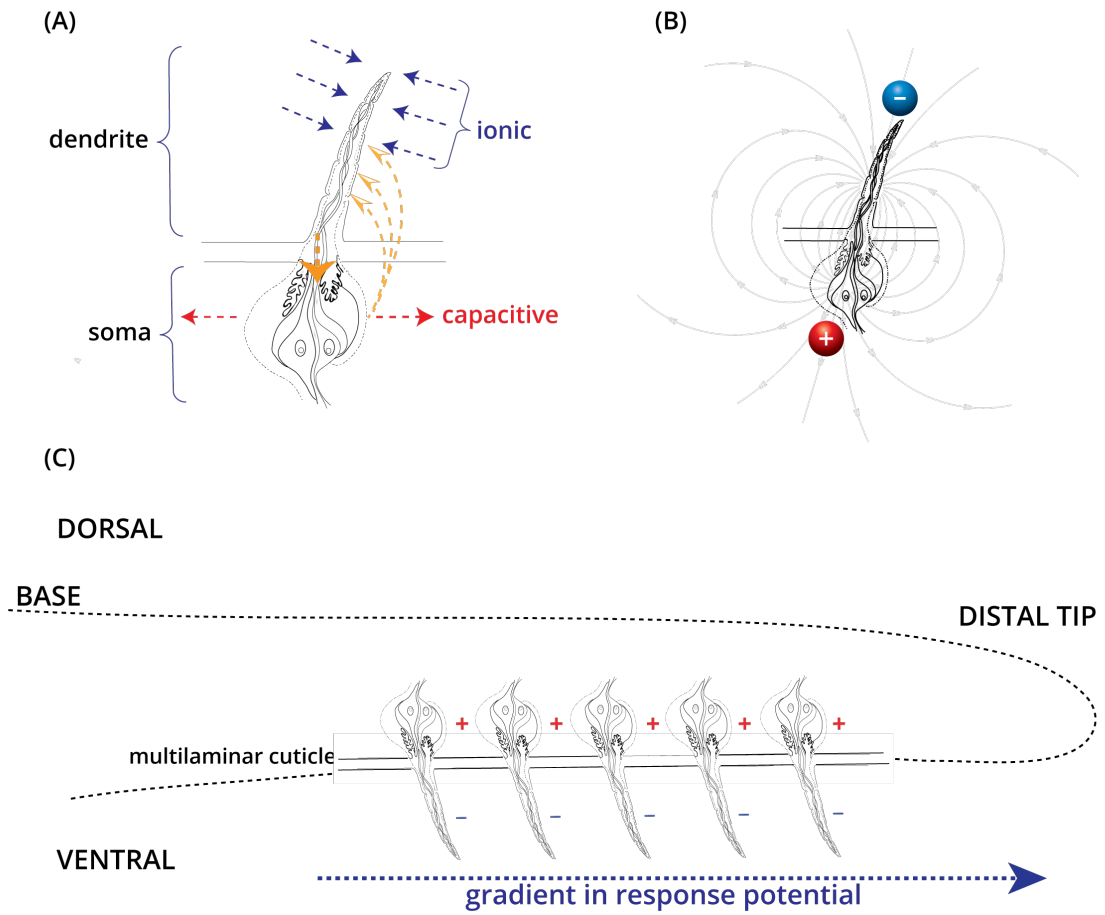

Figure 4-1 Bioelectric properties of the OSN unit housed within trichoid sensillum on moth antennae. **(A)** Each OSN can be divided into two distinct compartments, the dendrite and the soma. The OSN is activated via excitation of the receptor proteins embedded in the dendritic membrane by opening of ion channels and influx of cations into the dendrite (blue arrows). The sensillar lymph surrounding the dendrite becomes a current sink (red arrows). In contrast, the capacitive current of the soma (dashed yellow arrows) generates a current source in the sensillar lymph. The intracellular current flowing between the two compartments (dashed orange arrow) is equal and opposite to the current flowing in the sensillar lymph. **(B)** Theoretical representation of the electric field generated between the distal sensillum and soma. Inherent asymmetry of OSN and intra- and extracellular current flow contribute to the generation of an electrical dipole. **(C)** The organization of sensilla along the same plane and with the same directionality on the surface of the antenna is thought to further accentuate the dipole differential. Thus, during olfactory stimulation, a gradient in response potential generated along the length of the whole antenna becomes more negative towards the distal end of the antenna and is proposed to be responsible for the negative charging of the recording electrode. Adapted from Stengl (2010), Jacob (2018).

deflection is accompanied by a slower electrotonic[12] spread across the epithelial surface of the antenna that serves as a signal amplification mechanism [Nagai 1983a]. As a result, the EAG response is thought to arise from the transduction currents and spread from the stimulated antennal region across the antennal surface [Schneider 1969; Kaissling 1986]. As an extracellular recording technique, EAG is limited in its ability to quantitatively estimate the sensitivity of an insect to the chemicals tested. The recorded amplitude of the response does not necessarily correlate to the insect's ability to detect the chemical. In addition, EAG analysis can become even more complex for general odours which can stimulate several classes of different OSNs [Baker 2008].

4.1.2.2 Gas chromatography coupled electro-antennographic detection (GC-EAD)

The EAG recording technique can be coupled to gas chromatography (GC) [Struble and Arn 1984; Olsson and Hansson 2013]. Coupling of EAG to GC has resulted in the development of an extremely sensitive and specific detection system for the identification of pheromone components. This development alone has allowed for characterization of the large number of pheromone blends currently knowns for lepidopteran species [Löfstedt et al. 2016]. GC involves the separation of complex mixtures by means of the differential partitioning of compounds between a "stationary" phase and a "mobile" phase [Sparkman et al. 2011]. During GC separation, a volatile mixture is flash-evaporated into a stream of inert gas (mobile phase) moving through a long, capillary, glass, column tube modified with a semi-solid wax or polymer (solid phase). The separation of the mixture components depends on their affinity for the column components, as well as the temperature. The column is housed in an oven whose temperature can be precisely controlled. The effluent of the GC column is delivered to a detector that produces a DC voltage whose amplitude is proportional to the concentration of compound eluting from the column at a specific time. The most common detector is a flame ionization detector (FID), which is sensitive to all organic molecules. The output of the detector is normally displayed on an X-Y graph with the Y-axis representing detector voltage and the X-axis representing time. With the same column and GC operating conditions, a compound will always elute with the same retention time (t_r), hence retention time can be used for identification of unknown compounds. In GC-

[12] **electrotonus** in physiology refers to the passive spread of charge inside a neuron; passive means that voltage-dependent changes in membrane conductance do not contribute

EAD, the effluent from the end of the column is split in two, with one portion of the effluent delivered to an FID and the other passed into a stream of purified air and delivered to an insect's antenna [Struble and Arn 1984]. The EAD experimental set up resembles the EAG set up with the antennal preparation placed on a recording probe or recording electrodes in a stream of humidified air [van der Pers and Ockenfels 2004]. Antennal responses, detected as changes in voltage (mV) and FID signal, are coupled and plotted versus the time axis. Synchronous voltage changes in the FID and the EAG indicate olfactory sensitivity by the insect to the compound eluting at the characteristic retention time. The FID output can be used to confirm the presence, identity, and quantity of compounds exposed to the antenna, whereas the antennal (EAG) output indicates presence/absence of olfactory response to eluted compounds and provides a relative measure of the intensity of olfactory stimulation [Struble and Arn 1984]. Separation of mixtures into individual components prior to their contact with the antennal preparation ensures their purity and allows for their identification based on the retention times [van der Pers and Ockenfels 2004]. This technique has proven invaluable in identification of biologically-active compounds [Struble and Arn 1984; Löfstedt et al. 2016], as well as identification of their carbon-chain length [Roelofs et al. 1976; Roelofs and Cardé 1977], isomer status and activity [Cardé et al. 1977b; Linn and Roelofs 1981], and often detection of compounds that are in concentrations too low to be observed on the GC trace alone [Hill et al. 1975]. Once the prospective components of the pheromone blend are identified, their attractiveness, appropriate blend ratios and concentration can be tested using male behaviour as the ultimate diagnostic.

4.1.3 Evaluation of BAW behavioral response to female pheromone gland extracts

The male BAW behavioural response to the female pheromone gland extract components was used as a diagnostic measure during initial identification of major and minor pheromone components [Chisholm et al. 1975; Underhill et al. 1977a]. These early studies employed single tube olfactometer bioassays for evaluation of male behavioural response to either female pheromone gland extracts or synthetic mixtures of semiochemicals [Chisholm et al. 1975]. The male response was evaluated based on the observation of six "key" markers including; 1) antennal movement, 2) rapid wing vibration, 3) upwind flight, 4) extension and curvature of the abdomen, 5) clasper extension, and 6) copulatory attempts with other males. The activity of fractions resolved via GC was confirmed via olfactometer bioassays and EAG recordings. Chisholm et al. (1975) initially reported (*Z*)-11-hexadecenyl acetate (*Z*11-16Ac) as a major

attractant; however, traps baited with Z11-16Ac alone failed to attract BAW males in the field [Underhill et al. 1977a]. Underhill et al. (1977a) identified (*Z*)-9-tetradecenyl acetate (*Z*9-14Ac) as the minor active component of the female, pheromone blend necessary for male attraction. EAG analysis was carried out to confirm the carbon-chain length and determine the position and configuration of the double bond for both the major and the minor pheromone components [Chisholm et al. 1975]. The attractive ratio, defined as 19:1 of Z11-16Ac to Z9-14Ac, was determined based on field, lure-trapping experiments and field-cage experiments [Chisholm et al. 1975; Underhill et al. 1977a]. GC-EAD experiments were eventually used to confirm the activity of the pheromone components and to evaluate the attractiveness of the other components present in the female, pheromone gland extracts [Steck et al. 1984; Struble et al. 1984]. Struble et al. (1984b) reported the presence of Z7-12Ac, Z9-14OH, Z7-16Ac, Z9-16Ac and Z11-16OH, in addition to Z11-16Ac and Z9-14Ac; however, only Z11-16Ac and Z9:14Ac produced a response profile in GC-EAD experiments. Additional field-trapping experiments showed that among 25 known lepidopteran semio-chemicals tested as synthetic additives to BAW pheromone lures, Z5-12Ac, Z7-12Ac, Z7-14Ac and Z11:14OH affected specificity, but not potency, Z9-16OH and Z11-16Ald affected potency, but not specificity and Z11-16OH affected both potency and specificity. The presence of Z11-16OH, which is present in female pheromone glands as a precursor of Z11-16Ac, was reported as a particularly potent inhibitor of BAW male catches in trapping experiments [Steck et al. 1984]. Since the initial identification, no further work has been carried out on BAW pheromones. The GC-EAD profile responses, as well as much of the EAG results, were not included in these reports. The report by Steck et al. (1984) does refer to "ancillary flight tunnel experiments," however, no results and no data were reported for these studies. Since these initial reports, no further investigations have addressed the behavioural and electrophysiological responses of BAW males field populations to the female-produced pheromones. An extensive field-trapping study, including eight cutworm and armyworm species in western Canada, noted that BAW-specific blends used in lures during the study were less specific than lures for other species resulting in high by-catch of non-target species [Byers and Struble 1987]. In the same study, the authors also mention that the proximity of the traps baited with BAW-specific pheromone blends to canola fields increased specificity and decreased the number of non-target species in the traps.

As outlined in the minutes from the 2011 Western Committee of Crop Pests Annual Meeting, anecdotal evidence from farmers and agronomists suggested that BAW populations develop at different rates and respond differently to the synthetic pheromone lures utilized in pheromone traps across western Canada [2011]. The observed differences in development and male response to the commercially-available lures were identified as a potential cause for poor predictability of economically-relevant levels of infestations for BAW. Thus, the objective of this study was to investigate if any differences in the behavioural or physiological responses to pheromones exist among BAW populations. During the last major BAW outbreak (2011-2014), egg masses and pupae were collected from several distinct geographic locations across western Canada. The eggs and pupae were placed under standard rearing conditions and reared to produce adult moths. In addition to the AAFC-Davidson and AAFC-Vegreville populations used in the transcriptomic analysis (Chapter 3), an effort was also made to establish populations representative of AAFC-Regina and AAFC-Lethbridge. My experimental design involved behavioral wind tunnel and electrophysiological experiments with insects from all four field populations and the AAFC-Saskatoon laboratory-reared colony. However, before the wind tunnel set up and optimization was complete, the AAFC-Regina, AAFC-Lethbridge and AAFC-Vegreville populations collapsed for unknown reasons. Thus, the experiments described in Chapter 4 involve only the AAFC-Saskatoon colony and AAFC-Davidson populations.

4.2 MATERIALS AND METHODS

4.2.1 Pupal size assessment

Individual pupae were collected within 24 hours of pupation and weighed on a Mettler AE163 scale. The pupal weight data was analyzed with Statistix10 (Analytical Software, Florida, USA) using one-way ANOVA and Tukey's HSD all-pairwise multiple comparisons test for variance.

4.2.2 Scanning electron microscopy

M. configurata antennae were excised at the pedicel from female and male moths (aged 48h). Antennae were dehydrated using a 50, 70, 80, 90, 95 and 100% ethanol series for 30 min. After freeze-drying, the specimens were mounted on aluminium stubs with double-sided sticky tape and coated with gold-palladium. The antennae were viewed using a scanning electron microscope (Phenom G2Pure, Phenom-World, Eindhoven, Netherlands).

4.2.3 Wind tunnel bioassays

All wind tunnel experiments were carried out in a plexiglass wind tunnel (3 m x 1 m x 1 m (L x H x W)) (Figure 4-2). The temperature of the room was kept at 22 ± 3 ℃ and the relative humidity at a minimum of 50% ± 15% (adjusted with 2 commercial electric humidifiers). Illumination was provided by small LED IR source and one red incandescent light bulb to give a light intensity of of 0.5-0.7 lux). Wind speed was kept constant at 0.3 m/s. The odour plume was vented at the downwind end of the wind tunnel via a large exhaust duct. The floor of the wind tunnel was lined with white fabric marked by large (diameter=10 cm) red circles. A Canon XA 20 semi-professional video camera with IR light detector mounted 1.9 m directly above the wind tunnel (top view) was used to record each trial. The odour source was positioned using a metal stand with a holder, 50 mL Erlenmeyer glass flask, and a heavy rubber stopper with mounted alligator clip on a metal post. The alligator clip was used to hold the filter disk with the odour source. When not in use, the clip and disk were stored inside the vial and sealed by the rubber stopper (Figure 4-2 inset). To introduce the odour source, the rubber stopper was flipped to expose the alligator clip to the air flow and set in the opening of the flask. Once mounted upright for the odour release, the distance of the filter disk was 20 cm from the floor of the wind tunnel floor. The insect release stand was positioned in the horizontal centre of the wind tunnel 1.2 m downwind from the pheromone source. To ensure that the release cage was placed in the center of the odour plume, titanium tetrachloride ($TiCl_4$; ~200 μL) was applied onto a circular filter paper disk (Whatman Grade GF/D, 10 mm diameter; GE Healthcare Life Sciences) and mounted as for the odour source on the flask. The wind tunnel was switched on and the stand position adjusted until the release cage was in the center of the air plume visible due to the $TiCl_4$ smoke. The position of the stand with the release cage was marked. The tunnel was vented for at least 1 hour prior to carrying out any experiments. This test was performed prior to each set of experiments to ensure that the release cage was always positioned in the center of the air plume. One day preceding the wind tunnel flights, during the photophase, 2-4 day old male moths were transferred into individual 4 x 6 cm cylindrical mesh cages with a sugar-honey solution strip. The following day the mesh cages containing insects were placed in a dark insulated container and were transferred to the wind tunnel room. The insects were acclimatized for 1 h prior to the experiments before they were tested 4-7 hours into the scotophase.

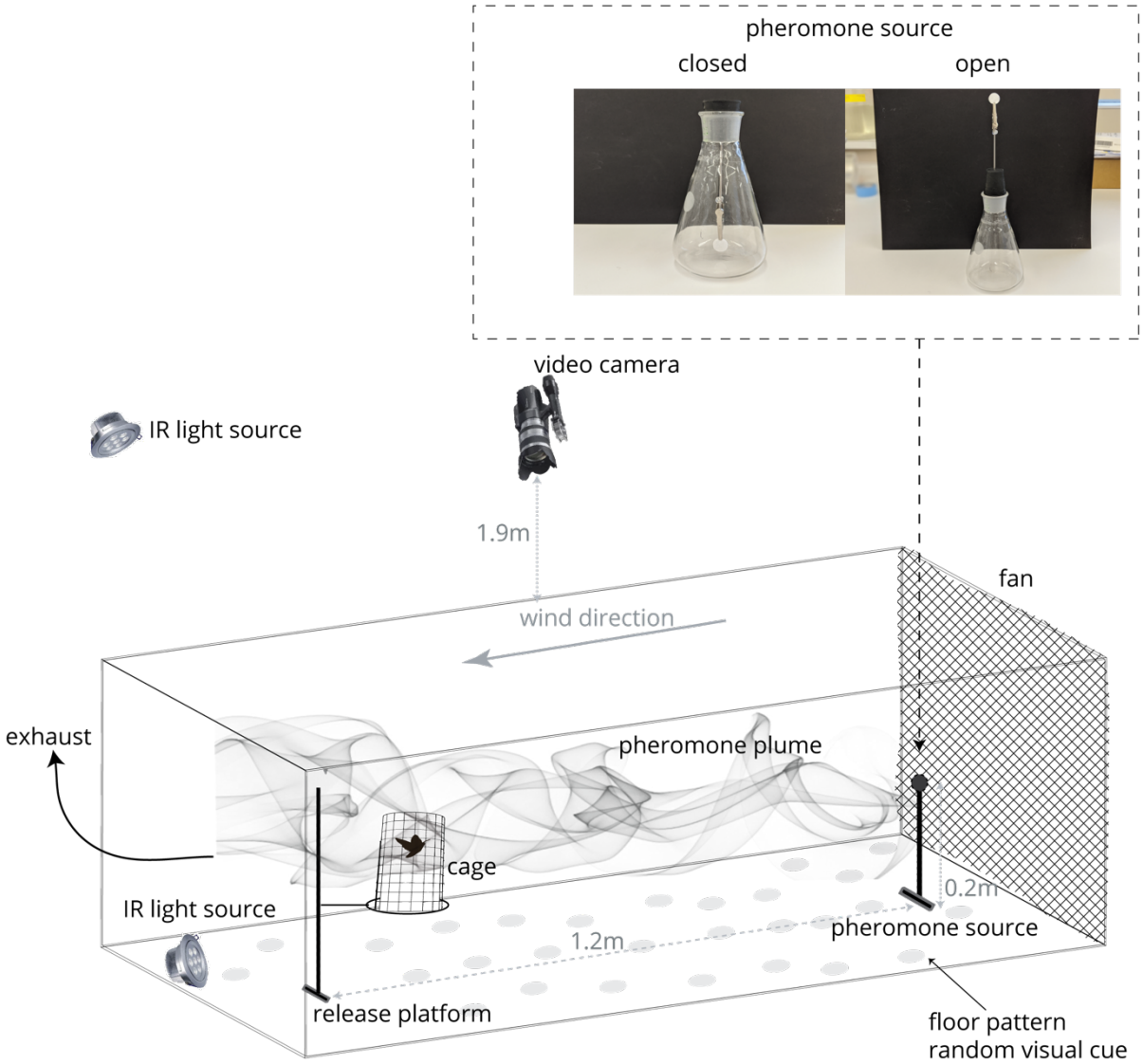

Figure 4-2 The experimental set-up for wind tunnel bioassay. Fine mesh placed in front of a flat blade fan was used to produce laminar air flow throughout the wind tunnel. The pheromone source was placed 1.2 m upwind from the release platform on which an open top cage with the moth could be placed. The entire area of the wind tunnel was captured with an IR sensitive Canon video camera positioned 1.9 m from the top side of the wind tunnel structure. The two IR sources, one placed on top of the tunnel and one directly behind the release platform, allowed for camera recording without affecting the light lux. The pheromone source was placed 20 cm from the floor base of the tunnel so that the floor pattern could be utilized by the moth as a navigation cue [Kuenen and Baker 1982b]. The tunnel was vented via exhaust fan downstream behind the release platform.

The blend ratio of 19:1 of Z11-16Ac and Z9-14Ac was previously described by Byers et al. and used as formulation for the commercially-available pheromone traps (Contech Enterprises, Canada) [Byers and Struble 1987]. Concentrated solutions of Z11-16Ac and Z9-14Ac were used to make volumetric dilutions in hexane until a concentration of 100 ng/μL for Z11-16Ac and 10 ng/μL for Z9-14Ac was achieved. The odour source was prepared by loading 950 ng of Z11-16Ac and 50 ng of Z9-14Ac (19:1 ratio) onto a circular filter paper disk (Whatman Grade GF/D, 10 mm diameter; GE Healthcare Life Sciences) and the hexane solvent evaporated in the fume hood for 5 min at room temperature. A control filter disk was also prepared by applying hexane only. The odour source disk was replaced every 30 min during the bioassay to ensure consistent release. The flask, rubber and alligator clip were rinsed with ethanol after each use and left in the fume hood to dry.

All recordings were collected between the 4^{th} and 7^{th} hour of scotophase as follows. The mesh cage with a male moth was placed in the wind tunnel and left for 1 min. The males were introduced in a quiescent state. The control disk with hexane was introduced for 30 s and the behavior of the moth was observed. Subsequently, the camera was switched on immediately prior to introduction of the odour source to the wind tunnel. Each recording was stopped at 4 min after the introduction of the pheromone source. The moth and the pheromone source were removed from the wind tunnel. The wind tunnel was vented for 4 min prior to introduction of the next insect. Responses to the pheromone source were based on five distinct markers along the flight track; 1) wing fanning, 2) flight initiation, 3) lock-on, during which the male flew near the base of the take-off platform while attempting to 'lock-on' to the odour plume, 4) directional flight, and 5) source contact, during which the male hovered within 10 cm or making contact with the source. The time data collected for each moth and corresponding to; 1) time of the wing fanning onset recorded from pheromone source introduction, 2) wing fanning duration prior to flight takeoff, 3) time required for plume lock-on, and 4) total flight duration was analyzed with Statistix10 (Analytical Software, Florida, USA) using Shapiro-Wilk normality test and Wilcoxon rank sum test.

4.2.4 Gas chromatography coupled electroantennographic detection (GC-EAD)

The GC-EAD analysis was carried out at Simon Fraser University with technical assistance from Regine Gries. The capillary gas chromatography analysis was carried out on Hewlett-Packard

5890 gas chromatograph fitted with a fused silica column (30 m x 0.25 mm coated with DB-5 (J&W Scientific, Folsom, California, USA) and a custom-built head-stage amplifier. A male insect antenna was gently "plucked" from the head. The basal end with intact nerve fibers was placed into the opening of a capillary glass reference electrode (1.0 x 0.58 x 100mm) (A-M Systems, Inc) filled with saline solution (in mmol/L: glucose 22.5, NaCl 25, KCl 172.0, KH_2PO_4 9.2, K_2HPO_4 10.8, $MgCl_2$ 3.0, $CaCl_2$ 1.0, HCl 1.5; pH 6.5) [Kaissling 1995]. The distal tip of the antenna was cut with spring micro-scissors and placed into the recording capillary electrode. The head stage amplifier was placed at the GC column outlet delivering eluate and cooled by a surrounding glass tube circulating cold water. One female gland equivalent in hexane was injected into the GC and the male response recorded with an analog printer. Prior to resolving a pheromone blend of interest, the column was calibrated by resolving a commercial standard containing 18-25 carbon chain compounds. In total, 10 male antennal preparations were tested for both AAFC-Saskatoon and AAFC-Davidson strains with extracts from 10 female pheromone glands from respective populations.

4.2.5 Electroantennography (EAG)

Synthetic pheromone components, (Z)-11-hexadecenyl acetate (Z11-16Ac) and (Z)-9-tetradecenyl acetate (Z9-14Ac), as well as Z11-16Ac precursor (Z)-11-hexadecenol (Z11-16OH) and cis-3-hexenyl acetate (3HAC) were used to prepare odour delivery cartridges. A solution of each volatile compound in hexane (concentration range 0.01-1000 μg) was applied as 10 μL to a small piece (2 cm x 0.5 cm) of filter paper folded into an accordion fold. The solvent was evaporated at room temperature and the filter paper was inserted into a glass Pasteur pipette. The cartridges were prepared fresh for each recording and the ends were sealed with dental wax when not in use.

Syntech probe holders and electro-conductive gel were used for electroantennographic detection. Individual antennae were excised from males and females and placed in electroconductive gel with the distal tip of the antennae clipped as for GC-EAD and contacting the recording probe. The antennal preparation with the probe was positioned in the middle of the humidified airstream and approximately 3 cm from the location where the odour stimulus was introduced. EAG signals from the antenna were amplified with a 10 X amplifier (Syntech), recorded and further processed with a PC-based signal-processing system (Syntech). The main airflow was adjusted

to ~1-2 mL/min. Odour stimulation was administered by injecting a puff of purified air (0.5 sec at 5 ml/min airflow) through an odour cartridge using an electronically controlled stimulus flow controller (Syntech).

The recordings were performed on antennae from 48-72 hour-old males. Each stimulus was followed by a 1 min recovery of the antennal preparation to allow the EAG signal to return to baseline and stabilize. Air and hexane were used as controls at the beginning and end of each experiment. Antennal preparations were stimulated with increasing amounts of the pheromone component. Each consecutive pheromone stimulation was followed by stimulus with 100 µg 3HAC. Each response to the pheromone component was normalized to the stimulus response from 3HAC using the following formula:

Equation 4-1 Normalized EAG response amplitude.

$$Response\ (mV) = \frac{R_P \times Avg(R_{3HAC})}{R_{3HAC}\ closest}$$

Where Rp is response to the pheromone stimulus (mV), R_{3HAC} is the response to 3HAC (mV) either as an average or the stimulus following the pheromone stimulus (R_{3HAC} closest). Only one pheromone component was tested per cohort per day to prevent contamination. All surfaces and probes were wiped with ethanol after completion of each experiment. All statistical analysis was carried out with Statistix10 (Analytical Software, Florida, USA). The data was analyzed with Shapiro-Wilk normality test to confirm the normal distribution. Parametric Levene's test was used to check for equal variances. The normalized responses to each pheromone component were analyzed using one-way ANOVA (significance level p=0.05) and Tukey's HSD all-pairwise comparison test. The normalized responses to each dose amount between the two populations were analyzed with a paired T-test (significance level p=0.05).

4.3 RESULTS

4.3.1 Pupal size assessment

AAFC-Saskatoon males were used during the initial set up of the wind tunnel and optimization of conditions. When exposed to the commercial BAW pheromone blend source placed upwind from the release platform, the males elicited classical wing fanning behaviour and would subsequently take off, but rather than flying towards the source they would drop off the platform and were unable to take off again. Only a small number of the AAFC-Saskatoon males (typically

1-2 out of 10) were able to take flight. In contrast, when males from the 3rd generation AAFC-Davidson and AAFC-Vegreville populations were tested under the same wind tunnel conditions they typically could successfully takeoff, fly and locate the pheromone source. While handling the insects, I observed considerable difference in body size between the AAFC-Saskatoon and the weight difference between the colony and the two field populations (Figure 4-3). To determine whether there is a significant body, I weighed both male and female pupae from AAFC-Saskatoon, AAFC-Davidson and AAFC-Vegreville populations, as well as two additional field populations AAFC-Regina and AAFC-Lethbridge. The pupal weights collected at 48 h post pupation were analyzed with one-way ANOVA and means for each population compared using Tukey HSD all-pairwise comparison test (Figure 4-4). Males (LM) and females (LF) from AAFC-Lethbridge had the lowest pupae weight (LM=0.2632±SE0.0102 g; LF=0.2938±SE0.0009 g), whereasAAFC-Saskatoon males (CM) and females (CF) had the highest pupal weight (CM=0.3291±SE0.0073 g; CF=0.3660±SE0.0009 g). The AAFC-Saskatoon pupal weights were significantly different for male pupae [$F(4,413)=10.97$, $p=0.00$] and female pupae [$F(4,435)=15.66$, $p=0.00$] from the other four BAW populations at the $p<0.05$ level. Furthermore, pupal weight mean for AAFC-Vegreville males was statistically different ($p<0.05$) from AAFC-Davidson, AAFC-Regina and AAFC-Lethbridge. A similar result was obtained for the female mean pupal weights (Figure 4-4).

4.3.2 Scanning electron microscopy (SEM) of BAW male antenna

Images acquired with the scanning electron microscope were visually inspected for sensillar content and arrangement on the male antenna from AAFC-Saskatoon, AAFC-Davidson and AAFC-Vegreville populations. The antennal sensillum content was analyzed based on previously described BAW antenna [Liu and Liu 1984]. Figure 4-5 contains images corresponding to male antenna from AAFC-Saskatoon and AAFC-Davidson populations. Visual inspection of the antenna did not show any differences in the sensillar content, arrangement and sensillar morphology between the populations studied.

Figure 4-3 Body size difference of BAW males. AAFC-Saskatoon (top), AAFC-Vegreville (bottom).

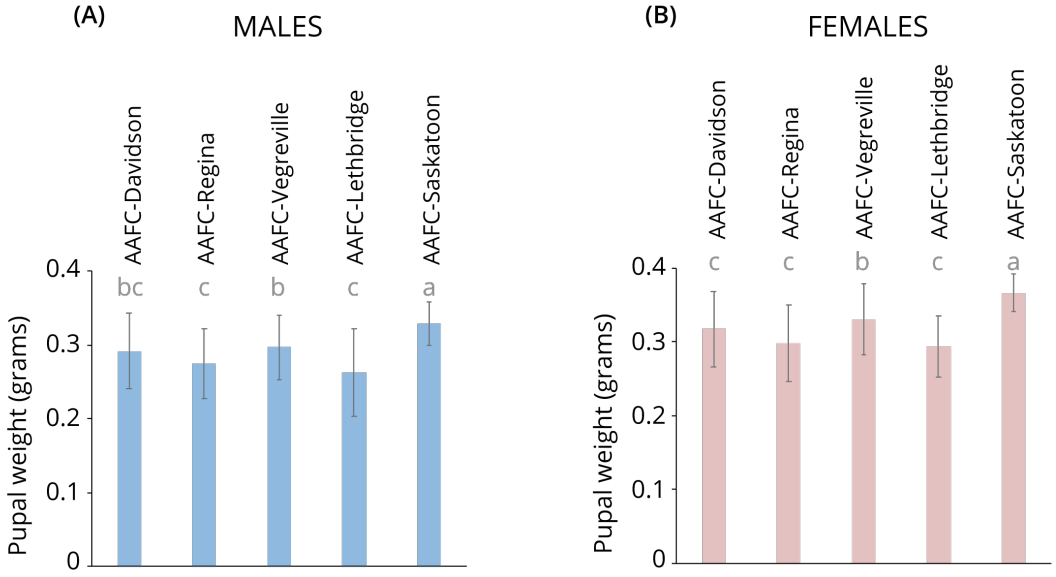

Figure 4-4 Pupal weight difference among five BAW populations. Mean pupal weights (grams) for **(A)** males and **(B)** females are displayed with errors bars corresponding to 1 standard deviation. Tukey's HSD all-pairwise comparison assigned the means into three distinct mean groups indicated with lower case letters (a, b, c) in grey.

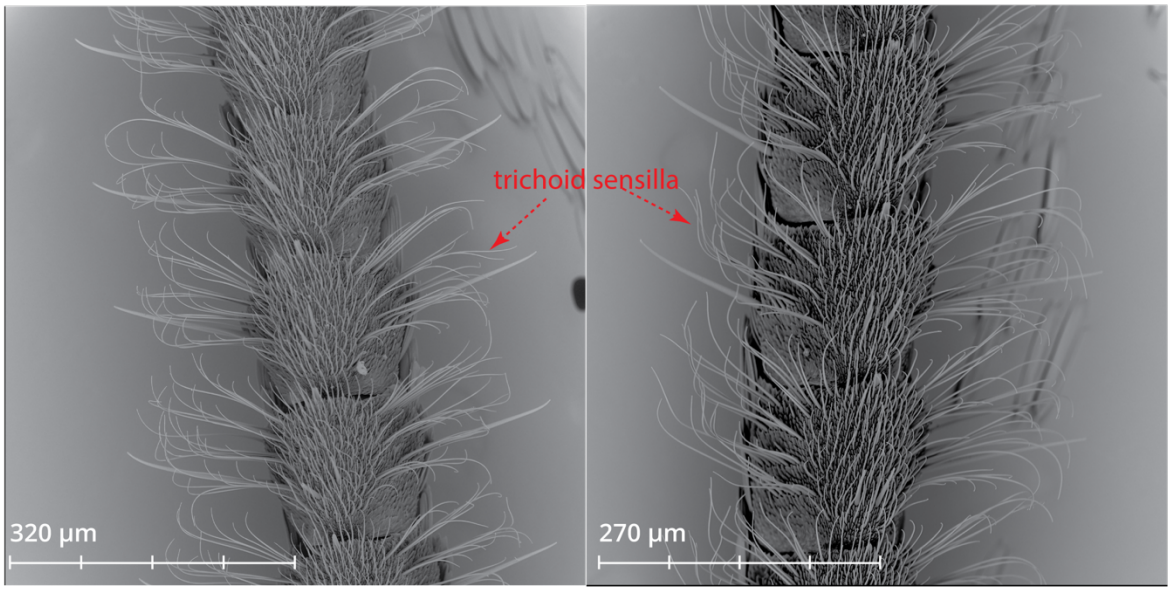

Figure 4-5 SEM images of the ventral surface of BAW male antenna. **(A)** AAFC-Saskatoon. **(B)** AAFC-Davidson. The antennal tissue was fixed on supporting medium in gold-palladium. Scale bars are provided for reference. Both antennae show characteristic arrangement of long trichoid sensilla types on each antennal segment.

4.3.3 Wind tunnel bioassays

The experimental set up of the wind tunnel for BAW pheromone attraction bioassays required optimization of several parameters critical to the experiments. Wind speed, light lux, distance of the release cage to the pheromone source and height of the pheromone source above floor were obtained from literature reports of wind tunnel bioassays for noctuid species of similar size and using unsaturated acetates in their pheromone blend [Baker and Linn 1984; Löfstedt et al. 1985b; Vickers 2002; Hemmann et al. 2008]. These parameters were not specified in the existing literature reporting behavioural responses to pheromones in BAW. While carrying out initial flights with moths in the wind tunnel, I observed that the temperature and humidity in the room housing the wind tunnel were susceptible to large fluctuations. When the temperature and humidity were tracked over a 30-day period during the month of June 2015 with a Nomad Omega OM-71 portable temperature and humidity tracker, the temperature range recorded was between 19 - 28 ± 0.8°C. The relative humidity range varied between 0 - 64 ± 3.5% with 18 out of 30 days being below 30%. According to Environment Canada historical weather records (https://climate.weather.gc.ca/historical_data) during the years 2011-2014, the average

temperature in Saskatoon, SK was reported to be 15.67°C, average wind speed 12.36 km/h and the average humidity 84% for months of July and August and time between 12:00 am and 3:00 am. To account for the large variation in wind tunnel room conditions, the humidity was adjusted with 2 commercial humidifiers and kept in the range of 50-70%. The temperature was manually adjusted with a thermostat and kept in the range of 20-22°C during the experiments. Early in the optimization stages, a commercially-available rubber septum lure (Contech) was used as a pheromone source; however, I observed that insects rarely undertook flight despite showing the classical wing fanning behaviour in response to the septum pheromone source. While testing AAFC-Saskatoon (n=10), AAFC-Davidson (n=8) and AAFC-Vegreville (n=5) moths on the same day and under the same wind tunnel conditions, all males from each population elicited wing fanning, but none of the males from any of the populations took flight in response to the pheromone septum. When the odour source was switched to a filter disk with synthetic Z11:16Ac and Z9:14Ac at a 19:1 ratio as 1000 ng total solution in hexane, upwind flight towards the pheromone source occurred consistently. This suggested that the concentration and release rate of the septum under wind tunnel conditions was not appropriate for this bioassay.

The behavioral responses from each male were observed under wind tunnel conditions and using synthetic Z11:16Ac and Z9:14Ac at a 19:1 ratio as the pheromone source. Both AAFC-Saskatoon and AAFC-Davidson males were able to successfully initiate wing fanning as a pre-flight warm-up and initiate flight in response to the pheromone source (Figure 4-6A). Tests on a separate cohort of males showed that the hexane control did not evoke wing fanning or flight initiation. AAFC-Saskatoon males were less likely to lock on to the pheromone plume, undertake directional flight, or successfully locate the pheromone source. Only one out of ten (n=10) AAFC-Saskatoon males contacted the pheromone source, in contrast to six AAFC-Davidson males. The time elapsed between the introduction of the pheromone source and each category of behaviour was measured and compared between the two populations (Figure 4-6B). Wilcoxon rank sum test showed that there was no significant difference in the median time required for wing fanning onset between AAFC-Saskatoon (med=24.5 sec) and AAFC-Davidson (med=26.0 sec) [Z=-0.04; $p > 0.05$ (p=1.00)] (Figure 4-6B(i)). No significant difference was detected in the duration of wing fanning before flight take-off between AAFC-Saskatoon males (med=38.5 sec) and AAFC-Davidson (med=35.5 sec) [Z=0.49; $p > 0.05$ (p=0.63)] (Figure 4-6B(ii)). Although there was no significant difference between the means in time

required for wing fanning prior to flight take-off, the AAFC-Saskatoon males had considerably more varied responses ranging from 6 to 123 sec, whereas AAFC-Davison male responses where more consistent ranging from 8 to 40 sec. The only AAFC-Saskatoon male that flew to the pheromone source took 6 sec to lock-on the plume and 10 seconds to reach the source (Figure 4-6B(iii and iv)). In contrast, the AAFC-Davidson males locked-on to the plume much faster (med=2 sec) and took more time to reach the source (med=13.5 sec).

4.3.4 Electrophysiological recordings

4.3.4.1 GC-EAD

A custom stage amplifier was used to record the EAD from the antennal preparation (Figure 4-7). In total, 10 BAW male antennal preparations were tested for each of the AAFC-Saskatoon and AAFC-Davidson populations. Pheromone glands from 10 females from each population were extracted as per the protocol described in materials and methods (Chapter 1) and pooled. Each antennal preparation was tested by injecting 2 μL of the concentrated pooled pheromone extract equivalent to approximately 1 female pheromone gland equivalent. The GC-EAD traces were printed on an analog printer and for this reason the results can be inspected visually, but peak amplitudes cannot be reliably calculated due to baseline differences between individual preparations (Figure 4-8). A total of 7 FID peaks were observed for each responding male from either the AAFC-Saskatoon or AAFC-Davidson populations. Based on their retention times, the peaks were identified as Z9-14Ac, saturated 14Ac, Z11-16OH (precursor of Z11-16Ac), palmitic acid (precursor), Z11-16Ac, saturated 16Ac and octadecanol (precursor). In both populations, the largest EAD response was recorded at a retention time (t_r) of ~8.6 min corresponding to Z11-16Ac. The second largest response was recorded at t_r ~7.5 min corresponding to Z9-14Ac. A much smaller response peak was also observed for Z11-16OH and palmitic acid. No compounds other than the pheromone gland components previously reported for BAW were detected [Struble et al. 1984]. Antennal preparations from both populations responded to the two pheromone components and Z11-16OH consistently and without observable differences in amplitude of the response. Antennal preparations from both subpopulations responded to the two pheromone components and Z11-16OH consistently and without observable differences in amplitude of the response. However, the antennal preparations from AAFC-Davidson subpopulation produced split EAG response peaks for Z9-14Ac and Z11-16Ac with 2 distinct subpeaks (Figure 4-8B). In each case the first peak corresponded to the pheromone component

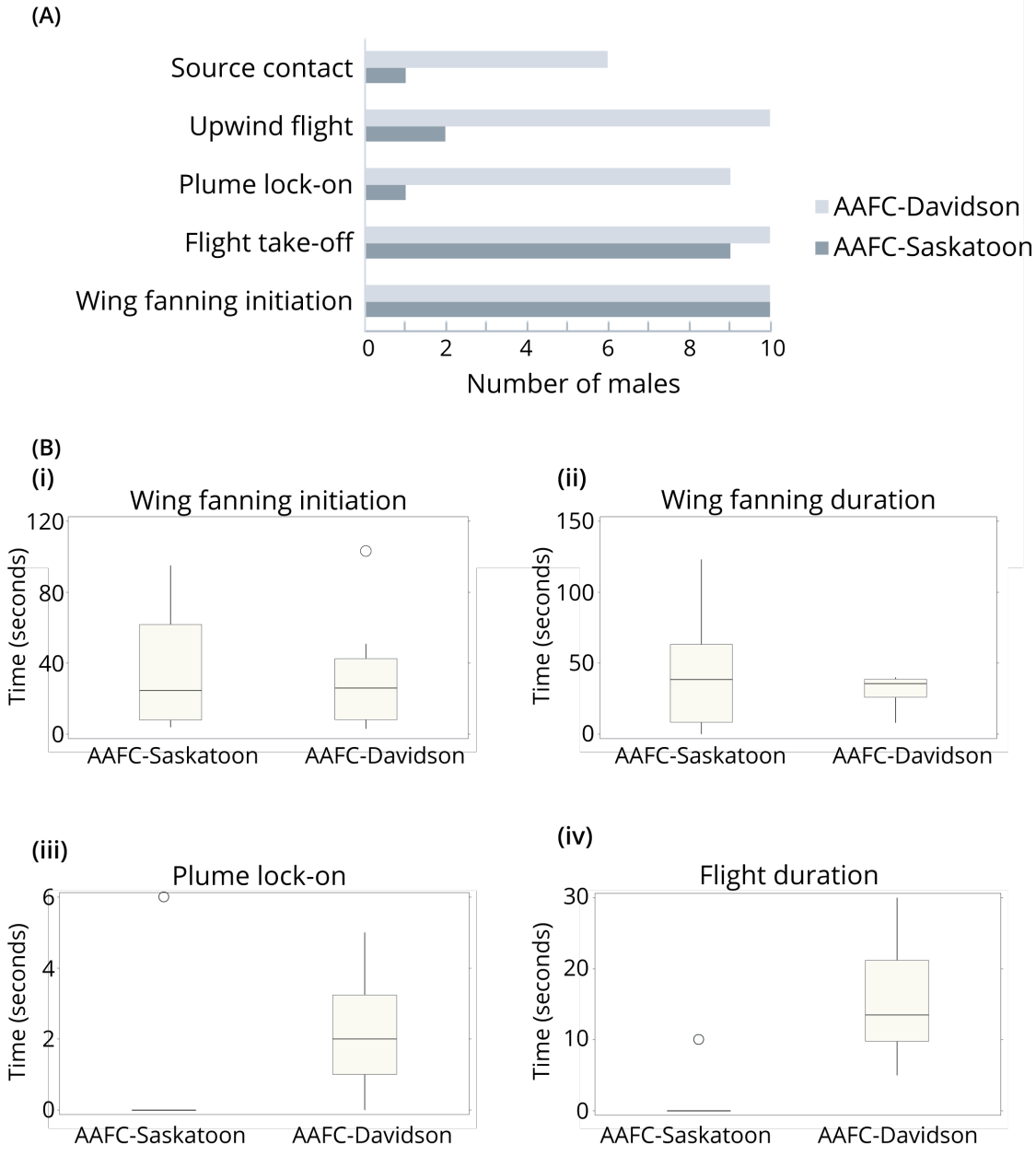
(A)
Source contact
Upwind flight
Plume lock-on
Flight take-off
Wing fanning initiation
0
2
4
6
8
10
Number of males
AAFC-Davidson
AAFC-Saskatoon
(B)
(i)
Wing fanning initiation
Time (seconds)
120
80
40
0
AAFC-Saskatoon
AAFC-Davidson
(ii)
Wing fanning duration
Time (seconds)
150
100
50
0
AAFC-Saskatoon
AAFC-Davidson
(iii)
Plume lock-on
Time (seconds)
6
4
2
0
AAFC-Saskatoon
AAFC-Davidson
(iv)
Flight duration
Time (seconds)
30
20
10
0
AAFC-Saskatoon
AAFC-Davidson

Figure 4-6 Wind tunnel bioassay for AAFC-Saskatoon and AAFC-Davidson males. **(A)** The number of males successfully performing a series of marked behaviours associated with pheromone-mediated mate-finding. The length of the bar corresponds to the number of males that successfully completed the marked behaviour from AAFC-Saskatoon (dark grey bar) and AAFC-Davidson (light grey bar) populations. Response evaluation to the pheromone source was based on five distinct markers along the flight track, 1) wing fanning, 2) flight take-off from the cage, 3) plume lock-on during which the male flew near the base of the takeoff platform while attempting to 'lock-on' to the odour plume, 4) upwind flight, and 5) source contact during which the male hovered within 10 cm or made contact with the source. **(B)** Box and whiskers plots of (i) the time required for wing fanning initiation from a quiescent state, (ii) the time required for wing fanning for pre-flight warm up, (iii) the time required for plume lock-on from flight take-off and (iv) the total duration of flight from take-off to reaching the source. The horizontal line within the box indicates the median, the boundaries of the box indicate the 25^{th}- and 75^{th} - percentile, and the whiskers indicate the highest and lowest values of the results. The outliers are indicated as open circles. Only one AAFC-Saskatoon male locked-on to the plume and successfully located the pheromone source. In contrast, nine AAFC-Davidson males locked-on to the plume with a median time of 2.0 sec and six males located the pheromone source with a median time of 13.5 sec.

and the second peak to the corresponding saturated acetate of 14Ac and 16Ac respectively. The subpeaks were not present for the EAD responses from AAFC-Saskatoon antennal preparations.

4.3.4.2 EAG

As the GC-EAD responses could not be quantified, I carried out EAG dose-response analysis with synthetic Z11-16Ac and Z9-14Ac using males from the AAFC-Saskatoon and AAFC-Davidson populations. Total antennal potential (mV) was measured at a concentration range of 0.01 μg to 1000 μg for each of the pheromone components with air and hexane stimulus as controls and the common plant volatile cis-3-hexenyl acetate (3HAC) as a reference stimulus for normalization (Figure 4-9). The antennal responses to air and hexane were measured prior to and post-stimulation with the pheromone components. One-way ANOVA analysis of the antennal responses to air and hexane controls prior to and post-pheromonal stimulation did not show the responses to be significantly different [$F(7, 32)=0.44$; $p=0.87$], suggesting that there was no observable deterioration of the antennal preparation during the course of the experiment. The normalized responses for the controls and responses to increasing amounts of each of the pheromone components were analyzed with one-way ANOVA and Tukey's HSD all-pairwise comparison to test for differences in response within each BAW population. Antennal preparations from AAFC-Saskatoon males had significant mean responses to Z11-16Ac at 10, 100 and 1000 μg doses [$F(9,40)=4.61$; $p=0.00$] (Figure 4-9A). For antennal preparations from AAFC-Davidson population, significant mean responses to Z11-16Ac were detected at 1, 10, 100 and 1000 μg [$F(9,40)=15.71$; $p=0.00$] (Figure 4-9A). When the mean normalized responses from antennal preparations of AAFC-Saskatoon males to Z9-14Ac were analyzed, no significant differences among the means for each dose-response were found [$F(9,40)=2.09$; $p=0.06$] (Figure 4-9B). In contrast, for antennal preparations from AAFC-Davidson males, significant mean responses were observed at 0.01, 1, 10, 100 and 1000 μg of Z9-14Ac [$F(9,40)=15.67$; $p=0.00$] (Figure 4-9B).

An independent sample t-test was performed to compare the mean responses for each dose amount between the AAFC-Saskatoon and AAFC-Davidson populations. When the responses to Z11-16Ac were compared between the two populations, significant difference was observed for the 0.01 μg [$t(8)=-3.02$; $p=0.02$] and 1 μg doses [$t(8)=-4.44$; $p=0.00$] (Figure 4-9A). However,

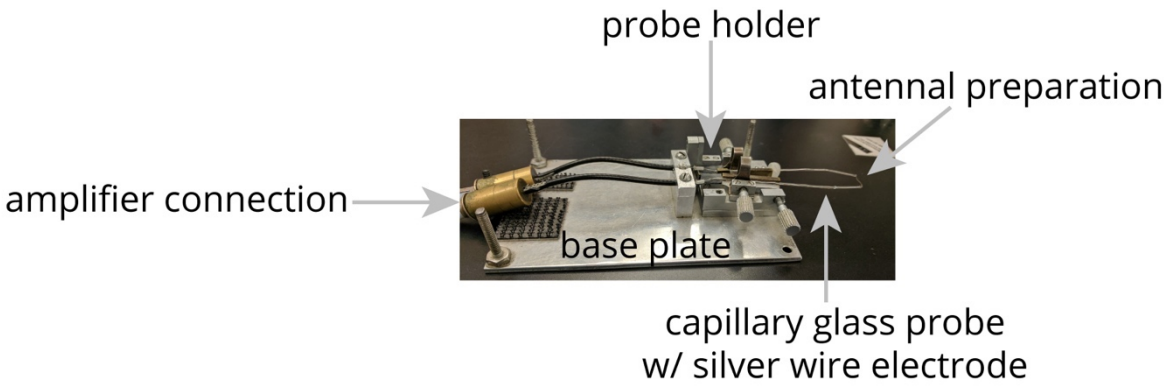

Figure 4-7 GC-EAD experimental setup. Custom probes and probe holder for the EAD recording of the individual pheromone gland components eluting from the GC column (Courtesy of Gries Lab, Simon Fraser University, Burnaby, British Columbia).

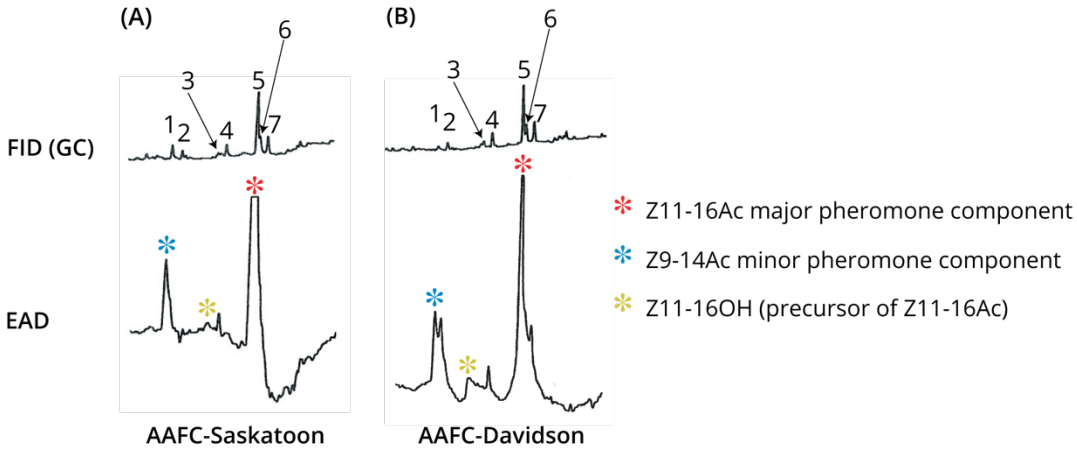

Figure 4-8 GC-EAD analysis for BAW male response to female pheromone gland extract. FID (GC)-EAD coupled traces for **(A)** AAFC-Saskatoon and **(B)** AAFC-Davidson BAW male antennal preparations responding to 1 female pheromone gland equivalent of the pooled female. Pheromone-gland extract. Only FID trace region where EAD responses were recorded are shown. FID traces show retention times of peaks eliciting a response from the antennal preparation and identified as; Z9-14Ac (1), saturated 14Ac (2), Z11-16OH, (3) palmitic acid (4), Z11-16Ac, (5) saturated 16Ac (6), and octadecanol (7). The EAD response peaks to Z11-16Ac (red), Z9-14Ac (blue) and Z11-16OH (yellow) are shown with asterisks.

because the normalized mean response to 0.01 μg was not significantly higher than the response to the controls for both BAW populations, the statistical significance detected for this dose between the populations is below the detection limits of the bioassay. The mean normalized responses to Z9-14Ac between the two populations were significantly different at the 10 μg [$t(8)=-2.70$; $p=0.03$]and 100 μg [$t(8)=-3.04$; $p=0.02$] doses.

4.5 DISCUSSION

This study aimed to investigate whether any differences with respect to behavioural and electrophysiological male response exist between BAW populations. Two early observations motivated the investigation of pupal weight among the populations. A marked difference in body size between adult male moths from the AAFC-Saskatoon and geographic field BAW populations was observed concurrently with an observation of poor flight performance from the AAFC-Saskatoon adult moths in the wind tunnel. As it is difficult to accurately assess the body weight of live adult moths, pupal weight was assessed instead. The mean pupal weight for the long-term reared colony from AAFC-Saskatoon was significantly higher than for the geographic field populations. The data also suggested that there might be smaller, but statistically significant, differences in pupal weight among the geographic field populations with pupae from AAFC-Regina and AAFC-Lethbridge being smaller than AAFC-Davidson and AAFC-Vegreville pupae. An important consideration for the pupal weight experiment is that it was carried out during an attempt to establish viable colonies under laboratory conditions. Thus, the pupal weight could reflect the nutritional state of individuals from each population and their ability to adapt to the laboratory diet and rearing conditions. Since AAFC-Regina, AAFC-Lethbridge and AAFC-Vegreville populations collapsed during efforts to establish viable colonies, I cannot exclude the possibility that the differences in pupal size were a result of poor diet adaptation. However, the body weight of the long-term reared AAFC-Saskatoon colony could contribute to the results obtained in the wind tunnel bioassays described below.

In wind tunnel bioassays, AAFC-Saskatoon males responded to synthetic pheromone blend with the stereotypic behaviour of wing fanning and initiated flight in search of the pheromone source, but unlike AAFC-Davidson males, they were unsuccessful in flying towards and reaching the pheromone source. The observed wing fanning and attempts to takeoff for flight suggest that the

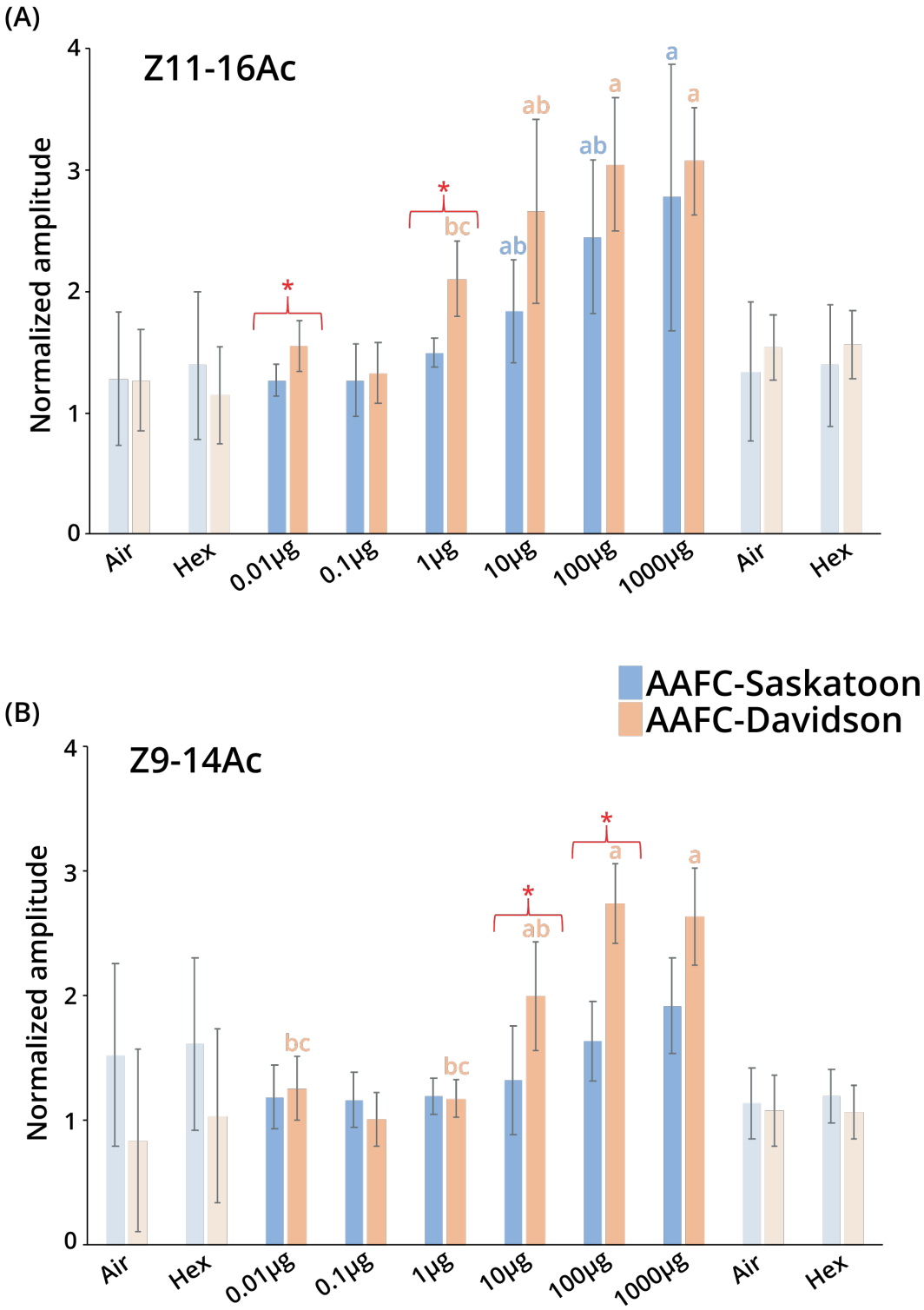
(A)
Z11-16Ac
Normalized amplitude
0
1
2
3
4
*
*
bc
ab
ab
ab
a
a
a
Air
Hex
0.01µg
0.1µg
1µg
10µg
100µg
1000µg
Air
Hex
(B)
AAFC-Saskatoon
AAFC-Davidson
Z9-14Ac
Normalized amplitude
0
1
2
3
4
*
*
bc
bc
ab
a
a
Air
Hex
0.01µg
0.1µg
1µg
10µg
100µg
1000µg
Air
Hex

Figure 4-9 EAG dose-response analysis for BAW male antenna from AAFC-Saskatoon and AAFC-Davidson. Mean normalized responses from AAFC-Saskatoon (n=5; blue bars) and AAFC-Davidson (n=5; orange bars) male moth antennal preparations to increasing amounts of **(A)** Z11-16Ac and **(B)** Z9-14Ac. Error bars correspond to 1 standard deviation. Each control and pheromone component response (mV) were normalized to 3HAC response (mV). The responses to the control (air) and hexane prior and post-pheromone stimulation are indicated by the lighter colours. One-way ANOVA and Tukey's HSD all-pairwise mean comparison analyses were performed to determine statistically-significant antennal responses within each population. For clarity, only responses that were significantly different from responses to the controls are indicated with colour-coded lower-case letters (a-c) for each population. Antennal preparations from AAFC-Saskatoon males showed significant responses to 10-1000 μg of Z11-16Ac, whereas AAFC-Davidson antennae also showed a significant response to the 1-1000 μg doses. No significant responses were detected from the AAFC-Saskatoon antennal preparations to Z9-14Ac. In contrast, AAFC-Davidson antennae showed significant responses at the 0.01, 1 and 10-1000 μg dose. An independent sample t-test was used to compare the means for each pheromone dose between the two populations. The dose amounts found significant between the two BAW populations are indicated with a red bracket and a star. The responses to Z11-16 were detected at 0.01 and 1 μg, whereas the responses to Z9-14Ac were detected at 10 and 100 μg between the two populations.

AAFC-Saskatoon males correctly detect the synthetic blend of pheromones used in the wind tunnel bioassay; however, their flight was impaired preventing them from reaching the pheromone source. Although, there was no significant difference for the median time required for the onset of wing fanning and median time spent on wing fanning between the two populations, AAFC-Davidson males appeared to be more efficient at these steps showing less variation in the time spent on pre-flight warm-up. AAFC-Davidson males required, on average, 10.5 seconds less than AAFC-Saskatoon males to take off. Significant differences were observed between the two populations in their ability to locate the pheromone plume and navigate to the pheromone source. Six out of ten AAFC-Davidson moths reached the pheromone source, in contrast to only one of ten AAFC-Saskatoon males. The percentage of AAFC-Davidson males reaching the pheromone source under wind tunnel conditions is in agreement with other published reports [Zhu et al. 1997; Vickers 2002]. Interestingly, the one AAFC-Saskatoon male that reached the source took a long time to lock-on the plume (6 sec) and flew directly at the source (10 sec) in comparison to AAFC-Davidson males, which required less time to lock on to the plume (2 sec), but more time to reach the pheromone source (13.5 sec). To assess whether the response observed from the AAFC-Saskatoon male was characteristic for males that were capable of flying within this population, the wind tunnel bioassay should be repeated with a larger cohort size. Nonetheless, the wind tunnel bioassay results suggest that work involving behavioural responses to female pheromones should not be carried out on the long-term, laboratory-reared *M. configurata* colony. To my knowledge, there are no reports in the literature comparing pheromone-mediated flight under wind tunnel conditions between a long-term, laboratory-reared and field populations of noctuid moths. Our current understanding of flight characteristics exhibited by noctuid moths navigating to a pheromone source is based on a handful of pest species, such as *H. virescens*, *A. segetum, T.ni and S. littoralis* [Cardé 2016]. At least for these species, colony-reared moths are often used in wind tunnel studies; however, the age of the colony is rarely specified. In one study investigating the adaptation of male moths to a mutant female-produced pheromone blend, the authors tested *T. ni* males taken from a seven-year-old laboratory colony [Zhu et al. 1997]. The success rate of these *T. ni* moths in reaching the pheromone source was reported to be between 50-60% and, thus, the "long-term colony effect" observed for BAW does not appear to manifest to the same degree in this species.

The differences in male response to the female-produced pheromones between the two populations were investigated in GC-EAD experiments. Based on the results obtained in Chapter 2 of this thesis, which showed that quantities of the major and minor pheromone components present in pheromone gland of individual BAW females vary, I used pooled gland extracts as the odour stimulus for the GC-EAD bioassay. Thus, the FID trace corresponding to the chemical content of the pooled gland extract and the concentration of the components were kept constant for each antennal preparation tested. The EAG traces corresponding to the male-response profile were consistently similar for both BAW populations investigated. In agreement with previously reported results, males from both BAW populations showed a large EAG response peak corresponding to Z11-16Ac and smaller peak corresponding to Z9-14Ac [Struble et al. 1984]. In contrast to previous reports, however, I also saw two small response peaks corresponding to Z11-16OH and likely a palmitic acid precursor. Although Struble et al. (1984b) reported the presence of Z11-16OH in the gland extracts, they did not report an antennal response to this component in GC-EAD studies. During field-trapping experiments, addition of Z11-16OH to a lure blend containing the two BAW pheromones resulted in complete inhibition of BAW male trap catches, but attracted another noctuid, *Discestra trifolli* (clover cutworm) [Steck et al. 1984]. The presence of Z11-16OH in pheromone blends of hetero-specific species may, therefore, inhibit BAW male pheromone attraction. Based on the analysis in Chapter 3 (Section 3.3.2.3 and Figure 3-9) of this thesis, both MconOR27 and MconOR29 were identified as putative pheromone receptors belonging to a subclade of Group 2 pheromone receptors known to be specific for Z11-16OH and Z9-14Ac. These receptor proteins are, therefore, candidates for binding and reception of Z11-16OH. In this study, the female pheromone glands were collected 3-4 hours into scotophase and about 1-2 hours before the commencement of female calling [Swailes et al. 1975; Howlader and Gerber 1986a]. Hence, the amount of Z11-16OH as precursor of Z11-16Ac is expected to be low in the pheromone gland at this time. Future experiments should address the levels of Z11-16OH in female pheromone glands during photophase, as well as the male response to Z11-16OH outside of the calling period and scotophase.

The differences in antennal responses to the major and minor pheromone components between the two BAW populations were highlighted in the EAG dose-response analysis. Although antennal preparations from both populations showed similar EAG responses to increasing amounts of the major pheromone Z11-16Ac, antennae from the AAFC-Davidson males showed

higher sensitivity and responded to the 1 μg dose, whereas antennae from AAFC-Saskatoon males did not. A major difference was observed between the two BAW populations in the dose-response profile to Z9-14Ac. Antennae from the AAFC-Saskatoon males failed to produce statistically-significant responses above the mean amplitude of responses to the experimental controls. In contrast, the antennae from AAFC-Davidson males produced significant responses at all dose amounts, except for 0.01 μg. The response to the minor pheromone component between the two populations was different at 10 and 100 μg amounts. The range (1-100 μg) of pheromone component evoking a significant response from an antennal preparation is consistent with studies in other noctuid species [Seabrook et al. 1987; Malo et al. 2000; Groot et al. 2005]. In response profiles for AAFC-Davidson antennal preparations, the mean response to the 0.1 μg dose was not significantly larger than the air and hexane controls, but the 0.01 μg dose was. The solutions of both neat pheromones in hexane were prepared as a serial dilution, thus, it is unlikely that an error affected the concentration of 0.1 μg dose since the 0.01 μg was not affected. The only plausible explanation would be that the stimulus cartridge was faulty affecting the delivery of the 0.1 μg dose amount to the antennal preparation.

The results of this study suggest that the long-term, laboratory-reared males are less sensitive to Z9-14Ac as compared to the BAW geographic field population. The loss of sensitivity to a pheromone component was previously observed in a laboratory strain of *T. ni* in which males adapted to a mutant female blend over 50 generations [Liu and Haynes 1994b]. Electrophysiological investigation found that the sensitivity of the OSN tuned to *Z*9-14Ac was attenuated in these males [Domingue et al. 2009]. This attenuation caused the action potential amplitudes from both *Z*9-14Ac and *Z*7-12Ac to be approximately equal, which in turn translated into mutant males being able to detect both mutant and original pheromone blends equally. Subsequent analysis revealed that although the adapted males were able to respond equally to both pheromone blends, overall, their sensitivity was lower than in wild-type males [Hemmann et al. 2008].

Based on the results presented in Chapter 3 (Section 3.3.2.3), the expression profile of genes coding for the five putative pheromone receptors (PRs) was not significantly different between the BAW populations investigated. However, three of the genes encoding putative PRs (*OR15*, *OR27*, and *OR29*) contained single nucleotide polymorphisms potentially affecting PR protein

function. The majority of the non-synonymous SNPs discovered in the coding sequences of OR genes appeared to be invariant in the AAFC-Saskatoon population as compared to the AAFC-Davidson and AAFC-Vegreville populations. For example, in the sequence coding for OR15, a SNP corresponding to amino acid position 122 and located immediately next to the predicted TMD2 resulted in phenylalanine (F; TTC) being detected with high allelic frequencies in the AAFC-Davidson (94%) and AAFC-Vegreville (88%) populations, whereas isoleucine (I; ATC) was predominant in the AAFC-Saskatoon population (74%). Single point mutations in the transmembrane domains of OR proteins were shown to alter both sensitivity and specificity of the ligand-binding kinetics of the receptor protein [Pellegrino et al. 2011; Leary et al. 2012]. Thus, SNPs, such as the one affecting amino acid position 122 in OR15, should be subject to further investigation as potential candidates related to the attenuation of sensitivity in the long-term, laboratory-reared colony.

Taken together with the results from the wind tunnel bioassays, the results suggest that the performance in response to the sex pheromones in the long-term, laboratory reared colony was altered relative to the performance of wild-moths. Colony rearing for insect production was shown to affect colony quality, including reductions in genetic variability and artificial selection that can affect phenotypic traits of ecological relevance [Grayson et al. 2015]. Colony-reared insects are often utilized in pheromone research; however, comparisons with wild populations are rarely investigated. The results of this study have profound implications for the design of future olfaction-based studies in BAW.

4.6 CONCLUSION

This study explored the behavioural and electrophysiological responses of BAW males from a long-term, laboratory-reared colony and a geographic field population to female pheromone gland extracts and synthetic pheromone components. The results indicate that both behavioural and electrophysiological responses in the long-term AAFC-Saskatoon laboratory colony are different from the responses of the AAFC-Davidson field population. The AAFC-Saskatoon males present the characteristic wing-fanning, excitation behaviour, but their flight is impaired. The higher body weight of the long-term, laboratory-colony insects may play a role in their ability to take off and fly. However, as indicated by electrophysiological data, their decreased sensitivity to the minor pheromone components may also contribute to their ability to lock on to

the plume and navigate towards the pheromone source. Although AAFC-Saskatoon colony males can detect pheromonal components extracted from females from conspecific BAW populations, their sensitivity to the minor, and to a lesser extent the major pheromone, component was found to be attenuated in EAD bioassays. This implies that behavioural work related to pheromone response in BAW males must be carried out with field-collected populations. This work also provides fundamental knowledge on the BAW male responses for consideration in the future design of BAW monitoring and control systems for this pest species.

CHAPTER 5. CONCLUSIONS AND DISCUSSION

5.1 SUMMARY AND LIMITATIONS OF THE THESIS RESEARCH

5.1.1 BAW pheromone gland and whole-head transcriptomes

Generation of BAW pheromone gland and whole-head reference transcriptomes is an important first step in characterization of the genetic architecture involved in pheromone production in females and pheromone reception in males. Due to the cyclical nature of BAW outbreaks, the genetic analysis of geographic BAW field populations is limited by the availability of time and genetic material. The established bioinformatic workflow, together with data sets of target sequences, will serve as a platform for further analyses during future outbreaks. In the female pheromone gland data, transcripts coding for enzymes involved in acyl chain modification (DESs, ß-oxidation enzymes) and a pgFAR constitute putative targets for future genetic analysis of variation among BAW populations. The three classes of receptor proteins identified within the BAW transcriptomic chemosensory data set are of special interest in the context of BAW olfaction-based behaviours and their implication in the design of integrated, pest-management strategies. The PR sequences identified are essential for future studies of BAW male sex-pheromone responses and design of improved monitoring strategies. The identification of the OR sequences in both sexes can serve as a starting point for studies on BAW responses to inhibitory compounds and host plant volatiles. The IR and GR receptors may be involved in behaviours, such as host plant selection and oviposition, and warrant further exploration.

Correct identification, characterization and annotation of the gene data sets is limited by inherent errors originating from the *de novo* transcriptome assembly. Tremendous progress has been made in *de novo* assembly of short RNA-Seq reads; however, large portions of the transcriptomes contain misassembled transcripts or key genes are missing altogether despite these recent improvements [Hölzer and Marz 2019]. In most recent assessments of *de novo* assemblers, Trinity was found to be the best-performing tool with the highest precision, recall and accuracy

[Voshall and Moriyama 2018]. However, even in a Trinity assembled transcriptome, only 41% of the contigs were accurately assembled, whereas60% were either erroneous or missing entirely from the transcriptome. Despite the high quality of the read input and the high quality of the final assembly, transcripts selected for downstream analysis may contain errors.

Identification of genes of interest relies on orthologous searches through the public sequence repositories and databases; however, the database collections are biased by factors responsible for the organism being chosen for sequencing and deposition in the public domain. Even with the rapid increase in the number of sequences from a wide range of species as a result of universal application of NGS, the database content is often overwhelmed by certain classes of sequences. This bias may lead to some species-specific sequences being perpetually missed from the analyses. In addition, mass processing and deposition of large data sets is often associated with a high number of erroneously-annotated, redundant or partial sequences being incorporated into the databases. These errors are propagated and affect systematic and comparative studies of orthologous genes from different species. The difficulties with accurate annotation of sequences are exacerbated by the lack of a unified nomenclature for genes, such as those corresponding to the pheromone gland enzymes or lepidopteran chemosensory components.

Tissue and sex-biased quantification of transcript abundance is used as a predictor of functional relevance in the investigated tissue; however, mRNA levels are not always an accurate predictor of actual protein accumulation [Evans 2015]. Stable mRNA with low abundance may produce the same amount of protein as a very abundant mRNA with short half-life [Tian et al. 2004]. Our current understanding of the relationship between mRNA levels and protein levels is limited and protein accumulation must be confirmed empirically.

The assessment of genetic variation present in genes coding for key chemosensory proteins among populations poses a great challenge for a non-model species, such as *M. configurata.* Without a reference genome and a library of defined molecular markers, such analysis was not be possible until recently. *De novo* calling of SNPs for the antennal read libraries corresponding to the three BAW populations was a proof-of-concept analysis. It resulted in identification of a library of non-synonymous SNPs assigned to sequences coding for BAW male chemosensory proteins and represented by population-specific allelic frequencies. The end result was a curated

list of candidate genes for which genetic variation may result in ecologically-important phenotypic variation.

A major limitation for this type of analysis was the lack of biological replicates for the antennal tissue read libraries from each BAW population. KisSplice analysis was carried out on normalized read libraries from each population and allelic frequencies for each identified SNP were calculated from read alignments to the SNP loci; however, determination of the statistical significance of the differential variant frequencies between populations was not possible without replication. Another limitation is related to the prediction of the impact of SNPs on protein function. Although the SNP calling is independent of transcriptome assembly and analysis, the SNP assignment to coding sequences does depend on transcript output from Trinity and ORF determination by Transdecoder and, thus, any errors originating from these tools would be inherent in the final step of the KisSplice analysis. Moreover, highly over- or under- represented transcripts within the transcriptome may have contributed to reporting of artifact SNPs. Currently, the only approach for confirming the SNPs predicted by KisSplice is the polymerase chain reaction amplification of the genomic regions and re-sequencing.

5.1.2 The BAW pheromone blend ratios do not vary significantly between the colony-reared and geographic field populations

The results from the chemical analysis of BAW female pheromone glands from two BAW populations were in agreement with previously-reported chemical content. The evaluation of the interindividual variation in pheromone production is imperative for studies on interpopulation differences, but has not previously been addressed in the literature. Despite large interindividual differences in the amounts of major and minor pheromone components present in the pheromone gland prior to the calling period, no significant differences were discovered in the mean component quantities and mean blend ratios between the females from the AAFC-Saskatoon and AAFC-Davidson populations. The mean ratios determined were higher than the ratio previously reported as maximally attractive in field-trap experiments and the difference observed should be investigated further. The obvious limitation of assessing pheromone gland content is that the amounts detected may vary from those actually emitted by females during calling. The differences in pheromone gland and effluvium content have been linked to the chemical properties of compounds and determined to be species-specific [Allison and Cardé 2016a]. For some female moths, the amount of pheromone content is not significantly different between the

gland and the effluvium. In other species, however, the amount of one or more of the pheromone components in the emissions varies from their concentration in the gland. Future analysis should address the content of the pheromone glands outside of the calling period, as well as content of the female effluvium at the time of calling.

5.1.3 Behavioural and electrophysiological responses are affected in a long-term, laboratory-reared BAW colony

Observation of behavioural responses to the synthetic blend of BAW pheromones under wind tunnel conditions suggests that the ability to locate a pheromone source is diminished in long-term, laboratory-reared males. The detection of the pheromone and pre-flight warm-up were not significantly different between males from the two populations; however, the AAFC-Davidson moths outperformed the AAFC-Saskatoon moths in location of the plume upon flight takeoff and navigation to the pheromone source. The inability of AAFC-Saskatoon males to sustain flight appeared to be the major factor responsible for the significantly different performance in the wind tunnel between the two BAW populations. The results of wind tunnel bioassays are inherently sensitive to environmental conditions, such as temperature, humidity and barometric pressure. As these factors were somewhat difficult to control in the room housing the wind tunnel, the comparative analysis of behaviour between the two populations was carried out on moths flown on the same day. The requirement to carry out the flights on the same day, together with the limited availability of AAFC-Davidson male moths, constrained the sample size for the bioassay.

The electrophysiological response of antennal preparation from the two populations to female pheromone extracts in the GC-EAD analysis showed nearly identical EAD response profiles to Z11-16Ac, Z9-14Ac and Z11-16OH. The only observed difference between the response profiles was the presence of smaller subpeaks within peaks corresponding to the major and minor pheromone component in the AAFC-Davidson EAD response. The subpeaks corresponded to saturated precursors of pheromone components and were absent from the AAFC-Saskatoon EAD response profile. This subtle difference in the EAD profiles may be an indication of a more discriminating response from the AAFC-Davidson moths. The EAD profiles from both populations indicated that the responses of BAW to its own pheromone components are relatively weak as compared to other species. The electrophysiological response to Z11-16OH from the female gland extracts has not been reported in the past; however, it is an important discovery in the context of field-trapping experiments suggesting that this compound is a potent inhibitor of

BAW male attraction [Steck et al. 1979]. Although the sensitivity of the instrument used for this experiment at Simon Fraser University was found to be superior to other experimental setups explored, the major limitation encountered was the analog rather than digital recording of the FID and EAD signals as the analog recordings are not conducive to subsequent evaluation of peak amplitudes.

An EAG dose-response study, with major and minor pheromone components tested independently, showed a statistically-significant attenuation of the antennal responses from the long-term, laboratory-reared colony to the minor pheromone component. The presence of the minor pheromone component is essential for the successful navigation to the pheromone source for BAW in the field [Underhill et al. 1977b]. In addition, antenna from AAFC-Saskatoon males produced significant responses only to higher concentrations of the major pheromone component, again suggesting attenuation of sensitivity at lower concentrations of Z11-16Ac. The genetic analysis presented in Chapter 3 did not show any differences in expression levels of the pheromone-specific receptor proteins between the two BAW populations. However, the SNP analysis produced a number of SNPs mapping to three PR sequences and showing different allelic frequencies between the populations. These SNPs represent potential targets for future investigations of the genetic basis underlying the observed attenuation of response in the AAFC-Saskatoon moths. Taken together, the results from behavioural and electrophysiological studies imply that long-term, laboratory colonies should not be used in olfaction-based bioassays.

EAG analysis is inherently limited to being an empirical rather than quantitative technique. Its limitation stems from the nature of recording a summed response from a population of OSNs, potentially involving different classes of OSNs and complex interactions for which theoretical explanation is lacking. An EAG response does not necessarily indicate a compound's ability to elicit a behavioural response. Although testing of the pheromone components independently rather than as a blend is informative, the responses may not be an accurate representation of the responses during pheromone-guided flight to a source. Furthermore, the concentrations of pheromone components used in the EAG dose-response bioassay may be outside of the biologically-relevant concentrations and bias the responses produced.

5.2 DISCUSSION AND FUTURE PROSPECTS

5.2.1 Informatics analysis serve as a platform for development of computational models for insect olfaction

The acquisition and analysis of datasets, including multi-level -omics and physiology from non-model species which are sampled from field populations, is a major challenge. Transcriptomic analysis is becoming an integral technique used as a starting point for characterization of the genetic architecture underlying olfaction in non-model insect species. The rapid accumulation of data prompts questions as to how can we maximize the use of this data and how can we move past the basic characterization stage. One of the major areas of interest regarding insect olfaction is the role of receptor proteins mediating the transduction process within the OSN. At present, there are hundreds of chemosensory receptor proteins being identified for which ligands are not known. The current approaches involving *in vivo* heterologous expression system in *Xenopus* oocytes [Wang et al. 2011] or expression systems in Drosophila "empty neurons" [Dobritsa et al. 2003] are not feasible based on the number of sequences identified. In addition, these approaches are hampered by limited success in expressing some of the receptor proteins within these expression systems. There is a pressing need for the development of high throughput screening methods for functional deorphanization of chemosensory receptor classes.

The recent finding of a correlation between prolonged exposure to high odorant concentrations and expression of genes encoding chemosensory receptors in mammals also has potential application in insects [Weid et al. 2015]. Based on this finding, a technique called DREAM (Deorphanization of receptors based on expression alterations of mRNA levels) is in the early stages of development and testing [Koerte et al. 2018]. The technique involves exposure to the odorant of interest and subsequent extraction of tissues. Polymerase chain reaction is used to screen for changes in the expression of receptor genes. It is predicted, however, that DREAM will be effective with some, but not the entire repertoire of receptors and, thus, other approaches are required.

The use of advanced algorithms and machine learning for *in silico* decoding of odour-receptor chemical pairings is likely one of the most promising approaches [Boyle et al. 2013]. This approach involves using computational identification of shared structural features from known ligands of individual receptors. The library of these features is then applied to screen *in silico* for new candidate ligands from a massive library of thousands of potential volatiles with biological

relevance to insects. Subsequently, the compound ligands, along with their activator or inhibitor status, can be assigned to their respective receptor. An extension of this approach is transcriptome profiling [Chapman et al. 2014] with artificial intelligence where gene characteristics are integrated with known structural features, expression levels and ligands to model patterns or profiles of the changing olfactory genetic landscape under varying experimental conditions.

5.2.2 The need for quantitative analysis of the female emissions as a function of time for determination of metabolic fluxes

The major question remaining in the field of pheromone biosynthesis is how and why the quantities of pheromone produced by either individuals or species vary so greatly. Answering this question will require a combination of genetic and molecular biology approaches. The current static analysis of pheromone components must give way to quantitative analysis of effluvium components as a function of time [Foster 2016]. The analytical tools required for this shift are available and do not differ greatly from the methods used in static gland quantification. Effective sample collection remains the major challenge; however, if quantification of total amounts of components produced during scotophase can be achieved and correlated to the quantities of precursors needed, ultimately the energetic cost of pheromone production in the female can be determined. Here, computational modelling may also be applied. The current characterization of the genetic architecture underlying biosynthetic pathways in the pheromone gland can be integrated with the knowledge of metabolic flux through the pheromone network [Nielsen 2003]. Modelling of metabolic fluxes from precursors to pheromone products under different conditions and interacting factors can be used to predict how the quantities produced are affected by changes in the network, such as mutations in biosynthetic genes, the nutritional state of the female or varying environmental conditions. Understanding gained from such analysis can then be applied to either improve current pest control strategies or to develop novel techniques.

5.2.3 The need for quantitative analysis of the male pheromone response

The evaluation of the number of OSNs expressing the same chemosensory receptor and exhibiting the same response profile to a given stimulus is challenging with EAG, but is the key parameter required for evaluation of the overall responsiveness of an antenna to a given odour. Exhaustive knowledge of the insect's response profiles to environmental chemicals requires the evaluation of all classes of OSNs. To address the limitations of EAG, an approach previously

utilized for the analysis of recordings from brain tissues is currently being adapted for insect olfactory studies [Jacob et al. 2017; Jacob 2018]. The properties of EAG recorded from insect antennae were shown to share a number of properties with local-field-potential (LFP) recordings [Jacob et al. 2017]. LFP recordings in brain tissues are dependent on the propagation of electrical fields through the extracellular medium [Bédard and Destexhe 2012]. Thus, in brain tissues, the original approach included recording of LFPs at multiple positions and modelling the electrical field to localize the activated neurons [Buzsáki et al. 2012]. Although propagation of LFP through the brain tissue is different from propagation of EAGs through the insect antenna, the main principles underlying the mechanism are similar [Jacob et al. 2017]. Accordingly, recording of EAG responses at multiple positions from insect antenna and applying the current source density (CSD) analysis was recently attempted in *D. melanogaster* [Jacob et al. 2017]. CSD analysis was pioneered in the 1950's to explore synaptic transmission in the nervous system [Pitts 1952]. With current progress in computing, CSD is being developed for interpretation of single-cell activity from the population recordings [Pettersen et al. 2006; Potworowski et al. 2012]. The CDS analysis applied to EAG recordings from an insect antenna produced reproducible and reliable maps of antennal activation in response to olfactory stimuli, which correlated well with previously-established individual OSN response characterization [Jacob 2018]. A major advantage of the CSD analysis is that peak amplitude generated from EAG data can be used to quantify the olfactory responses by correlating the number of responsive OSNs and their response level. This approach is particularly useful in insects with uneven sensillar distribution. Sampling of the EAGs at multiple locations across the antennal surface and subsequent CSD analysis could satisfy the need for a fully quantitative method for evaluation and screening of total antennal activation to a given stimulus. In addition, the information from this type of analysis could be integrated with the modelling experiments described above to fill a major knowledge gap in our understanding of the insect olfactory system.

Design of improved or novel pest-specific control strategies utilizing the principles of pheromone communication requires intrinsic knowledge of the factors that shape the female signal production and the male response. In addition, consideration of the effects of long-term rearing of laboratory insects on ecologically-relevant traits is imperative when applying research conclusions to field populations with the goal of developing pest management strategies. Although the -omic data currently generated may seem overwhelming, its integration with our

current knowledge of physiology, neuroanatomy and neuroethology should allow for effective modeling of the olfactory network. If successful, this type of approach could lessen the current challenge of working with non-model and laboratory-reared insects and contribute to our understanding of how populations evolve in response to environmental factors, such as narrowing host plant range, climate change or pesticide application.

APPENDIX

Appendix Table A-1. Electronic File Name: Table A-1.

Manually curated insect sequence and accession number lists used in the phylogenetic analysis.

File Type: Microsoft Excel (.xlsx)

File Size: 78 KB

Tabs: CSP, CXE, DES, FAR, GR, IR, OBP, OR

Appendix Table A-2. Electronic File Name: Table A-2.

M. configurata female pheromone gland biosynthesis and transport sequence data summary.

File Type: Microsoft Excel (.xlsx)

File Size: 164 KB

Tabs: Table Legend, PBAN-R, ACC, FAS, DES, ACO, ECH, ACD, KCT, 3HCD, FAR, FAT, CSP, OBP

Appendix Table A-3. Electronic File Name: Table A-3

M. configurata male and female whole-head chemosensory sequence data summary.

File Type: Microsoft Excel (.xlsx)

File Size: 164 KB

Tabs: Table Legend, CSP, GR, IR, OBP, ODE, OR, SNMP

Appendix Table A-4. Primer and probe sequences for digital droplet PCR experiments

Name	Trinity ID		Sequence	Start	Length	Tm	GC Percent	Amplicon
MconOR01	TRINITY_DN36907_c0_g1_i1	Forward Primer	ACCGCTAACTACGTTCCAAATA	846	22	62	41	
		Probe	TGCGAAATAAACGGATAAACGTCGAGT	878	27	67	41	
		Reverse Primer	TCAGGAGGTCGCTGTAGTAA	970	20	62	50	
		Product						125
MconOR03	TRINITY_DN42966_c0_g1_i1	Forward Primer	GCCAGCACCTTTGGACTATTAC	873	22	63	50	
		Probe	TCCTGGTACCAAACCAACAAGGAACC	964	26	68	50	
		Reverse Primer	TGCAAGCAGGTTGCTCTTATC	990	21	63	48	
		Product						118
MconOR07	TRINITY_DN44077_c0_g1_i1	Forward Primer	TGAATGGGACCAGCATCTATTT	488	22	62	41	
		Probe	ACGGCTACACTCCATTTCATAAGGAACC	521	28	68	46	
		Reverse Primer	CCCAAGACTGTCTGGATTGAC	590	21	62	52	
		Product						103
MconOR11	TRINITY_DN46688_c3_g1_i1	Forward Primer	TAGCGAGTGGATACCGAGAT	990	20	62	50	
		Probe	TGAAACTCTTCAGAGAACGTGCCG	1031	24	66	50	
		Reverse Primer	CCTGAAACCATGATTGGGATTG	1076	22	62	45	
		Product						87
MconOR12	TRINITY_DN47475_c0_g1_i1	Forward Primer	CAGACTGGGTCTATGCTGATTC	1055	22	62	50	
		Probe	CAAAGGGTTTCTGAGCGCGCATC	1129	23	68	57	
		Reverse Primer	AGTAACCCTTGGCGCTAAAT	1150	20	62	45	
		Product						96
MconOR14	TRINITY_DN48521_c0_g1_i1	Forward Primer	CAGCTTTGTTGACCGCATAAA	762	21	62	43	
		Probe	TTTCAGGGTTAGCTCGTAAGCGACC	819	25	68	52	
		Reverse Primer	CGGTTGAATGCCTCTAGAACT	875	21	62	48	
		Product						114
MconOR15	TRINITY_DN48934_c0_g2_i5	Forward Primer	GCAGTGCTTCTGGTGTACTT	964	20	62	50	
		Probe	TTCCACCAAGTGAGCGAGTGTCTT	988	24	68	50	
		Reverse Primer	AGCGCTTTCTGGTCCATTT	1049	19	62	47	
		Product						86
MconOR21	TRINITY_DN50162_c6_g1_i6	Forward Primer	CCTATGGTGCTGATAGCTGTAAA	466	23	62	43	
		Probe	ACGAAAGAGTTTGTGATGTTGCTGCC	499	26	68	46	
		Reverse Primer	TACGCAAAGGGCCAGTATTT	581	20	62	45	
		Product						116
MconOR22	TRINITY_DN50417_c1_g1_i3	Forward Primer	CACTGTTCTCTTCTTCACCCATAC	240	24	63	46	
		Probe	TTCGCATTCAGCGCAAAGAATCCC	299	24	68	50	
		Reverse Primer	GCTGTTTGACTGGTTCCATACT	342	22	63	45	
		Product						103
MconOR27	TRINITY_DN52074_c5_g1_i4	Forward Primer	GACCGATGCTGTTCGTGTATTA	920	22	62	45	
		Probe	CATGTTCCATCAGGCAAGCGGTTG	942	24	68	54	
		Reverse Primer	AGTGGCACATATCGCATAAGG	1025	21	62	48	
		Product						106
MconOR39	TRINITY_DN53702_c5_g2_i2	Forward Primer	TGTAAGCACCGTGTCATCTG	873	20	62	50	
		Probe	AGGTTTCTTTCAGCTCCATCGCCA	917	24	68	50	
		Reverse Primer	CGGCAATCTGGTACGCTATAA	967	21	62	48	
		Product						95
MconOR42	TRINITY_DN53928_c1_g1_i1	Forward Primer	CATCGCATCTCCCACTTCTT	460	20	62	50	
		Probe	TGTCGGTCAAATGTTAAGTGGTCTCTTTCT	492	30	68	40	
		Reverse Primer	AAGCCTCCACTAGCATAGTTTC	581	22	62	45	
		Product						122
MconOR44	TRINITY_DN54106_c3_g1_i1	Forward Primer	CCCTAGGAAAGTTCAAAGAGAGG	527	23	62	48	
		Probe	TACCTTTCTGTGCCTGTGCTGGAA	583	24	68	50	
		Reverse Primer	GCAAAGAGGAACATACGCATATAAA	642	25	62	36	
		Product						116
MconOR45	TRINITY_DN54218_c0_g1_i2	Forward Primer	CTACGGCTTCGATCTACGATAC	882	22	61	50	
		Probe	TATTTATCTGCCGTGCCGCTATGCA	933	25	68	48	
		Reverse Primer	CCACTGACATGGCTTTCAAC	982	20	61	50	
		Product						101
EF-1		Forward Primer	AACCACCCTGGTCAAATCTC	1042	20	62	50	
		Probe	CACACAGCTCACATTGCCTGCAAA	1090	24	68	50	
		Reverse Primer	CGACGGTCCACTTTCTCTTT	1145	20	62	50	
		Product						104
RPS13		Forward Primer	AGCACTTGGAACGCAACA	299	18	62	50	
		Probe	AGGACAAGGACAGCAAATTCAGGCT	320	25	68	48	
		Reverse Primer	GCACGCTCTTTGTCTTGTAGTA	403	22	62	45	
		Product						105
RPS20		Forward Primer	ACAGAAGCTCCGTGTTAAGG	147	20	62	50	
		Probe	CAACCAAGATCCTCCGCATCACCA	182	24	68	54	
		Reverse Primer	CGATGACTCGCTTGTGGAT	280	19	62	53	
		Product						134

REFERENCES

Agnihotri AR, Roy AA, Joshi RS (2016) Gustatory receptors in Lepidoptera: chemosensation and beyond. Insect Mol Biol 25:519–529

Allison JD (2006) Heritable variation in the sex pheromone of the almond moth, *Cadra cautella*. J Chem Ecol 32:621–641

Allison JD, Cardé RT (2016a) Variation in Moth Pheromones: Causes and Consequences. In: Allison JD, Cardé RT (eds) Pheromone Communication in Moths. University of California Press, Oakland, California, pp 33–50

Allison JD, Cardé RT (2016b) Pheromones: Reproductive Isolation and Evolution in Moths. In: Allison JD, Cardé RT (eds) Pheromone Communication in Moths. University of California Press, Oakland, California, pp 19–32

Anamika K, Verma S, Abhay J, Aarti D (2016) Transcriptomic Profiling Using Next Generation Sequencing - Advances, Advantages, and Challenges. In: Next Generation Sequencing - Advances, Applications and Challenges. IntechOpen, pp 112–151

Anderson P, Sadek MM, Hansson BS (2003) Pre-exposure modulates attraction to sex pheromone in a moth. Chem Senses 28:285–291

Andersson MN, Löfstedt C, Newcomb RD (2015) Insect olfaction and the evolution of receptor tuning. Front Ecol Evol 3:691

Ando T, Inomata S-I, Yamamoto M (2004) Lepidopteran Sex Pheromones. In: Schulz S (ed) The Chemistry of Pheromones and Other Semiochemicals II. Springer, Berlin, pp 51–96

Ando T, Yamakawa R (2011) Analyses of lepidopteran sex pheromones by mass spectrometry. Trends Anal Chem 30:990–1002

Angeli S, Ceron F, Scaloni A, et al (1999) Purification, structural characterization, cloning and immunocytochemical localization of chemoreception proteins from *Schistocerca gregaria*. Eur J Biochem 262:745–754

Anglade P, Stockel J, Cooperators IWGO (1984) Intraspecific sex-pheromone variability in the European corn borer, *Ostrinia nubilalis* Hbn. (Lepidoptera, Pyralidae). Agronomie 4:183-187.

Arenas M (2015) Trends in substitution models of molecular evolution. Front Genet 6:319

Baker TC (2008) Balanced olfactory antagonism as a concept for understanding evolutionary shifts in moth sex pheromone blends. J Chem Ecol 34:971–981

Baker TC, Cardé RT (1979) Analysis of pheromone-mediated behaviors in male *Grapholitha molesta*, the oriental fruit moth (Lepidoptera: Tortricidae). Environ Entomol 8:956–968

Baker TC, Domingue MJ, Myrick AJ (2012) Working range of stimulus flux transduction determines dendrite size and relative number of pheromone component receptor neurons in moths. Chem Senses 37:299–313

Baker TC, Hansson BS (2016) Moth Sex Pheromone Olfaction: Flux and Flexibility in the Coordinated Confluences of Visual and Olfactory Pathways. In: Allison JD, Cardé RT (eds) Pheromone Communication in Moths. University of California Press, Oakland, California, pp 148–180

Baker TC, Hansson BS, Löfstedt C, Lofqvist J (1988) Adaptation of antennal neurons in moths is associated with cessation of pheromone-mediated upwind flight. Proc Natl Acad Sci USA 85:9826–9830

Baker TC, Linn CE (1984) Wind Tunnels in Pheromone Research. In: Hummel HE, Miller TA (eds) Techniques in Pheromone Research. Springer, New York, pp 75–110

Baker TC, Quero C, Ochieng SA, Vickers NJ (2006) Inheritance of olfactory preferences II. Olfactory receptor neuron responses from *Heliothis subflexa* x *Heliothis virescens* hybrid male moths. Brain Behav Evol 68:75–89

Baker TC, Vickers NJ (1997) Pheromone-Mediated Flight in Moths. In: Cardé RT, Minks AK (eds) Insect Pheromone Research: New Directions. Springer US, Boston, MA, pp 248–264

Baker TC, Vogt RG (1988) Measured behavioural latency in response to sex-pheromone loss in the large silk moth *Antheraea polyphemus*. J of Exp Biol 137:29–38

Baker TC, Willis MA, Haynes KF, Phelan PL (1985) A pulsed cloud of sex pheromone elicits upwind flight in male moths. Physiol Entomol 10:257–265

Baker TC, Zhu JJ, Millar JG (2016) Delivering on the promise of pheromones. J Chem Ecol 42:553–556

Bengtsson BO, Löfstedt C (2007) Direct and indirect selection in moth pheromone evolution: population genetical simulations of asymmetric sexual interactions. Biol J Linn Soc 90:117-123

Benton R (2009) Molecular basis of odor detection in insects. Ann NY Acad Sci 1170:478–481

Benton R, Sachse S, Michnick SW, Vosshall LB (2006) Atypical membrane topology and heteromeric function of *Drosophila* odorant receptors *in vivo*. PLoS Biology 4:e20

Benton R, Vannice KS, Gomez-Diaz C, Vosshall LB (2009) Variant ionotropic glutamate receptors as chemosensory receptors in *Drosophila*. Cell 136:149–162

Benton R, Vannice KS, Vosshall LB (2007) An essential role for a CD36-related receptor in pheromone detection in *Drosophila.* Nature 450:289–293

Berg BG, Zhao X-C, Wang G (2014) Processing of pheromone information in related species of heliothine moths. Insects 5:742–761

Bernsel A, Viklund H, Hennerdal A, Elofsson A (2009) TOPCONS: consensus prediction of membrane protein topology. Nucleic Acids Res 37:W465–W468

Bédard C, Destexhe A (2012) Modeling local field potentials and their interaction with the extracellular medium. In: Brette R, Destexhe A (eds) Handbook of Neural Activity Measurement. Cambridge, pp 136–191

Bigiani A, Scalera G, Crnjar R, et al (1989) Distribution and function of the antennal olfactory sensilla in *Ceratitis capitata* Wied. (Diptera, Trypetidae). Ital J Zool 56:305–311

Binyameen M, Jankuvová J, Blaženec M, et al (2014) Co-localization of insect olfactory sensory cells improves the discrimination of closely separated odour sources. Funct Ecol 28:1216-1223

Bjostad LB, Wolf WA, Roelofs WL (1987) Pheromone biosynthesis in lepidopterans: desaturation and chain shortening. In: Prestwich GD, Blomquist GJ (eds) Pheromone Biochemistry. Academic Press, pp 77–120

Blomquist GJ, Figueroa-Teran R, Aw M, et al (2010) Pheromone production in bark beetles. Insect Biochem Mol Biol 40:699–712

Blomquist GJ, Jurenka R, Schal C, Tittiger C (2012) Pheromone Production: Biochemistry and Molecular Biology. In: Gilbert LI (ed) Insect Endocrinology. Academic Press, San Diego, pp 523–567

Bolger AM, Lohse M, Usadel B (2014) Trimmomatic: a flexible trimmer for doi: 10.1093/bioinformatics/btu170

Boyle SM, Mcinally S, Ray A (2013) Expanding the olfactory code by *in silico* decoding of odor-receptor chemical space. eLife 2:e01120

Bracken GK (1984) Within plant preferences of larvae of *Mamestra configurata* (Lepidoptera: Noctuidae) feeding on oilseed rape. Can Entomol 116:45–49

Bracken GK (1987) Relation between pod damage caused by larvae of bertha armyworm, *Mamestra configurata* Walker (Lepidoptera: Noctuidae), and yield loss, shelling, and seed quality in canola. Can Entomol 119:365–369

Bracken GK, Bucher GE (1977) An estimate of the relation between density of bertha armyworm and yield loss on rapeseed, based on artificial infestations. J Econ Entomol 70:701–705

Brito NF, Moreira MF, Melo ACA (2016) A look inside odorant-binding proteins in insect chemoreception. J Insect Physiol 95:51–65

Bryant DM, Johnson K, DiTommaso T, et al (2017) A tissue-mapped Axolotl *de novo* transcriptome enables identification of limb regeneration factors. Cell Rep 18:762–776

Bucher GE, Bracken GK (1976) The bertha armyworm, *Mamestra configurata* (Lepidoptera: Noctuidae). Artificial diet and rearing technique. Can Entomol 108:1327–1338

Bultin RK, Ritchie MG (1989) Genetic coupling in mate recognition systems: what is the evidence? Biol J Linn Soc 37:237–246

Buskirk JV, Willi Y (2006) The change in quantitative genetic variation with inbreeding. Evolution 60:2428–2434

Butenandt A, Beckman R, Stamm D, Hecker E (1959) Uber den sexuallockstoff des seidenspinner *Bombyx mori*, reidarstellung und constitution. Zeitschrift fur Naturforschung B 14:283–284

Buzsáki G, Anastassiou CA, Koch C (2012) The origin of extracellular fields and currents - EEG, ECoG, LFP and spikes. Nat Rev Neurosci 13:407–420

Byers JA (2006) Pheromone component patterns of moth evolution revealed by computer analysis of the Pherolist. J Anim Ecol 75:399–407

Byers JR, Struble DL (1987) Monitoring population levels of eight species of noctuids with sex-attractant traps in southern Alberta, 1978-1983: specificity of attractants and effect of target species abundance. Can Entomol 119:541–556

Callahan FE, Vogt RG, Tucker ML, et al (2000) High level expression of "male specific" pheromone binding proteins (PBPs) in the antennae of female noctuid moths. Insect Biochem Mol Biol 30:507–514

Cao S, Liu Y, Guo M, Wang G (2016) A conserved odorant receptor tuned to floral volatiles in three heliothinae species. PloS ONE 11:e0155029

Cardé AM, Baker TC, Cardé RT (1979) Identification of a four-component sex pheromone of the female oriental fruit moth, *Grapholitha molesta* (Lepidoptera: Tortricidae). J Chem Ecol 5:423–427

Cardé RT (2016) Moth Navigation along Phermone Plumes. In: Allison JD, Cardé RT (eds) Pheromone Communication in Moths. University of California Press, Oakland, California, pp 181–198

Cardé RT, Cardé AM, Hill AS, Roelofs WL (1977a) Sex pheromone specificity as a reproductive isolating mechanism among the sibling species *Archips argyrospilus* and *A. mortuanus* and other sympatric tortricine moths (Lepidoptera: Tortricidae). J Chem Ecol 3:71–84

Cardé RT, Doane CC, Baker TC, et al (1977b) Attractancy of optically active pheromone for male gypsy moths. Environ Entomol 6:768–772

Cardé RT, Elkinton JS (1984) Field Trapping with Attractants: Methods and Interpretation. In: Hummel HE, Miller TA (eds) Techniques in Pheromone Research. Springer New York, New York, NY, pp 111–129

Cardé RT, Haynes KF (2004) Structure of the pheromone communication channel in moths. In: Millar JG, Cardé RT (eds) Advances in Insect Chemical Ecology. Cambridge University Press, Cambridge, pp 283–332

Cardé RT, Willis MA (2008) Navigational strategies used by insects to find distant, wind-borne sources of odor. J Chem Ecol 34:854–866

Chapman RW, Reading BJ, Sullivan CV (2014) Ovary transcriptome profiling via artificial intelligence reveals a transcriptomic fingerprint predicting egg quality in striped bass, *Morone saxatilis*. PloS ONE 9:e96818–10

Chertemps T, François A, Durand N, et al (2012) A carboxylesterase, Esterase-6, modulates sensory physiological and behavioral response dynamics to pheromone in *Drosophila*. BMC Biol 10:56

Chisholm MD, Steck WF, Arthur AP, Underhill EW (1975) Evidence for cis-11-hexadecen-1-ol acetate as a major component of the sex pheromone of the bertha armyworm, *Mamestra configurata* (Lepidoptera: Noctuidae). Can Entomol 107:361–366

Cho S, Mitchell A, Mitter C, et al (2008) Molecular phylogenetics of heliothine moths (Lepidoptera: Noctuidae: Heliothinae), with comments on the evolution of host range and pest status. Syst Entomol 33:581–594

Choo Y-M, Pelletier J, Atungulu E, Leal WS (2013) Identification and characterization of an antennae-specific aldehyde oxidase from the navel orangeworm. PloS ONE 8:e67794

Coates BS, Dopman EB, Wanner KW, Sappington TW (2018) Genomic mechanisms of sympatric ecological and sexual divergence in a model agricultural pest, the European corn borer. Curr Opin Insect Sci 26:50–56

Collins RD, Cardé RT (1985) Variation in and heritability of aspects of pheromone production in the pink bollworm moth, *Pectinophora gossypiella* (Lepidoptera: Gelechiidae). Ann Entomol Soc Am 78:229–234

Conesa A, Götz S, García-Gómez JM, et al (2005) Blast2GO: a universal tool for annotation, visualization and analysis in functional genomics research. Bioinformatics 21:3674–3676

Conesa A, Madrigal P, Tarazona S, et al (2016) A survey of best practices for RNA-seq data analysis. Genome Biol 17:13

Cossé AA, Campbell MG, Glover TJ, et al (1995) Pheromone behavioral responses in unusual male European corn borer hybrid progeny not correlated to electrophysiological phenotypes of their pheromone-specific antennal neurons. Experientia 51:809–816

Crespo JG, Goller F, Vickers NJ (2012) Pheromone mediated modulation of pre-flight warm-up behavior in male moths. J Exp Biol 215:2203–2209

Crespo JG, Vickers NJ, Goller F (2013) Female pheromones modulate flight muscle activation patterns during preflight warm-up. Journal of Neurophysiology 110:862–871

Crnjar R, Scalera G, Liscia A, et al (2011) Morphology and EAG mapping of the antennal olfactory receptors in *Dacus oleae*. Entomol Exp App 51:77–85

Croset V, Rytz R, Cummins SF, et al (2010) Ancient protostome origin of chemosensory ionotropic glutamate receptors and the evolution of insect taste and olfaction. PLoS Genet 6:e1001064–33

David CT, Kennedy JS (1987) The steering of zigzagging flight by male gypsy moths. Naturwissenschaften 74:194–196

de Bruyne M, Baker TC (2008) Odor detection in insects: volatile codes. J Chem Ecol 34:882-897

de Kramer JJ (1985) The electrical circuitry of an olfactory sensillum in *Antheraea polyphemus*. J Neurosci 5:2484

de Kramer JJ, Kaissling KE, Keil T (1984) Passive electrical properties of insect olfactory sensilla may produce the biphasic shape of spikes. Chem Senses 8:289–295

Deng Y, Zhang W, Farhat K, et al (2011) The stimulatory Gα(s) protein is involved in olfactory signal transduction in *Drosophila.* PloS ONE 6:e18605

Ding B-J, Löfstedt C (2015) Analysis of the *Agrotis segetum* pheromone gland transcriptome in the light of sex pheromone biosynthesis. BMC Genomics 16:711

Dobritsa AA, van der Goes van Naters W, Warr CG, et al (2003) Integrating the molecular and cellular basis of odor coding in the *Drosophila* antenna. Neuron 37:827–841

Dolzer J, Krannich S, Fischer K, Stengl M (2001) Oscillations of the transepithelial potential of moth olfactory sensilla are influenced by octopamine and serotonin. J of Exp Biol 204:2781-2794

Domingue MJ, Haynes KF, Todd JL, Baker TC (2009) Altered olfactory receptor neuron responsiveness is correlated with a shift in behavioral response in an evolved colony of the cabbage looper moth, *Trichoplusia ni*. J Chem Ecol 35:405–415

Domingue MJ, Musto CJ, Linn CE, et al (2007) Evidence of olfactory antagonistic imposition as a facilitator of evolutionary shifts in pheromone blend usage in *Ostrinia* spp. (Lepidoptera: Crambidae). J Insect Physiol 53:488–496

Dopman EB (2010) Genetic hitchhiking associated with life history divergence and colonization of North America in the European corn borer moth. Genetica 139:565–573

Dopman EB, Bogdanowicz SM, Harrison RG (2004) Genetic mapping of sexual isolation between *E* and *Z* pheromone strains of the European corn borer (*Ostrinia nubilalis*). Genetics 167:301–309

Dopman EB, Pérez L, Bogdanowicz SM, Harrison RG (2005) Consequences of reproductive barriers for genealogical discordance in the European corn borer. Proc Natl Acad Sci USA 102:14706–14711

Dopman EB, Robbins PS, Seaman A (2010) Components of reproductive isolation between North American pheromone strains of the European corn borer. Evolution 64:881–902

Du JW, Löfstedt C, Löfqvist J (1987) Repeatability of pheromone emissions from individual female ermine moths *Yponomeuta padellus* and *Yponomeuta rorellus*. J Chem Ecol 13:1431-1441

Duménil C, Judd G, Bosch D, et al (2014) Intraspecific variation in female sex pheromone of the codling moth *Cydia pomonella*. Insects 5:705–721

Durand N, Chertemps T, Maibeche-Coisne M (2014) Antennal carboxylesterases in a moth, structural and functional diversity. Commun Integr Biol 5:284–286

Ekblom R, Galindo J (2011) Applications of next generation sequencing in molecular ecology of non-model organisms. Heredity (Edinb) 107:1–15

El-Sayed AM (2014) The Pherobase: Database of insect pheromones and semiochemicals www.pherobase.com

Eliyahu D, Applebaum S, Rafaeli A (2003) Moth sex-pheromone biosynthesis is inhibited by the herbicide diclofop. Pestic Biochem and Phys 77:75–81

Erlandson MA (2013) *Mamestra configurata* Walker, Bertha armyworm (Lepidoptera: Noctuidae). In: Mason PG, Gillespie D (eds) Biological control programmes against insects and weeds in Canada, 2001-2012. Wallingford, pp 228–232

Erlandson MA (1990) Biological and biochemical comparison of *Mamestra configurata* and *Mamestra brassicae* nuclear polyhedrosis virus isolates pathogenic for the bertha armyworm, *Mamestra configurata* (Lepidoptera: Noctuidae). J Invertebr Pathol 56:47–56

Erlandson MA, Mori BA, Coutu C, et al (2019) Examining population structure of a bertha armyworm, *Mamestra configurata* (Lepidoptera: Noctuidae), outbreak in western North America: Implications for gene flow and dispersal. PloS ONE 14:e0218993

Evans TG (2015) Considerations for the use of transcriptomics in identifying the "genes that matter" for environmental adaptation. J Exp Biol 218:1925–1935

Evenden ML, Spohn BG, Moore AJ, et al (2002) Inheritance and evolution of male response to sex pheromone in Trichoplusia ni (Lepidoptera: Noctuidae). Chemoecology 12:53–59

Fang N, Teal PEA, Tumlinson JH (1995a) PBAN regulation of pheromone biosynthesis in female tobacco hornworm moths, *Manduca sexta* (L.). Arch Insect Biochem Physiol 29:35-44

Fang N, Teal PEA, Tumlinson JH (1995b) Correlation between glycerolipids and pheromone aldehydes in the sex pheromone gland of female tobacco hornworm moths, *Manduca sexta* (L.). Arch Insect Biochem Physiol 30:321–336

Faucheux MJ (2011) Antennal sensilla in adult males of five species of Coleophora (Coleophoridae): Considerations on their structure and function. Nota Lepidopterologica 34:93–101

Feng B, Guo Q, Zheng K, et al (2017) Antennal transcriptome analysis of the piercing moth *Oraesia emarginata (*Lepidoptera: Noctuidae). PloS ONE 12:e0179433

Fitt GP (1989) The ecology of heliothis species in relation to agroecosystems. Ann Rev Entomol 34:17–53

Fleischer J, Pregitzer P, Breer H, Krieger J (2018) Access to the odor world: olfactory receptors and their role for signal transduction in insects. Cell Mol Life Sci 75:485–508

Forstner M, Gohl T, Gondesen I, et al (2008) Differential expression of SNMP-1 and SNMP-2 proteins in pheromone-sensitive hairs of moths. Chem Senses 33:291–299

Foster SP (2016) Towards a quantitative paradigm for sex pheromone production in moths. In: Allison JD, Cardé RT (eds) Pheromone Communication in Moths. University of California Press, Oakland, California, pp 121–135

Foster SP, Anderson KG (2015) Sex pheromones in mate assessment: analysis of nutrient cost of sex pheromone production by females of the moth *Heliothis virescens*. J of Exp Biol 218:1252–1258

Fujii T, Ito K, Katsuma S, et al (2010a) Molecular and functional characterization of an acetyl-CoA acetyltransferase from the adzuki bean borer moth *Ostrinia scapulalis* (Lepidoptera: Crambidae). Insect Biochem Mol Biol 40:74–78

Fujii T, Nakano R, Takubo Y, et al (2010b) Female sex pheromone of a lichen moth *Eilema japonica* (Arctiidae, Lithosiinae): Components and control of production. J Insect Physiol 56:1986–1991

Fujii T, Namiki S, Abe H, et al (2011) Sex-linked transcription factor involved in a shift of sex pheromone preference in the silkmoth *Bombyx mori*. Proc Natl Acad Sci USA 108:18038–18043

Fujii T, Suzuki MG, Kawai T, et al (2007) Determination of the pheromone-producing region that has epoxidation activity in the abdominal tip of the Japanese giant looper, *Ascotis selenaria* cretacea (Lepidoptera: Geometridae). J Insect Physiol 53:312–318

Fujii T, Yamakawa R, Terashima Y, et al (2013) Propionates and acetates of chiral secondary alcohols: novel sex pheromone components produced by a lichen moth *Barsine expressa* (Arctiidae: Lithosiinae). J Chem Ecol 39:28–36

Galizia CG, Rössler W (2010) Parallel olfactory systems in insects: anatomy and function. Ann Rev Entomol 55:399–420

Gardiner A, Butlin RK, Jordan WC, Ritchie MG (2009) Sites of evolutionary divergence differ between olfactory and gustatory receptors of *Drosophila*. Biol Lett 5:244–247

Gemeno C, Haynes KF (2000) Periodical and age-related variation in chemical communication system of black cutworm moth, *Agrotis ipsilon*. J Chem Ecol 26:329–342

Gemeno C, Moore AJ, Preziosi RF, Haynes KF (2001) Quantitative genetics of signal evolution: a comparison of the pheromonal signal in two populations of the cabbage looper, *Trichoplusia ni.* Behav Genet 31:157–165

Gerber GH, Howlader MA (1987) The effects of photoperiod and temperature on calling behaviour and egg development of the bertha armyworm, *Mamestra configurata* (Lepidoptera: Noctuidae). J Insect Physiol 33:429–436

Glaser N, Gallot A, Legeai F, et al (2013) Candidate chemosensory genes in the stemborer *Sesamia nonagrioides*. Int J Biol Sci 9:481–495

Glover T, Campbell M, Robbins P, Roelofs W (1990) Sex-linked control of sex pheromone behavioral responses in European corn-borer moths (*Ostrinia nubilalis*) confirmed with TPI marker gene. Arch Insect Biochem Physiol 15:67–77

Goldman AL, van der Goes van Naters W, Lessing D, et al (2005) Coexpression of two functional odor receptors in one neuron. Neuron 45:661–666

Gomez-Diaz C, Bargeton B, Abuin L, et al (2016) A CD36 ectodomain mediates insect pheromone detection via a putative tunnelling mechanism. Nat Comm 7:11866

Gong D-P, Zhang H-J, Zhao P, et al (2007) Identification and expression pattern of the chemosensory protein gene family in the silkworm, *Bombyx mori*. Insect Biochem Mol Biol 37:266–277

Gong D-P, Zhang H-J, Zhao P, et al (2009) The odorant binding protein gene family from the genome of silkworm, *Bombyx mori*. BMC Genomics 10:332

Gould F, Estock M, Hillier NK, et al (2010) Sexual isolation of male moths explained by a single pheromone response QTL containing four receptor genes. Proc Natl Acad Sci USA 107:8660–8665

Gould F, Groot AT, Vasquez GM, Schal C (2017) Sexual communication in Lepidoptera: A need for wedding genetics, biochemistry and molecular biology. In: Goldsmith MR, Marec F (eds) Molecular Biology and Genetics of Lepidoptera. CRC Press, Florida, pp 169–193

Grabherr MG, Haas BJ, Yassour M, et al (2011) Full-length transcriptome assembly from RNA-Seq data without a reference genome. Nat Biotechnol 29:644–652

Grant AJ, O'Connell RJ, Eisner T (1989) Pheromone-mediated sexual selection in the moth U*tetheisa ornatrix*: Olfactory receptor neurons responsive to a male-produced pheromone. J Insect Behav 2:371–385

Grapputo A, Thrimawithana AH, Steinwender B, Newcomb RD (2018) Differential gene expression in the evolution of sex pheromone communication in New Zealand's endemic leafroller moths of the genera *Ctenopseustis* and *Planotortrix.* BMC Genomics 19:94

Grayson KL, Parry D, Faske TM, et al (2015) Performance of wild and laboratory-reared gypsy moth (Lepidoptera: Erebidae): A comparison between foliage and artificial diet. Environ Entomol 44:864–873

Groot A, Gemeno C, Brownie C, et al (2005) Male and female antennal responses in *Heliothis virescens* and *H. subflexa* to conspecific and heterospecific sex pheromone compounds. Environ Entomol 34:256–263

Groot AT (2014) Circadian rhythms of sexual activities in moths: a review. Front Ecol Evol 2:1-21

Groot AT, Estock ML, Horovitz JL, et al (2009) QTL analysis of sex pheromone blend differences between two closely related moths: Insights into divergence in biosynthetic pathways. Insect Biochem Mol Biol 39:568–577

Groot AT, Horovitz JL, Hamilton J, et al (2006) Experimental evidence for interspecific directional selection on moth pheromone communication. Proc Natl Acad Sci USA 103:5858–5863

Groot AT, Schofl G, Inglis O, et al (2014) Within-population variability in a moth sex pheromone blend: genetic basis and behavioural consequences. Proc Biol Sci 281:20133054-20133054

Groot AT, Ward C, Wang J, et al (2004) Introgressing pheromone QTL between species: towards an evolutionary understanding of differentiation in sexual communication. J Chem Ecol 30:2495–2514

Große-Wilde E, Gohl T, Bouché E, et al (2007) Candidate pheromone receptors provide the basis for the response of distinct antennal neurons to pheromonal compounds. Eur J Neurosci 25:2364–2373

Große-Wilde E, Kuebler LS, Bucks S, et al (2011) Antennal transcriptome of *Manduca sexta*. Proc Natl Acad Sci USA 108:1–14

Große-Wilde E, Stieber R, Forstner M, et al (2010) Sex-specific odorant receptors of the tobacco hornworm *Manduca sexta*. Front Cell Neurosci 4:1-7

Haas BJ, Papanicolaou A Fau Yassour M, Yassour M Fau Grabherr M, et al (2013) *De novo* transcript sequence reconstruction from RNA-seq using the Trinity platform for reference generation and analysis. Nat Protocols 8:1750–2799 (Electronic)

Haas BJ, Zody MC (2010) Advancing RNA-Seq analysis. Nat Biotechnol 28:421–423

Hagström AK, Liénard MA, Groot AT, et al (2012) Semi–selective fatty acyl reductases from four heliothine moths influence the specific pheromone composition. PloS ONE 7:e37230

Hallberg E, Hansson BS, Steinbrecht RA (1994) Morphological characteristics of antennal sensilla in the European cornborer *Ostrinia nubilalis* (Lepidoptera: Pyralidae). Tissue Cell 26:489–502

Hallberg E, Subchev M (1997) Unusual location and structure of female pheromone glands in *Theresimima (= Ino) ampelophaga* Bayle-Berelle (Lepidoptera : Zygaenidae). Int J Insect Morphol & Embryol 25:381–389

Hallem EA, Carlson JR (2006) Coding of odors by a receptor repertoire. Cell 125:143–160

Hallem EA, Dahanukar A, Carlson JR (2006) Insect odor and taste receptors. Ann Rev Entomol 51:113–135

Hallem EA, Ho MG, Carlson JR (2004) The molecular basis of odor coding in the *Drosophila* antenna. Cell 117:965–979. doi: 10.1016/j.cell.2004.05.012

Hansson BS (1995) Olfaction in Lepidoptera. Experientia 51:1003–1027

Hansson BS, Hallberg E, Löfstedt C, Steinbrecht RA (1994) Correlation between dendrite diameter and action potential amplitude in sex pheromone specific receptor neurons in male *Ostrinia nubilalis* (Lepidoptera: Pyralidae). Tissue and Cell 26:503–512

Hansson BS, L Fstedt C, Roelofs WL (1987) Inheritance of olfactory response to sex pheromone components in *Ostrinia nubilalis*. Naturwissenschaften 74:497–499

Hansson BS, Stensmyr MC (2011) Evolution of insect olfaction. Neuron 72:698–711

Hansson BS, Tóth M, Löfstedt C, et al (1990) Pheromone variation among eastern European and a western Asian population of the turnip moth *Agrotis segetum*. J Chem Ecol 16:1611–1622

Hashimoto K, Yoshizawa AC, Okuda S, et al (2008) The repertoire of desaturases and elongases reveals fatty acid variations in 56 eukaryotic genomes. J lipid Res 49:183–191

Hashimoto T (1996) Peroxisomal Oxidation: enzymology and molecular biology. Ann NY Acad Sci 804:86–98

Haupt SS, Sakurai T, Namiki S, et al (2010) Olfactory Information Processing in Moths. In: Menini A (ed) The Neurobiology of Olfaction. Boca Raton(FL): CRC Press/Taylor & Francis, Florida

Haynes KF (2016) Genetic Control of Moth Sex Pheromone Signal and Response. In: Allison JD, Cardé RT (eds) Pheromone Communication in Moths. University of California Press, Oakland, California, pp 98–109

Haynes KF, Gaston LK, Pope MM, Baker TC (1984) Potential for evolution of resistance to pheromones: Interindividual and interpopulational variation in chemical communication system of pink bollworm moth. J Chem Ecol 10:1551–1565

Haynes KF, Hunt RE (1990a) Interpopulational variation in emitted pheromone blend of cabbage looper moth, *Trichoplusia ni*. J Chem Ecol 16:509–519

Haynes KF, Hunt RE (1990b) A mutation in pheromonal communication system of cabbage looper moth, *Trichoplusia ni*. J Chem Ecol 16:1249–1257

He P, Zhang Y-F, Hong D-Y, et al (2017) A reference gene set for sex pheromone biosynthesis and degradation genes from the diamondback moth, *Plutella xylostella*, based on genome and transcriptome digital gene expression analyses. BMC Genomics 18:262

Hegdekar BM (1983) Effect of latitude on the critical photoperiod for diapause induction in the bertha armyworm, *Mamestra configurata* (Lepidoptera: Noctuidae). Can Entomol 115:1039–1042

Hemmann DJ, Allison JD, Haynes KF (2008) Trade-off between sensitivity and specificity in the cabbage looper moth response to sex pheromone. J Chem Ecol 34:1476–1486

Hildebrand JG, Shepherd GM (1997) Mechanisms of olfactory discrimination: converging evidence for common principles across phyla. Ann Rev Neurosci 20:595–631

Hill AS, Cardé RT, Kido H, Roelofs WL (1975) Sex pheromone of the orange tortrix moth, *Argyrotaenia citrana* (Lepidoptera: Tortricidae). J Chem Ecol 1:215–224

Hill AS, Roelofs WL (1981) Sex pheromone of the saltmarsh caterpillar moth, *Estigmene acrea*. J Chem Ecol 7:655–668

Hill MP, Macfadyen S, Nash MA (2017) Broad spectrum pesticide application alters natural enemy communities and may facilitate secondary pest outbreaks. PeerJ 5:e4179

Hill WG, Armando C (1992) Artificial selection experiments. Ann Rev Ecol Syst 23:287–310

Hokkanen HMT, Menzler-Hokkanen I (2017) Use of Entomopathogenic Fungi in the insect Pest Management of *Brassica* Oilseed Crops. In: Reddy GVP (ed) Integrated Management of Insect Pests on Canola and Other Brassica Oilseed Crops. Wallingford, pp 373–382

Hopf TA, Morinaga S, Ihara S, et al (2015) Amino acid coevolution reveals three-dimensional structure and functional domains of insect odorant receptors. Nat Comm 6:6077

Howlader MA, Gerber GH (1986a) Calling behavior of the bertha armyworm, *Mamestra configurata* (Lepidoptera: Noctuidae). Can Entomol 118:735–743

Howlader MA, Gerber GH (1986b) Effects of age, egg development, and mating on calling behavior of the bertha armyworm, *Mamestra configurata* Walker (Lepidoptera: Noctuidae). Can Entomol 118:1221–1230

Hölzer M, Marz M (2019) *De novo* transcriptome assembly: A comprehensive cross-species comparison of short-read RNA-Seq assemblers. GigaScience 8:1-16

Huang X, Chen X-G, Armbruster PA (2016) Comparative performance of transcriptome assembly methods for non-model organisms. BMC Genomics 17:523

Hughes DT, Wang G, Zwiebel LJ, Luetje CW (2014) A determinant of odorant specificity is located at the extracellular loop 2-transmembrane domain 4 interface of an *Anopheles gambiae* odorant receptor subunit. Chem Senses 39:761–769

Hunt RE, Haynes KF (1990) Periodicity in the quantity and blend ratios of pheromone components in glands and volatile emissions of mutant and normal cabbage looper moths, *Trichoplusia ni*. J Insect Physiol 36:769–774

Ikeda Y, Okamura-Ikeda K, Tanaka K (1985) Purification and characterization of short-chain, medium-chain, and long-chain acyl-CoA dehydrogenases from rat liver mitochondria. Isolation of the holo- and apoenzymes and conversion of the apoenzyme to the holoenzyme. J Biol Chem 260:1311–1325

Ishida Y, Ishibashi J, Leal WS (2013) Fatty acid solubilizer from the oral disk of the blowfly. PloS ONE 8:e51779

Ishida Y, Leal WS (2005) Rapid inactivation of a moth pheromone. Proc Natl Acad Sci USA 102:14075–14079

Ishida Y, Leal WS (2008) Chiral discrimination of the Japanese beetle sex pheromone and a behavioral antagonist by a pheromone-degrading enzyme. Proc Natl Acad Sci USA 105:9076–9080

Itagaki H, Conner WE (1988) Calling behavior of *Manduca sexta* (L.) (Lepidoptera: Sphingidae) with notes on the morphology of the female sex pheromone gland. Ann Entomol Soc Am 81:798–807

Jacob V (2018) Current source density analysis of electroantennogram recordings: a tool for mapping the olfactory response in an insect antenna. Front Cell Neurosci 12:287

Jacob V, Scolari F, Delatte H, et al (2017) Current source density mapping of antennal sensory selectivity reveals conserved olfactory systems between tephritids and *Drosophila*. Sci Rep 7:1–13

Jacquin E, Jurenka RA, Ljungberg H, et al (1994) Control of sex pheromone biosynthesis in the moth *Mamestra brassicae* by the pheromone biosynthesis activating neuropeptide. Insect Biochem Mol Biol 24:203–211

Jacquin-Joly E, François M-C, Burnet M, et al (2002) Expression pattern in the antennae of a newly isolated lepidopteran Gq protein alpha subunit cDNA. Eur J Biochem 269:2133–2142

Jacquin-Joly E, Legeai F, Montagné N, et al (2012) Candidate chemosensory genes in female antennae of the noctuid moth *Spodoptera littoralis*. Int J of Biol Sci 8:1036–1050

Jacquin-Joly E, Vogt RG, François M-C, Nagnan-Le Meillour P (2001) Functional and expression pattern analysis of chemosensory proteins expressed in antennae and pheromonal gland of *Mamestra brassicae*. Chem Senses 26:833–844

Jeong SE, Rosenfield C-L, Marsella-Herrick P, et al (2003) Multiple acyl-CoA desaturase-encoding transcripts in pheromone glands of *Helicoverpa assulta*, the oriental tobacco budworm. Insect Biochem Mol Biol 33:609–622

Jin X, Ha TS, Smith DP (2008) SNMP is a signaling component required for pheromone sensitivity in *Drosophila*. Proc Natl Acad Sci USA 105:10996–11001

Jones PL, Pask GM, Rinker DC, Zwiebel LJ (2011) Functional agonism of insect odorant receptor ion channels. Proc Natl Acad Sci 108:8821–8825

Jones WD, Cayirlioglu P, Kadow IG, Vosshall LB (2007) Two chemosensory receptors together mediate carbon dioxide detection in *Drosophila.* Nature 445:86–90

Joseph J, Dunn FA, Stopfer M (2012) Spontaneous olfactory receptor neuron activity determines follower cell response properties. J Neurosci 32:2900–2910

Jurenka R (2004) Insect Pheromone Biosynthesis. In: The Chemistry of Pheromones and Other Semiochemicals I. Springer, Berlin, Heidelberg, pp 97–132

Jurenka R, Rafaeli A (2011) Regulatory role of PBAN in sex pheromone biosynthesis of heliothine moths. Front Endocrinol (Lausanne) 2:46

Jurenka RA (2003) Biochemistry of Female Moth Sex Pheromones. In: Blomquist GJ, Vogt RG (eds) Insect Pheromone Biochemistry and Molecular Biology. Elsevier, Amsterdam, pp 53–80

Jurenka RA, Haynes KF, Adlof RO, et al (1994) Sex pheromone component ratio in the cabbage looper moth altered by a mutation affecting the fatty acid chain-shortening reactions in the pheromone biosynthetic pathway. Insect Biochem Mol Biol 24:373–381

Jurenka RA, Jacquin E, Roelofs WL (1991) Stimulation of pheromone biosynthesis in the moth *Helicoverpa zea*: action of a brain hormone on pheromone glands involves Ca^{2+} and cAMP as second messengers. Proc Natl Acad Sci USA 88:8621–8625

Jørgensen K, Kvello P, Almaas TJ, Mustaparta H (2006) Two closely located areas in the suboesophageal ganglion and the tritocerebrum receive projections of gustatory receptor neurons located on the antennae and the proboscis in the moth *Heliothis virescens*. J Comp Neurol 496:121–134

Kaissling K (1986) Chemo-electrical transduction in insect olfactory receptors. Ann Rev Neurosci 9:121–145

Kaissling K-E (2014) Pheromone reception in insects. In: Neurobiology of Chemical Communication. CRC Press, pp 99–146

Kaissling K-E (2013) Kinetics of olfactory responses might largely depend on the odorant–receptor interaction and the odorant deactivation postulated for flux detectors. J Comp Physiol A 199:879–896

Kaissling K-E (2009) Olfactory perireceptor and receptor events in moths: a kinetic model revised. J Comp Physiol A 195:895–922

Kaissling K-E (1995) Single unit and electroantennogram recordings in insect olfactory organs. In: Spielman AI, Brand JG (eds) Experimental Cell Biology of Taste and Olfaction. Florida, pp 361–377

Kaissling KE (1998a) Flux detectors versus concentration detectors: two types of chemoreceptors. Chem Senses 23:99–111

Kaissling KE (1998b) Pheromone deactivation catalyzed by receptor molecules: a quantitative kinetic model. Chem Senses 23:385–395

Kaissling KE (2001) Olfactory perireceptor and receptor events in moths: A kinetic model. Chem Senses 26:125–150

Kanzaki R, Arbas E, Hildebrand J (1991a) Physiology and morphology of descending neurons in pheromone-processing olfactory pathways in the male moth *Manduca sexta*. J Comp Physiol A 169:

Kanzaki R, Arbas EA, Hildebrand JG (1991b) Physiology and morphology of protocerebral olfactory neurons in the male moth *Manduca sexta*. J Comp Physiol A 168:281–298

Karlson P, Luscher M (1959) "Pheromones": a new term for a class of biologically active substances. Nature 183:55–56

Karner T, Kellner I, Schultze A, et al (2015) Co-expression of six tightly clustered odorant receptor genes in the antenna of the malaria mosquito *Anopheles gambiae*. Front Ecol Evol 3 :1–8

Karpati Z, Tasin M, Cardé RT, Dekker T (2013) Early quality assesment lessens pheromone specificity in moth. PNAS 110:7377–7382

Kay LM, Stopfer M (2006) Information processing in the olfactory systems of insects and vertebrates. Semin Cell Dev Biol 17:433–442

Kárpáti Z, Dekker T, Hansson BS (2008) Reversed functional topology in the antennal lobe of the male European corn borer. J of Exp Biol 211:2841–2848

Kárpáti Z, Olsson S, Hansson BS, Dekker T (2010) Inheritance of central neuroanatomy and physiology related to pheromone preference in the male European corn borer. BMC Evol Biol 10:286

Kennedy JS, Ludlow AR, Sanders CJ (1980) Guidance system used in moth sex attraction. Nature 288:475–477

Kennedy JS, Marsh D (1974) Pheromone-regulated anemotaxis in flying moths. Science 184:999–1001

Kijima H, Goshima S, Kazawa T, et al (1995) Free ion concentrations in receptor lymph and role of transepithelial voltage in the fly labellar taste receptor. J Comp Physiol A 177:123–133

Kim KS, French BW, Sumerford DV, Sappington TW (2007) Genetic diversity in laboratory colonies of western corn rootworm (Coleoptera: Chrysomelidae), including a nondiapause colony. Environ Entomol 36:637–645

Kim Y-J, Nachman RJ, Aimanova K, et al (2008) The pheromone biosynthesis activating neuropeptide (PBAN) receptor of *Heliothis virescens*: Identification, functional expression, and structure–activity relationships of ligand analogs. Peptides 29:268–275

Kiyota R, Arakawa M, Yamakawa R, et al (2011) Biosynthetic pathways of the sex pheromone components and substrate selectivity of the oxidation enzymes working in pheromone glands of the fall webworm, *Hyphantria cunea*. Insect Biochem Mol Biol 41:362–369

Knipple DC, Rosenfield C-L, Nielsen R, et al (2002) Evolution of the integral membrane desaturase gene family in moths and flies. Genetics 162:1737–1752

Koerte S, Keesey IW, Khallaf MA, et al (2018) Evaluation of the DREAM Technique for a High-Throughput Deorphanization of Chemosensory Receptors in Drosophila. Frontiers in Molecular Neuroscience 11:149

Koh T-W, He Z, Gorur-Shandilya S, et al (2014) The *Drosophila* IR20a clade of ionotropic receptors are candidate taste and pheromone receptors. Neuron 83:850–865

Koutroumpa FA, Karpati Z (2014) Shifts in sensory neuron identity parallel differences in pheromone preference in the European corn borer. Front Ecol Evol 2:65

Krieger J, Grosse-Wilde E, Gohl T, Breer H (2005) Candidate pheromone receptors of the silkmoth *Bombyx mori*. Eur J Neurosci 21:2167–2176

Krieger J, Grosse-Wilde E, Gohl T, et al (2004) Genes encoding candidate pheromone receptors in a moth (*Heliothis virescens*). Proc Natl Acad Sci USA 101:11845–11850

Kuenen LPS, Baker TC (1981) Habituation versus sensory adaptation as the cause of reduced attraction following pulsed and constant sex pheromone pre-exposure in *Trichoplusia ni*. J Insect Physiol 27:721–726

Kuenen LPS, Baker TC (1982a) The effects of pheromone concentration on the flight behaviour of the oriental fruit moth, *Grapholitha molesta*. Physiol Entomol 7:423–434

Kuenen LPS, Baker TC (1982b) Optomotor regulation of ground velocity in moths during flight to sex pheromone at different heights. Physiol Entomol 7:193–202

Kuenen LPS, Gilbert C, Siegel J (2014) Flying slower: Floor pattern object size affects orthokinetic responses during moth flight to sex pheromone. J Insect Behav 27:581–592

Kuenen LPS, Siegel JP (2015) Measure your septa release ratios: pheromone release ratio variability affected by rubber septa and solvent. J Chem Ecol 41:303–310

Kumar BN, Taylor RW, Pask GM, et al (2013) A conserved aspartic acid is important for agonist (VUAA1) and odorant/tuning receptor-dependent activation of the insect odorant co-receptor (ORCO). PloS ONE 8:e70218

Lacey MJ, Sanders CJ (1992) Chemical composition of sex pheromone of oriental fruit moth and rates of release by individual female moths. J Chem Ecol 18:1421–1435

LaForest S, Wu W, Löfstedt C (1997) A genetic analysis of population differences in pheromone production and response between two populations of the turnip moth, *Agrotis segetum*. J Chem Ecol 23:1487–1503

Laish-Farkash A, Glikson M, Brass D, et al (2010) A novel mutation in the HCN4 gene causes symptomatic sinus bradycardia in Moroccan Jews. J Cardiovasc Electrophysiol 21:1365-1372

Lamb RJ, Turnock WJ, Hayhoe HN (1985) Winter survival and outbreaks of bertha armyworm, *Mamestra configurata* (Lepidoptera: Noctuidae), on canola. Can Entomol 117:727–736

Landolt PJ (2000) New chemical attractants for trapping *Lacanobia subjuncta*, *Mamestra configurata*, and *Xestia c-nigrum* (Lepidoptera: Noctuidae). J Econ Entomol 93:101–106

Langmead B, Salzberg SL (2012) Fast gapped-read alignment with Bowtie 2. Nat Methods 9:357–359

Larkin MA, Blackshields G, Brown NP, et al (2007) Clustal W and Clustal X version 2.0. Bioinformatics 23:2947–2948

Larsson MC, Domingos AI, Jones WD, et al (2004) Or83b encodes a broadly expressed odorant receptor essential for *Drosophila* olfaction. Neuron 43:703–714

Lassance J-M (2016) The European Corn Borer *Ostrinia nubilalis*. In: Allison JD, Cardé RT (eds) Pheromone Communication in Moths. University of California Press, Oakland, California, pp 242–253

Lassance J-M, Bogdanowicz SM, Wanner KW, et al (2011) Gene genealogies reveal differentiation at sex pheromone olfactory receptor loci in pheromone strains of the European corn borer, O*strinia nubilalis*. Evolution 65:1583–1593

Lassance J-M, Groot AT, Liénard MA, et al (2010) Allelic variation in a fatty-acyl reductase gene causes divergence in moth sex pheromones. Nature 466:486–489

Lassance J-M, Löfstedt C (2013) Chemical communication: a jewel sheds light on signal evolution. Curr Biol 23:R346–R348

Laue M, Maida R, Redkozubov A (1997) G-protein activation, identification and immunolocalization in pheromone-sensitive sensilla trichodea of moths. Cell Tissue Res 288:149–158

Leal WS (2013) Odorant reception in insects: roles of receptors, binding proteins, and degrading enzymes. Ann Rev Entomol 58:373–391

Leal WS, Chen AM, Ishida Y, et al (2005) Kinetics and molecular properties of pheromone binding and release. Proc Natl Acad Sci USA 102:5386–5391

Leary GP, Allen JE, Bunger PL, et al (2012) Single mutation to a sex pheromone receptor provides adaptive specificity between closely related moth species. Proc Natl Acad Sci USA109:14081–14086

Letunic I, Bork P (2007) Interactive Tree Of Life (iTOL): an online tool for phylogenetic tree display and annotation. Bioinformatics 23:127–128

Levy SE, Myers RM (2016) Advancements in next-generation sequencing. Ann Rev Genomics Hum Genet 17:95–115

Li B, Dewey CN (2011) RSEM: accurate transcript quantification from RNA-Seq data with or without a reference genome. BMC Bioinformatics 12:323

Li B, Fillmore N, Bai Y, et al (2014) Evaluation of *de novo* transcriptome assemblies from RNA-Seq data. Genome Biol 15:663–21

Li S, Picimbon J-F, Ji S, et al (2008) Multiple functions of an odorant-binding protein in the mosquito *Aedes aegypti*. Biochem Biophys Res Commun 372:464–468

Lienard MA, Strandh M, Hedenstrom E, et al (2008) Key biosynthetic gene subfamily recruited for pheromone production prior to the extensive radiation of Lepidoptera. BMC Evol Biol 8:270. doi: 10.1186/1471-2148-8-270

Liénard MA, Hagström AK, Lassance J-M, Löfstedt C (2010) Evolution of multicomponent pheromone signals in small ermine moths involves a single fatty-acyl reductase gene. Proc Natl Acad Sci USA 107:10955–10960

Liénard MA, Wang H-L, Lassance J-M, Löfstedt C (2014) Sex pheromone biosynthetic pathways are conserved between moths and the butterfly *Bicyclus anynana*. Nat Comm 5:212

Linn C Jr, Poole K, Zhang A, Roelofs W (1999) Pheromone-blend discrimination by European corn borer moths with inter-race and inter-sex antennal transplants. J Comp Physiol A 184:273–278

Linn C Jr., O'Connor M, Roelofs W (2003) Silent genes and rare males: A fresh look at pheromone blend response specificity in the European corn borer moth, *Ostrinia nubilalis*. J Insect Sci 3:1–6

Linn CE Jr., Bjostad LB, Du JW, Roelofs WL (1984) Redundancy in a chemical signal: behavioral responses of male *Trichoplusia ni* to a 6-component sex pheromone blend. J Chem Ecol 10:1635–1658

Linn CE, Campbell MG, Roelofs WL (1987) Pheromone components and active spaces: What do moths smell and where do they smell it? Science 237:650–652

Linn CE, Campbell MG, Roelofs WL (1988) Temperature modulation of behavioural thresholds controlling male moth sex pheromone response specificity. Physiol Entomol 13:59–67

Linn CE, Gaston LK (1981) Behavioral function of the components and the blend of the sex pheromone of the cabbage looper, *Trichoplusia ni*. Environ Entomol 10:751–755

Linn CE, Roelofs WL (1981) Modification of sex pheromone blend discrimination in male Oriental fruit moths by pre-exposure to (E)-8-dodecenyl acetate. Physiol Entomol 6:421–429

Linn CE, Roelofs WL (1983) Effect of varying proportions of the alcohol component on sex pheromone blend discrimination in male Oriental fruit moths. Physiol Entomol 8:291–306

Linn CE, Young MS, Gendle M, et al (1997) Sex pheromone blend discrimination in two races and hybrids of the European corn borer moth, *Ostrinia nubilalis*. Physiol Entomol 22:212-223

Liu C, Zhang J, Liu Y, et al (2014) Expression of SNMP1 and SNMP2 genes in antennal sensilla of *Spodoptera exigua* (Hübner). Arch Insect Biochem Physiol 85:114–126

Liu HJ, Liu TP (1984) Sensilla on the antennal flagellum of the bertha armyworm moth, *Mamestra configurata* Walker (Lepidoptera: Noctuidae): a scanning electron microscope study. Ann Entomol Soc Am 77:236–245

Liu Y, Gu S, Zhang Y, et al (2012) Candidate olfaction genes identified within the *Helicoverpa armigera* antennal transcriptome. PloS ONE 7:e48260

Liu Y-B, Haynes KF (1994a) Temporal and temperature-induced changes in emission rates and blend ratios of sex pheromone components in *Trichoplusia ni*. J Insect Physiol 40:341–346.

Liu Y-B, Haynes KF (1994b) Evolution of behavioral responses to sex pheromone in mutant laboratory colonies of *Trichoplusia ni*. J Chem Ecol 20:231–238

Lopez-Maestre H, Brinza L, Marchet C, et al (2016) SNP calling from RNA-seq data without a reference genome: identification, quantification, differential analysis and impact on the protein sequence. Nucleic Acids Res 44:e148

Löfstedt C (1990) Population variation and genetic control of pheromone communication systems in moths. Entomol Exp App 54:199–218

Löfstedt C, Herrebout WM, Menken SBJ (1991) Sex pheromones and their potential role in the evolution of reproductive isolation in small ermine moths (Yponomeutidae). Chemoecology 2:20–28

Löfstedt C, Kozlov MV (1997) A Phylogenetic Analysis of Pheromone Communication in Primitive Moths. In: Cardé RT, Minks AK (eds) Insect Pheromone Research. New York, pp 473–489

Löfstedt C, Lanne BS, Löfqvist J, et al (1985a) Individual variation in the pheromone of the turnip moth, *Agrotis segetum*. J Chem Ecol 11:1181–1196

Löfstedt C, Linn CE, Löfqvist J (1985b) Behavioral responses of male turnip moths, *Agrotis segetum*, to sex pheromone in a flight tunnel and in the field. J Chem Ecol 11:1209–1221

Löfstedt C, Löfqvist J, Lanne BS, et al (1986) Pheromone dialects in European turnip moths *Agrotis segetum*. Oikos 46:250

Löfstedt C, Wahlberg N, Millar JG (2016) Evolutionary Patterns of Pheromone Diversity in Lepidoptera. In: Allison JD, Cardé RT (eds) Pheromone Communication in Moths. University of California Press, Oakland, California, pp 51–87

Lucas P, Renou M (1992) Electrophysiological study of the effects of deltamethrin, bioresmethrin, and DDT on the activity of pheromone receptor neurones in two moth species. Pestic Biochem and Phys 43:103–115

Lundin C, Käll L, Kreher SA, et al (2007) Membrane topology of the Drosophila OR83b odorant receptor. FEBS Lett 581:5601–5604

Ma PWK, Ramaswamy SB (2003) Biology and ultrastructure of sex pheromone-producing tissue. In: Insect Pheromone Biochemistry and Molecular Biology. Elsevier, pp 19–51

Mafra-Neto A, Cardé RT (1995) Effect of the fine-scale structure of pheromone plumes: pulse frequency modulates activation and upwind flight of almond moth males. Physiol Entomol 20:229–242

Maida R, Ziegelberger G, Kaissling KE (2003) Ligand binding to six recombinant pheromone-binding proteins of *Antheraea polyphemus* and *Antheraea pernyi*. J Comp Physiol B 173:565–573

Malo EA, Renou M, Guerrero A (2000) Analytical studies of *Spodoptera littoralis* sex pheromone components by electroantennography and coupled gas chromatography–electroantennographic detection. Talanta 52:525–532

Mao A, Zhou J, Bin Mao, et al (2016) Sex pheromone recognition and characterization of three pheromone-binding proteins in the legume pod borer, *Maruca vitrata* Fabricius (Lepidoptera: Crambidae). Sci Rep 6:503

Martin JP, Beyerlein A, Dacks AM, et al (2011) The neurobiology of insect olfaction: Sensory processing in a comparative context. Prog Neurobiol 95:427–447

Mason PG, Arthur AP, Olfert OO, Erlandson MA (1998) The bertha armyworm (*Mamestra configurata*) (Lepidoptera: Noctuidae) in Western Canada. Can Entomol 130:321–336

Mason PG, Turnock WJ, Erlandson MA, et al (2002) *Mamestra configurata* Walker, Bertha armyworm (Lepidoptera: Noctuidae). In: Mason PG, Huber J (eds) Biological control programmes against insects and weeds in Canada, 1980-2000. CAB International Publishing, Wallingford, pp 169–176

Matsumoto S (2010) Molecular mechanisms underlying sex pheromone production in moths. Biosci, Biotech, Biochem 74:223–231

Matsuoka K, Tabunoki H, Kawai T, et al (2006) Transport of a hydrophobic biosynthetic precursor by lipophorin in the hemolymph of a geometrid female moth which secretes an epoxyalkenyl sex pheromone. Insect Biochem Mol Biol 36:576–583

McCloskey C, Isman MB (1993) Influence of foliar glucosinolates in oilseed rape and mustard on feeding and growth of the bertha armyworm, *Mamestra configurata* (Walker). J Chem Ecol 19:249–266

McNeil JN (1991) Behavioral ecology of pheromone-mediated communication in moths and its importance in the use of pheromone traps. Ann Rev Entomol 36:407–430

Millar J (2014) The devil is in the details. J Chem Ecol 40:517–518

Miller JR, Gut LJ (2015) Mating disruption for the 21st century: matching technology with mechanism. Environ Entomol 44:427–453

Miller JR, Mori K, Roelofs WL (1977) Gypsy moth field trapping and electroantennogram studies with pheromone enantiomers. J Insect Physiol 23:1447–1453

Miller JR, Roelofs WL (1980) Individual variation in sex pheromone component ratios in two populations of the redbanded leafroller moth, *Argyrotaenia velutinana*. Environ Entomol 9:359–363

Miller JR, Roelofs WL (1978) Sustained-flight tunnel for measuring insect responses to wind-borne sex pheromones. J Chem Ecol 4:187–198

Miura N, Atsumi S, Tabunoki H, Sato R (2005) Expression and localization of three G protein alpha subunits, Go, Gq, and Gs, in adult antennae of the silkmoth (*Bombyx mori*). J Comp Neurol 485:143–152

Miyamoto T, Yamamoto M, Ono A, et al (1999) Substrate specificity of the epoxidation reaction in sex pheromone biosynthesis of the Japanese giant looper (Lepidoptera: Geometridae). Insect Biochem Mol Biol

Montagné N, de Fouchier A, Newcomb RD, Jacquin-Joly E (2015) Advances in the identification and characterization of olfactory receptors in insects. Prog Mol Biol Transl Sci 130:55–80

Mori K, Harada H, Zagatti P, et al (1991) Pheromone synthesis, CXXVI. Synthesis and biological activity of four stereoisomers of 6,10,14-trimethyl-2-pentadecanol, the female-produced sex pheromone of rice moth (*Corcyra cephalonica*). Liebigs Annalen der Chemie 1991:259–267

Morse D, Meighen E (1986) Pheromone biosynthesis and the role of functional groups in pheromone specificity. J Chem Ecol 12:335–351

Morse D, Meighen E (1987) Biosynthesis of the acetate ester precursor of the spruce budworm sex pheromone by an acetyl CoA: fatty alcohol acetyltransferase. Insect Biochem 17:53–59

Mosbah A, Campanacci V, Lartigue A, et al (2003) Solution structure of a chemosensory protein from the moth *Mamestra brassicae*. Biochem J 369:39–44

Moto K, Yoshiga T, Yamamoto M, et al (2003) Pheromone gland-specific fatty-acyl reductase of the silkmoth, Bombyx mori. Proc Natl Acad Sci USA 100:9156–9161

Mucignat-Caretta C (2014) Neurobiology of Chemical Communication. In: Mucignat-Caretta C (ed) Frontiers in Neuroscience. CRC Press/Taylor & Francis, Boca Raton (FL) 2014:1-22

Murlis J, Elkinton JS, Cardé RT (1992) Odor plumes and how insects use them. Ann Rev Entomol 37:505–532

Murlis J, Jones CD (1981) Fine-scale structure of odour plumes in relation to insect orientation to distant pheromone and other attractant sources. Physiol Entomol 6:71–86

Nagai T (1981) Electroantennogram response gradient on the antenna of the European corn borer, *Ostrinia nubilalis*. J Insect Physiol 27:889–894

Nagai T (1983a) Spread of local electroantennogram response of the European corn borer, *Ostrinia nubilalis*. Pestic Biochem and Phys 19:291–298

Nagai T (1983b) On the relationship between the electroantennogram and simultaneously recorded single sensillum response of the european corn borer, *Ostrinia nubilalis*. Arch Insect Biochem Physiol 1:85–91

Nakagawa T, Pellegrino M, Sato K, et al (2012) Amino acid residues contributing to function of the heteromeric insect olfactory receptor complex. PloS ONE 7:e32372

Nakagawa T, Vosshall LB (2009) Controversy and consensus: noncanonical signaling mechanisms in the insect olfactory system. Curr Opin Neurobiol 19:284–292

Nardi JB, Miller LA, Walden KKO, et al (2003) Expression patterns of odorant-binding proteins in antennae of the moth *Manduca sexta*. Cell Tissue Res 313:321–333

Nicholson C (1973) Theoretical analysis of field potentials in anisotropic ensembles of neuronal elements. IEEE Trans Biomed Eng BME-20:278–288

Nielsen J (2003) It is all about metabolic fluxes. J Bacteriol 185:7031–7035

Ning C, Yang K, Xu M, et al (2016) Functional validation of the carbon dioxide receptor in labial palps of *Helicoverpa armigera* moths. Insect Biochem Mol Biol 73:12–19

Oakeshott JG, Claudianos C, Russell RJ, Robin GC (1999) Carboxyl/cholinesterases: a case study of the evolution of a successful multigene family. BioEssays 21:1031–1042

Olberg R, Willis M (1990) Pheromone-modulated optomotor response in male gypsy moths, *Lymantria dispar* L.: Directionally selective visual interneurons in the ventral nerve cord. J Comp Physiol A 167:707-714

Olivier V, Monsempes C, François MC, et al (2011) Candidate chemosensory ionotropic receptors in a Lepidoptera. Insect Mol Biol 20:189–199

Olsson SB, Hansson BS (2013) Electroantennogram and Single Sensillum Recording in Insect Antennae. In: Pheromone Signaling. Humana Press, Totowa, NJ, Totowa, NJ, pp 157–177

Olsson SB, Kesevan S, Groot AT, et al (2010) Ostrinia revisited: Evidence for sex linkage in European Corn Borer *Ostrinia nubilalis* (Hubner) pheromone reception. BMC Evol Biol 10:285

Omasits U, Ahrens CH, Müller S, Wollscheid B (2013) Protter: interactive protein feature visualization and integration with experimental proteomic data. Bioinformatics 30:884–886

Ono T (1993) Effect of rearing temperature on pheromone component ratio in potato tuberworm moth, *Phthorimaea operculella*, (Lepidoptera: Gelechiidae). J Chem Ecol 19:71–81

Ono T, Charlton RE, Cardé RT (1990) Variability in pheromone composition and periodicity of pheromone titer in potato tuberworm moth, *Phthorimaea operculella* (Lepidoptera: Gelechiidae). J Chem Ecol 16:531–542

Ozsolak F, Milos PM (2011) RNA sequencing: advances, challenges and opportunities. Nat Rev Genet 12:87–98

Pellegrino M, Steinbach N, Stensmyr MC, et al (2011) A natural polymorphism alters odour and DEET sensitivity in an insect odorant receptor. Nature 478:511–514

Pelosi P, Iovinella I, Felicioli A, Dani FR (2014) Soluble proteins of chemical communication: an overview across arthropods. Front Physiol 5:320

Pelosi P, Iovinella I, Zhu J, et al (2018) Beyond chemoreception: diverse tasks of soluble olfactory proteins in insects. Biol Rev 93:184–200

Pelosi P, Zhou JJ, Ban LP, Calvello M (2006) Soluble proteins in insect chemical communication. Cell Mol Life Sci 63:1658–1676

Percy-Cunningham JE, Macdonald JA (1987) Biology and Ultrastructure of Sex Pheromone–Producing Glands. In: Prestwich GD, Blomquist GJ (eds) Pheromone Biochemistry. Academic Press, pp 27–75

Perera OP, Shelby KS, Popham HJR, et al (2015) Generation of a transcriptome in a model lepidopteran pest, *Heliothis virescens*, using multiple sequencing strategies for profiling midgut gene expression. PloS ONE 10:e0128563

Pettersen KH, Devor A, Ulbert I, et al (2006) Current-source density estimation based on inversion of electrostatic forward solution: Effects of finite extent of neuronal activity and conductivity discontinuities. J Neurosci Methods 154:116–133

Phelan PL (1992) Evolution of Sex pheromones and the Role of Asymmetric Tracking. In: Roitberg BD, Isman MB (eds) Insect Chemical Ecology An Evolutionary Approach. New York, pp 265–314

Phelan PL, Baker TC (1987) Evolution of male pheromones in moths: reproductive isolation through sexual selection? Science 235:205–207

Phelan PL, Baker TC (1990) Comparative study of courtship in twelve phycitine moths (Lepidoptera: Pyralidae). J Insect Behav 3:303–326

Phelan PL, Miller JR (1982) Post-landing behavior of alate *Myzus persicae* as altered by (E)-β-farnesene and three carboxylic acids. Entomol Exp App 32:46–53

Picimbon J-F, Dietrich K, Krieger J, Breer H (2001) Identity and expression pattern of chemosensory proteins in *Heliothis virescens* (Lepidoptera, Noctuidae). Insect Biochem Mol Biol 31:1173–1181

Pickett JA, Wadhams LJ, Woodcock CM (1997) Developing sustainable pest control from chemical ecology. Agric Ecosyst Environ 64:149–156

Pitts W (1952) Investigation of synaptic transmission. In: Foerster HV (ed) Cybernetics, *Trans. 9th Conf. Josiah Macy Foundation*. New York, pp 159–166

Potworowski J, Jakuczun W, Łęski S, Wójcik D (2012) Kernel Current Source Density Method. Neural Comput 24:541–575

Rafaeli A, Jurenka RA (2003) 5 - PBAN Regulation of Pheromone Biosynthesis in Female Moths. In: Blomquist G, Vogt R (eds) Insect Pheromone Biochemistry and Molecular Biology. Academic Press, San Diego, pp 107–136

Raina AK, Wergin WP, Murphy CA, Erbe EF (2000) Structural organization of the sex pheromone gland in *Helicoverpa zea* in relation to pheromone production and release. Arthropod Struct Dev 29:343–353

Ray A, van der Goes van Naters W, Shiraiwa T, Carlson JR (2007) Mechanisms of odor receptor gene choice in *Drosophila*. Neuron 53:353–369

Regier JC, Brown JW, Mitter C, et al (2012) A molecular phylogeny for the leaf-roller moths (Lepidoptera: Tortricidae) and its implications for classification and life history evolution. PloS ONE 7:e35574

Reisenman CE, Lei H, Guerenstein PG (2016) Neuroethology of olfactory-guided behavior and its potential application in the control of harmful insects. Front Physiol 7:271

Renou M (2014) Pheromones and General Odor Perception in Insects. In: Mucignat-Caretta C (ed) Neurobiology of Chemical Communication. CRC Press, Boca Raton, Florida, pp 23–56

Ribeiro JMC, Genta FA, Sorgine MHF, et al (2014) An insight into the transcriptome of the digestive tract of the bloodsucking bug, *Rhodnius prolixus*. PLoS Negl Trop Dis 8:e2594

Ritchie MG (1996) The shape of female mating preferences. Proc Natl Acad Sci USA 93:14628-14631

Robertson G, Schein J, Chiu R, et al (2010) *De novo* assembly and analysis of RNA-seq data. Nat Methods 7:909–912

Robertson HM, Warr CG, Carlson JR (2003) Molecular evolution of the insect chemoreceptor gene superfamily in *Drosophila melanogaster*. Proc Natl Acad Sci USA 100:14537–14542

Roelofs W, Cardé A, Hill A, Cardé R (1976) Sex pheromone of the threelined leafroller, *Pandemis limitata*. Environ Entomol 5:649–652

Roelofs W, Glover T, Tang XH, et al (1987) Sex pheromone production and perception in European corn borer moths is determined by both autosomal and sex-linked genes. Proc Natl Acad Sci USA 84:7585–7589

Roelofs WL (1984) Electroantennogram assays: rapid and convenient screening procedures for pheromones. In: Hummel HE, Miller TA (eds) Techniques in Pheromone Research. Springer, New York, pp 131–159

Roelofs WL, Cardé RT (1977) Responses of Lepidoptera to synthetic sex pheromone chemicals and their analogues. Ann Rev Entomol 22:377–405

Roelofs WL, Liu W, Hao G, et al (2002) Evolution of moth sex pheromones via ancestral genes. Proc Natl Acad Sci USA 99:13621–13626

Roelofs WL, Rooney AP (2003) Molecular genetics and evolution of pheromone biosynthesis in Lepidoptera. Proc Natl Acad Sci USA 100:9179–9184

Rogers ME, Krieger JR, Vogt RG (2001) Antennal SNMPs (sensory neuron membrane proteins) of lepidoptera define a unique family of invertebrate CD36-like proteins. J Neurobiol 49:47-61

Rogers ME, Sun M, Lerner MR, Vogt RG (1997) SNMP1, a novel membrane protein of olfactory neurons of the silk moth *Antheraea polyphemus* with homology to the CD36 family of membrane proteins. J Biol Chem 272:14792–14799

Rule GS, Roelofs WL (1989) Biosynthesis of sex pheromone components from linolenic acid in arctiid moths. Arch Insect Biochem Physiol 12:89–97

Ruther J (2014) Pheromone research - still something to write home about. J Chem Ecol 40:215---289

Ryan MF (2002) The chemoreceptive organs: structural aspects. In: Ryan MF (ed) Insect Chemoreception. Kluwer Academic Publishers, Boston, pp 113–140

Rytz R, Croset V, Benton R (2013) Ionotropic receptors (IRs): chemosensory ionotropic glutamate receptors in *Drosophila* and beyond. Insect Biochem Mol Biol 43:888–897

Sacomoto GAT, Kielbassa J, Chikhi R, et al (2012) KISSPLICE: *de-novo* calling alternative splicing events from RNA-seq data. BMC Bioinformatics 13 Suppl 6:S5

Samuelson DWS, Jurenka RA, Cripps C, et al (1988) Fatty acids in insects: Composition, metabolism, and biological significance. Arch Insect Biochem Physiol 9:1–33

Sasaerila Y, Gries G, Khaskin G, Gries R (1997) Identification of sex pheromone components of nettle caterpillar, *Setothosea asigna*. J Chem Ecol 23:2187–2196

Sato K, Pellegrino M, Nakagawa T, et al (2008) Insect olfactory receptors are heteromeric ligand-gated ion channels. Nature 452:1002–1006

Schal C (1986) Effects of temperature and light on calling in the tiger moth *Holomelina lamae (*Freeman) (Lepidoptera: Arctiidae). Physiol Entomol 11:75–87

Schal C, Sevala V, Cardé RT (1998) Novel and highly specific transport of a volatile sex pheromone by hemolymph Lipophorin in Moths. Naturwissenschaften 85:339–342

Schneider D (1957) Electrophysiological investigation on the antennal receptors of the silk moth during chemical and mechanical stimulation. Experientia 13:89–91

Schneider D (1992) 100 years of pheromone research. Naturwissenschaften 79:241–250

Schneider D (1969) Insect olfaction: deciphering system for chemical messages. Science 163:1031

Schneider D, Schulz S, Priesner E, et al (1998) Autodetection and chemistry of female and male pheromone in both sexes of the tiger moth *Panaxia quadripunctaria*. J Comp Physiol A 182:153–161

Schulz MH, Zerbino DR, Vingron M, Birney E (2012) Oases: robust *de novo* RNA-seq assembly across the dynamic range of expression levels. Bioinformatics 28:1086–1092

Seabrook WD, Linn CE, Dyer LJ, Shorey HH (1987) Comparison of electroantennograms from female and male cabbage looper moths (*Trichoplusia ni*) of different ages and for various pheromone concentrations. J Chem Ecol 13:1443–1453

Sheck AL, Groot AT, Ward CM, et al (2006) Genetics of sex pheromone blend differences between *Heliothis virescens* and *Heliothis subflexa*: a chromosome mapping approach. J Evol Biol 19:600–617

Silbering AF, Rytz R, Grosjean Y, et al (2011) Complementary function and integrated wiring of the evolutionarily distinct *Drosophila* olfactory subsystems. J Neurosci 31:13357–13375

Silva-Brandão KL, Horikoshi RJ, Bernardi D, et al (2017) Transcript expression plasticity as a response to alternative larval host plants in the speciation process of corn and rice strains of *Spodoptera frugiperda*. BMC Genomics 18:107

Simão FA, Waterhouse RM, Ioannidis P, et al (2015) BUSCO: assessing genome assembly and annotation completeness with single-copy orthologs. Bioinformatics 31:3210–3212

Smith-Unna R, Boursnell C, Patro R, et al (2016) TransRate: reference-free quality assessment of *de novo* transcriptome assemblies. Genome Res 26:1134–1144

Sparkman OD, Penton ZE, Kitson FG (2011) Chapter 2 - Gas Chromatography. In: Sparkman OD, Penton ZE, Kitson FG (eds) Gas Chromatography and Mass Spectrometry (Second Edition). Academic Press, Amsterdam, pp 15–83

Steck W, Underhill EW, Chisholm MD, et al (1979) Sex pheromone traps in population monitoring of adults of the bertha armyworm, *Mamestra configurata* (Lepidoptera: Noctuidae). Can Entomol 111:91–95

Steck WF, Bailey BK, Underhill EW (1984) Effects of some semiochemicals on the sex pheromone of the bertha armyworm, *Mamestra configurata* (Lepidoptera: Noctuidae). Can Entomol 116:619–623

Steinbrecht RA (1997) Pore structures in insect olfactory sensilla: A review of data and concepts. Int J Insect Morphol & Embryol 26:229–245

Steinbrecht RA, Laue M, Ziegelberger G (1995) Immunolocalization of pheromone-binding protein and general odorant-binding protein in olfactory sensilla of the silk moths *Antheraea* and *Bombyx*. Cell Tissue Res 282:203–217

Stengl M (2010) Pheromone transduction in moths. Front Cell Neurosci 4:1-15

Stengl M, Funk NW (2013) The role of the coreceptor Orco in insect olfactory transduction. J Comp Physiol A 199:897–909

Stengl M, Hildebrand JG (1990) Insect olfactory neurons in vitro: morphological and immunocytochemical characterization of male-specific antennal receptor cells from developing antennae of male *Manduca sexta*. J Neurosci 10:837–847

Strandh M, Johansson T, Ahrén D, Löfstedt C (2008) Transcriptional analysis of the pheromone gland of the turnip moth, *Agrotis segetum* (Noctuidae), reveals candidate genes involved in pheromone production. Insect Mol Biol 17:73–85

Struble DL, Arn H (1984) Combined Gas Chromatography and Electroantennogram Recording of Insect Olfactory Responses. In: Hummel HE, Miller TA (eds) Techniques in Pheromone Research. Springer New York, pp 161–178

Struble DL, Ayre GL, Byers JR (1984) Minor sex-pheromone components of *Mamestra configurata* (Lepidoptera: Noctuidae) and improved blends for attraction of male moths. Can Entomol 116:103–105

Su C-Y, Menuz K, Carlson JR (2009) Olfactory perception: receptors, cells, and circuits. Cell 139:45–59

Suckling DM (2016) Monitoring for Surveillance and Management. In: Allison JD, Cardé RT (eds) Pheromone Communication in Moths. University of California Press, Oakland, California, pp 345–356

Sun Y-L, Huang L-Q, Pelosi P, Wang C-Z (2012) Expression in antennae and reproductive organs suggests a dual role of an odorant-binding protein in two sibling *Helicoverpa* species. PloS ONE 7:e30040

Svensson MGE, Bengtsson M, Löfqvist J (1997) Individual variation and repeatability of sex pheromone emission of female turnip moths *Agrotis segetum*. J Chem Ecol 23:1833–1850

Swailes GE, Struble DL, Holmes ND (1975) Use of traps baited with virgin females for field observations on the bertha armyworm (Lepidoptera: Noctuidae). Can Entomol 107:781–784

Talluri S, Bhatt A, Smith DP (1995) Identification of a *Drosophila* G protein alpha subunit (dGq alpha-3) expressed in chemosensory cells and central neurons. Proc Natl Acad Sci USA 92:11475–11479

Tang JD, Charlton RE, Card RT, Yin C-M (1992) Diel periodicity and influence of age and mating on sex pheromone titer in gypsy moth, *Lymantria dispar* (L.). J Chem Ecol 18:749-760

Teal PEA, Tumlinson JH (1987) The role of alcohols in pheromone biosynthesis by two noctuid moths that use acetate pheromone components. Arch Insect Biochem Physiol 4:261–269

Teal PEA, Tumlinson JH (1988) Properties of cuticular oxidases used for sex pheromone biosynthesis by *Heliothis zea*. J Chem Ecol 14:2131–2145

Tegoni M, Campanacci V, Cambillau C (2004) Structural aspects of sexual attraction and chemical communication in insects. Trends Biochem Sci 29:257–264

Tian Q, Stepaniants SB, Mao M, et al (2004) Integrated genomic and proteomic analyses of gene expression in mammalian cells. Mol Cell Proteom 3:960–969

Tillman JA, Seybold SJ, Jurenka RA, Blomquist GJ (1999) Insect pheromones-an overview of biosynthesis and endocrine regulation. Insect Biochem Mol Biol 29:481–514

Tobin TR (1981) Pheromone orientation: role of internal control mechanisms. Science 214:1147

Toth M, Löfstedt C, Blair BW, et al (1992) Attraction of male turnip moths *Agrotis segetum* (Lepidoptera: Noctuidae) to sex pheromone components and their mixtures at 11 sites in Europe, Asia, and Africa. J Chem Ecol 18:1337–1347

Toth M, Szöcs G, van Nieukerken EJ, et al (1995) Novel type of sex pheromone structure identified from *Stigmella malella* (Stainton) (Lepidoptera: Nepticulidae). J Chem Ecol 21:13–27

Touhara K, Vosshall LB (2009) Sensing odorants and pheromones with chemosensory receptors. AnnRev Physiol 71:307–332

Turnock WJ (1985) Developmental, survival, and reproductive parameters of bertha armyworm, *Mamestra configurata* (Lepidoptera: Noctuidae) on four plant species. Can Entomol 117:1267–1271

Turnock WJ, Braken GK (1989) Effects of low non-freezing tempertures on pupae of two species of diapausing, freeze-intolerant insects. Cryo-letters 10:189–196

Ulmer B, Gillott C, Erlandson M (2001) Feeding preferences, growth, and development of *Mamestra configurata* (Lepidoptera: Noctuidae) on *Brassicaceae*. Can Entomol 133:509-519

Underhill EW, Steck WF, Chisholm MD (1977a) A sex pheromone mixture for the bertha armyworm moth, *Mamestra configurata*: (*Z*)-9-Tetradecen-1-ol acetate and (*Z*)-11-hexadecen-1-ol acetate. Can Entomol 109:1335–1340

Underhill EW, Steck WF, Chisholm MD (1977b) A sex pheromone mixture for the bertha armyworm moth, *Mamestra configurata*: (Z)-9-tetradecen-1-ol acetate and (Z)-11-hexadecen-1-ol acetate. Can Entomol 109:1335–1340

van der Pers J, Ockenfels P (2004) Electroantennography. Ockenfels SYNTECH GmbH

van Dijk EL, Auger H, Jaszczyszyn Y, Thermes C (2014) Ten years of next-generation sequencing technology. Trends Genet 30:418–426

van Nieukerken EJ, Kaila L, Kitching IJ, et al (1999) Order Lepidoptera Linnaeus, 1758. In: Zhang, Z.-Q. (Ed.) Animal biodiversity: An outline of higher-level classification and survey of taxonomic richness. 1–10

Vasquez GM, Syed Z, Estes PA, et al (2013) Specificity of the receptor for the major sex pheromone component in *Heliothis virescens*. J Insect Sci 13:1–12

Vickers NJ (2006a) Winging It: moth flight behavior and responses of olfactory neurons are shaped by pheromone plume dynamics. Chem Senses 31:155–166

Vickers NJ (2006b) Inheritance of olfactory preferences I. Pheromone-mediated behavioral responses of *Heliothis subflexa* x *Heliothis virescens* hybrid male moths. Brain Behav Evol 68:63–74

Vickers NJ (2006c) Inheritance of olfactory preferences III. Processing of pheromonal signals in the antennal lobe of *Heliothis subflexa* x *Heliothis virescens* hybrid male moths. Brain Behav Evol 68:90–108

Vickers NJ (2002) Defining a synthetic pheromone blend attractive to male *Heliothis subflexa* under wind tunnel conditions. J Chem Ecol 28:1255–1267

Vickers NJ, Baker TC (1992) Male *Heliothis virescens* maintain upwind flight in response to experimentally pulsed filaments of their sex pheromone (Lepidoptera: Noctuidae). J Insect Behav 5:669–687

Vickers NJ, Christensen TA (2003) Functional divergence of spatially conserved olfactory glomeruli in two related moth species. Chem Senses 28:325–338

Vogt RG, Chertemps T (2005) Molecular Basis of Pheromone Detection in Insects. In: Vogt RG, Chertemps T (eds) Comprehensive Molecular Insect Science. pp 753–803

Vogt RG, Große-Wilde E, Zhou J-J (2015) The Lepidoptera odorant binding protein gene family: Gene gain and loss within the GOBP/PBP complex of moths and butterflies. Insect Biochem Mol Biol 62:142–153

Voshall A, Moriyama EN (2018) Next-generation assembly: Strategies adn performance analysis. In: Abdurakhmonov IY (ed) Bioinformatics in the Era of Post Genomics and Big Data. pp 16–36

Vosshall LB, Hansson BS (2011) Unified nomenclature system for the insect olfactory coreceptor. Chem Senses 36:497–498

Wang G, Vasquez GM, Schal C, et al (2011) Functional characterization of pheromone receptors in the tobacco budworm *Heliothis virescens.* Insect Mol Biol 20:125–133

Wang H-L, Ming Q-L, Zhao C-H, Wang C-Z (2008) Genetic basis of sex pheromone blend difference between *Helicoverpa armigera* (Hübner) and *Helicoverpa assulta* (Guenée) (Lepidoptera: Noctuidae). J Insect Physiol 54:813–817

Wang H-L, Zhao C-H, Wang C-Z (2005) Comparative study of sex pheromone composition and biosynthesis in *Helicoverpa armigera, H. assulta* and their hybrid. Insect Biochem Mol Biol 35:575–583

Wang Z, Gerstein M, Snyder M (2009) RNA-Seq: a revolutionary tool for transcriptomics. Nat Rev Genet 10:57–63

Wanner KW, Nichols AS, Allen JE, et al (2010) Sex pheromone receptor specificity in the European corn borer moth, *Ostrinia nubilalis*. PloS ONE 5:e8685

Wanner KW, Willis LG, Theilmann DA, et al (2004) Analysis of the insect os-d-like gene family. J Chem Ecol 30:889–911

Watanabe K, Toba G, Koganezawa M, Yamamoto D (2011) Gr39a, a highly diversified gustatory receptor in *Drosophila*, has a role in sexual behavior. Behav Genet 41:746–753

Weeraddana CDS, Evenden ML (2018) Canola nutrition and variety affect oviposition and offspring performance in the generalist herbivore, *Mamestra configurata* (Lepidoptera: Noctuidae). J Econ Entomol 111:1702–1710

Weid Von Der B, Rossier D, Lindup M, et al (2015) Large-scale transcriptional profiling of chemosensory neurons identifies receptor-ligand pairs in vivo. Nat Neurosci 18:1455–1463

Wicher D (2018) Tuning insect odorant receptors. Front Cell Neurosci 12:94

Wicher D, Schafer R, Bauernfeind R, et al (2008) *Drosophila* odorant receptors are both ligand-gated and cyclic-nucleotide-activated cation channels. Nature 452:1007–1011

Willett CS, Harrison RG (1999) Insights into genome differentiation: pheromone-binding protein variation and population history in the European corn borer (*Ostrinia nubilalis*). Genetics 153:1743–1751

Willis MA, Baker TC (1988) Effects of varying sex pheromone component ratios on the zigzagging flight movements of the oriental fruit moth, *Grapholita molesta*. J Insect Behav 1:357–371

Willis MA, Baker TC (1984) Effects of intermittent and continuous pheromone stimulation on the flight behaviour of the oriental fruit moth, *Grapholita molesta*. Environ Entomol 9:341-358

Willis MA, David CT, Murlis J, Cardé RT (1994) Effects of pheromone plume structure and visual stimuli on the pheromone-modulated upwind flight of male gypsy moths (*Lymantria dispar*) in a forest (Lepidoptera: Lymantriidae). J Insect Behav 7:385–409

Wilson-Sanders SE (2011) Invertebrate models for biomedical research, testing, and education. 52:126–152

Witzgall P (1997) Modulation of Pheromone-Mediated Flight in Male Moths. In: Insect Pheromone Research. Springer, Boston, MA, Boston, MA, pp 265–274

Wu J, Baldwin IT (2010) New insights into plant responses to the attack from insect herbivores. Ann Rev Genet 44:1–24

Wu W, Zhu J, Millar J, Löfstedt C (1998) A comparative study of sex pheromone biosynthesis in two strains of the turnip moth, *Agrotis segetum*, producing different ratios of sex pheromone components. Insect Biochem Mol Biol 28:895–900

Wyatt T (2014) Introduction to Chemical Signaling in Vertebrates and Invertebrates. In: Neurobiology of Chemical Communication. CRC Press, pp 1–22

Wylie HG, Bucher GE (1977) The bertha armyworm, *Mamestra configurata* (Lepidoptera: Noctuidae). Mortality of immature stages on the rape crop, 1972-1975. Can Entomol 109:823–837

Xie Y, Wu G, Tang J, et al (2014) SOAP *de novo*-Trans: *de novo* transcriptome assembly with short RNA-Seq reads. Bioinformatics 30:1660–1666

Xu W, Anderson A (2015) Carbon dioxide receptor genes in cotton bollworm *Helicoverpa armigera*. Naturwissenschaften 102:10741

Xu W, Papanicolaou A, Liu NY, et al (2015) Chemosensory receptor genes in the Oriental tobacco budworm *Helicoverpa assulta*. Insect Mol Biol 24:253–263

Yamakawa R, Do ND, Kinjo M, et al (2011a) Novel components of the sex pheromones produced by emerald moths: identification, synthesis, and field evaluation. J Chem Ecol 37:105–113

Yamakawa R, Kiyota R, Taguri T, Ando T (2011b) (5R,7R)-5-Methylheptadecan-7-ol; a novel sex pheromone component produced by a female lichen moth, *Miltachrista calamine*, in the family Arctiidae. Tetrahedron Lett 52:5808–5811

Yang K, Huang L-Q, Ning C, Wang C-Z (2017) Two single-point mutations shift the ligand selectivity of a pheromone receptor between two closely related moth species. eLife 6:155

Yew JY, Chung H (2015) Insect pheromones: an overview of function, form, and discovery. Prog Lipid Res 59:88–105

Zerbino DR, Birney E (2008) Velvet: Algorithms for *de novo* short read assembly using de Bruijn graphs. Genome Res 18:821–829

Zhang C, Zhang B, Lin L-L, Zhao S (2017) Evaluation and comparison of computational tools for RNA-seq isoform quantification. BMC Genomics 18:583

Zhang D-D, Löfstedt C (2015) Moth pheromone receptors: gene sequences, function, and evolution. Front Ecol Evol 3:51

Zhang DD, Löfstedt C (2013) Functional evolution of a multigene family: orthologous and paralogous pheromone receptor genes in the turnip moth, *Agrotis segetum*. PloS ONE 8:e77345

Zhang H-J, Anderson AR, Trowell SC, et al (2011) Topological and functional characterization of an insect gustatory receptor. PloS ONE 6:e24111

Zhang J, Walker WB, Wang G (2015a) Pheromone reception in moths: from molecules to behaviors. Prog Mol Biol Transl Sci 130:109–128

Zhang J, Yan S, Liu Y, et al (2015b) Identification and functional characterization of sex pheromone receptors in the common cutworm (*Spodoptera litura*). Chem Senses 40:7–16

Zhang Y-N, Jin J-Y, Jin R, et al (2013) Differential expression patterns in chemosensory and non-chemosensory tissues of putative chemosensory genes identified by transcriptome analysis of insect pest the purple stem borer *Sesamia inferens* (Walker). PloS ONE 8:e69715

Zhang Y-N, Ye Z-F, Yang K, Dong S-L (2014) Antenna-predominant and male-biased CSP19 of *Sesamia inferens* is able to bind the female sex pheromones and host plant volatiles. Gene 536:279–286

Zhong H, Li F, Chen J, et al (2017) Comparative transcriptome analysis reveals host-associated differentiation in *Chilo suppressalis* (Lepidoptera: Crambidae). Sci Rep 7:124

Zhu J, Chastain BB, Spohn BG, Haynes KF (1997) Assortative mating in two pheromone strains of the cabbage looper moth, *Trichoplusia ni*. J Insect Behav 10:805–817

Zhu J, Kozlov MV, Philipp P, et al (1995) Identification of a novel moth sex pheromone in *Eriocrania cicatricella* (Zett.) (Lepidoptera: Eriocraniidae) and its phylogenetic implications. J Chem Ecol 21:29–43

Zhu J, Löfstedt C, Bengtsson BO (1996a) Genetic variation in the strongly canalized sex pheromone communication system of the European corn borer, *Ostrinia nubilalis* Hübner (Lepidoptera; Pyralidae). Genetics 144:757–766

Zhu JW, Zhao CH, Lu F, et al (1996b) Reductase specificity and the ratio regulation of *E/Z* isomers in pheromone biosynthesis of the European corn borer, *Ostrinia nubilalis* (Lepidoptera: Pyralidae). Insect Biochem Mol Biol 26:171–176

(2011) Western Committee of Crop Pests Annual Meeting www.westernforum.org